Plant-Based Cheese Analogues

and

Value-Added, High-Fiber Soymilk Gels Containing Okara

by

Jing Sy

A thesis

presented to the University of Waterloo

in fulfillment of the

thesis requirement for the degree of

Master of Applied Science

in

Chemical Engineering

Waterloo, Ontario, Canada, 2022

Author's Declaration

This thesis consists of material all of which I authored or co-authored: see Statement of Contributions included in the thesis. This is a true copy of the thesis, including any required final revisions, as accepted by my examiners.

I understand that my thesis may be made electronically available to the public.

Statement of Contributions

Jing Sy was the sole author of Chapters 1, 2, 3, 6, and 7, which were written under the supervision of Dr. Christine Moresoli and were not written for publication.

This thesis consists in part of two manuscripts written for publication. Exceptions to sole authorship of materials are as follows:

Research presented in Chapters 4 and 5:

Dr. Christine Moresoli was the supervisor, primary co-investigator, and the grant acquirer of Natural Sciences and Engineering Research Council (NSERC) which supported the work. Dr. Tizazu Mekonnen was the co-author of both manuscripts, who provided valuable resources for the execution of the work and advice related to the projects.

This research was conducted at the University of Waterloo by Jing Sy under the supervision of Dr. Christine Moresoli. Jing Sy contributed to the study by forming research hypothesis, designing experimentation, developing methods for characterizations, conducting experiments, analyzing and interpreting results. The initial drafts of the manuscripts were written by Jing Sy, which were reviewed by all co-investigators, and edited by Dr. Christine Moresoli and Jing Sy.

Chapter 4:

Dr. Christine Moresoli is the corresponding author of the manuscript presented in Chapter 4. Jing Z. Sy and Dr. Tizazu H. Mekonnen are the co-authors. The breakdown of authors' contributions is as follows:

- Jing Sy: conceptualization, methodology, experimentation, analysis, writing – original draft and editing.
- Christine Moresoli: conceptualization, methodology, experimentation, analysis, writing – original draft review and editing, supervision, funding acquisition.
- Tizazu Mekonnen: FTIR, mechanical and viscoelastic characterization – methodology and analysis, revised draft – review and editing.

Chapter 5:

Dr. Christine Moresoli is the corresponding author of the manuscript presented in Chapter 5. Jing Z. Sy and Dr. Tizazu H. Mekonnen are the co-authors. The breakdown of authors' contributions is as follows:

- Jing Sy: conceptualization, investigation, methodology, experimentation, data curation, formal analysis, writing – original draft and editing.
- Christine Moresoli: conceptualization, investigation, methodology, data curation, formal analysis, writing – original draft review and editing, supervision, funding acquisition.
- Tizazu Mekonnen: mechanical and viscoelastic characterization – methodology and analysis, revised draft – review and editing.

Abstract

In this work, the potential of adding soy okara modified by heat or citric acid or their combination into soymilk to create whole soybean gels was examined. The purpose of the treatments was to improve the compatibility of okara with the soy protein matrix by targeting the insoluble components of okara. The changes to okara as well as the physicochemical and structural properties of the okara-containing soymilk gels were examined. Subsequently, selected commercial dairy and vegan cheeses along with soybean derived products were analyzed to establish baseline textural profiles.

Soymilk gels containing okara subjected to heat treatment (95 °C, 1 h) had similar properties to the untreated okara-containing soymilk gels. In contrast, citric acid (CA) modified okara (3:5 w/w citric acid:okara) showed remarkable alterations in structure where esterification reactions occurred in the insoluble constituents of okara based on FTIR results. The changes to CA okara were also confirmed by TGA results. The soymilk gel containing CA okara displayed the highest Young's modulus (up to 30 kPa) among all gels, and decent true fracture stress reaching over 4 kPa. It also had a homogeneous and protein-continuous structure indicating the enhanced compatibility of okara with the soy protein matrix. The okara subjected to citric acid and subsequent heat treatment (CAH) had more than double the soluble solids content when compared to the CA okara, indicating significant hydrolysis of okara. The soymilk gels containing CAH okara had extremely high mechanical strength where fracture was not observed under compressive load used in this study. The gel prepared with the insoluble portion of CAH okara displayed coarse-stranded network which may explain the considerable water syneresis observed with this gel. This study demonstrates the benefits of modifying okara with citric acid to improve its integration with the soy protein matrix and produce homogeneous and protein rich high-fiber soybean gel product.

Limited similarities exist between the commercial vegan mozzarella style cheese and the conventional pizza or fresh mozzarella regarding their mechanical and viscoelastic properties. The commercial vegan cheddar and mozzarella style cheeses displayed high mechanical strength and viscoelastic rigidity with a compact structure possessing excellent water holding capacity. As expected, due to their different processing conditions, distinct characteristics were observed among the dairy cheeses, *i.e.*, pizza and fresh mozzarella, and panner. Pizza mozzarella and

paneer had considerably higher mechanical strength whereas the fresh mozzarella had a significantly softer texture that closely resembled tofu products. The extra and medium firm tofu had considerably weaker mechanical strength, gel rigidity and low water holding capacity, contrasting the other commercial products.

The okara-containing soymilk gels developed in this study had resembling viscoelastic properties and comparable mechanical firmness as affirmed by Young's modulus to the commercial tofu products. However, the lower true fracture stress of the okara-containing soymilk gels reflects the considerable differences in composition and processing compared to the commercial products. Overall, these results demonstrate the potential of the high-fiber soymilk gels containing okara as substitutes to the existing commercial tofu products and eventually even as dairy cheese analogues.

Acknowledgements

I would like to offer my sincere gratitude to my supervisor, Prof. Christine Moresoli for her all-time guidance and support. She shaped me to become a better researcher I am now. She taught me to be a critical thinker and a meticulous individual. Beyond that, she is always considerate. She cares not only for my success but also supports me personally even as a friend whom I deeply respect.

Furthermore, I would like to give my special thanks to Prof. Tizazu Mekonnen for providing valuable advice and resources that contributed greatly to our research work. I would also like to thank Prof. Alexander Penlidis for taking the time to review our work and providing feedback.

I am also exceedingly grateful for all those who have helped me during my studies. I would like to make mention of Dylan Jubinville and Rohan Shorey for their assistance with the training of FTIR, mechanical and rheology equipment. I would also like to thank my colleague and my friend, Xuan Nguyen, who also helped conduct the mechanical and rheological tests of a commercial product as presented in this work.

Finally, but the most importantly, I would like to express my deepest appreciation to my beloved husband and my dearest friend, Serubbabel Sy, for his unconditional love and unceasing care. I would also like to make mention of my parents and grandparents who have always been my support and safe harbor.

Dedication

To my God and the Father of all, who is over all and through all and in all.

Table of Contents

List of Figures

List of Tables

List of Abbreviations

Abbreviations	Full Name
SPC	Soy protein concentrate
SPI	Soy protein isolate
pI	Isoelectric point
TAG	Triglyceride
NSP	Non-starch polysaccharide
GDL	Glucono-delta-lactone
TGase	Transglutaminase
MTGase	Microbial transglutaminase
DP	Degree of polymerization
MDF	Micro-sized okara fiber
NDF	Nano-sized okara fiber
SHP	Sodium hypophosphite
SSPS	Soluble soybean polysaccharides
ISPS	Insoluble soybean polysaccharides
HMP	High methoxyl pectin
CMC	Carboxymethyl cellulose
EDTA	Ethylenediaminetetraacetic acid
WPI	Whey protein isolate
DS	Dried solids on filter paper
DSWL	Dried solids in washing liquid
DI	Deionized
TPA	Texture profile analyzer
LVR	Linear viscoelastic region
TGA	Thermogravimetric analysis
DTG	Derivative thermogravimetry
WHC	Water-holding capacity
FTIR	Fourier-transform infrared spectroscopy

SDS-PAGE	Sodium dodecyl sulphate-polyacrylamide gel electrophoresis
SEM	Scanning electron microscope
CLSM	Confocal laser scanning microscopy
NMR	Nuclear magnetic resonance
HSQC-NMR	Heteronuclear single quantum coherence-nuclear magnetic resonance
HPAEC	High-performance anionic exchange chromatography

List of Symbols

Symbols	Meaning
$\sigma(t)$	True stress at time t
$l(t)$	Height of specimen during compression at time t
$F(t)$	Force of specimen during compression at time t
l_0	Original height of the specimen
A_0	Original cross-sectional area of the specimen
ϵ	True strain
E	Young's modulus
σ_{frac}	True fracture stress
ϵ_{frac}	True fracture strain
G'	Storage modulus
G"	Loss modulus
$\tan \delta$	Tangent delta
G*	Complex modulus
γ_L	Linearity limit or yield strain if strain sweep test is performed)
G_0'	Storage modulus at 1 rad/s
$G_0"$	Viscous modulus at 1 rad/s
ω	Angular frequency
n'	Degree of ω on G'
n"	Degree of ω on G"
W_t	Initial mass of specimen
W_r	Mass of released water during centrifugation

1.0 Introduction

1.1 Research Motivation and Objective

The demand for plant-based cheeses, also known as plant cheese analogues, has increased drastically over the years because of the rising dietary shifts to plant-based foods in general populations in views of environmental, health, and animal-welfare considerations. Current commercial plant cheeses often fall short in terms of their nutritional content when compared to conventional dairy cheeses. Plant-based cheeses lack proteins and consist primarily of carbohydrates and fats. There is limited knowledge on their physicochemical properties in the scientific literature. which limits the development of plant cheese analogues to have textural profiles comparable to traditional dairy cheeses. Therefore, there is a need to develop plant cheeses with high protein content and to better understand the texture profiles of commercial cheeses and related products.

Soy proteins are extensively studied plant proteins owing to their high nutritional value, essential amino-acid composition and economic advantages [1]. Soybeans are comprised of about 40% of protein on dry weight basis [2]. Tofu, also known as the soybean curd, is a gel-like product often induced by heat and coagulants, and thus resembling the production of dairy cheeses. It has increasingly attracted more consumers especially in recent years due its plant-based origin, high protein content (~8%), low saturated-fat (~0.7%) and minimal cholesterol content. In conventional tofu production, soybeans, either dehulled or hull-on, are soaked, ground, then filtered to recover and separate the soluble content, soymilk, from the insoluble residue, okara. The soymilk portion is then gelled to produce tofu while the okara is discarded as waste or used as animal feed [3]. Consequently, a growing body of research attempts to incorporate okara back into the tofu production because of its high dietary fiber and protein contents. However, there are challenges in creating homogeneous okara-containing soy tofu, or whole soybean gels, with desired texture attributes. Okara is comprised mostly of insoluble dietary fibers possessing a fibrous structure and large and irregularly shaped particles. These characteristics tend to limit the interactions between okara and the heat-denatured proteins, and thus the resulting gel is often coarse while possessing low strength [4]–[6]. Therefore, whole soybean gels are known to be chalky and sandy in texture [7].

1

Various techniques in literature have been employed to resolve the poor texture imparted by okara in whole soybean gels. Examples include physical treatments such as high-speed shearing, ultrasound, and high-pressure homogenization treatment as well as enzymatic treatments, *e.g.*, using transglutaminase and cellulose to increase protein coagulation and to hydrolyze cellulose in okara, respectively [4], [5], [8]–[12]. Nonetheless, the properties of the treated okara tofu remain inferior as compared to traditional tofu prepared without okara, including discontinuous network and lower gel strength [5], [12], [13]. Hence, there remains a need to improve the homogeneity and strength of okara soymilk gels.

Citric acid, an inexpensive weak acid was selected in this study to modify the okara fibers. Citric acid has been used to promote ester-bond formation in lignocellulosic materials [14]–[16]. It is therefore hypothesized that the carboxylic groups of citric acid may act as reactive sites for esterification reactions with the hydroxyl groups present in the okara fibers, and thus enhancing the compatibility of okara with the protein matrix. Citric acid may also assist with the solubilization of the insoluble fibers present in okara and facilitate the okara incorporation within the protein matrix. As a result, modification of okara with citric acid was examined as means to improve its compatibility with the protein matrix and create homogeneous soy gels with good mechanical strength.

The objective of this study was three-fold. Firstly, the effect of citric acid on okara-containing soymilk gels was investigated. Secondly, a mapping of physicochemical properties of commercial products including dairy cheeses, soybean-based products, and plant-based cheese analogues was established as baseline. Finally, the citric-acid-treated okara soymilk gels were compared with the commercial tofu products. Mechanical, viscoelastic, and structural properties were assessed to portray the textural attributes of the various products.

1.2 Thesis Structure

This main content of the thesis is organized into seven sections. The first and the last sections served as introduction and conclusion of the studies discussed in this thesis, respectively.

Chapter 2 encapsulates the research background which was developed based on the literature review of existing publications. Section 2.1 begins with the review of dairy cheeses and cheese analogues and serves as the background information for the study of commercial cheeses and related products in the manuscript outlined in chapter 5. Section 2.2 provides an overview of

food texture and its processing within the mouth. The following sections, sections 2.3-2.7 cover soybeans, tofu, okara, okara-containing whole soybean gels, and specific treatments of soy okara. These sections serve as background for the development of the research on citric acid treatment of okara which will be expanded in the manuscript outlined in chapter 4. This section is followed by the discussion of different characterizations used in this thesis, thermogravimetric analysis (TGA), Fourier transform infrared spectroscopy (FTIR), mechanical compression, rheology, water holding capacity (WHC), and morphology, as outlined in section 2.8. Section 2.9 entails the statistical analysis methods of the experimental data produced in this study.

Chapter 3 illustrates the preliminary experimentations conducted for the preparation of okara-containing soymilk gels. The experimentation presented in sections 3.1-3.7 was designed to explore and finalize the experimental conditions to be employed for the study detailed in chapter 4. Investigations focused on hypothesis testing, determining ingredient concentration and processing conditions, as well as developing techniques.

Chapters 4 and 5 encompass two submitted manuscripts. Specifically, chapter 4 contains the study of soy okara modification *via* citric acid treatment. This study illustrates a novel technique for the development of homogeneous okara-containing soymilk gel driven by waste reduction and value-added benefits. Chapter 5 outlines the study of the investigation of several commercial food products. The study provides the baseline of selected texture attributes of existing commercial dairy, soy, and imitation cheese products.

Lastly, chapter 6 entails the comparison of the okara soymilk gels and the commercially available tofu products.

2.0   Literature Review

2.1 Cheese

2.1.1   Dairy Cheeses

2.1.1.1 Classification

Cheeses are fermented milk-based food products, produced in a wide range of flavors and forms [17]. They are commonly classified according to their texture, which varies with the degree of moisture. In Canada, cheese products are generally categorized according to cheese firmness by the Canadian Dairy Information Center (CDIC) as summarized in **Table 2-1**.

Table 2-1 Cheese requirements according to different textures (according to statistics published on CDIC website)

Cheese type according to firmness	Moisture on fat-free basis
Soft fresh cheese	≥ 80%
Soft cheese	≥ 67%, and < 80%
Semi-soft cheese	≥ 62%, and < 67%
Firm cheese	≥ 50%, and < 62%
Hard cheese	< 50%

In Canada, mozzarella cheese is the second highest cheese production closely following cheddar cheese production according to the CDIC (**Table 2-2**). Hence, it is of our interest to study the properties of mozzarella.

Table 2-2 Cheese production (in kilogram) by variety in Canada (adapted based on statistics published on the CDIC website)

Cheese variety	2014	2015	2016	2017	2018	2019
Cheddar	143,070	146,810	155,139	162,355	173,478	163,583
Mozzarella	120,157	129,663	143,932	147,137	147,732	151,374
Cream	37,906	37,316	41,171	39,005	40,237	43,283
Cottage	24,094	21,362	21,397	23,339	23,528	23,255
Swiss & Emmental	10,184	10,827	10,551	7,787	8,651	9,302
Parmesan	9,006	9,752	10,776	11,271	11,919	12,559
Ricotta	5,712	6,650	8,352	8,886	9,375	9,316
Monterey Jack	8,330	7,843	9,361	10,950	11,054	12,234
Havarti	7,348	7,382	7,296	7,583	7,572	7,639
Feta	5,909	6,978	7,674	7,927	7,934	8,719
Gouda	3,045	3,475	X	2,880	2,992	3,141
Brick	2,922	2,630	3,272	3,604	3,910	3,933
Provolone	3,294	3,442	3,774	3,885	4,441	3,798
Friulano & Casata	522	X	X	760	760	X
Colby	334	X	X	X	X	407
Others	51,558	52,086	53,946	59,912	56,712	62,446
Total	433,391	446,216	476,641	497,281	510,250	514,989

2.1.1.2 Mozzarella

Mozzarella cheese is an un-ripened cheese. It is smooth and elastic with a long stranded parallel-oriented fibrous protein structure without evidence of curd graduals. The cheese is rindless and may be formed into various shapes [18].

Mozzarella is made by "pasta filata" processing. The milk is curdled initially by a bacteria starter followed by enzyme rennet. The curd with suitable pH is then kneaded and stretched until the it is smooth and free from lumps. When it is still warm, the curd is cut and moulded, then firmed by cooling. Other processing techniques, which give final products with the same physical, chemical and organoleptic characteristics are allowed [18].

Generally, mozzarella cheeses are categorized into two groups, low moisture (pizza) and high moisture (fresh). The low moisture mozzarella cheese is a firm/semi-hard homogeneous cheese

without holes and is suitable for shredding and heating to be consumed melted [18]. Sometimes it is also referred to as "low-moisture part-skim" and is made by souring fresh mozzarella a little longer, and then carefully drying it out. Low moisture mozzarella has a moisture content in the range of 45 to 52% range [19], while its fat content should be greater or equal than 30% on a dry matter basis [19]. Because of its lower moisture content, it has a longer shelf life and saltier taste. The lower moisture also lends the cheese to better browning and stretching abilities when heated, which makes it a popular choice for pizza and lasagna.

The high moisture or fresh mozzarella cheese is a soft cheese with overlying layers that may form pockets containing liquid of milky appearance. The fresh mozzarella can have moisture content as much as 60% by weight and sometimes even higher. The fat content of high moisture mozzarella is typically greater or equal than 45% on a dry matter basis [19]. The cheese has a near white colour [18]. It is often packaged in water or hand-wrapped fresh in plastic wrap and should be consumed within one week of production. Upon heating, water evaporates and may settle as a "soupy" or "puddle". This mozzarella does not work well in most heated foods, and is best eaten cold and fresh, such as in caprese salad.

2.1.1.3 Paneer

Paneer is a soft acid-set fresh cheese of Indian-origin made from cow or buffalo milk [20], classified as soft cheese. Paneer has relatively high fat content, 22-25% and moderate protein content (16-18%), low carbohydrate content (2-2.5%) and minerals (1.5-2%) [21]. The appearance of paneer is white and uniform with a mild acidic and sweet taste. Because of its compact texture, it is often used in Indian cuisine as a meat substitute [22].

Paneer is generally made by curdling milk with a fruit- or vegetable-derived acid, such as lemon juice. Typically, buffalo milk with 6% fat is heated at around 80 °C for 5 min and cooled to 70 °C before coagulation with 1% citric acid solution. The mixture is continuously stirred for complete separation of the curd from the whey. The curd is then collected in an open-bottom hoop and pressed for 15-20 min using a weight. The pressed curd is then cut into small pieces and immersed in pasteurized chill water for 2-3 h then drained to be packaged [22].

2.1.2   Cheese Analogues

Cheese analogues or imitation cheeses are food products with substitution where milk fat, protein or both may be partially or entirely replaced by non-milk-based components, primarily of plant

origin. The benefits of cheese analogue production include the selection of lower cost ingredients, ease of manufacture, and fewer requirements of equipment and manpower [23]. Beside these, a plant-based diet has shown to reduce farmland use by 3.1 million-hectare, greenhouse gas emissions by 6.6 billion metric tons of CO_2-equivalent, acidification by 50%, and eutrophication by 49% [24]. Recently, plant-based cheese analogues experienced a 28% growth in sale from 2019 to 2020 reaching $1.9 billion in USA [25].

There are two basic types of processes for manufacturing cheese substitutes (**Figure 2-1**). The first type is the use of liquid "milk" to initiate the conventional cheesemaking process. Products produced are often referred to as filled cheese. The second type is referred to as cheese analogues, which are obtained by blending various raw materials using techniques similar to the manufacture of processed cheeses. The majority of cheese substitutes are manufactured by the blending technique [26].

CHEESE SUBSTITUTES (= IMITATES) TYPES

FILLED CHEESES		CHEESE ANALOGUES		
Skimmed milk, butterfat, vegetable oil	Skimmed milk, vegetable oil	(a) Synthetic e.g. soya protein, soya oil, artificial flavour	(b) Partial dairy e.g. casein/ates, soya oil, artificial flavour	(c) Dairy e.g. casein/ates, butter oil, EMC

conventional cheese manufacturing methods (matured products)

processed cheese manufacturing methods (non-matured products)

Figure 2-1 Types of cheese substitutes [26]. Reprinted from *Cheese Analogues: A Review*, **11**, H. Bachmann, 505-515, 2001, with permission from Elsevier.

Soy-based cheese analogues have received considerable attention in the research community owing to the high nutritional value, essential amino-acid composition and economic advantages

associated with the use of soy proteins [27]. Researchers have studied soy proteins in plant cheese analogues for complete or partial substitution of dairy cheeses.

Most studies have used the blending technique for producing the soybean mozzarella cheese analogues [28], [29], [30]. The soy protein is typically sourced from full-fat and/or defatted soy flour, soy protein concentrate (SPC), or soy protein isolate (SPI). Some thickening agents such as gelatin, guar gum, and gum arabic are used along with fat, *e.g.*, hydrogenated shortening. These ingredients are then blended with water or soy base, heated into a slurry, and then tempered in ice-water bath for one day to produce a solid cheese-like mass [28], [29], [30].

According to Yand and Taranto [29], increased fat content can enhance the hardness of the analogue gels while the cohesiveness and springiness values are not affected as observed with texture profile analyzer (TPA) [28]. Moreover, samples prepared with soy base at natural pH (7.5) had the highest hardness, while adjusting the pH tended to result in a softer gel and also weakened the adhesiveness and cohesiveness. Furthermore, sample prepared with SPI as the source of soy protein exhibited a gel texture similar to the natural mozzarella cheese and increasing the amount of SPI resulted in enhanced stretchability, hardness, and adhesiveness. The addition of salts or electrolytes tends to weaken forces between charges which in turn led to reduced gel rigidity. The gel formation with a 2% NaCl was retarded even at a 40% gelatin concentration while the gel network was strengthened with 2% $CaCl_2$ by cross-linking between soy protein molecules *via* the calcium ions.

The effects of protein concentration, processing temperature, and mixing rate or shear rate of progel, the mixture subjected to heat treatment prior to solidification, were studied [30]. Heating at 80 °C for 30 min changes a slurry of soybean globulin (≥ 8% concentration, w/v) from solution to the progel state, followed by the formation of a gel through cooling at 4 °C for 1 h. A gel was formed at 8-14% protein concentration upon heat treatment of the slurry for 10 to 30 min at 70-100 °C with subsequent cooling. A gel was otherwise not formed when the slurry was heated to 125°C. When using a protein concentration above 17%, the gels formed were firm, resilient, self-supporting, and less susceptible to disruption by over-heating [30].

2.2 Food Texture and Oral Processing

Texture is a critical quality for food materials. This is illustrated by the study where fresh and unseasoned foods were pureed in a blender to eliminate textural clues and given to a blindfolded panel (young adults of normal weight) who were asked to identify foods solely based on flavour [31]. Their results showed that only 4% of panel correctly identified cabbage, 7% cucumber, 15% pork, 17% cream cheese, and 22% rice [31]. This confirms the essential role of the texture attributes in the cognition of foods.

Texture is the integration of both mechanical and thermal properties perceived in both oral and pharyngeal phases of the consuming process [32]. Sensory attributes expressed by consumers or experts to describe the properties of the food can be grouped according to the stage in the oral processing at which they are perceived [33]: pre-fracture, first bite, chew down and residual after swallowing (oral coating) (**Figure 2-2**).

The first stage is the pre-fracture of a food. This stage begins with the visual examination which creates an expectation of the texture of the food to be consumed. A variety of sensory perception is generated during the handling of the food with cutlery or fingers before it is placed into the mouth. This stage ends when the food is placed in the mouth. The sensory attributes associated with this stage generally relates with rheological parameters measured under small or large deformation [33].

Following the pre-fracture stage, foods are placed in mouth for the first bite. During the first bite, the product is either compressed between the tongue and the palate or bitten with the incisors until the product falls apart. Several sensory attributes can be generated from this stage. For example, the sensory "firmness" characterized during this stage generally correlates well with mechanical properties such as Young's modulus, stress at fracture and energy to fracture. Recoverable energy quantifies the amount of strain energy stored in the gel network which corelates with the sensory "crumbliness". Food gels with a high recoverable energy typically have fast fracture propagation, which contributes to higher chewing frequencies [33].

The next stage is the chew-down period and is generally the longest stage of the oral process. The most significant change occurring in this stage is the reduction in particle size. The food particle size observed by the sensory panel correlated with the closing duration and opening velocity of the jaw. Textural attributes generated from mechanical testing that intends to capture

changes in this stage may not provide good correlation with the sensory evaluations, because conditions such as temperature, moisture due to saliva, chewing movements, and food deformation rates are often not well mimicked by conventional instruments [34].

Residuals or oral coatings of foods after swallowing is due to food particles or residues adhering to the tongue, teeth, and oral tissues. Oral coatings have been hypothesized to significantly influence the perception of taste and mouth-feel attributes, however, the mechanism of the formation of oral coatings is still unknown, Overall, viscosity has been shown to be a key indicator of the initial amount of residue or oral coating, whereas salivary flow rate has little impact [33].
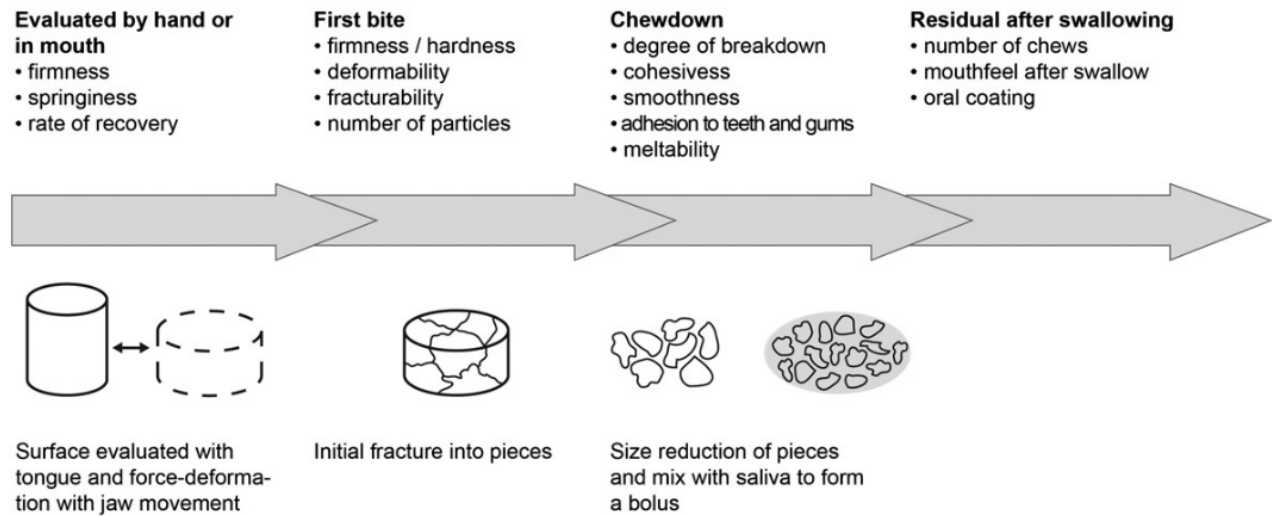
Figure 2-2 Schematic representation of the different stages in the oral processing of soft- and semi-solid foods and their associated sensory attributes [33]. Reprinted from *Microstructure, texture and oral processing: New ways to reduce sugar and salt in foods*, **18**, M. Stieger and F. Velde, 334-348, 2013, with permission from Elsevier.

The perceived food texture tends to have a good association with foods' mechanical behaviour mainly during the initial stages, *i.e.*, first bites of oral processing [35]. On the other hand, sensory perceptions that occur in later stages of chewing after the food has been broken down and been mixed with saliva, *e.g.*, viscoelasticity, crunchy and sticky, have not been adequately correlated with properties characterized by instrumentation [35]. Consequently, the measurement of the properties associated with the initial bites with mechanical compression test are important to obtain information on the perceived texture of foods.

Rheological measurements can provide information on the viscoelastic properties of food material include small deformation dynamic oscillation and large deformation compression [36]. Both the large-scale deformation and the small deformation dynamic oscillation will be discussed in detail as mechanical compression (section 2.8.3) and rheological properties (section 2.8.4), respectively.

2.3 Soybeans

Soybean seed is made up of embryo, accounting for 90% of the seed weight, as well as hull. Soybean consists of about 40% protein and 20% fat on a dry matter basis [2]. Carbohydrate and ash are the remaining components, constituting about 26% and 5% by weight, respectively [37]. Around 16.5% of the total carbohydrate is made up by dietary fibre [37].

2.3.1 Soy Protein

Soy proteins can be classified into four groups: 2S, 7S, 11S and 15S, based on their sedimentation coefficients which reflects their size.

The 2S soy protein fraction consists of low molecular mass polypeptides in the range of 8000-20,000 Da. The main components in this fraction include Bowman-Brik and Kunitz trypsin inhibitors, cytochrome C, and α-conglycinin [38], [39]. The 7S fraction contains polypeptides in the range of 180-210 kDa, which mainly include β-conglycinin, ϒ-conglycinin, and α-amylase [40]. The 11S fraction consists of glycinin, in a molecular mass of 320-360 kDa. In the present thesis, (11S and glycinin) and (7S and β-conglycinin) are used interchangeably. Lastly, the 15S fraction is identified as a dimer of glycinin [41].

Approximately 30-40% of total proteins of soybeans are composed of glycinin and β-conglycinin, respectively [42]. Glycinin is composed of five types of subunits and divided into three groups: group I ($A_{1a}B_{1b}$, $A_{1b}B_2$, A_2B_{1a}), group IIa ($A_5A_4B_3$), and group IIb (A_3B_4) [43]. β-conglycinin consists of three N-glycosylated subunits: α', α and β, assembled in a non-random set of seven forms, $α'β_2$, $αβ_2$, $αα'β$, $α_2β$, $α_2α'$, $α_3$, and $β_3$ [44]. The subunits α', α and β are associated via hydrophobic interactions [45]. Comparatively, β-conglycinin has a lower content of sulfur containing amino acids, hence, minimal disulfide bonds are formed to stabilize the structure of β-conglycinin [46].

Soy proteins can also be categorized into two groups based on their particle size, which are the particulate proteins with diameter of greater than 40 nm and the soluble proteins with diameter less than 40 nm [47]. Around 40% of raw soymilk consist of soluble proteins, while nearly 50% of the soy protein exist as particles [47]. Particulate proteins are formed by the aggregation of dissociated soy protein subunits upon thermal treatment whereas soluble proteins are composed of small and stable oligomer subunits which are disulfide-linked aggregates of A subunits of 11S [48]–[50].

A variety of soy protein products are available according to their degree of processing and protein content and include defatted or full-fat soy flour. soy protein concentrate (SPC) and soy protein isolate (SPI). SPC and SPI are made by first removing the fat from soybeans, then the water-soluble non-protein components are removed. SPC contains at least 65% protein on a dry basis. SPI contains the highest protein content, about 90% of crude protein.

2.3.1.1 Amino Acids

The amino acid composition of the two main subunits of soy proteins, 7S and 11S, measured according to two methods, aqueous phase and AOT reverse micelle extractions, is presented in **Table 2-3** [51]. Overall, proteins in soymilk have a well-recognized deficiency of the essential sulfur amino acids like cysteine and methionine but are relatively rich in lysine.

Table 2-3 Amino acid composition of 7S and 11S globulins by aqueous phase and AOT reverse micelle (with bis(2-ethylhexyl) sodium sulfosuccinate as amphophilic surfactant and with isooctane as organic solvent) extraction (g/100 g protein) [51]. Adapted from *Analysis of the Amino Acids of Soy Globulins by AOT Reverse Micelles and Aqueous Buffer*, **165**, X. Zhao et al., 802-813, 2011, with permission from Springer Nature.

Amino acid	Globulin with aqueous buffer extraction		Globulin with AOT reverse micelle extraction	
	7S	11S	7S	11S
Non-essential amino acids (NEAA)				
Aspartic acid	11.31±0.01	10.73±0.01	11.30±0.02	11.75±0.02
Serine	4.40±0.01	4.44±0.01	4.38±0.01	5.17±0.01
Glutamic acid	20.78±0.02	18.59±0.05	22.24±0.01	21.98±0.03
Glycine	2.64±0.05	3.68±0.01	2.18±0.01	4.17±0.01
Alanine	2.66±0.02	3.17±0.02	2.29±0.02	3.48±0.01
Cystine	0.90±0.01	1.48±0.01	0.55±0.01	1.42±0.01
Tyrosine	2.77±0.02	3.32±0.01	2.58±0.01	3.62±0.01
Proline	4.37±0.02	4.69±0.01	4.47±0.01	4.98±0.01
Arginine	7.45±0.03	6.51±0.03	7.93±0.01	6.69±0.01
Histidine	2.41±0.01	2.38±0.01	2.22±0.01	2.55±0.01
Total NEAA	59.6	58.99	60.14	65.81
Essential amino acids (EAA)				
Leucine	7.33±0.01	6.86±0.03	7.40±0.03	7.75±0.02
Valine	3.51±0.01	4.03±0.02	3.00±0.02	4.05±0.01
Phenylalanine	5.43±0.01	4.66±0.02	5.58±0.02	5.21±0.03
Lysine	5.52±0.02	4.56±0.01	5.65±0.01	4.93±0.03
Isoleucine	3.78±0.02	3.54±0.01	3.77±0.03	3.70±0.03
Methionine	0.56±0.01	1.09±0.01	0.26±0.01	1.04±0.01
Threonine	2.51±0.03	3.05±0.01	1.59±0.01	3.27±0.02
Total EAA	28.28	27.79	27.25	29.95

2.3.1.2 Functional and Physical Properties

Functional properties of proteins are the physicochemical properties describing their behaviour in food systems during preparation, processing, storage, and consumption [52]. Functional characteristics are essential in determining the quality of the final food product, as well as in facilitating food processing. The common functional properties of proteins generally include gelation, interfacial properties, and film formation [53].

During gelation, high concentration of globular proteins unfolds upon heating, or when placed in environments with extreme pH conditions or ionic strength. The denatured polypeptide chains will aggregate to form thermally irreversible gels. The properties of the gels can be affected by many factors, including the degree of protein unfolding, as well as the extent and kinetics of aggregation of the polypeptide chains [53]. Protein unfolding induced by heating will lead to interactions among polypeptide chains. Intermolecular and inter-particle forces between macromolecules in the protein mixture can be either attractive or repulsive. The balance between these forces will determine the stability of protein molecules in the aqueous solution. Hydrogen bonds, ionic attraction, van der Waals forces, disulfide bonds, and hydrophobic forces all are examples of the molecular interactions involved in the aggregation and gelation of proteins and contributing to the stability of the protein gel network [54], [55]. In addition, the size of protein aggregates has also been recognized as an important element in the gelling ability of proteins [56], [57].

Covalent bonds, such as disulfide bonds, play a significant role in the structure and functional behavior of soy proteins, especially concerning the 11S globulin subunits, due to the presence of higher concentration of sulfur-containing amino acids in this fraction [46], [58]. Non-covalent interactions, such as hydrophobic interactions, hydrogen bonds, electrostatic attractions are involved in protein-protein and protein-solvent interactions, and eventually can impact the overall properties of the protein. Hydrophobic interactions are the fundamental forces in stabilizing the native structure of soy proteins, strengthening proteins' emulsifying and foaming abilities [52]. Hydrogen bonds are essential in stabilizing the internal structure of proteins in α-helix and β-sheet structures. While electrostatic interactions between charged proteins can be affected by the addition of salts and counterions.

Proteins are also used to stabilize oil-in-water emulsions accredited to their ability to adsorb at the oil-water and air-water interfaces. Soymilk is an emulsion of fine lipid droplets released from soybean seeds, measuring several hundred nanometers in size dispersed in water. The dispersion of oil droplets is extremely stable because they are encapsulated by phospholipids and the protein oleosin [59]. Generally, soymilk has a pH value far from the isoelectric point (pI) of the protein, and electrostatic repulsion is attributed to the stabilization of oil droplets against flocculation and coalescence [53]. When the pH of soymilk is close to the pI of the proteins, electrostatic

repulsive forces become insufficient to prevent protein aggregation, but stabilization can be achieved through steric repulsion between the adsorbed protein layers. Albeit in many cases the adsorbed protein layer is too thin to provide such stabilization [53].

The film formation of proteins has received increasing attention because of their potential use in biodegradable packaging such as edible films to enhance the shelf life of fruits or vegetables. Protein films can also contain bioactive compounds such as essential oils, organic acid, bacteriocins and enzymes [53]. Functional characteristics specific to soy proteins are summarized in **Table 2-4**.

The functional characteristics of proteins reflect their intrinsic physical attributes. The physical behavior of proteins is determined by their amino acid composition, molecular size, primary structure, and protein conformation, the charge distribution, the extent of inter- and intra-molecular binding, and the environment [52].

Table 2-4 Functional properties of soy proteins in different food systems [52]. Reprinted from *Functional properties of soy proteins*, **56**, J. E. Kinsella, 242-258, with permission from John Wiley and Sons.

Functional property	Mode of action	Food system
Solubility	Protein solvation, pH dependent	Beverages
Water absorption and binding	Hydrogen-bonding of HOH, entrapment of HOH, no drip	Meats, sausages, breads, cakes
Viscosity	Thickening, HOH binding	Soups, gravies
Gelation	Protein matrix formation and setting	Meats, curds, cheese
Cohesion-adhesion	Protein acts as adhesive material	Meats, sausages, baked goods, pasta products
Elasticity	Disulfide links in gels deformable	Meats, bakery
Emulsification	Formation and stabilization of fat emulsions	Sausages, bologna, soup, cakes
Fat adsorption	Binding of free fat	Meats, sausages, donuts
Flavour-binding	Adsorption, entrapment, release	Simulated meats, bakery
Foaming	Forms stable films to entrap gas	Whipped toppings, chiffon desserts, angel cakes
Colour control	Bleaching of lipoxygenase	Breads

2.3.2 Lipids

The primary fatty acids present in soybean oil are palmitic (16:0), stearic (18:0), oleic (18:1), linoleic (18:2) and linolenic (18:2) acids, taking up approximately 10%, 4%, 18%, 55%, and 13% of soybean oil, respectively [60]. Lipids are present in soymilk in the form of oil bodies. Triglycerides (TAG) are the main constituent (>90%) of the floating lipid fraction of the soymilk [61]. The oil bodies in the soymilk are made up with the non-polar TAG core, coated by phospholipid monolayer and embedded with oleosins, which in turn stabilize the oil bodies [59]. Thus, the oil bodies can maintain their well-defined structure throughout the soymilk production [59].

The oil bodies, and subunits of soy proteins, β-conglycinin and glycinin change upon heating (**Figure 2-3**). In raw soymilk, most of the oil bodies are present in the particulate fraction of soymilk [61]. During heating, when temperature increases to 65-75 °C, some oil droplets and subunits of β-conglycinin are liberated from the particulate fraction into soluble fraction. At 75-95 °C, most lipids start to be liberated and shifted to the floating fraction [61]. When a coagulant is incorporated, the oil bodies at first are attached with the original glycinin-rich protein particles, and subsequently with β-conglycinin-rich protein particles which are newly formed from soluble proteins [62]. Hence, the lipid is involved in the coagulation of soymilk gel and become a component of the gel [63].
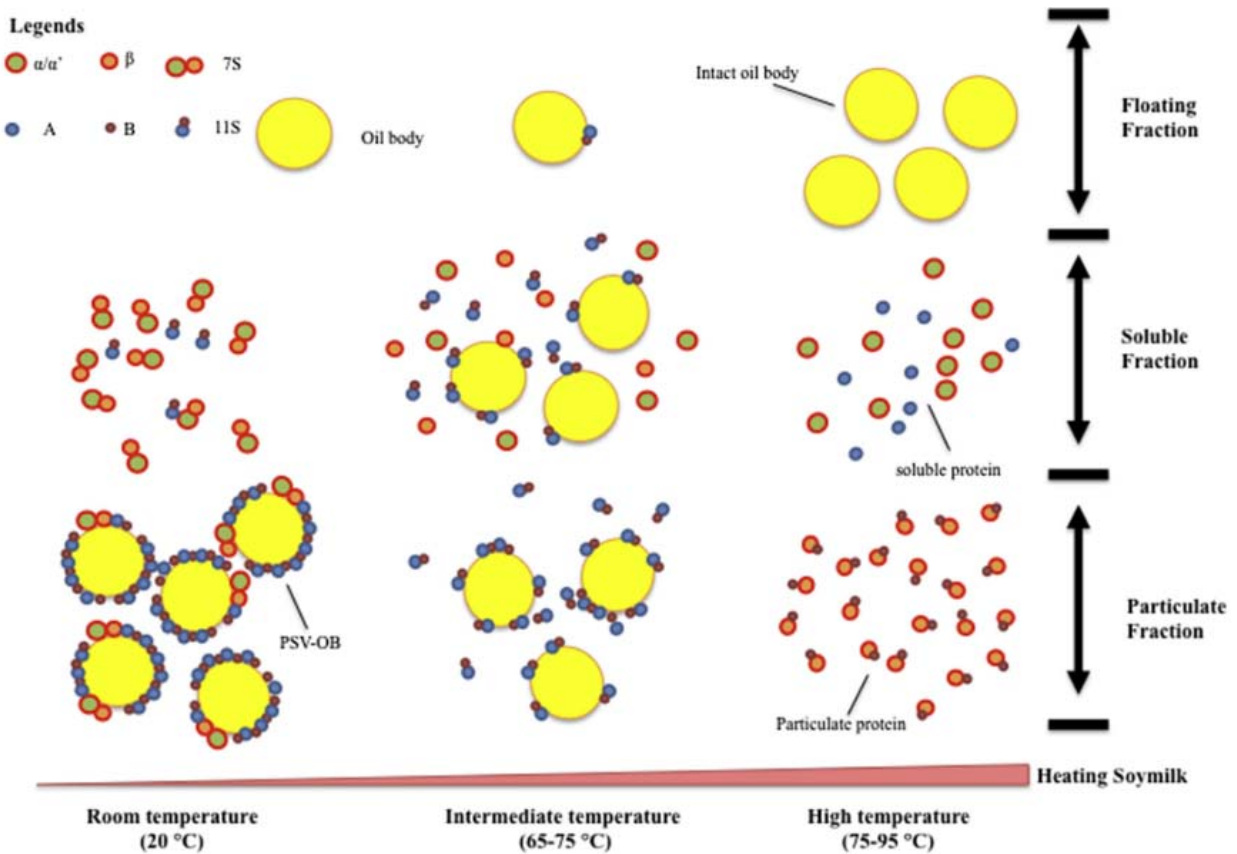
Figure 2-3 Formation of soymilk particles when heating raw soymilk. PSV-OB refers to protein storage vacuoles-oil body complex [63]. Reprinted from Particle formation and gelation of soymilk: Effect of heat, **54**, X. Peng et al., 138-147, 2016, with permission from Elsevier.

2.3.3   Carbohydrates

In soybeans, the carbohydrate constituents consist mainly of 20-30% non-starch polysaccharides (NSP) as well as about 10% free sugars, such as mono-, di- and oligosaccharides [64]. NSP consist of around 8% cellulose with the remaining being non-cellulosic, hemicellulose and pectic polysaccharides [64] whereas free sugar is composed of 5% sucrose, 4% stachyose, and 1% raffinose [64].

The major constituents of NSP will be discussed in detailed in sections 2.5.1, 2.5.2 and 2.7.2.

2.3.4   Minerals

Soybeans are a good source of minerals. According to the U.S. Department of Agriculture (USDA), for every half cup of cooked soybeans, there are 88 mg of calcium, 4 mg of iron, 74 mg

of magnesium, 0.4 mg of copper and 1 mg of zinc. Soybeans are also rich in B-vitamins, including 1.4 mg niacin (B3), 0.2 mg pyridoxine (B6), and 47 µg of folic acid (B9).

2.4 Soymilk Gels (Tofu)

In general, gels are characterized by a relatively high viscosity, plasticity, and elasticity. Protein gels including soymilk gels are consisted of three-dimensional matrices or networks of intertwined, partially associated polypeptides, in which water is entrapped [52]. The ability of proteins to form gels enables the matrix to retain water, lipids, sugars, and other ingredients, which serves as a structural basis of many textured foods, such as tofu.

The principal factors responsible for soy protein aggregation and the formation of a gel network include pH, temperature, pressure, protein concentration and presence and type of coagulant. Heating results in denaturation and unfolding of proteins to expose their functional groups. The addition of coagulants promotes protein gelation and the network formation. In this section, the mechanism of soy protein aggregation as a result of heating and the use of coagulants will be examined. Lastly, the soy protein gel network will be reviewed.

2.4.1   Heat-Induced Gelation

Non-network and network proteins are the two types of proteins participating in a gel network. Non-network proteins are the protein diffusing out of the gel to the bulk solution, and they are not engaged in the gel network but entrapped in the gel matrix as soluble components after gelation [65]–[67]. On the other hand, network proteins are the protein remaining in the gel network after non-network proteins have diffused into the bulk solution. Non-network proteins are composed mainly of A polypeptides in forms of monomer, dimer, trimer, polymer and undissociated AB subunits, as well as a few 7S α' and α subunits as aggregates cross-linked via hydrophobic interactions [65].

For heat-induced soy protein gels formed at 85 – 100 °C, the storage modulus of viscoelastic testing, G', was strongly and proportionally related to the amount of network proteins and the size of protein aggregates [67]. The quantity of network proteins increased when heated at higher temperatures, which resulted in raising G' value [67], [68]. It was attributed to increased number of strands or thickening of the strands in the network of the gel [67]. Furthermore, as the denaturation degree of glycinin increased, the non-network proteins in the gel network decreased [65]. Since the non-network proteins were removed from gel network through diffusion, the

storage modulus remained the same, suggesting that the non-network protein had no major effect on the elastic behaviour of the gel.

The effect of NaCl addition (0 – 0.5 M) was investigated for heat-induced SPI gel formed at a temperature range of 30 – 85 °C [69]. Increasing the ionic strength is equivalent to decreasing the net charge density of the protein, which shifts the pH towards the isoelectric point (pI) of the protein. It was found that although the addition of NaCl led to an increased rate of the gelation process, it did not alter the stiffness of the gel at steady state [69].

2.4.2   Coagulants and Mechanisms

Protein molecules can carry positive or negative net charges depending on the pH and ionic strength of the solution. At neutral pH, proteins in soymilk are negatively charged. In the absence of salts or acids, the electrical double layer is formed around the protein, creating repulsive forces between them. Therefore, repulsive forces dominate in the protein-water mixture and prevent protein aggregation. The addition of salts or acids can reduce the thickness of electrical double layers and thus decrease the electrostatic repulsion between the proteins. Consequently, the attractive interactions become sufficiently strong compared to the repulsive forces and the protein molecules tend to flocculate in the aqueous solution [70]. The aggregation of protein molecules is mainly driven by hydrophobic interactions, and a 3D gel structure is subsequently formed [71].

2.4.2.1 Salts

The unfolding of proteins upon thermal denaturation leads to the exposition of the hydrophobic core of the protein, enabling proteins to aggregate *via* hydrophobic interactions. At neutral pH however, proteins carry a net negative charge, and thus the electrostatic repulsive forces are keeping the proteins from interacting further and thereby form more aggregates [72].

In salt-induced protein coagulation, the salts reduce the electrostatic repulsion between the charged soy proteins, causing them to aggregate with cations, such as Ca^{2+} or Mg^{2+}. These ions act as bridges between the charged adjacent carboxylic groups on neighboring protein molecules *via* electrostatic interactions, promoting the gelation process [73], [74]. Hydrophobic interactions, electrostatic interactions, hydrogen bonds and disulfide bonds are involved in the formation of a continuous three-dimensional network [74].

Commonly used salt coagulants are: (1) "nigari-type" or chloride-type coagulant such as magnesium chloride ($MgCl_2$) and calcium chloride ($CaCl_2$); (2) sulfate-type coagulants such as calcium sulfate ($CaSO_4$) and magnesium sulfate ($MgSO_4$) [75].

The two most frequently used salt coagulants are nigari (or bittern), traditionally made from seawater [74] and containing mostly magnesium chloride combined with little or no calcium chloride, and gypsum (calcium sulfate $CaSO_4$). Nigari is more soluble than calcium sulfate and tends to induce rapid coagulation [76], [77] by visual observation [78], which not only may result in a hard-to-control processing, but also may lead to a nonuniform tofu with poor water holding capacity (WHC) [77]. A slower gelation often facilitates the formation of highly elastic fine-stranded protein gels, whereas a fast-gelling rate gives rise to fast precipitation producing a less uniform network [79]. Nigari tofu is softer, less chewy, cohesive, and springy as compared to gypsum tofu (**Table 2-5**), which might be ascribed to its rapid coagulation rate, and thus captures larger amount of water.

The hardness of salt-induced tofu follows the order of $CaCl_2 > CaSO_4 > MgCl_2 > MgSO_4$ for the same concentration of coagulant used [78]. Albeit $CaSO_4$ and $MgCl_2$ tofu were similar in hardness with merely a 0.02-N difference [78]. Further, the coagulating strength of salts used for soymilk curdling to produce tofu follows the order of $CaCl_2 > MgCl_2 > CaSO_4 > MgSO_4$ [75].

The texture of tofu can also be influenced by the coagulant concentration. When the concentration of the coagulant, $MgCl_2$, increased above 0.2%, the breaking stress of tofu increased, reaching a maximum value when the concentration was about 0.4% [80]. Increasing the coagulant concentration generally leads to a harder gel texture [79], [80]. However, the breaking stress of tofu generally does not increase further after reaching the maximum value [79], [81]. The optimum concentration of salt coagulant tends to vary significantly between different studies.

The cooperation effect of multiple salt coagulants was investigated for SPI emulsion gels by incorporating various concentrations of $MgCl_2$, $MgSO_4$ or $CaSO_4$ [82]. They found that a low concentration (5 mM) of Mg^{2+} in addition to $CaSO_4$ promoted the production of stronger gels with increased firmness. Meanwhile, compact protein aggregates were formed in the mixed-coagulant system, and the resultant gel had enhanced homogeneity and resistance to deformation.

However, when more than 5 mM of Mg^{2+} was added, the gel structure became coarser with large protein aggregates formed due to excessive protein aggregation [82].

Table 2-5 Comparison of coagulation rate, texture, microstructure, and taste of tofu coagulated by different salt coagulants. [Refer to **Table S. 10** for supporting data used for this comparison].

Coagulant	Coagulation rate[a]	Texture	Microstructure	Taste
Gypsum ($CaSO_4$)	Slower (> 8 min for curd formation) [78]	Harder [83], [78], [84] chewier, more cohesive [83], [84], slightly less springy [83]	Larger pores, more uniformly rounded [83], [84], fewer in number [83]	Better taste and flavour with uncooked gypsum tofu than uncooked nigari tofu [83]
Nigari (bittern, mostly $MgCl_2$)	Rapid [74], [78], [77]	Softer [83], [78], [84], less chewy, less cohesive [83], [84], slightly springier [83]	Slightly more compact than gypsum [84], smaller pores with irregular size and shape [83]	Higher sensory score with cooked nigari tofu than cooked gypsum tofu [83]
Epsom ($MgSO_4$)	Slower (> 8 min for curd formation) [78]	Softest amongst salt-induced tofu [78]	-	Less acceptable overall (flavour, mouthfeel) than gypsum tofu [85]
Calcium chloride ($CaCl_2$)	Rapid [78]	Hardest amongst salt-induced tofu [78]	-	-

[a] Possibly based on visual observations [78], [86]

2.4.2.2 Acids

Some commonly used acid coagulants include glucono-δ-lactone (GDL), lemon juice and acetic acid. Among these, GDL is the most common coagulant in tofu processing, and is used specifically for silken or soft tofu because of the rapid coagulation, allowing the capture of large amount of water [83]. GDL leaves a slightly sweet taste in the finished product [87]. In addition, GDL-induced tofu tends to have slightly higher gel strength as opposed to the lower gel strength of tofu induced by citric acid or adipic acid [87].

During GDL gelation, protons are released that neutralize the negative charges of soy protein aggregates which facilitates coagulation *via* hydrophobic and electrostatic interactions in forming a continuous three-dimensional network [74]. Vinegar and lemon juice, on the other hand, coagulate soy proteins by lowering the pH of the system to promote protein aggregation [85]. Lowering the pH of a solution containing soy proteins lowers the repulsion forces between protein molecules while facilitating protonation of the carboxyl groups of β-conglycinin. The β-conglycinin subunit will thus undergo denaturation leading to an increased number of exposed β-strands. These strands can then create bonds, promoting the formation of rigid gels at acidic pH values [88]. Generally, acid coagulants will cause higher aggregation of β-conglycinin, while salt coagulants cause more glycinin to aggregate [89].

In contrast to salt-induced tofu, the breaking stress of GDL-induced tofu increases even when the GDL concentration is higher than the desired quantity needed to produce homogeneous network [81]. The hardest and most cohesive tofu gels were formed when using 8 g/L of GDL at coagulation temperatures of 60 and 80 °C [58]. Comparatively, GDL-induced tofu tends to be softer than salts-induced tofu [83], [84], [90] and does not form cracks in the curd, giving a smooth appearance, whereas $CaSO_4$-tofu tends to have more cracks possessing a heterogeneous structure [81].

2.4.2.3 Enzymes

Enzymatic treatment has recently been considered for inducing aggregation and gelation of soy proteins and improving their functional properties [5]. Transglutaminase (TGase) or microbial transglutaminase (MTGase) is one of the most used enzymes for this application. TGase has been frequently used to induce gelation of milk casein or casein micelles effectively. More recently, it has been increasingly used for coagulation of soybean proteins such as glycinin and β-conglycinin subunits [91].

TGase catalyzes an acyl transfer reaction between the γ-carboxyamide groups of peptide-bound glutamine residues as the acyl donor and the primary amino groups in a variety of amine compounds as the acyl acceptor, *e.g.*, peptide-bound ε-amino groups of lysine residues [91], [92]. As a result, cross-links or ε-(γ-glutamyl)lysine isopeptide bonds and high molecular weight proteins are formed. The crosslinking reaction can be divided in two stages. In the primary stage, the spatial structure of the protein destabilizes due to covalent linkages, while the hydrophobic

22

regions of the protein are partially exposed. In the latter stage, the destabilized proteins undergo further crosslinking and aggregation with one another as promoted mainly by hydrophobic interactions [91]. Covalent cross-linking is identified as the main regime for the gelation of native soy proteins [91].

Increasing the enzyme concentration can increase the number of cross-links formed, especially at TGase concentration above 3% w/v [91]. Glycinin was the more readily cross-linked with MTGase than β-conglycinin [93]. Glycinin is primarily accounted for the formation of the initial gel network, resulting a network with increased gel strength. β-conglycinin on the other hand, is associated with the viscous property of the tofu gel [93].

Generally, TGase-induced so gels tend to have a more homogeneous structure as compared to $CaSO_4$- or GDL-induced tofu [94]. In terms of texture properties, tofu gel coagulated with TGase can have a much harder texture than gels coagulated with salt or acid coagulants. Nonetheless, depending on the cultivar and variety of soybeans, texture of the final gel can have a wide variability [94]. On the negative side, TGase can be considerably more costly than the salt and the acid coagulants.

2.4.3   Protein Network

The processing conditions such as pH, ionic strength, protein concentration and heating procedures can influence the heat denaturation of globular soy proteins, causing them to associate into either stranded-aggregate or particulate-aggregate type of network (**Figure 2-4**), or both [95], [96]. Stranded-aggregate network involves arrangement of proteins into highly branched "string of beads" structure to produce a transparent gel, whereas the particulate-aggregate network involves the association of protein particles to produce a turbid gel [97]. When the ionic strength of the solution is low, and/or the pH is far from the pI of the protein, electrostatic repulsion dominates, resulting in the formation of nanometer-sized strand-like aggregates. On the contrary, at high ionic strength, and/or pH is close to pI, electrostatic repulsion will lessen, resulting the formation of particulate gels with an opaque appearance [98]. A mixed type of network is the combination of both arrangements.

Particulate or mixed type of network is often observed with ion- and acid-induced soy protein gels [71], [99], [100]. As for MTGase-induced soymilk gels, the type of network it produces depends on the heating methods of soymilk. Particulate protein network was observed when

using the conventional one-step heating at 95 °C, whereas a random type of protein aggregation was noted when using the two-step heating method, *i.e.*, heating at 75 °C for 5 min then 95 °C for 5 min [101].
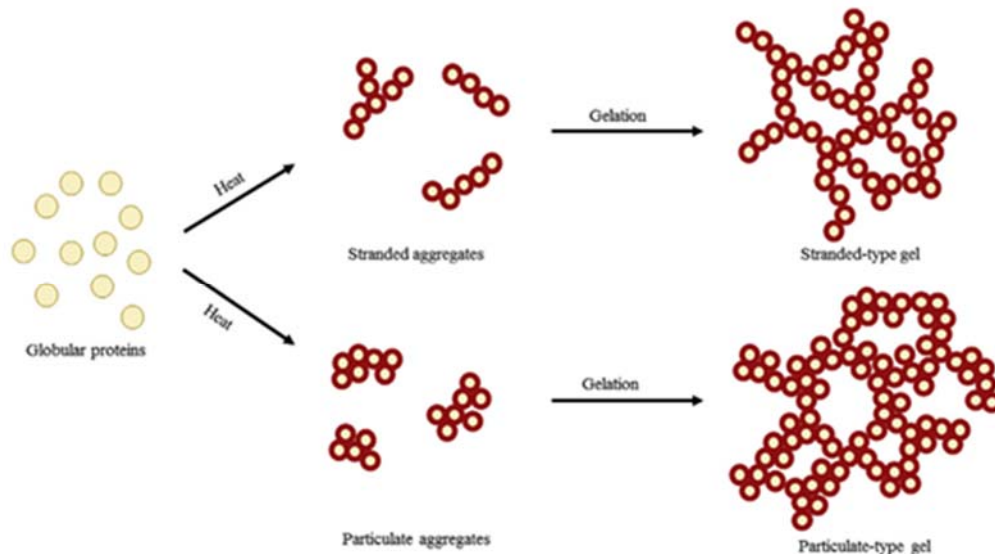
Figure 2-4 Schematic of stranded and particulate type of gels formed by globular proteins. The circles without or with thick red borders respectively represent the native or denatured soy proteins [63]. Reprinted from *Particle formation and gelation of soymilk: Effect of heat*, **54**, X. Peng et al., 138-147, 2016, with permission from Elsevier.

2.5 Soy Okara

Soy okara is the insoluble by-product in tofu production separated from the soymilk which is extracted from soybeans. On average, every pound of dry soybeans made into soymilk or tofu generates about 1.1 pounds of okara with around 80% moisture [102]. It is characterized by its coarse and fibrous texture. Okara is burnt or dumped in landfills as waste or used as animal feed [3]. Hence, incorporating okara back into foods has been of interest because of its high nutritional value, *i.e.*, high amount of dietary fiber, bioactive contents, and antioxidant activity [103].

In the following sections, the composition of okara will be discussed first, followed by the polysaccharide content of the okara fibers.

2.5.1 Okara Composition

Dry okara contains about 50% fiber, 25% protein, 10% lipid, 8-12% fat and 3% ash [104], [104]. The proximate composition of okara depends on the amount of water used to grind soybeans and whether more water is added to further extract residual components [3]. If low levels of water were employed in the extraction process, there would be less soymilk resulted and less soluble components extracted [3].

Since most of the water-soluble protein is extracted in the soymilk, okara consists of primarily non-extractable proteins [105]. Proteins in okara usually interact tightly with non-starch polysaccharides, *e.g.*, soybean cellulose, hemicellulose, lignin, which are located inside the intact plant cells, making the recovery of the proteins from okara difficult [106].

Okara contains soluble and non-soluble dietary fibers of the soybean cotyledon which are primarily non-starch [107]. The majority of the okara fiber consists of cellulose and hemicellulose [108], along with some pectin and lignin from the cell wall [109]. The fiber content is reported to be 12.1% hemicellulose, 5.6% cellulose, 11.7% lignin, and 0.16% phytic acid [3]. The detailed information concerning the polysaccharide components of okara will be presented in the following section.

2.5.2 Polysaccharide Constituents of Okara and Its Structure

As alluded to in the preceding section, okara is an irregularly shaped material that contains cellulose, hemicellulose, lignin, pectic substances, and proteins. Cellulose as the major structural component of the okara is the core of the matrix. Within the crystalline and amorphous regions of cellulose, strong intra- and intermolecular hydrogen bonds make cellulose highly insoluble while possessing high mechanical strength [110]. Hemicellulose links with cellulose microfibrils *via* hydrogen bonds, and this network forms the strong backbone of the plant cell wall [111]. Cellulose-hemicellulose frames are embedded in the amorphous matrices of pectic substances of okara [6]. Lignin can be found in the cell surface and acts as the barrier to keep away from outside environment [111].

Cellulose is made up of β-D-glucopyranose units linked via β-(1,4) glycosidic bonds [112]. The cellulose chains are composed of 500 – 1400 D-glucose units arranged in microfibrils, called cellulose fibrils. They are embedded in a lignocellulosic matrix making them difficult to be accessed [112]. Cellulose is made up with both the crystalline and non-crystalline regions, with a

degree of polymerization (DP) of cellulose is 500 – 1400, which is the number of glucose units [112].

Hemicellulose is a heterogeneous polysaccharide containing a variety of monosaccharides including xylans, xyloglucan, mannans, and glucomannans [112]. The degree of polymerization of hemicellulose is significantly lower than cellulose, around 100 – 200, suggesting a higher degree of complex substituents [112]. Hemicellulose is amorphous in nature possessing weak physical strength such that it can be hydrolyzed with dilute acids, bases, or enzymes [113].

Lignin is a complex polysaccharide that is abundantly present in lignocellulosic materials. It is amorphous aromatic, composed of phenylpropanoid building units such as p-coumaryl, coniferyl and sinapyl alcohol [112]. Lignin binds hemicellulose to cellulose in plant cell walls and is responsible for their hydrophobicity and structural rigidity of plant materials [112].

The main component of the dietary fibre in okara is ruptured cotyledon cells [114]. The cell wall of the soybean cotyledon is comprised of a series of polysaccharides, which are cross-linked with proteins and lignin. The primary cotyledon cell wall contains pectin, hemicellulose and microfibrils of cellulose crosslinked with proteins [115]. The secondary cell wall is within the primary wall containing cellulose and hemicellulose and is also capable of protein binding [115]. Cells are held together by adhesive substances found in the middle lamella, *i.e.*, the extra-cellular space between cells, composing mostly of pectin as well as some glycine and hydroxyproline-rich proteins [116].

The microstructure of okara as visualized by confocal laser scanning microscopy (CLSM) is presented in **Figure 2-5** where fluorochrome acridine orange was used as the staining dye possibly because of its affinity for lignin in fibrous materials [117]. The fibrous insoluble okara was extracted by centrifugation of the soy slurry (soybean:water=1:6) using a high shear mixer at 80 °C [118]. Cell wall material and intact cells were present in the soy slurry (**Figure 2-5**). The cell walls of disrupted cells are robust, making the network difficult to compress [118].
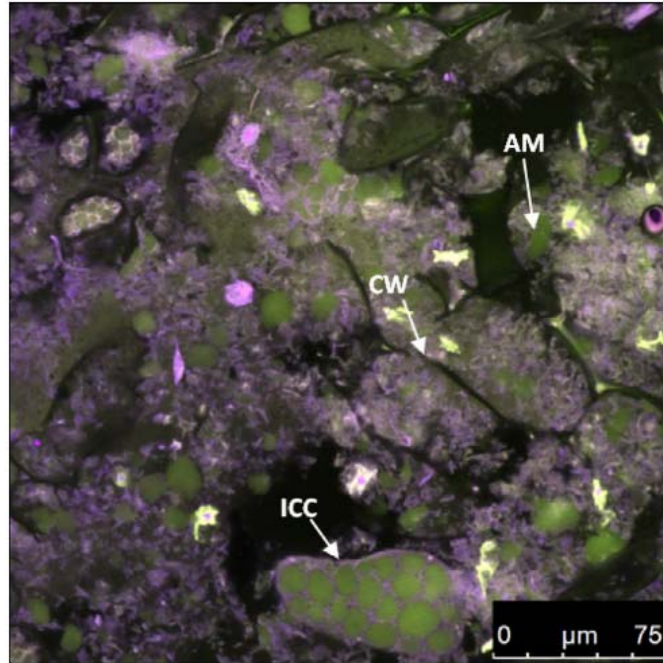
Figure 2-5 CLSM image of okara extracted at 80 °C. Intact cotyledon cells (ICC), cell walls of disrupted cells (CW) and agglomerates material (AM in green, most likely protein bodies) are annotated. Fibrous materials appear as a combination of blue and red emission, *i.e.*, purple [118]. Reprinted from an open-sourced article.

2.6 Tofu Gel Prepared with Soy Okara

The high dietary fiber content and excellent nutritional value of okara has gained growing interest in research. The potential of producing okara-added tofu products, also known as whole soybean curd, is widely investigated in recent years. Okara tofu is made by either coagulating the soybean slurry [9], or by first separating okara from the soymilk with subsequent coagulation of the soymilk with a fraction of the extracted okara [5], [119]. Other types of okara tofu products have been created by adding okara to an SPI dispersion as the protein substitute to soymilk [8], [11].

The production of whole soybean curd appears to be challenging in providing desired texture attributes because of the large particle size of okara fiber [9]. Moreover, soybean fibers reduce the crosslinking of heat-denatured proteins and thereby weaken the textural properties of soybean curd, resulting in a coarse gel [5]. As a result, whole soybean curd containing okara has low gel strength and disrupted three-dimensional network [73].

27

A variety of methods to improve the gelling properties of whole soybean curd have focused on the modification of the okara fiber. These techniques include TGase for enhanced protein crosslinking, ultra-high pressure for finer homogenization of okara, and milling, grinding, or shearing to reduce the size of okara for the ease of its incorporation in the network [5], [8], [11]. The purpose of these techniques is generally two-fold, which is to increase the crosslinking degree of soy protein, and/or to reduce the size of the okara fibers [4].

The improvement of texture, water holding capacity and rheological properties of whole soybean tofu remains unclear. Some publications report inferior properties for whole-soybean tofu when compared to traditional tofu [9], while other studies reported improvements [5], [119]. The consensus of the results is an improvement of the textural properties *e.g.*, hardness, springiness, cohesiveness, *etc.*, water-holding capacity (WHC), surface hydrophobicity, free sulfhydryl group contents [8], as well as viscoelastic properties (G' and G'') [11] of the whole soybean curd with decreased mean particle size of okara.

In this section, each type of the okara treatment techniques will be discussed in detail to obtain an idea of the state of the current research and help identify any existing gaps.

2.6.1   Enzymatic Treatment

Enzymatic treatment improves the homogeneity and gel strength of okara-containing tofu. Two enzymes are commonly used for this application. Transglutaminase (TGase) is used for the crosslinking of the proteins and assists with their coagulation. Cellulase has been employed to hydrolyze the cellulosic constituents of the okara fiber [9], [12].

TGase is often used in addition to coagulants such as GDL [5] and calcium chloride [10] to increase the protein coagulation that was retarded by the addition of okara fibers. Soybeans are firstly ground in water to create a slurry. The slurry is either used intact to preserve the whole okara constituents [10], or only a fraction of okara components is utilized [5]. Often, the okara-containing soymilk is subsequently subjected to a high-pressure homogenizer or a high-speed mill to increase the fineness of the okara particles. Then, TGase is added with other coagulants to coagulate the mixture, resulting a curd upon incubation. The okara-containing tofu was found to possess lower gel strength, higher WHC than traditional tofu [5]. The gel strength and WHC of TGase-induced tofu improved significantly [5]. According to protein solubility measurements of the okara-containing tofu, the degree of protein crosslinking was lower when compared to tofu

28

without okara and TGase-induced okara-tofu [5]. This confirms that the presence of okara reduces the crosslinking degree of soy proteins and thereby leads to a heterogeneous structure. In contrast, TGase-induced okara-containing tofu had the lowest solubility in all bond-disrupting buffers, suggesting that the covalent bond formed between glutamine and lysine residues played the dominant role in TGase-induced protein network [5]. Moreover, the microstructure of the tofu showed that the addition of TGase strengthened the binding intensity of protein network which resulted in a denser structure [10]. It was suggested that okara particles decreased the continuity of the aggregated protein network. However, TGase could promote the formation of aggregates of the protein phase allowing them to wrap around the okara particles [5].

SPI has been considered as an alternative protein source to soybean to produce okara-containing tofu, induced with the acid of microbial transglutaminase (MTGase) where high-pressure homogenization was also employed [11]. It was reported that the proportion of 6% w/v of SPI of and 60% w/v could imitate the actual protein to okara ratio found in the whole soybean [11]. It was shown that the G' of the SPI gels containing larger amounts of okara was slightly higher than SPI-only gel, indicating enhanced gel rigidity. The FTIR analysis suggested that okara influenced the composition of the protein secondary structure based on the areas under the amide I spectra. A prevalence of β-sheet and random coils was observed in the secondary structure of the okara-containing tofu [11].

In summary, the use of TGase as a coagulant for the okara-containing soybean gel improves the uniformity and gel strength of the network compared to untreated okara soybean gel. TGase solely acted on the protein phase by generating covalent bonds to increase the crosslinking degree of proteins. By virtue of such reactions, this approach reduced the weak gel strength commonly observed with okara tofu. However, the root cause of poor compatibility of okara fiber with the remaining protein network is not addressed by the TGase treatment.

Lastly, the enzymatic treatment of whole soybean curd with cellulase combined with high-pressure homogenization [9] or superfine grinding with ultrasonic treatment [12] has been investigated. It was reported that the enzymatic hydrolysis of cellulose in okara along with high-pressure homogenization modified the okara structure and reduced its size, which led to lower polymerization degree of cellulose components in okara and increased the content of soluble polysaccharides in the whole soybean slurry [9]. Moreover, the surface area of okara particles

and the hydroxyl groups content increased [9]. Generally, the higher the cellulase concentration (up to 9 U/g) the higher the gel strength of the whole soybean curd up to a maximum cellulase concentration (*e.g.*, 14 U/g) where the gel strength was weakened, which could be caused by the presence of glucose preventing the thermal denaturation of the proteins due to the occurrence of Maillard reactions [12]. The microstructure, the whole soybean curd treated with cellulase unveiled discontinuous protein network where pores and lumps were observed [12]. Hence, it remains unclear whether the cellulase treatment has a positive effect on the homogeneity of the overall network.

2.6.2   Milling, Shearing, Ultrasound Treatment, and Homogenization

Various methods have been investigated to improve the homogeneity of okara-containing tofu, including treatments of okara by milling [13], [108], [119], high-speed shearing [4], ultrasound [8], and homogenization [9], [11] to reduce its particle size.

The effect of okara particle size was investigated to a large extent for coagulant-induced whole soybean tofu. Adding okara to the soymilk protein matrix was found to retard the formation of disulfide bonds between SH groups as well as the hydrophobic interactions, but this negative effect could be mitigated by reducing the particle size of okara [106]. The size of the okara can be reduced to 380 µm to 370 nm via pulverization or high energy milling [119]. The tofu prepared with the decreased okara size (75-180 µm) had better gel strength and sensory scores even compared to the okara-free tofu [106]. Similarly, the SPI gel prepared with wet-ground okara had slightly increased breaking stress, strain, and WHC compared to the SPI gel with untreated okara [108]. The nano-sized okara was well distributed in the gel matrices and provided less gritty mouthfeel than the micro-sized okara [108]. The study published by Ullah et al. reported different observations where the TPA texture properties of okara tofu were negatively affected when nano-sized okara (NDF, 370 nm) was added. In contrast, the tofu gel prepared with the micro-sized okara (MDF, 110 µm) had higher hardness, springiness, chewiness, and cohesiveness as compared to those gels containing nano-sized okara [13]. However, whether nano-sized or micro-sized okara was added, all TPA texture parameters decreased as compared to the okara-free tofu. Moreover, with the increasing concentration of the various-sized okara, textural properties of the tofu gel were reduced [13]. In terms of the microstructure, the addition of up to 20% of MDF okara did not alter significantly the continuous

phase although sheet-like fragments irregularly distributed within the gel matrix could be observed (**Figure 2-6**). The aggregated fragments were more obvious when the MDF okara concentration increased to 30-40% and the number of cavities in the continuous phase increased considerably. Similarly, the addition of 10-20% NDF okara also resulted in irregular network with large cavities [13].
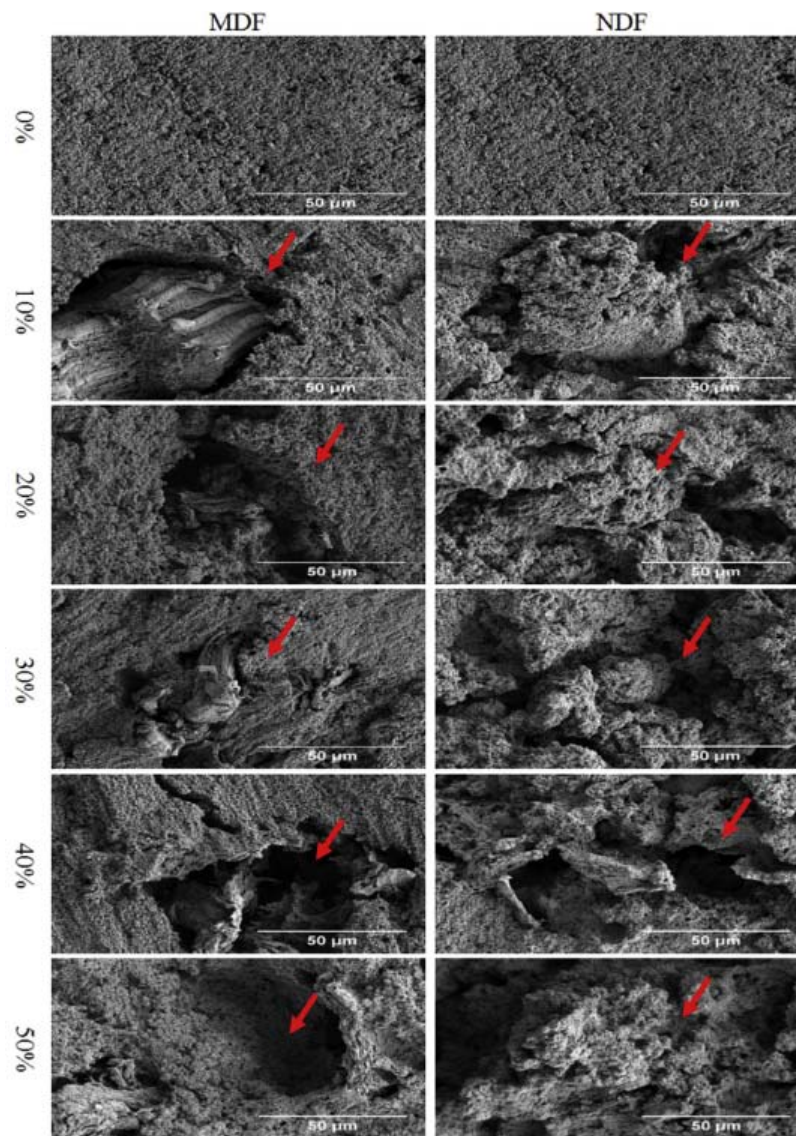
Figure 2-6 Scanning electron microscopy images of tofu prepared with micro-sized (MDF) and nano-sized (NDF) okara at different volumetric ratios as denoted by the numerical values in the row [13]. Reprinted from *Influence of okara dietary fiber with varying particle sizes on gelling properties, water state and microstructure of tofu gel*, **89**, I. Ullah et al., 512-522, 2019, with permission from Elsevier.

The effect of high-speed shearing, obtained by homogenization, was used in the fabrication of whole soybean curd starting with soybean flour containing okara dispersed in water [109]. The shearing led to the breakdown of okara cell layers according to the measurement of okara solubility, which led to a change in fiber composition from the insoluble to the soluble fraction [109]. The gel strength and WHC of the okara soy gel decreased with high-speed shearing compared to the untreated okara gel [4] The higher the shearing speed and duration, the weaker the gel strength and the lower the WHC were noted [4]. Although the size of okara fibers was reduced by shearing, the resulting gel network was looser and less connected based on SEM images [4]. It was believed that shearing may have destroyed the structure of native protein, thereby weakening the gel strength. Hence, the challenge was to maintain the native structure of the protein during okara shearing. Hence, the okara fiber was micronized separately. The research team claimed that the separate treatment of okara produced an ordered gel network, which offered higher resistance to destructive compressing and better WHC, but the results were not shown [4].

Ultrasound treatment utilized for enzymatically hydrolyzed okara fibers in hope to improve the microstructural and physicochemical properties of okara tofu [8]. Okara was first ground in a high-speed grinder and mixed with SPI and water, and then treated with ultrasound at 500-800 W for 20 min. The treated okara suspension was subsequently incubated with trypsin solution. According to FTIR profiles, the okara fibers were largely decomposed into oligosaccharides as the power density of ultrasound increased [8]. The okara fibers appeared fragmented with a flaky and staked structure after ultrasound treatment, contrasting a smooth surface without the ultrasound treatment. As the ultrasound power increased to 500 W, irregularly shaped okara particles were observed with nonuniform pores [8]. It was similarly reported that the whole soybean curd treated with ultrasonic disruption had large lumps unevenly distributed in the gel network [12].

High-pressure homogenization has been investigated for treating okara fiber. It is often combined with other treatments, such as enzymatic treatment [9], [11]. The combined treatment of high-pressure homogenization and cellulase induced cellulose hydrolysis in the whole cotyledon soymilk, and thereby disintegrated the fiber into smaller particle size which had larger specific surface area with larger amount of hydroxyl groups on its surface [9]. However, the size

of insoluble particles in the whole cotyledon milk remained significantly larger than in the traditional soymilk, which was believed to hinder the formation of protein gel network [9]. According to confocal laser scanning microscopy (CLSM) imaging, untreated okara had the largest particle size and was composed of numerous fiber strands [108]. Homogenization sheared and fractured the okara fibers into smaller bundles and decreased the clustering of okara as the homogenization pressure increased [108].

In summary, mixed results of the benefits of the various treatments are reported in the literature. It remains unclear whether the reduction of okara particle size has a positive or negative effect on the gel strength and homogeneity of the structure. Moreover, the poor compatibility of okara with the protein network was once again not addressed by these techniques as for the enzymatic treatment, which is believed to be the primary reason for the coarse network associated with whole soybean curd.

2.6.3   Okara Coating

The coating of okara has been investigated as means to enhance interactions of okara with the gel matrix. One proposed approach reported in the literature is *via* layer-by-layer coating of the okara with chitosan and pectin [120]. Chitosan deposition unto okara was achieved by elevating pH of the dispersion from 4 to 6.5 while pectin coating was based on electrostatic interaction with the deposited chitosan at pH 4.5. The chitosan-coated okara was positively charged with similar hydration capacity and water suspendability to the untreated okara. As the okara was further coated with pectin, it became negatively charged with increased hydration capacity and water suspendability. The untreated okara had coarse surfaces, whereas the chitosan-pectin coated okara displayed smoother surface with no apparent cracks [120]. Although the study represents an effective strategy, the technique can be extensive and laborious, involving costs that likely surpass the value of okara itself.

2.6.4   Research Gaps in the Production of Whole Soybean Gels

The quality of okara-containing tofu remains inferior when compared to traditional tofu with the absence of okara. Okara tofu possesses a lower gel strength and a coarse and discontinuous gel structure [5], [12], [13]. Hence, there is a need to improve the homogeneity and strength of the okara soymilk gels.

As discussed in the previous sections, different methods have been investigated to address the gel-disruptive nature of okara fibers. Physical treatments are used to reduce the particle size of okara fiber, which include high-speed shearing, high-intensity ultrasound treatment, high-pressure homogenization, or excessive pulverization of okara fiber. Moreover, enzyme treatments, *e.g.*, TGase and cellulase, have been investigated either to increase the crosslinking degree of the protein by inducing covalent interactions [5], [10], [11], or to hydrolyze the cellulose components within okara [9], [121], [122]. Combinations of both physical and enzymatic treatments have also been reported [12].

The poor interaction between the insoluble fiber of okara with the soy proteins is believed to be the fundamental issue responsible for the coarse structure and weak strength of okara-containing soymilk gel [123]. Current studies have had limited success in addressing this issue despite the effort to either increase the crosslinking degree of soy proteins or reduce the okara size to compensate for the inferior gel quality [4]. For example, Wei et al. coated the okara particles with chitosan and pectin to improve its compatibility with the soymilk gel network [120], however, this extensive technique adds challenges to the overall process. Consequently, there remains a need to improve the compatibility of okara fiber with the food protein matrix *via* a simple and economical process. The proposed technique will be reviewed in detail in the following sections.

2.7 Acid Treatment of Soy Okara

As previously discussed, the homogeneity and strength of the okara soymilk gels needs improvements. The treatment of okara with food-grade acid could disrupt its tight fiber structure and increase its compatibility with the protein gel matrix *via* reactions such esterification and acid hydrolysis. This technique has been investigated primarily with lignocellulosic and polymeric materials, but it has not been considered in the context of soy okara for the production of high-fiber value-added tofu product. The acid treatment of a lignocellulosic materials will be reviewed in this section.

2.7.1 Promotion of Esterification Reaction

A large body of research has reported the use organic acid such as citric acid to promote esterification reaction between carboxylic groups of the acid and the hydroxyl groups of

cellulosic materials. Particularly, citric acid has been considered as a bond promoter with wood or polymeric materials to improve their functionalities.

Esterification of wood increases decay resistance against microbial attacks such as fungi [124], [125]. It can also assist in minimizing the moisture absorption of wood, swelling or shrinkage, and susceptibility to photodegradation [125]. Oleic acid was used for the esterification of lignin, which caused hydrogen bonds to decrease and resulted increased chain flexibility of lignin as well as a lower glass transition point for improved processibility of lignin [126]. Citric acid can also be used as a chemical-bonding wood adhesive by mixing wood powder with 20% citric acid powder and poured into the molds and hot-pressed at 180 °C and 4 MPa for 10 min [127]. It was found that citric acid functions as a clamp connecting wood powder particles *via* covalent bonds [127].

Beside wood materials, the application of using organic acid for the promotion of esterification reaction has also been extended to polymeric materials. For example, cellulose which was used as reinforcing fillers in polypropylene (PP) composites has been modified by citric acid to increase carboxyl content on cellulose surface *via* esterification reaction to improve its compatibility with hydrophobic polymeric matrices [128], [129]. Furthermore, cellulose has also been modified by strong acids such as oxalic acid [130] and a mixture of hydrochloric acid and nitric acid [131] to render more carboxylic acid groups on its surface as reactive sites.

Citric acid has also been considered as a mean to overcome the poor water resistance of hydrophilic polysaccharide films by facilitating the formation of ester bonds between its tri-carboxyl groups and the hydroxyl groups of polysaccharides, at an average reaction temperature (80-100 °C). The cross-linking between citric acid and the polysaccharides was attributed to the covalent inter- and intra-molecular ester linkages between hydroxyl groups of polysaccharides, nanofiber, glycerol and three carboxyl groups of citric acid, which led to the possible formation of mono-, di- and tri-esters [132]. This application has been extended to edible films, where 0-30% citric acid was used to strengthen the films made with soybean residues, and the crosslinking between citric acid and the soybean fibers was examined by FTIR and supported by the lower water uptake of the film [133].

2.7.2   Acid Hydrolysis

Acid hydrolysis is commonly conducted as the mean to assess the sugar content of lignocellulosic materials because of the fast reaction rate and less structural alterations [134], [135]. Traditionally, two sequential hydrolysis process is adopted [134]. The first hydrolysis involves the use of strong acids, followed by the second hydrolysis with diluted acids. This two-step process initiates the disruption of the crystalline cellulose, and subsequently promotes the hydrolysis of polysaccharides for the release of sugars [134]. This technique reveals that acids can promote the release of smaller-molecular-weight polysaccharides from larger polysaccharides including fibers.

In the same fashion, okara polysaccharides can be hydrolyzed when treated with acid. However, strong acids such as sulfuric and hydrochloric acid are not suited for food applications. Therefore, food-grade acids will be considered, and they are typically weak and organic acids. For okara fibers, acid treatment may promote the extraction of soluble (SSPS) and insoluble soybean polysaccharides (ISPS), as well as pectic substances of soybean materials. The extraction process of these substances and their properties will be discussed in the following sections.

2.7.2.1 Acid Extraction of Soluble Soybean Polysaccharides (SSPS)

Weak-acid extraction of okara at 120 $^{\circ}$C and pH 3-3.5 generates two fractions, which are the soluble soybean polysaccharide (SSPS), and the insoluble soybean polysaccharide (ISPS) [136], [137]. By heating the residual of SPI at 120 °C for 1.5 h under pH 5 using hydrochloride acid, 45% yield of SSPS extraction can be achieved [138].

SSPS is an anionic polysaccharide that is comprised of 49.7%-mol galactose, 19.8%-mol galacturonic acid, 18.5%-mol arabinose, 5.1%-mol rhamnose, 2.9%-mol xylose, 2.0%-mol glycose, and 2.0%-mol fructose [139] and has a pectin-like structure [140]. The structure of SSPS however is different from that of pectin because of its short backbone and long complex branches, and the highly branched structure leads to globular shape of SSPS [141]. The main backbone consists of homogalacturonan and rhamnogalacturonan. It is believed to be a peptide-bound polysaccharide, that is, peptides are covalently attached to the main carbohydrate chain [140]. The presence of long side chains makes SSPS a compact molecule. The galacturonic acid backbone (~18%) contributes to its acidic properties with a negative charge when pH > 3.0

36

[141]. In addition to the negatively charged galacturonan chains, the highly branched neutral sugar chains consisting of galactan and arabinan contribute to the formation of a thick hydrated layer on the surface of protein particles [142].

The linear or globular molecular structures of SSPS also play an important role in their protein-stabilizing properties under acidic conditions [143]. The compact structure and the small dimension of SSPS (*i.e.*, ~100 nm) enables its stabilization of milk proteins without causing undesired increase in thickness or viscosity [142]. In fact, SSPS could be used in any kind of salty or sweet food solution without rheological changes during storage [138].

The monosaccharide composition of SSPS is predominantly comprised of arabinose, galactose, and galacturonic acid, but many other monosaccharides like fucose, rhamnose, xylose and glucose are also present [144]. The soluble soybean backbone consists of long-chain rhamnogalacturonan and short-chain homogalacturonan, which are composed of the diglycosyl repeating unit, -4)-α-D-GalpA-(1-2)-α-L-Rhap-(1 [144]. The neutral sugar size chains of β-1, 4-galactans, branched with fucose and arabinose residues, and α-1, 3- or 1,5-arabinans are linked to the C-4 side of rhamnose residues in the rhamnogalacturonan as illustrated in **Figure 2-7** [145]. However, the full aspect of their structure is not fully known [145].
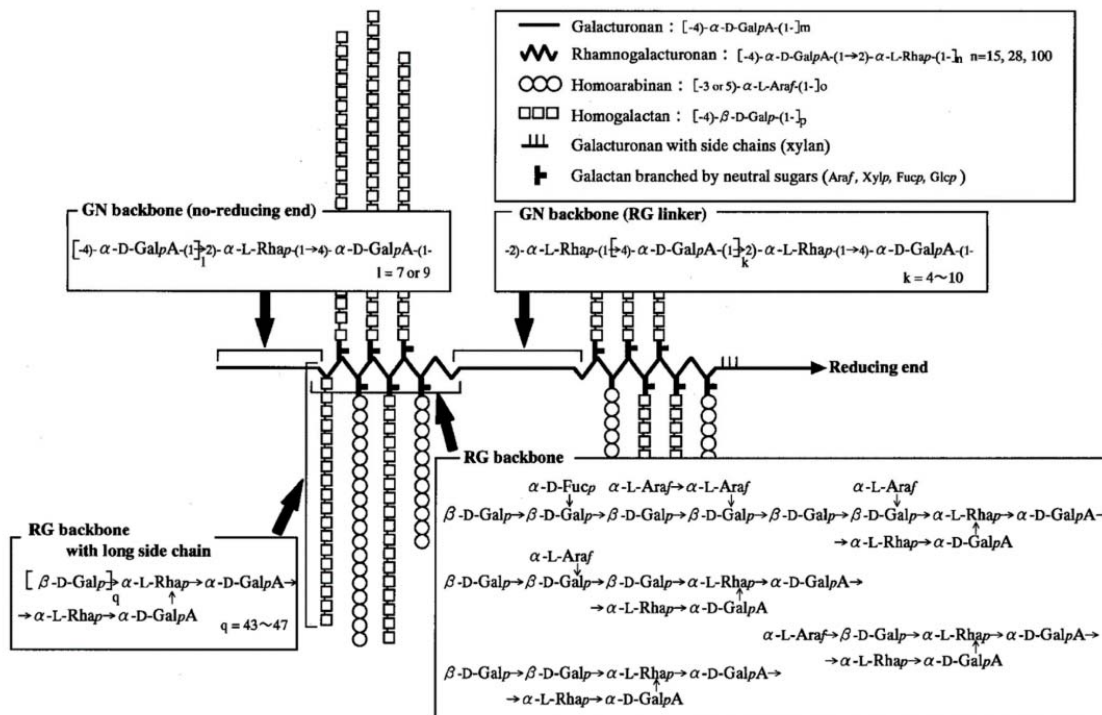
Figure 2-7 Structure of main fracture of soluble soybean polysaccharide [145]. Reprinted from *Soluble soybean polysaccharide*, H. Maeda and A. Nakamura, Handbook of Hydrocolloid, 693-709, 2009, with permission from Elsevier.

The molecular weight of SSPS influences its functional characteristics. The weight-average molecular weight (M_w) of SSPS is 2.54×10^6 g/mol, which is close to some commercial gums such as guar gum (1.45×10^6 Da), xanthan gum (4.05×10^6 Da), gellan gum (1.64×10^6 Da) and locust bean gum (1.6×10^6 Da) [144]. The number-average molecular weight (M_n) of SSPS is 5.54×10^5 g/mol [144]. Polydispersity index (PDI = M_w/M_n) of SSPS is 4.5, while the PDI of biopolymers is commonly ranged from 1.16 to 2.86. This suggests that SSPS is less uniform than the commercial hydrocolloids, such as guar gum (PDI=1.21) and Arabic gum (PDI=1.26) [144].

SSPS has been found to have emulsifying property [146]. The emulsifying activities of SSPS has been attributed to the proteinaceous materials that are bound to carbohydrate, adsorbing onto the oil and water (O/W) interface as an anchor, and the carbohydrate contributes mainly to emulsion stability by steric repulsion, preventing flocculation of the oil droplets by forming a hydrated layer. The number of molecules adsorbed onto the oil droplets is in the order of sugar beet pectin < SSPS < gum Arabic [146].

One of the most well-studied characteristics of SSPS is its ability to stabilize acidified milk drinks. Acidified milk drinks commonly refer to a large category of dairy products such as fruit-juice-containing milk or directly acidified milk drinks and yogurt drinks with an approximate pH range of 3.4 – 4.6 [147]. As pH of such product is brought close to the isoelectric point (pI) of the protein, the electrostatic repulsion between the protein molecules is reduced, and thus leading to aggregation and sedimentation of proteins in the product. To resolve this issue, one solution was to use negatively charged hydrocolloids to bind with the positively charged protein molecules, thereby creating a new steric repulsion between the hydrocolloids (**Figure 2-8**). SSPS can be used as such anionic polysaccharide to effectively adsorb onto and fully cover the surface of the protein and restore the steric hindrance and electrostatic repulsion at low pH [147]. High methoxyl pectin (HMP), SSPS, and carboxymethyl cellulose (CMC) are the stabilizers commonly used for this application. It was found that SSPS have similar monosaccharide composition to HMP. The main structural difference is that SSPS have longer side chains due to the presence of larger number of neutral monosaccharides as compared to HMP. Moreover, SSPS have a globular form that enabled them to stabilize acidified drinks without increasing viscosity or thickness. These might explain SSPS's superior stabilizing ability as it was able to stabilize acidified milk drinks at pH < 4, whereas HMP loses its stabilization effect in this pH range [147].
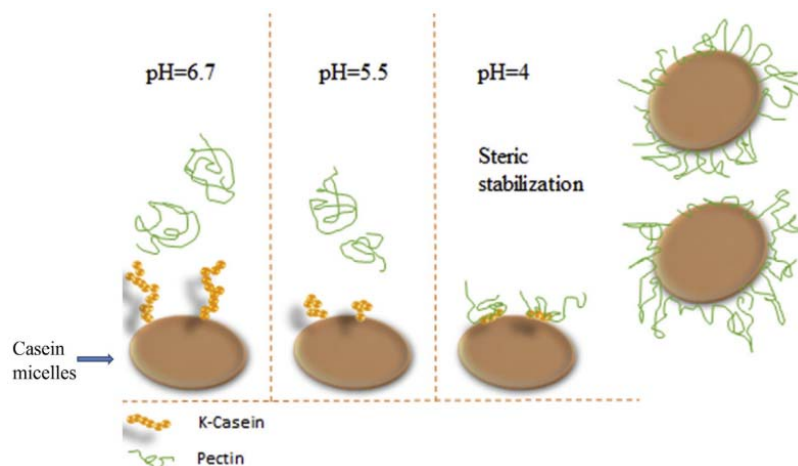
Figure 2-8 A schematic illustration of the replacement of k-caseins with pectin at different pH values, and caseins coated with pectin molecules [148]. Reprinted from *Recent advances in application of different hydrocolloids in dairy products to improve their techno-functional properties*, **88**, M. Yousefi and S. M. Jafari, 468-483, 2019, with permission from Elsevier.

The gelling behaviour of SSPS was also examined in tofu-type gels. The study by Lan et al. studied the effect of SSPS on the formation of GDL-induced gel with 10% w/v SPI and 0-16% w/w SSPS [149]. It was suggested that SSPS conjugated with SPI *via* the Maillard reaction based on characterizations such as sodium dodecyl-sulfate polyacrylamide gel electrophoresis (SDS-PAGE), grafting degree, color change, and infrared analyses. After incorporating SSPS, the dominant interaction of the soy protein gel changed from non-covalent to electrostatic interaction as evaluated by protein dissolution analysis. Both the mechanical strength and water holding capacity (WHC) of the SPI gel decreased as the SSPS concentration increased. Moreover, larger protein aggregates and pores were observed in the microstructure of SPI gel at higher SSPS concentration [149].

<div align="center">

2.7.2.2 Acid Extraction of Insoluble Soybean Polysaccharides (ISPS)

</div>

The insoluble soybean polysaccharide (ISPS) as the other fraction of okara can be obtained by heating okara in weak acidic conditions [136]. ISPS is consisted of high concentrations of polysaccharides and proteins. The compositional analyses of ISPS allowed inference of the presence of carbohydrates covalently attached to proteins in a glycoprotein matrix, *i.e.*, arabino-galactan-proteins and glucomannan-proteins [136]. ISPS possesses loose structure with porous and wrinkled surface as observed by SEM [150]. Owing to these structural characteristics of ISPS, their ability to capture water or oil was otherwise enhanced. Additionally, the free hydroxyl groups of ISPS can act as water holding sites as well [150].

Several treatments were studied to increase the superficial hydrophobicity of ISPS in order to strengthen the absorption of the macromolecules at the oil-water interface by exposing internal sites of the polysaccharide and protein structures [136]. These treatments include high-pressure homogenization and ultrasonic sonication, and via these treatments the rigidity of the interfacial film increased [136]. Moreover, these treatments could solubilize certain compounds in okara, *i.e.*, the low molecular weight polysaccharide or peptides fragments, which could interfere negatively in the formation of the interface during the emulsification process [136].

The emulsifying ability of ISPS as a Pickering stabilizer was most studied. A Pickering emulsion is stabilized by solid particles that are adsorbed onto the surface between two phases. Treatments such as alkaline treatment, ultrasonic alkaline treatment, steam-cooking alkaline treatment, ultrasonic-assisted steam-cooking alkaline treatment have been used to improve the structural

and emulsifying properties of ISPS [150]. By rupturing ISPS *via* these treatments, increases in hydroxyl groups, porosity, and surface area of ISPS were observed, which led to enhanced WHC, swelling capacity, and oil holding capacity [150].

Additionally, ISPS are also capable to stabilize SPI emulsion at low protein concentrations, *i.e.*, less than 0.4 wt% [151]. This phenomenon was likely ascribed to the electrostatic interaction between ISPS and SPI, as well as the unique structure of ISPS that enabled them to function as emulsifier and thickener.

2.7.2.3 Acid Extraction of Pectic Substances

Pectic polysaccharides are one of the major polysaccharides in plant cell walls. Acid hydrolysis can facilitate the extraction of pectic substances in lignocellulosic materials [152]. Although there have not been studies conducted concerning the extraction of pectin from okara specifically, studies had been conducted for other food masses that contain hemicellulose, cellulose, lignin and pectic substances.

Conventionally, strong inorganic acids such as nitric acid, sulfuric acid or hydrochloric acid are commonly used in the extraction of pectin from lignocellulosic material. But the use of strong acids can generate toxic derivatives for health and environment [153]. Therefore, organic acids such as acetic acid, ascorbic acid and citric acid are alternative acids used to avoid the negative drawbacks. However, the release of pectin by organic acids is slower as compared to inorganic acid due to their low protonation capacity [153]. Hence, longer reaction time is often necessary to achieve similar yields. Alternatively, the processing temperature may be increased if prolonged processing time is to be avoided [153]. A higher extraction temperature (*i.e.*, 121 °C) could yield about three-time larger amounts of soybean pectin as compared to a much lower temperature (*i.e.*, room temperature) [142]. However, the soybean pectin extracted at room temperature had better-preserved native molecular characteristics, which was evident by an increased molar mass, and the protein moieties were covalently linked to pectin moieties *via* O-linkage [142].

Citric acid was employed as a weak acid to extract pectin from cocoa pod [153], [154]. Cocoa pod is a lignocellulosic waste, containing cellulose, hemicellulose, lignin, pectin, and other compounds [153], [154]. Pectin was extracted from the liquid fraction of hydrothermally processed cocoa pods at 120 °C for 10 min that was treated by 2% w/v citric acid [145].

41

Similarly, by subjecting okara fibers to organic acid such as citric acid, hydrolysis of larger-molecular-weight polysaccharides of okara (*e.g.*, cellulose, hemicellulose, lignin) may be hydrolyzed into smaller saccharides. Meanwhile, SSPS, ISPS, and pectin may be generated during this process.

2.7.3 Citric acid chelation

Citric acid has also been used as a chelator for the extraction of pectin. Research has shown that pectin and glucan may be harder to hydrolyze among all the soybean carbohydrates [155]. Therefore, to stabilize the calcium-ion-bridged junctures in pectin, chelators could be used to treat soybean meals for easier hydrolysis. Some common chelators are ethylenediaminetetraacetic acid (EDTA), sodium hexametaphosphate (HMP) and citric acid. The enzymatic hydrolysis of soybean meal occurred when a relatively mild thermal treatment was employed, *i.e.*, 90 °C for 2 h, with the help of chelators [155]. In comparing these three chelators, citric acid was found to be the most effective in facilitating the enzymatic hydrolysis, while EDTA decreased the hydrolysis activity [155].

Hence, hydrolysis of okara with citric acid may have increased effectiveness as it acts to destabilize the calcium junctures in pectin.

2.7.4 Rationale For the Use of Citric Acid

Citric acid is an economical, food-grade acid and is commonly used in food production [153], [156]. Unlike strong acids such as sulfuric acid and hydrochloric acid, citric acid does not release harmful substances. Structurally, citric acid is a polycarboxylic-structured acid with two primary and one tertiary carboxylic acid groups (**Figure 2-9**), and the tertiary group is less reactive than the primary groups [157]. The pKa value of the three carboxylic acid groups of citric acid are 3.1, 4.7, and 6.4 [158].
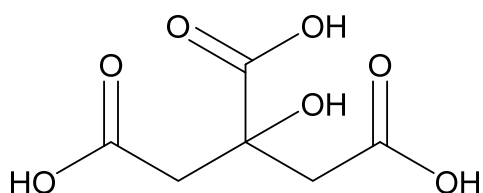
Figure 2-9 Chemical structure of citric acid [Created in Chem Draw, ACS document 1996-1].

As discussed in previous sections, acid treatment provides several potential benefits for the modification of soy okara. Firstly, the carboxylic groups of citric acid can react with the hydroxyl groups of the okara fiber constituents, *i.e.*, hemicellulose, cellulose, lignin and pectin, inducing the formation of covalent ester bonds, which may act to strengthen the network of the whole soybean gel. Secondly, citric acid treatment can facilitate the hydrolysis of the insoluble fiber of okara and generate smaller-weight saccharides. Since insoluble fiber creates a heterogeneous and coarse gel structure [5], citric acid hydrolysis may improve the compatibility of soybean polysaccharides with the remaining protein matrix. Moreover, citric acid hydrolysis may also facilitate the extraction of pectic substances present in okara while producing soluble and insoluble polysaccharides that possess different properties. Lastly, citric acid may act as chelator and stabilize the calcium-ion-bridged pectic structure, and thereby easing the extraction of pectic substances of okara fiber.

2.8 Characterizations

This section provides background overview concerning the characterizations adopted for the analysis of all the relevant data. The characterizations include thermogravimetric analysis (TGA), Fourier transform infrared spectroscopy (FTIR), mechanical compression, rheological test, water holding capacity (WHC), and morphological evaluations.

2.8.1 Thermogravimetric Analysis (TGA)

Thermogravimetric analysis (TGA) provides information on the composition profile of food materials obtained from the thermal stability of its constituents [159]. In particular, the mass loss over temperature will reveal the thermal stability of the constituents of a material. Generally, for food materials, about 5-15 mg of samples were heated from 20-35 °C to 200-700 °C [159]–[161].

The thermal decomposition profiles of materials can be divided in temperature ranges that can be assigned to classes of constituents. Generally, the first stage is assigned to the temperature region lower than 150 °C. This is associated with the weight loss caused by the evaporation of water and other volatile materials [162]. The following stages can vary depending on the main constituents of the sample tested. For example, the temperature range of 240 to 400 °C typically corresponds to the degradation of backbone peptide bonds of proteins in protein-rich materials [163], [164].

As for polysaccharide-rich materials that contain minimal protein, *e.g.*, starch, the same temperature range could be ascribed to thermal decomposition of polysaccharides [165].

A typical food product can be composed of protein, carbohydrate, and fat while lignocellulosic are composed of cellulose, hemicelluloses and lignin. At the temperature range of 150-250 °C, non-cellulosic material decomposes [166], such as hemicellulose [167], [168]. At temperature around 250-380 °C, cellulose depolymerization begins because of the hydration and decomposition of glycosidic linkages where major weight loss occurs rapidly [168]. At temperatures above 380 °C, the degradation of amorphous phases of hemicellulose and lignin as well as the crystalline cellulose takes place [166]. Because lignin is difficult to decompose, it is responsible for the formation of char residue present above 600 °C [166], [169].

The derivative thermogravimetry (DTG) curve represents the rate of weight change over the change in temperature of a specimen. If most weight loss occurs at a lower temperature, it indicates that the sample is relatively heat sensitive, and vice versa. The examination and comparison of the degradation peaks, weight loss of each stage, residual mass at the final temperature, provides information of the composition and stability of materials.

2.8.2   Fourier Transform Infrared Spectroscopy (FTIR)

Fourier transform infrared spectroscopy (FTIR) is a non-destructive, fast, and reliable technique that provides information on the functional groups of the chemical constituents of a material. FTIR requires very little sample preparation. For solid specimen, about 2 mg of sample is ground together with 200 mg potassium bromide (KBr) using a mortar and pestle, then compressed into pellets. FTIR spectra can then be collected using wavenumber range of 400 to 4000 cm^{-1}. A KBr pellet is often used to serve as the background spectrum and subtracted from the sample spectra.

Depending on the type of material and the functional groups associated with the material, absorption bands at certain wavelength are considered. In the context of soy milk and okara, the absorption bands in the regions of 3650-3100, 3000-2750, 1750-1540, and 1200-950 cm^{-1} are of particular interest. The broad band in the region of 3650-3100 cm^{-1} is ascribed to O-H stretching of hydrogen in the hydroxyl group [170]. The bands at ~2920 and ~2854 cm^{-1} are assigned to C-H vibration stretching in polysaccharides [171]. Bands at ~1742 and ~1645 cm^{-1} represent the stretching vibrations of esterified and unesterified carboxyl groups, respectively [172]. The band at ~1645 cm^{-1} can also represent the amide I bond of protein molecules [173], [174]. The band at

~1540 cm^{-1} is ascribed to amide II bond [173], [174]. The region 1200-950 cm^{-1} is the so-called fingerprint region, where the position and intensity of the bands differ for each polysaccharide type [175].

By analyzing the changes of intensities of absorption bands at a specific wavenumber, changes of the associated functional groups of a material can be inferred. For example, if the band intensity at 1742 cm^{-1} increases while the one at 1645 cm^{-1} decreases, then one can infer that some free or unesterified carboxylic groups are converted to esterified carboxylic groups. Depending on the available functional groups in the specimen, this phenomenon may be a result of the occurrence of esterification reactions.

2.8.3   Mechanical Compression

2.8.3.1 Methods

Food texture can be evaluated by two main types of methods, sensory evaluation and instrumental analysis [34]. Sensory evaluation, also considered as the "gold standard" in texture evaluation is a subjective evaluation as food texture is evaluated directly by humans [176]. In contrast, instrumental analysis is an objective evaluation based on physics and/or chemistry, and as the name implies, it is conducted by an equipment. Consequently, between the sensory and instrumental results, differences are often observed [34]. These differences can relate to the steps of the chewing process replicated by the instrument, which typically captures pre-fracture stage or first bites, which is different than for sensory evaluation that captures the entire oral processing stages. Moreover, conditions such as temperature, moisture due to saliva, chewing movements, and food deformation rates are often poorly reproduced with conventional instruments [34]. To eliminate the gap between subjective and objective methods, it becomes necessary to examine the physical changes that foods undergo during oral processing by using human physiological measurements an alternative category. In this method, sensors are attached to human subjects who eat the food. As a result, the output values from the sensors are objective, similar to instrumental analysis, while the mode of oral processing is the same as for the sensory evaluations [34].

Instrumental analysis can be further categorized into three types: fundamental, empirical and imitative methods. Fundamental methods involve the measurement of well-defined physical properties, such as Young's modulus, shear modulus, bulk modulus and Poisson's ratio (for

solids) and viscosity (for liquids) [176]. The measurement is limited to homogeneous and isotropic materials. Foods with an anisotropic structure (*e.g.*, meats) are difficult to analyze accurately. Generally, the limitation of fundamental methods is the difficulty in correlating the measured properties to the textural characteristics perceived by humans. Empirical tests, on the other hand, tend to provide better correlations to the sensory scores [177]. However, the measured variables are often ill-defined as they are developed from practical experience associated with some element of textural quality. Some examples of empirical tests include Magness-Taylor puncture tester for fruit hardness and the Kramer Shear Press for hardness of processed fruits [34]. Lastly, imitative methods attempt to simulate the conditions to which the food is subjected to human action. The instrument mimics human movements, and the empirical parameters help explain the texture perceived by humans [34]. Texture Profile Analysis (TPA) is a common and widely used technique and will be discussed in section 3.3.3.

2.8.3.2 Uniaxial Compression

Uniaxial compression test is an example of a fundamental method for texture evaluation based on well-defined physical properties of food. It provides large deformation measurement, meaning that fracture of a food material is induced through motions such as compression in order to evaluate the human mastication behaviour [32], [178]. Large deformation measurements provide information complementary to those obtained in the small deformation range. Measurements in the small deformation range are within the linear viscoelastic region, which do not necessarily reflect the human mastication behaviour [32], [179], [180]. Consequently, measurements made in the large deformation regime are more relevant to the use of food materials in practice and eating experience.

Uniaxial compression performed under large-deformation conditions is when the food material is compressed once and all the way until fracture. Fracture stress represents the maximum stress at which the food breaks down upon strain [32]. The fracture stress is sometimes referred to as the gel strength in the food industry. The true fracture stress is the applied load divided by the instantaneous cross-sectional area of the specimen at fracture, which gives a good indicator of mastication effort [181]. The fracture strain, which is the strain corresponding to the fracture point of the material, indicates the resistance to deformation of a food material [182]. A high fracture strain implies that the material is relatively resistant to compressive deformation.

One can also determine the elastic modulus, also known as the Young's modulus, which is located within the linear region of the stress-strain relation and is determined by the initial slope of the force-deformation curve between stress and strain [32].

The fracture stress and Young's modulus have different physical meanings. The elastic modulus is related to "firmness" or "hardness" whereas, the fracture stress or fracture force is related to "toughness" or "chewiness", which is a complex textural sensation that includes "springiness" and "cohesiveness" in addition to "firmness" [32]. Thus, if a food material possesses high Young's modulus, it indicates that the material is firm in texture. If high fracture stress is demonstrated, it suggests that the material has a high gel strength.

During compression, the cross-sectional area of a soft food material may change over time. Consequently, the engineering stress is not an adequate representation of the actual stress as it does not take account of the change in surface area. Therefore, true fracture stress and strain, which are also known as Hencky stress and strain should be considered. The measured mechanical properties from the uniaxial compression are summarized in **Table 2-6**.

Table 2-6 Mechanical properties for uniaxial compression test.

Parameters	Definition	Mathematical representation	References
True Fracture Stress $\sigma(t)$ (Pa or kPa)	True stress measured at material's fracture point Fracture point for foods is the maximum compression force or stress [183]–[185]	$$\sigma(t) = \frac{F(t)}{A_0} \times \frac{l(t)}{l_0}$$ l_0 and A_0: original height and cross-sectional area of the gel, respectively; $l(t)$ and $F(t)$: height and force of the gel at time t	[182]–[184], [186], [187]
True fracture strain ϵ (-)	True strain measured at material's fracture point	$$\epsilon = -\ln\left(\frac{l(t)}{l_0}\right)$$	[182]–[184], [186], [187]
Young's modulus E (N/m², Pa or kPa)	Linear region of the true stress-strain curve located between one and two-thirds of the way to the point of maximum true stress	$$E = \frac{2/3\sigma_{frac} - 1/3\sigma_{frac}}{2/3\epsilon_{frac} - 1/3\epsilon_{frac}}$$ σ_{frac}: true fracture stress; ϵ_{frac}: true fracture strain	[182], [184], [188], [189]

Texture profile analysis (TPA) is an imitative method for the evaluation of food textures [190]. It has been prevailingly adopted as the method for evaluating textural attributes of food material in expansive food research mainly because of the ease of operation and analysis of the results.

One of the major differences between uniaxial compression analysis and TPA is that the former was conducted until the sample is fractured whereas, TPA is performed with two-cycle compression, where a lower deformation (*e.g.*, 40%) is used for the first compression cycle, so that the food material has not permanently deformed to proceed to the second cycle.

In TPA test, a force-time graph is generated, illustrated in **Figure 2-10** as an example. Based on the graph, a number of texture attributes can be measured, including the so-called hardness, cohesiveness, springiness, chewiness, *etc*. (**Table 2-7**).
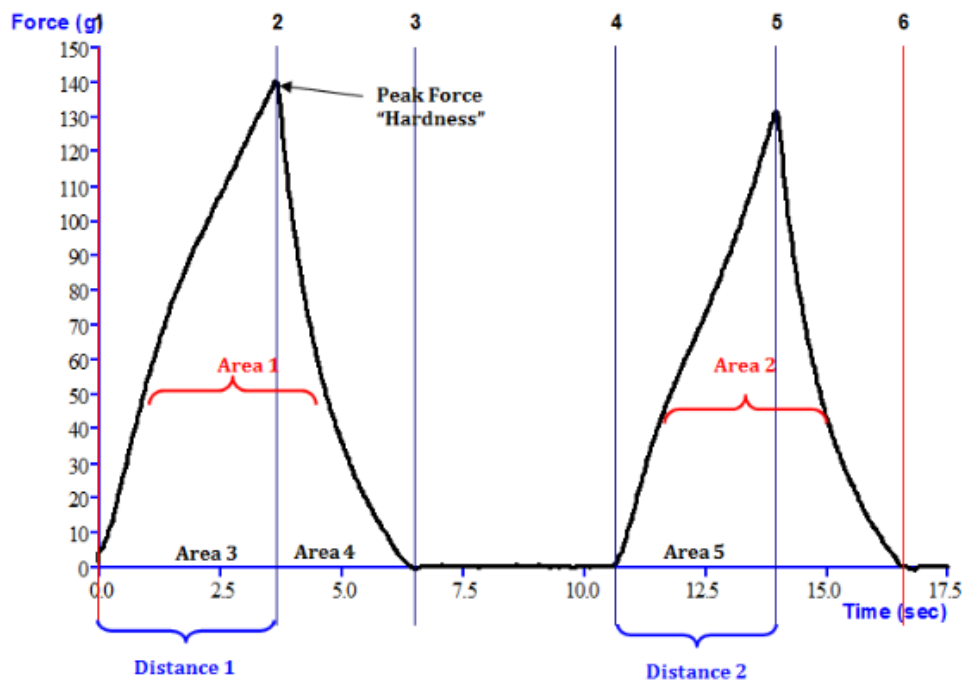
Figure 2-10 A typical TPA force versus time plot (adopted from TTC website).

Table 2-7 Measurements of TPA parameters (adapted from TTC website).

Parameter	Expression	Measurement (based on **Figure 2-10**)
Hardness	Maximum force of the 1st compression	Maximum force of the 1st compression
	Note: The hardness need not occur at the point of deepest compression, although it typically does for most products.	
Fracturability	Degree to which a product falls apart	Force at the 1st peak
	Note: Not all products fracture; but when they do fracture the Fracturability point occurs where the plot has its first significant peak (where the force falls off) during the probe's first compression of the product.	
Cohesiveness	Wellness of a product to withstand the 2nd deformation relative to the 1st one	Area 2/Area 1
Springiness	Wellness of a product to spring back after deformation during the 1st compression after targeted wait time between strokes	Distance 2/Distance 1
	Note: The spring-back is measured at the downstroke of the second compression. In some cases, an excessively long wait time will allow a product to spring back more than it might under the conditions being researched (*e.g.*, one would not wait 60 seconds between chews).	
Gumminess (semi-solids only)	Cohesive and sticky	Hardness x Cohesiveness
	Note: Gumminess is mutually exclusive with chewiness since a product would not be both a semi-solid and a solid at the same time.	
Chewiness (solids only)	Elastic resistance	Hardness x Cohesiveness x Springiness
Resilience	Wellness a product resists to spring back to original height	Area 4/Area 3
	Note: Resilience is measured on the withdrawal of the first penetration, before the waiting period is started. Resilience can be measured with a single compression; however, the withdrawal speed must be the same as the compression speed.	

The settings of the TPA test are crucial because soft food materials are very sensitive to deformation conditions. Many food products can tolerate low stresses, but they tend to be permanently deformed beyond the point of plastic deformation, for instance, at strains greater than 50%. A study reported by TTC conducted with a commercial tofu (type unknown), the texture varied significantly according to the strain conditions (**Table 2-8**). The "hardness" of the commercial tofu increased significantly with increasing strain, whereas springiness, cohesiveness and resilience were negatively influenced. The permanent deformation of the commercial tofu was achieved at and beyond 50% strain.

Similar observations are reported in other studies where the measured TPA attributes varied significantly according to testing conditions. Differences of the textural measurements were related mostly to the different percent deformation. Specifically, decreasing the percent deformation from 75% to 50% resulted in decrease "hardness" and "gumminess" and increase "springiness" and "cohesiveness" [191]. The use of different compression speed can also affect the measurements where the higher the compression speed, the higher the "hardness" value [191]. On the other hand, "cohesiveness" was influenced to a lesser extent by compression speed conditions [191].

In summary, the textural measurements obtained by TPA are strongly affected by the testing conditions. Consequently, caution should be given when conducting TPA tests as well as analyzing TPA results.

Table 2-8 Calculated TPA results of commercial tofu (data obtained from the TTC website)

	Strain	25%	50%	75%
Primary parameters	Hardness (g)	1609	3427	7613
	Springiness (%)	99.6	91.9	76.1
	Cohesiveness (%)	89.5	50.4	30.1
	Resilience (%)	52.1	20.2	7
Secondary parameters	Fracturability (g)	-	3427	2946
	Gumminess	N/A		
	Chewiness	1434	1587	1742

As previously discussed, the major difference between the uniaxial compression method and the two-cycle compression conditions of the TPA method is the degree of sample deformation. Samples that undergo uniaxial compression are deformed until fracture whereas in TPA, samples generally do not reach their fracture point. As a result, uniaxial compression is more robust because all samples are expected to fracture during the test while in a TPA test results are dependent on the percent deformation, compression speed, and size of the specimen [191], [192].

Although TPA may be a simple and convenient method for textural evaluations, this test has major methodological limitations and thereby cannot be recognized as a coherent method [192]. The parameters generated from TPA, such as "hardness", "bitterness", and "cohesiveness" are somewhat related to the properties defined in material science and other disciplines. Therefore, it has been suggested that the TPA parameters be replaced by mechanical and other physical properties recognized in material science, including "yield stress", "strain at failure", and "stiffness" [192].

Overall, uniaxial compression test is comparatively a more robust technique for measuring the texture attributes of food materials. The well-defined engineering properties include the true fracture stress, true fracture strain and Young's modulus, and they have strong correlations to the perceived food texture [32].

2.8.4   Rheology

Rheology is the science of the flow and deformation behaviour of substances. The rheological measurements provide information about the behaviour of a matter under stress.

The small amplitude oscillatory shear test provides information on the super-molecular distances (*e.g.*, nanometer to micrometer range) and relationships between levels of structures and structural organization in a material [180]. Small-deformation tests provide indirect information about gel strength and microstructure [94] and useful information on food texture and the initial stage of the oral processing [32].

In a dynamic rheological test, the material of interest is subjected to a controlled oscillation. Different types of dynamic tests can be set up by changing one or more experimental variables: strain (or stress) amplitude, temperature, time, or frequency of oscillation [193]. Dynamic rheological tests include stress or strain sweep, temperature sweep, time sweep, and frequency

sweep. In the context of gel materials, the strain and frequency sweep tests can be used to examine the effect of angular frequency on storage modulus (G') and loss modulus (G") where G' relates to the ability of a material to store energy elastically and G" relates to the ability of a material to dissipate stress through heat. Tangent delta (tan δ) refers to the viscoelasticity index of a material.

2.8.4.1 Strain or Stress Amplitude Sweep

Strain or stress amplitude sweep test is performed by measuring the dynamic shear moduli (G', G'', G*) as a function of increased strain or stress while the frequency is fixed [193]. The strain sweep test is performed under controlled shear deformation, whereas the stress sweep test is performed with controlled shear stress. The objective of each test is to determine the critical point beyond which the dynamic shear moduli become dependent on the input variable, strain, also known as the yield strain [194]. Conducting the strain or stress sweep is the first step in dynamic mechanical analysis.

Amplitude sweep tests describe the behaviour of dispersions, pastes, and gels. Amplitude sweep tests generally describe the deformation behaviour of samples in the non-destructive range and at determining the upper limit of this range. For amplitude sweep tests, the conditions increase step-wide from one measuring point to the next while keeping the frequency at a constant value.

The results of amplitude sweep tests are presented as strain (or shear stress) plotted on the x-axis and storage modulus G' and loss modulus G'' plotted on the y-axis (**Figure 2-11**). Typically, the x-axis or both axes are on logarithmic scale. The frequency at which the test is conducted should be low enough to not break the structure of the material, and 1 Hz is the typical frequency.

Amplitude sweep tests are often performed to determine the linear viscoelastic region (LVR). The LVR indicates the range where the material structure is not destroyed. The limiting value of the LVR, is often called the linearity limit or yield strain if strain sweep was performed, as denoted by γ_L in **Figure 2-11**.

The G' and G" profiles in the LVR provides information on the material properties. A material will display gel-like or solid structure, termed as a viscoelastic solid material, if G' > G". If G'' > G', the material displays a fluid structure, termed a viscoelastic liquid (**Figure 2-11**). This terminology is valid only for the selected experimental conditions, the pre-set frequency. For all

subsequent oscillatory tests, measurements should be obtained at strain or stress levels within the LVR. Prior to examining an unknown material by oscillatory test, an amplitude sweep test is normally performed first to determine the limit of the LVR.
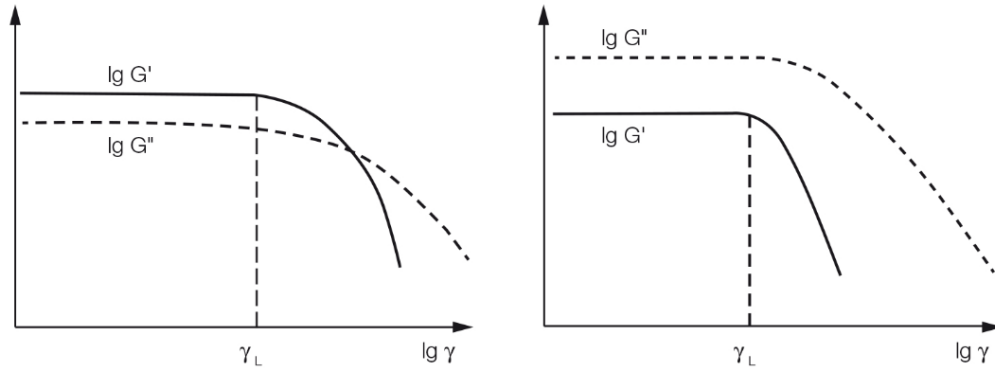
Figure 2-11 Example of two amplitude sweeps diagrams. The functions of G' and G'' show constant plateau values within the LVE region. Left: G' > G'' in the LVE region, indicating sample has a gel-like or solid structure. Right: G'' > G' in the LVE region, suggesting sample is fluid (adopted from the Anton Paar website).

2.8.4.2 Frequency Sweep

Frequency sweep test is performed when a sinusoidal strain or stress of fixed amplitude is imposed on the material, and the dynamic shear moduli are determined over a wide range of frequency [193]. The resultant plot is known as the "mechanical spectrum" of the material. This is the most versatile rheological test to characterize the viscoelastic behaviour of materials. Most rheometers can measure dynamic properties from 0.01 to 100 Hz. High frequencies are used to simulate fast motion on short timescales, while low frequencies simulate slow motion on long timescales or at rest.

Frequency sweep tests can be conducted under controlled strain or controlled shear stress. The preferred method for conducting frequency sweep test is from maximum to minimum frequencies, as this often results in a shorter testing period due to shorter adjustment time of the controller. Frequency sweep test results are presented as plots of the angular frequency on the x-axis and G' and G'' on the y-axis. Typically, the x-axis or both axes are on a logarithmic scale. The selected shear-strain or shear-stress amplitude must be within the LVR. The frequency sweep test provides information on the rigidity of the material under small-deformation

53

conditions [195]. A strong dependence of G' and G'' on frequency suggests a "weak gel" behaviour [195].

Typical preparation of solid gel-like food materials will consist of the taking a specimen in the center portion of the sample to avoid edge effects. The cutting motion should be slow and gentle to minimize any surface shear which may affect measurements. As an example, a specimen thickness of 1.5-mm is suitable for 1-mm measuring gap when using parallel plate geometry. The specimen should not be too thick, otherwise the high axial compression force resulting from loading may induce permanent damage to the structure of the sample. The specimen should not be too thin. The additional thickness will allow for adequate axial force to expel any air bubbles that may be present within the specimen. The "trimming position" should be used to optimize the sample filling. When trimming specimens, a vertical trim is often implemented. As the top plate displaces from the trimming position to the measurement position, the sample should have an appropriate filling with a bulged edge (**Figure 2-12**). The specimen should be allowed to rest at room temperature for about one hour to achieve thermal equilibrium when the test is conducted at room temperature.
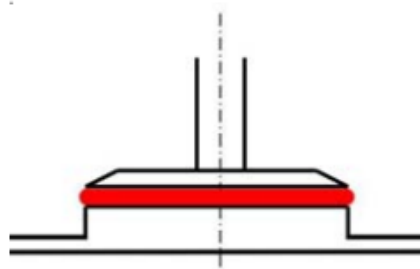
Figure 2-12 Correct sample filling with parallel plate geometry (adopted from the Thermo Scientific website).

2.8.4.4 Analysis of Rheological Data

In the amplitude sweep test, the sudden decrease in the storage modulus (G') indicates breakage of bonds within the gel network, resulting in transition from linear to nonlinear behaviour [195]. Moreover, the behaviour of a gel material can be reflected from the magnitude of G'. Typically, a weaker gel tends to have lower G'. Additionally, the limit the LVR provides information on samples' resistance to shearing motion [195]. The greater the linearity limit the more resistant the gel is to shear.

The frequency sweep results can be represented with a power law model to characterize the dependence of G' and G'' on the angular frequency (ω) [195]. The power law model is presented by **Equation 1** and **Equation 2**.

$$G' = G_0' \omega^{n'} \qquad \qquad \text{Equation 1}$$

$$G'' = G_0'' \omega^{n''} \qquad \qquad \text{Equation 2}$$

Where, G_0' (Pa) and G_0'' (Pa) are the storage and viscous moduli at 1 rad/s, respectively. G_0' is the energy stored and recovered per cycle of sinusoidal shear deformation. Based on the dynamic moduli versus angular frequency plots on logarithmic scale, constant parameters, G_0', G_0'', n', and n'' can be determined by linear regression.

G_0' reflects the rigidity of the material which is associated with the formation of an elastic gel structure. A higher G_0' value usually relates to denser network accounting for higher rigidity of the gel structure [195]. G_0'' is the energy dissipated or lost as heat per cycle of sinusoidal strain and indicates the extension of the viscous element in the material [195]. The exponents n' and n'' (both dimensionless) denote the influence degree of ω on both moduli. The dynamic moduli of a "weak" gel typically have higher dependence on ω, and thus higher n' and n'' values, and vice versa for a "strong" gel [195].

Some other parameters, such as $tan\ \delta$ (=G''/G'), indicates weak- or strong-gel behaviour. A $tan\ \delta$ value of greater or equal than 0.1 belonged to the so called "weak" gels [196], [197]. Furthermore, based on the magnitude of G' and G'', a "weak" gel behaviour may be suggested if the magnitude of G' is less than 10 times that of G'' [197].

2.8.5 Water Holding Capacity (WHC)

Water in foods is generally categorized into three types, free water, bound water, and entrapped water [198]. Free water is the water that can be extracted easily from foods by squeezing, cutting or pressing. Bound water is the water that cannot be extracted easily, and has structural bounding with the food structure, and is unable to act as a solvent. An example of bound water is the water present in pine tree needles, where the water cannot be squeezed out, and is not affected by extreme desert heat or winter freeze. In fact, even upon dehydration, food can still contain bound water. Whereas, entrapped water is immobilized in capillaries or cells, but can be released upon

cutting or damage and will flow freely. In short, entrapped water has properties of free water but not the properties of bound water.

The water associated with proteins structure can generally be divided into two main types, absorbed water, *i.e.*, water bound to the protein molecule, which is no longer available as a solvent, and retained water, *i.e.*, water trapped in the protein matrix or a corresponding co-matrix of polysaccharide and/or fat [199]. The absorbed water is more tightly bound to the protein molecules and largely influenced by the physicochemical parameters directly affecting the proteins, as well as the surface properties of the protein molecules interact with the dissolving solution. The retained water is influenced by the water immobilization associated with the establishment of structures [199]. This water is not free water, which is more commonly retained by a co-matrix that contributes to gel formation.

Water-holding capacity (WHC), or sometimes referred to as water hydration capacity, water absorption, water-imbibing, and water-binding, represents the amount of water that can be bound or retained by a protein matrix under defined conditions [199]. In other words, the WHC is mostly determined by the amount of absorbed and the retained water [199]. In the context of gels, the WHC is the ability to effectively immobilize water through the capillary effects of the gel matrix [200]. Gels with large pores or coarse structure tend to bind water to a lesser extent because of low capillary forces [201]. Hence, the WHC reflects to a certain degree the three-dimensional structure of a gel. Nonetheless, WHC not only depends on pore and capillary size, but also on the charges of the protein molecules, associated forces (*e.g.*, hydrophobic interactions, hydrogen bonds, S-S bonds, Van der Waals' forces), and surrounding medium (*e.g.*, ionic strength, pH, temperature, etc.) [199]. Low molecular weight species, such as lactones, minerals (*e.g.*, sodium chlorides) have been reported to significantly influenced the WHC [202].

There exist a number of definitions of WHC. For protein-based materials, the WHC can be defined as the total amount of water that can be absorbed by 1 g of dry protein [203]. For meat products, the WHC can be defined as the ability to retain its own water or water added during the application of any force [204].

Different methods have been established to measure the WHC, including Baumann apparatus, capillary volumeter method, filtration method, *etc.* [199]. Out of all the different techniques, centrifugation is the most widely used in publications for food protein gels.

WHC of food materials is most frequently measured *via* centrifugation and estimated with two different methods. The first method is based on the mass of the gel after centrifugation divided by the initial mass of the gel [123], [205]. The second method is based on the mass of water remaining in the gel after centrifugation divided by the mass of water initially present in the gel [5], [94], [206]. In principle, both estimation methods represent the ability of water retainment of a gel material. Practically however, the second method is significantly more difficult to implement, since the mass of water of the gel must be estimated, which implies a drying step and thus can lead to increased experimental errors. Hence, the first method is the preferred method.

Prior to centrifugation, gel samples are cut into the same shape to eliminate its effect on the WHC. The initial mass of the sample is recorded as W_t, and then the sample is centrifuged at room temperature at selected centrifugal forces. Different centrifugal forces may be investigated to examine their effect on WHC. After centrifugation, the mass of released water is measured and recorded as W_r. Subsequently, the WHC can be calculated based on **Equation 3**.

$$WHC\ (\%) = 100\% \times \frac{W_t - W_r}{W_t} \qquad\qquad \textbf{Equation 3}$$

Where, W_t is the mass of the initial sample (g), and W_r is the mass of the released water (g).

Because of the various factors contributing to the WHC of a food material, it could be quite challenging as regards to data interpretation. Generally, WHC reflects the three-dimensional structure of a gel network as it characterizes a gel's ability to immobilize water. Hence, a loose and porous structure tends to have poorer WHC, whereas if the network is more compact and homogeneous, an enhanced WHC would be expected. Additionally, the constituents of a food system, interactions, as well as environmental factors can also influence WHC measurements. Unless each of these factors are carefully controlled, many causes may be related to a reduced or elevated WHC.

2.8.6   Morphology

2.8.6.1 Macrostructure

The macrostructure of soft food materials can be obtained by visual examination which will provide an initial assessment of its homogeneity and porosity. The internal macrostructure can be visualized by preparing a cross section of the food material via careful cutting, and imaging. The porosity and uniformity of the material cross-section can be examined by generating a binary image. The mean cell size, cell density, and void fraction are the frequently used measurements for the porosity analysis [120], [207]. The mean cell size can be automatically generated based on the detection of pores in the binary image. The cell density is the ratio of the number of pores to the total cross-section area. The void fraction is the ratio of the total pore area to the total cross-section area [202]. Generally, a higher mean cell size, cell density, and/or void fraction of a material suggests a more porous and heterogeneous structure.

2.8.6.2 Microstructure

2.8.6.2.1   Comparison of Imaging Methods

Microstructure imaging provides details of the morphology of a soft food material beyond porosity and homogeneity such as the observation of discontinuity at a molecular level. Many options for microstructural analyses are available. The most two common options for soft and hydrated food applications are scanning electron microscopy (SEM) and confocal laser scanning microscopy (CLSM).

SEM is used to examine the surface of the specimen. This method requires extensive sample preparation for products with high water content materials such as foods to minimize artifacts. Rapid freezing below -80 °C seems to be the most suitable procedure for food materials, minimally changing the original structure of the sample [208]. The traditional approach for imaging a three-dimensional biological structure is to immobilize the specimen by chemical fixation or freezing and cutting thin sections which are examined sequentially to provide a three-dimensional reconstruction [209]. However, slicing may cause damage to the material structure by shear and compression forces and sectioning requires tedious fixation and embedding, which may introduce artifacts [208].

CLSM greatly enhances the ability to obtain sharp, resolved images from selected levels within relatively thick, three-dimensional objects [208]. Compared with SEM, CLSM has lower resolution but requires minimal specimen preparation that avoids the necessity to cut sections of

specimens and thereby allows for visual examination of three-dimensional structures in live specimens [210]. *Confocal* means that the image is obtained from the focal plane only, with noise resulting only from sample thickness being removed optically. *Laser scanning* means that the images are acquired point by point under localized laser excitation rather than with the full sample illumination, as in conventional widefield microscopy [210]. Optical sectioning is one of the main advantages of this technique since physical slicing is no longer necessary. Its non-invasive sample preparation permits the observation of physiologically active structures. Living systems can be selectively labeled and dynamic experiments including structural changes can be monitored during the imaging. CLSM also allows for fluorescence imaging which has been proven to be the most powerful microscopic technique in biological applications and in microscopy of food materials [208].

2.8.6.2.2 Confocal Laser Scanning Microscopy (CLSM)

Microstructural analysis of food materials can be related to their mechanical properties, which can be related to their sensory properties [211]. CLSM as the microstructural imaging method for the evaluation of the morphology of food gel samples will be discussed in this section.
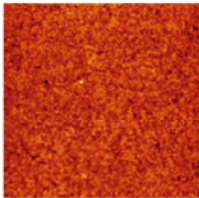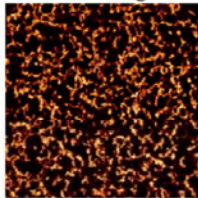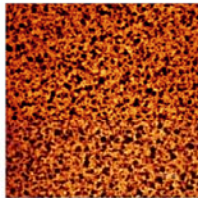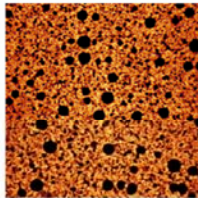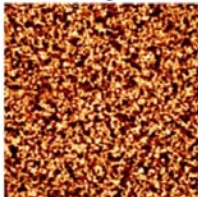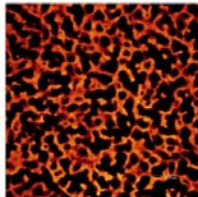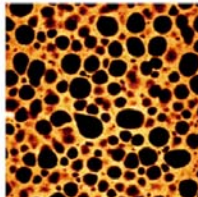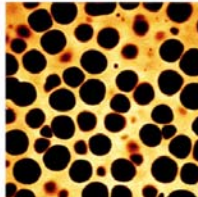
The microstructure of food gels obtained by CLSM can be classified on a micrometer length scale into homogeneous and phase-separated types. Phase-separated microstructures containing proteins can be further divided into protein continuous, bicontinuous, and coarse stranded [211].

As an example, CLSM was used to visualize the types of microstructures for different formulations of whey protein isolate (WPI)/polysaccharide mixed gels (**Table 2-9**). The protein network, stained by Rhodamine B, is depicted as bright areas, while dark areas represent the non-protein phase which is called the serum phase. In some formulation, phase separation was observed on a micrometer scale, likely the outcome of the gelation of mixed biopolymer solutions. The phase separation is driven by the incompatibility between proteins and polysaccharides, which is a fundamental property of many protein-polysaccharide mixtures. Homogeneous, protein continuous, and bicontinuous gels tend to reveal a distinct fracture, where the fracture occurs along only a few crack planes through the protein or serum phase [212]. In contrast, coarse-stranded gels tend to display multiple fractures at several places accompanied by coarsening of the network, leading to a vague fracture surface at CLSM length scale [211]. Homogeneous, protein continuous, and bicontinuous gels tend to reveal a distinct fracture, where

the fracture occurs along only a few crack planes through the protein or serum phase [212]. Whereas coarse-stranded gels tend to display multiple fractures at several places and are accompanied by coarsening of the network, leading to a vague fracture surface at CLSM length scale [211].

Table 2-9 Classification of microstructures of protein (whey protein isolate) and protein/polysaccharide mixed gels by CLSM [212]. Reprinted from *Breakdown properties and sensory perception of whey proteins/polysaccharide mixed gels as a function of microstructure*, **21**, L. van den Berg et al., 961-976, 2007, with permission from Elsevier.

	Microstructure			
	Homogeneous	Coarse stranded	Bicontinuous	Protein continuous
Length scale[a] (μm)	< 1	1	10	10
Thickness of protein phase[a] (μm)	< 1	1-3	3-15	3-10
Examples:	WPI 9-3	0.05% κ-carrageenan	0.025% gellan	0.05% locust bean
	0.01% gellan	0.09% pectin	0.04% gellan	0.1% locust bean gum
				0.14% pectin

The CLSM image represent a total surface of 160 μm × 160 μm
[a] Resolution of the CLSM equipment is typically < 1μm

Labeling of specific functional groups with fluorescence dyes allows the visualization of these groups. Fluorescent labeling is accomplished by using a reactive derivative of the fluorophore that creates covalent links to the functional groups of the proteins, such as amine or thiol groups [213].

The selection of a suitable dye for protein and polysaccharide phases is critical. The staining of polysaccharide constituent presents numerous challenges, which includes the selection of appropriate dye for targeted polysaccharide as well as the sensitivity of the selected dye. The simultaneous staining of two constituents, *i.e.*, polysaccharide and protein, can introduce crosstalk, which is the overlapping of the signals, and can eventually affect the quality of the imaging. Consequently, staining only a single phase, *e.g.*, the protein phase is more easily achievable and will enable the visualization of the protein constituents [212]. The distribution of the polysaccharide phase can be inferred accordingly.

Rhodamine B is commonly use for staining of soy proteins [118], [214], [215]. Rhodamine B has been extensively used either in its free form, *e.g.*, for thermometry or viscometry with its fluorescence intensity or lifetime or conjugated to macromolecules, such as proteins. The fluorescence properties of Rhodamine B can be affected by environmental conditions such as solvent polarity, viscosity or temperature. For instance, higher temperature results in lower fluorescence intensity [213]. Whey proteins or polysaccharides may also affect the fluorescent properties of Rhodamine B. The lifetime of Rhodamine B increases at elevated protein or polysaccharide concentrations [213].

For protein staining, a quantity of 10 μL of a 0.1% w/w Rhodamine B is suitable to stain 1 mL of protein dispersion [215], [216]. Typical excitation wavelength for Rhodamine B is 543 nm (He/Ne laser) while the emission is often recorded between 600 and 700 nm [214], [215].

2.9 Statistical Analysis

Statistical analysis tools are essential when conducting experimentation. Two types of statistical errors are considered. Type I error is the incorrect rejection of a true null hypothesis, denoted by symbol α. Type II error is the failure to reject a false null hypothesis, denoted by symbol β.

The multiple comparison test, or namely, the "post-hoc" test, allows for the simultaneous statistical comparison across more than two groups of data. The test can be categorized into two classes, *i.e.*, single-step and stepwise procedures. The single-step procedure assumes one hypothetical type I error rate, α, under which almost all pairwise comparisons are performed. This suggests that every comparison is independent [217]. Tukey and Bonferroni methods are examples of the single-step procedure. The stepwise procedure can be further divided into step-up and step-down methods. This procedure handles type I error according to previously selected

comparison results. Each comparison is performed only when the previous comparison is statistically significant. This method generally improves the statistical power of the process while preserving the type I error rate throughout [217]. Duncan test is an example of the stepwise procedure.

In the literature, the Tukey method, Bonferroni method, and Duncan test are common multiple comparison tests. The Tukey method uses pairwise post-hoc testing to determine if there is a difference between the mean of all possible pairs using the t-distribution. This test uses balanced data, meaning that the sample counts between groups are the same [217]. The Bonferroni method uses thresholds based on the t-distribution, which is more rigorous than the Tukey test, and tolerates type I error. However, the disadvantage of this method is its conservative approach, making the adjusted α often smaller than required. Therefore, this method often fails to detect real differences [217]. The Duncan test uses an error level for the entire collection of tests rather than an error rate for each individual test. This test provides significant levels for the difference between any pair of means, regardless of whether a significant F value results from the initial analysis of variance. Thus, Duncan test is criticized by statisticians for being too liberal. In the analysis, means are significantly different if $p \leq 0.05$, and not significant different if $p \geq 0.05$ [218].

3.0   Preliminary Experimentations

This section outlines the preliminary experimentations exploring the conditions for the preparation of gels based on visual analysis and defining the experimental conditions to conduct extensive characterization of the gels. In this study, protein aggregation by heating without coagulation addition was selected because of its simplicity. It was decided to limit the amount of water for the dispersion of the proteins extracted from whole soybeans by producing a protein concentrated soymilk mixture.

3.1 Formation of Soymilk Gel

The first condition investigated was the ratio of soybean to water during the initial soaking of soybean. The initial points were the soybean to water ratio ranging between 1:5 and 1:11 used in traditional tofu production [219] and the conditions for inducing protein aggregation. Several publications, including the one by Wu et al. report the ability to induce the gelation by heat of 18% w/v soy protein isolate (SPI), a high protein content source which is significantly more costly than raw soybean [220]. Assuming 36% protein content in soybeans, we decided to select a ratio of soybean to water to be 1:2 v/v, *i.e.*, ~3:8 w/v. This would result in the soy protein to water ratio that is close to the 18% protein concentration of the SPI heat-induced gels reported by Wu et al. [220]. It is hypothesized that by increasing the protein concentration the proximity between the protein molecules would be increased, affording more opportunities for proteins to associate, aggregate *via* hydrophobic interactions, thereby resulting in a gel network in the absence of coagulants.

The first experiment investigated the protein gelation with the reduced water approach (soybean: water = 1:2 v/v). The experimental procedure is outlined in **Figure 3-1**. Two samples were prepared for comparison, the whole soybean dispersion (1A), *i.e.*, okara-containing soymilk, and the soymilk only (1B) (**Figure 3-1**). Gelation occurred for both samples upon heating (**Figure 3-1**), confirming that a tofu-like material could be produced without the use of coagulant. The material made with the soymilk containing okara (*1A*) appeared like a firm tofu without water syneresis (**Figure 3-1**). Although sample *1A* appeared to be crumbly, it did not crumble easily in hands or with a knife. In fact, the structure held together well. The material prepared with soymilk only (sample *1B*), showed obvious syneresis (**Figure 3-1**). The exuded water was discarded using a home-made tofu press. After 30 min of pressing, the texture of the sample

resembled a medium-firm tofu but had a coarse and porous structure (**Figure 3-1**) and the sample did not crumble easily in hands or with a knife. This suggests that the fiber of the okara in sample *1A* was capable of immobilizing water in the protein matrix, as affirmed by the study where insoluble fiber was found to stabilize the moisture phase of SPI gels [123].
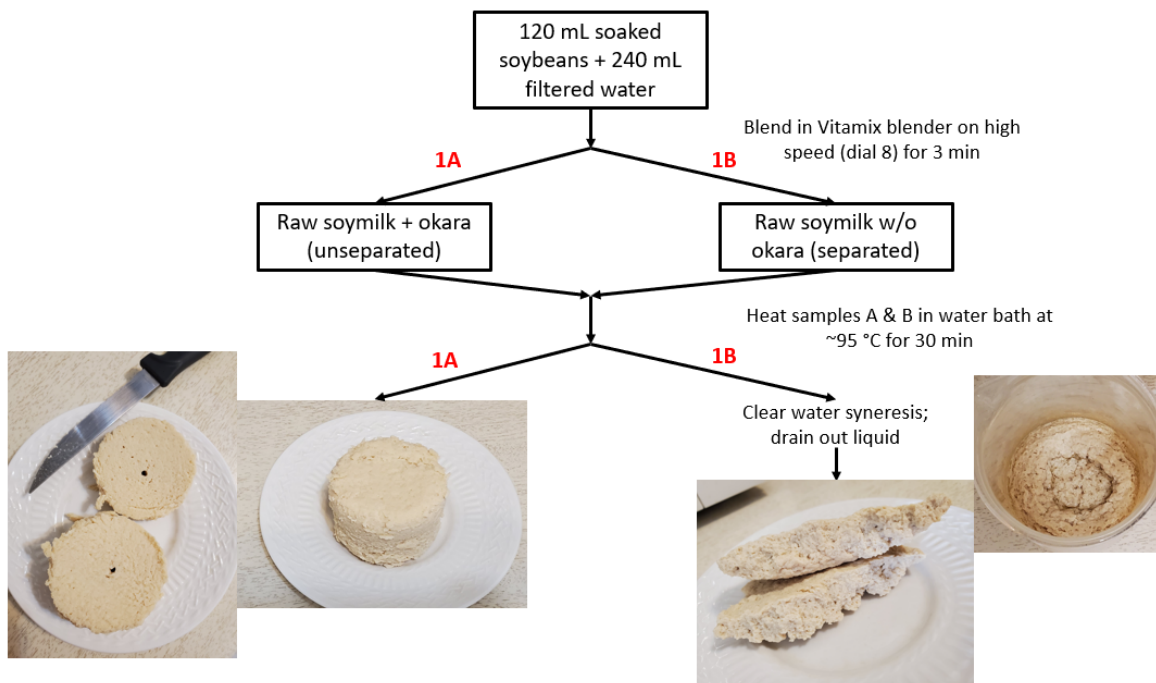
Figure 3-1 Experimental procedure of heat-induced soybean gels with (1A) and without (1B) okara.

3.2 Preparation of Soymilk Gels with Wet Okara

The second set of conditions investigated was the addition of citric acid to soymilk and the preparation of gel products with different combinations of soymilk and okara.

The methodology is detailed as follows. Dried soybeans (Nupak) of 120 mL (about 90 g) were soaked in water overnight at room temperature, and dehulled. The soybeans were ground at 1:2 v/v bean to water ratio in a high-speed commercial blender (Waring E11524) on high speed for 2 min for complete pulverization. The insoluble soybean solids (okara) were separated from the soymilk by passing through a cheese cloth bag (Scengclos, Woodridge, IL). Both the net weights of raw soymilk and wet okara were recorded to calculate the amount of wet okara in soymilk, which was 23.1% wet okara in raw soymilk by weight.

Four samples were prepared for comparison. Sample *2A* contained 60 mL raw soymilk with 10% w/v (6 g) of citric acid. The pH was measured to be 2-3 using a pH paper. Sample *2B* contained 60 mL raw soymilk only. Sample *2C* consisted of 60 mL raw soymilk with 8.22 g of wet okara, which makes 50% wet okara by weight. Sample *2D* consisted of 60 mL raw soymilk with 16.44 g of wet okara, which makes 100% wet okara by weight. All samples were placed in a water bath at 95 °C and heat-treated for 30 min to form into a gel. Afterwards, they were cooled completely at room temperature and taken out of the beaker for visual observations.

All samples formed self-supporting gels (**Figure 3-2**). Sample *2A* was barely self-standing. It could be due to the strong repulsive forces between positively charged proteins in acidic environment (pH 2-3). Sample *2B* possessed a soft texture resembling silken tofu and broke in hands easily (**Figure 3-3**). The strongest to the weakest gel based on finger press was *2D* > *2C* > *2B*. The strongest gel was heterogenous (sample *2D*) and contained the highest amount of okara (100%), suggesting that insoluble fiber of okara imparted strength and confirmed that okara indeed coarsens the gel matrix [5].

In summary:

1. The addition of 10% w/v citric acid impacted the protein phase resulted in a weakened structure (sample *2A*).
2. Soymilk gel containing the highest okara content (100% okara, sample *2D*) was stronger by touch but much coarser in structure as compared to the gel with lower okara content (50% okara, sample *2C*). This shows that okara strengthen the protein network but may hinder protein interactions negatively impacting the homogeneity of the gel.
3. The separation of okara from soymilk and its subsequent addition to soymilk enables the preparation of soymilk gels with different okara content.
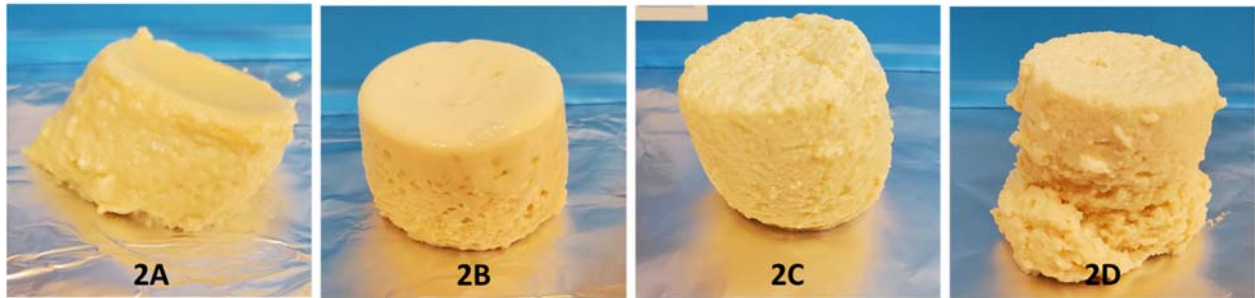
Figure 3-2 Visual appearance of self-supporting gels. From left to right are samples 2A, 2B, 2C, and 2D.
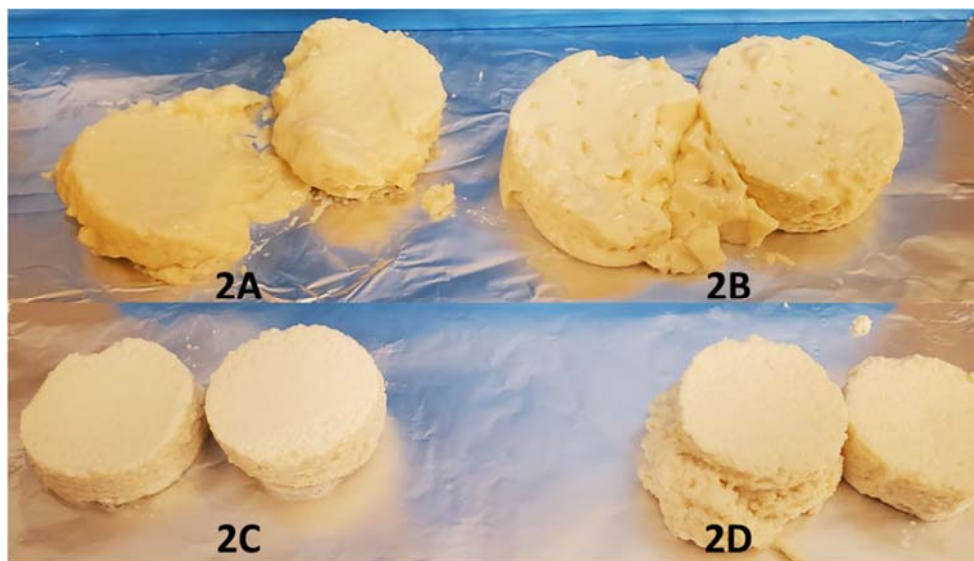
Figure 3-3 Cross-section of samples 2A (top left), 2B (top right), 2C (bottom left), and 2D (bottom right).

3.3 Preparation of Soymilk Gels with Dried Okara

The experimentation in the previous section employed okara in its wet state. In this section the okara in its dry state was investigated. Hence, a drying step was added, and soymilk gels were prepared with dried okara before heat treatment.

The preparation of soymilk and okara was the same as in the previous section (3.2). The tendency of the wet okara to cluster into a large lump was reduced by manually breaking the okara into smaller clusters to facilitate water evaporation during drying. Clusters of the wet okara were dried in a conventional oven at 110 °C for 1.5 h or until completely dried. The dried okara

clusters were ground in a coffee grinder for 1 min to obtain a powdered form (**Figure 3-4**). The mass of raw soymilk and dry okara were measured to be 313 g and 20 g, respectively, resulting a concentration of 6.4% dry okara in raw soymilk by weight.

Three different samples were prepared. Sample *3A* was 60 mL raw soymilk only. Sample *3B* consisted of 60 mL raw soymilk and 50% dry okara (1.92 g). Sample *3C* was composed of 60 mL raw soymilk and 100% dry okara (3.83 g). All samples except sample *3A* were mixed with a magnetic stirrer for 30 min on medium speed. Samples were then heated in 95 °C water bath for 30 min to induce gel formation. After heat treatment, all samples were immediately placed in a cold-water bath for about 10 min before transfer to a beaker for visual analyses.
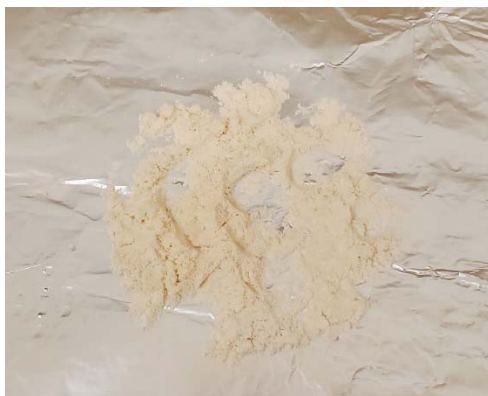
Figure 3-4 Dry okara after grinding.

All samples prepared with the dry okara appeared softer than those prepared with the wet okara (**Figure 3-5**). The sample containing only soymilk (*3A*) was softer than the one prepared previously (section 3.2). This experimental variation could be a result of a shorter cooling time. The visual analysis of the interior of sample *3C* was liquid-like while outside was set indicating that the cooling in cold water bath may probably not set completely the gel affecting the gel strength. It shows that the experimental conditions should be carefully controlled to avoid unnecessary experimental variations.

Because of the above results, gel samples with similar formulations were prepared a second time. The sample formulations were the same as previously except that samples were cooled at room temperature, instead of a cold-water, before their transfer to a beaker. The samples produced in this experiment were labelled with "*R*" denoting reproduced experimentation. All samples

formed into gels (**Figure 3-6**). By touch, the gel strength was in the order of sample ***3C-R > 3B-R > 3A-R***. These observations unveiled the following points:

1. Confirmation of the effect of the insoluble fiber of okara in imparting strength to the gel. The higher the okara content, the higher the gel strength.
2. The appearance of the gels with the dry okara was more homogeneous and less coarse when compared to gels prepared with wet okara. This could be due to the smaller particle size of the dried okara obtained by grinding (**Figure 3-4**). The removal of water during the drying of okara may also have affected its structure, such as protein components.

Based on the above observations, dry okara will be adopted moving forward for the preparation of gels with a more uniform matrix. A lower drying temperature could be considered to minimize potential effects on the okara structure.
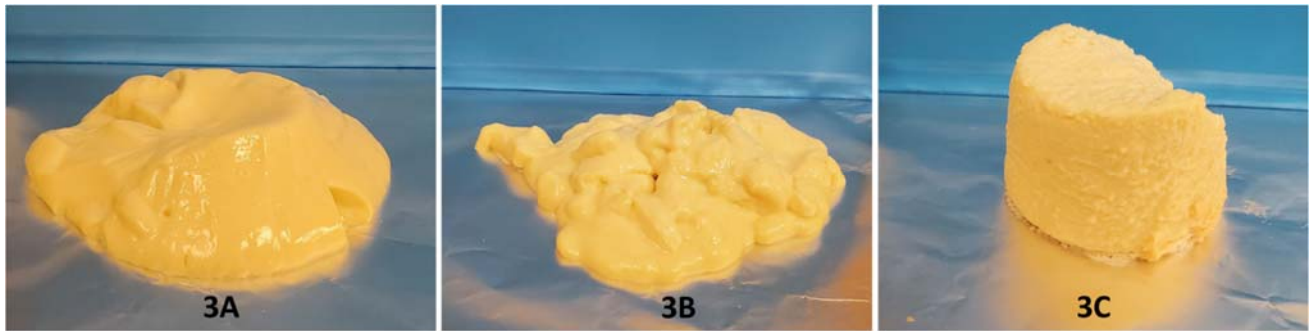
Figure 3-5 Physical appearance of samples 3A, 3B, and 3C from left to right. All samples were immediately cooled in cold water bath after heating and were not heated all the way through.

Figure 3-6 Physical appearance of replicate samples 3A-R, 3B-R, and 3C-R from left to right. Samples were cooled at room temperature. Samples were completely set.

3.4 Citric Acid Treatment of Okara

In this section, the effect of citric acid treatment on okara will be investigated by evaluating the gel strength by touch and homogeneity by visual appearance.

According to previous studies, the insoluble fiber content, hemicellulose and lignin, of okara can be hydrolyze by acid treatment [221], [222]. Acid treatment hydrolyzes the long chain polysaccharide chain to smaller saccharides which increases their solubility [218]. Esterification reactions among the citric acid, proteins, and fibers may also take place when citric acid is used [128], [129], [223], thereby promoting the compatibility of okara within the soymilk matrix.

The experimental procedure is illustrated in **Figure 3-7**. Four samples were prepared based on the methodology developed by Plazzotta et al. and Bader Ul Ain et al. [107], [221], to examined: 1) the effect of the state of okara, wet and dry, on gel formation (samples *4A* vs *4C*, *4B* vs *4D*), and 2) the effect of rinsing okara on the gel formation (*4A* vs *4B*, *4C* vs *4D*). The rinsing step was to assist in removing the excess citric acid. Specifically, after treating okara with citric acid, sample *4B* was rinsed with deionized (DI) water while sample *4A* was not rinsed. Both samples *4A* and *4B* were centrifuged to separate the insoluble components and both gel samples *4A* and *4B* were prepared with wet okara. Gel samples *4C* and *4D* were prepared with okara dried under fume hood and ground using a coffee grinder. The dried okara was then added to soymilk. Samples *4D* and *4C* were prepared with and without rinsing with DI water, respectively.

One more sample, sample *4-C* was used and denoted as the control sample, consisting of soymilk dispersion with 100% wet okara heated at 95 $^\circ$C for 40 min to form a whole soybean gel. The term 100% okara refers to the entirety of extracted okara and was added to the proportional amount of soymilk.
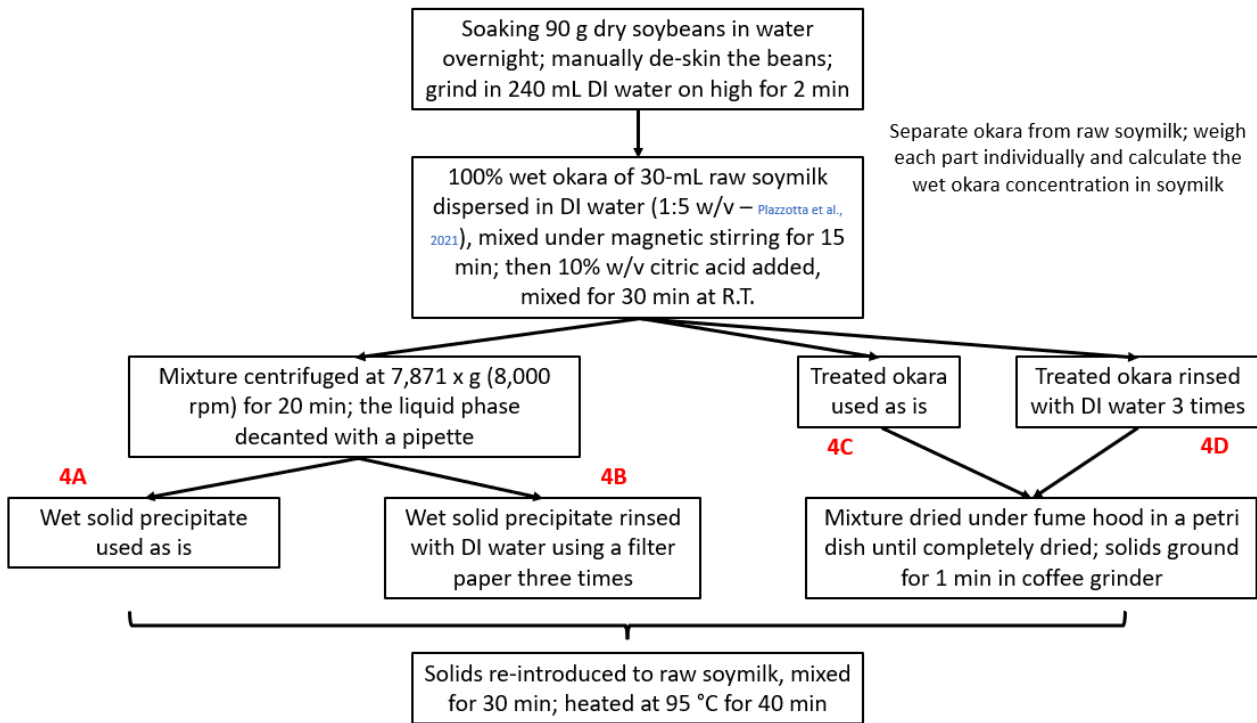
Figure 3-7 Experimental overview of samples prepared using different citric acid treatment methods.

The various phases obtained after centrifugation of the samples and the measured pH are illustrated in **Figure 3-8** and **Figure 3-9**, respectively. The control sample (*4-C*) and samples *4A* and *4B* formed into self-standing gels (**Figure 3-10**). Sample *4A* was very uniform with no visible large pores, appeared much smoother than the control sample, no syneresis was visible but was very fragile and could easily be broken with minimum finger force (**Figure 3-11**). On the other hand, sample *4B* had a crumbly structure with larger pores, showed significant water syneresis (~3.9 g of released water weight) and formed into a stronger gel as compared to the control sample by touch (**Figure 3-11**). The reason could be because of the large amount of gas bubbles generated by the high-speed stirring (**Figure 3-9**). Therefore, a degassing method or a lower stirring speed should be considered to reduce the effect of gas bubble on the creation of pores in the gel.

These observations demonstrate the following points:

1. The washing of okara prior to its addition to the soymilk had a significant effect on the gel formation. The pH of the soymilk with the unwashed okara was notably lower

compared to the washed okara sample. The soymilk gel prepared with unwashed okara was homogeneous, but had significantly weaker strength as compared to the gel with washed okara. It could be due to the increased repulsive force between the protein molecules at a lower pH, resulting in a weaker gel, as observed previously (**Figure 3-2**). The gel prepared with the washed okara had large pores and severe water syneresis.

2. A degassing method or a lower mixing speed should be employed, and the foaming effect accompanied by stirring on the pore size of the gels should be investigated.
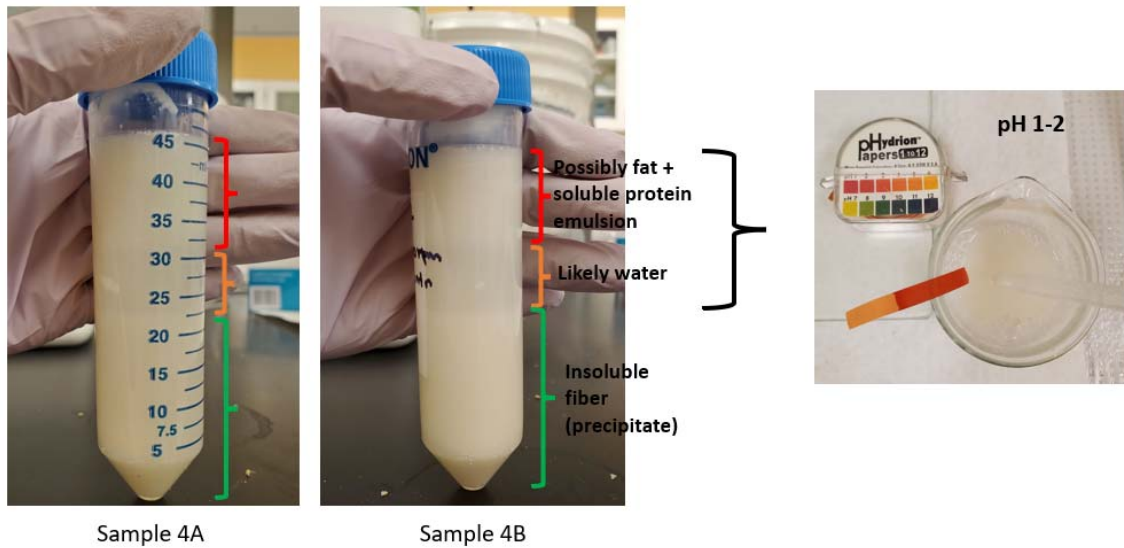
Figure 3-8 Phase separation observed after centrifugation of samples 4A and 4B and their measured pH.

Figure 3-9 pH of control sample, 4-C (left, 100% wet okara added to soymilk), and samples 4A (middle, labelled as 1) and 4B (right, labelled as 2), prior to heat treatment. Heavy foam was noted on top of sample 4B, which could have attributed to the gel's large pore size.
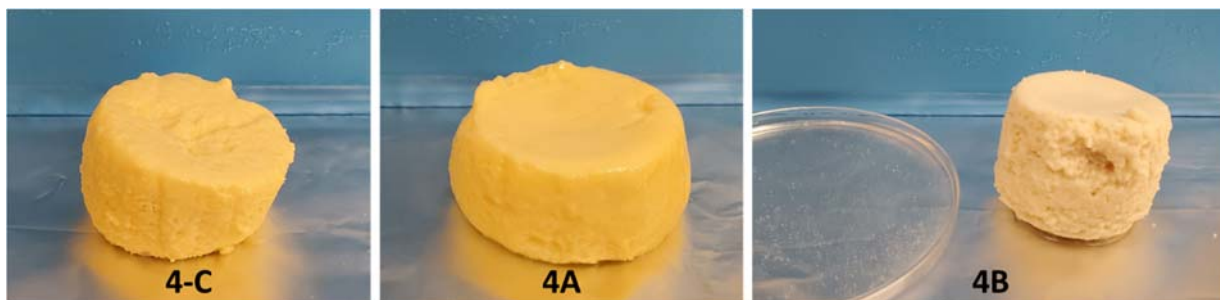
Figure 3-10 Control sample (4-C), sample 4A and 4B. Sample 4B had clear syneresis of water (3.9 g of water released).

Figure 3-11 Cross-section of control sample (4-C), samples 4A (unwashed) and 4B (washed).

The okara in samples *4C* and *4D* was dried in a fume hood for two days (**Figure 3-12**). The dried okara and citric acid mixture formed into a polymer-like "membrane" in sample *4C* that possessed an elastic texture as in "fruit rolls" (**Figure 3-13**). One can envision that the insoluble fibers of the okara with citric acid treatment may have been partially converted to soluble fibers. At acidic pH (pH 2-3), most soluble fiber should be protonated and reduce the repulsive forces among the negatively charged soluble fiber such that as to assemble and form into a gel network, similar as the mechanism in the making of fruit rolls.

In contrast, the okara of sample *4D* had formed into hard crystal-like material (**Figure 3-13**). This can likely be attributed to the water rinsing which removed some soluble fibers generated by the citric acid treatment, and thereby only the insoluble fibers remained. Hence, unlike the elastic gel-like material formed for the okara without rinsing (sample *4C*), hard crystal-like solids were consequently produced with the washing step (sample *4D*).

After heat treatment, both samples *4C* and *4D* formed into gels (**Figure 3-14**). Sample *4C* formed into a cohesive gel without water syneresis. Sample *4D* possessed large pores accompanied with some water syneresis (**Figure 3-15**). Preliminary mechanical test of samples

4C and *4D* (data not shown) showed that sample *4D* had doubled the fracture stress as that of sample *4C*, as ascribed to the washing step. This could be due to the high mechanical force of the remaining insoluble fiber content.

These observations demonstrated the following points:

1. Gels formed with washed okara (samples *4B* and *4D*) had large pores where there was also water syneresis. Comparatively, water syneresis was not observed with all other okara-containing gels (samples *4A* and *4C*). These observations could reflect the removal of the soluble fiber by the water washing such that the washed okara contains primarily insoluble fibers, which is known to have poor compatibility with the protein matrices [5].
2. Although the washed okara resulted in a coarse soymilk okara gel with syneresis, the strength of the gel was higher than that of the unwashed-okara soymilk gel. This is likely due to the high mechanical strength of the insoluble fiber imparted to the overall gel network.
3. The soymilk gels prepared with dried okara (sample *4C* and *4D*) had higher gel strength by touch as compared to the gels prepared with wet okara (sample *4A* and *4B*). The reason could be due to the excess water present in the wet okara which reduces the protein concentration of the mixture producing a weaker gel.
4. Soymilk gels prepared with unwashed, citric-acid-treated okara (samples *4A* and *4C*) appeared to be more homogenous and cohesive in comparison to the soymilk gel prepared with 100% untreated wet okara, indicating an improved compatibility of acid-treated okara with the protein matrix. This shows that the citric acid treatment can be a promising technique to employ for the modification of the okara.

Figure 3-12 Visual observation of citric acid treated okara dispersion, samples 4C (unwashed, left) and 4D (washed, right), prior to drying.
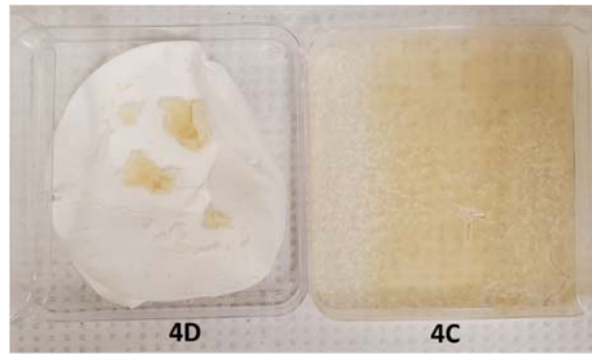
Figure 3-13 Visual observation of sample 4C (unwashed) and 4D (washed), dried under fume hood. Okara Dried sample 4C (right) illustrated a membrane-like, elastic texture. Dried sample 4D (left) became hard "crystals" that were small in quantity after drying.
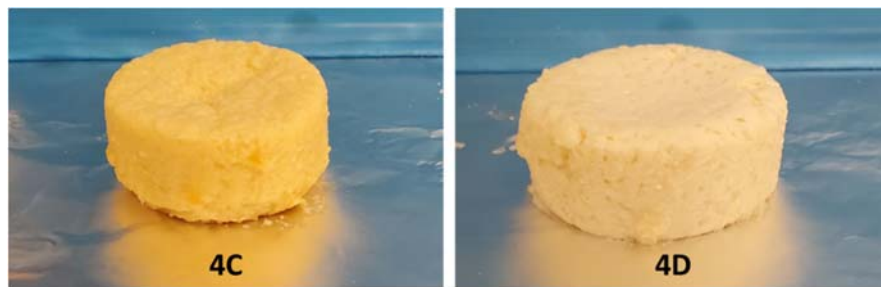
Figure 3-14 Visual appearance of sample 4C (left) and 4D (right) after gelling with soymilk under heat treatment at 95 ^{o}C for 40 min.
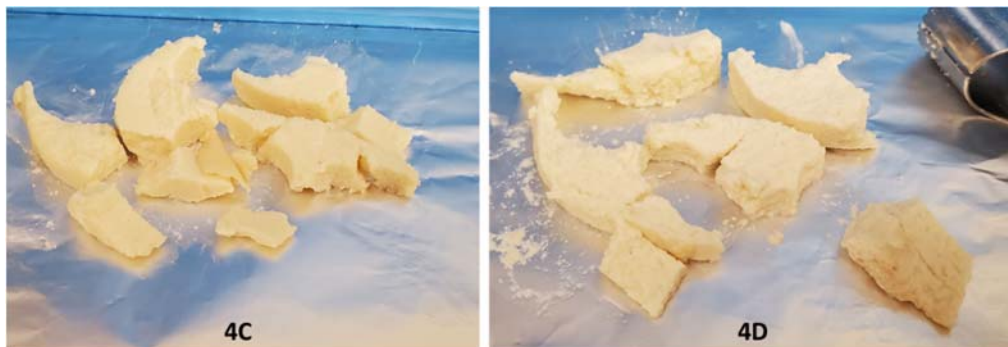
Figure 3-15 Cross-section of destructed sample 4C (left) and 4D (right). Sample 4C was more homogenous with small pores. Sample 4D had larger pores with some water syneresis.

3.5 Okara Washing *via* Gravitational Filtration

In this section, the solid content of the washed and unwashed okara samples is reported as a follow-up experiment to the observations presented in section 3.4 which helps investigate the change in soluble and insoluble solids of okara upon citric acid treatment.

We hypothesize that citric acid could hydrolyze insoluble fibers and convert them into soluble fibers. Consequently, the washing step may lead to the removal of most soluble fibers which should be recoverable in the washing liquids. Thus, the objective in this section was to examine whether soluble solids are present in the washing liquid *via* drying.

In this experiment, three sets of samples were investigated. Set 1 contained wet okara (denoted as **5-1**). Set 2 contained citric acid treated wet okara (denoted as **5-2**). Set 3 consisted of citric acid and heat treated wet okara (denoted as **5-3**). Each set included unwashed okara (denoted as "**A**") and washed okara (denoted as "**B**") performed according to section 3.4. The method for sample preparation was the same as described previously (section 3.4) and is illustrated in **Figure 3-16**. For sample sets **5-2** and **5-3**, the okara dispersion was prepared with 1:5 w/w wet okara in DI water, with 10% w/w citric acid and 30 min magnetic stirring at room temperature. For sample set **5-3**, an additional heat treatment was performed on the okara dispersion at 100 °C for 1 h, to examine the effect of heat on okara.

The washing step was based on gravitational filtration as illustrated in **Figure 3-17**. A filter paper (Whatman #1, Cat No 1001 090) was placed in the funnel to collect the insoluble solids. The washing liquid collected on the bottom of the flask had a milky colour. After treatment, all samples were dried under fume hood. The dried solid collected on top of the filter was denoted as "**DS**" while the dried solid collected in the washing liquid was denoted as "**DSWL**". Samples **5-1A**, **5-2A** and **5-3A** were dried for two days, while samples **5-2B (DS)** and **5-3B (DS)** took three days to completely dry, and the remaining samples took up to one week to dry completely. The weight of the insoluble and soluble fractions is presented in **Table 3-1**.
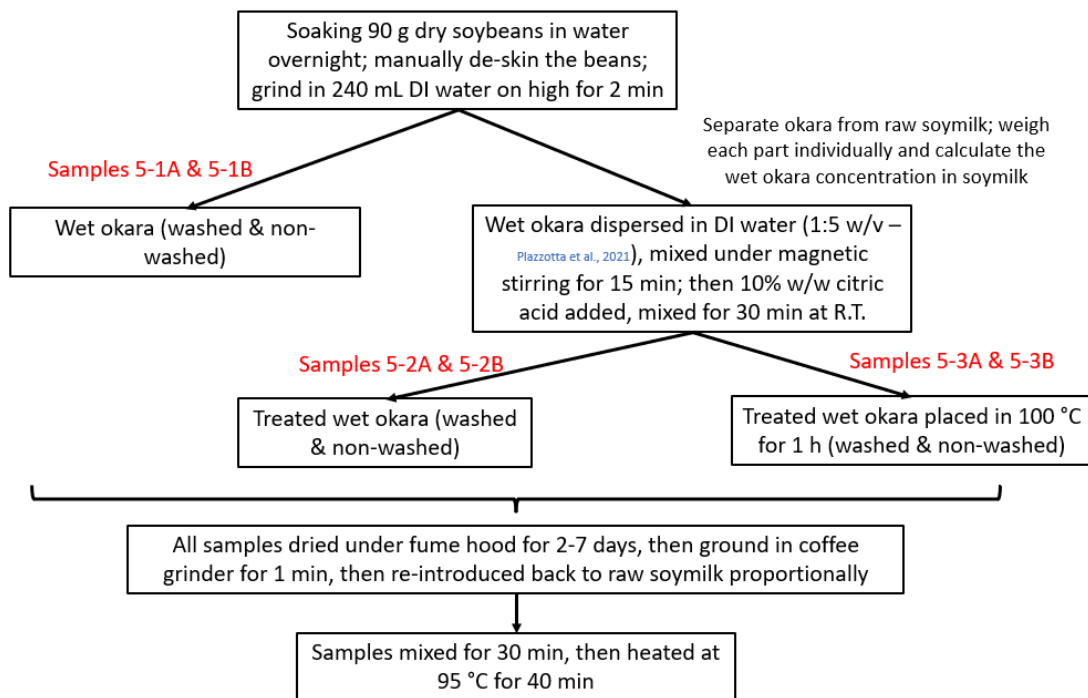
Figure 3-16 Flow chart of experimental procedure for the analysis of the solids content during the washing of okara.

Figure 3-17 Gravitational filtration set-up for the washing of the okara. A filter (Whatman #1) was used with the funnel to collect insoluble solids, and the washing liquids was later dried to collect the soluble solids.

Upon the citric acid treatment, the quantity of recovered solids in the washing liquid increased significantly, based on the differences in weights of samples **5-1B** and **5-2B** (**Table 3-1**). With the additional heat treatment, the quantity of solids in the washing liquid (**DSWL**) increased further, which was accompanied with a decreased solid quantity on the filter paper (**DS**). This analysis indicates that insoluble fibers of okara was converted to soluble fibers upon both the citric acid treatment and the additional heat treatment.

Table 3-1 Solids content for three sets of okara samples with and without subsequent washing.

Sample	Wash	Mass (g)							
		Wet okara	Water for dispersion	Citric acid	Total dispersion before drying	Water for washing	Total washing liquid (WL)	Dried solids on filter (DS)	Dried solids in washing liquid (DSWL)
5-1	A	10	-	-	-	-	-	2.4	-
	B	10	-	-	-	40	17.9	2.0	0.2
5-2	A	10	50	6	64.7	-	-	8.6	-
	B	10	50	6	-	20	49.0	4.2	4.3
5-3	A	10	50	6	62.1	-	-	8.8	-
	B	10	50	6	-	20	49.8	2.9	5.7

A: non-washed; B: washed

The solids content of the okara samples without washing **5-1A**, **5-2A** and **5-3A**, exhibited distinct characteristics after drying (**Figure 3-18**). Sample **5-1A** was the dried okara. Samples **5-2A** and **5-3A** were both treated with citric acid, with sample **5-3** subjected to additional heat treatment at 100 °C for 1 h. Both **5-2A** and **5-3A** formed an elastic material with high strength. The dried solids of okara with additional heating (sample **5-3A**) had a more continuous "membrane"-like network, whereas the one without additional heat treatment (sample **5-2A**) showed discontinuities in the elastic network. This indicates the higher conversion of insoluble to soluble solids with the additional heat treatment. This is supported by the larger mass of dried solids recovered in the washing liquid of sample **5-3B** as compared to sample **5-2B**.

The solids remaining on the filter paper (**DS**) for samples **5-1B** and **5-2B** formed small clusters (**Figure 3-18**). Sample **5-1B** was crumblier, while sample **5-2B** was harder. For sample **5-3B**, an elastic network adhering to the filter paper was present (**Figure 3-19**). It could relate to residual soluble solids that were larger than the pore size of the filter paper and thus were left behind.

This supports the effect of the additional 1-h heat treatment in facilitating the hydrolysis of the insoluble fiber into soluble fiber.

The solids of the washing liquid (*DSWL*) produced a thin layer on the petri dish for all three samples (**Figure 3-18**). A very small quantity (~0.16 g) of light, flaky, brittle, and thin material was left in sample *5-1B*. It is likely to be the dried soy protein particles since no treatment was performed. A thicker layer of material that formed an elastic film was observed for samples *5-2B* and *5-3B*.
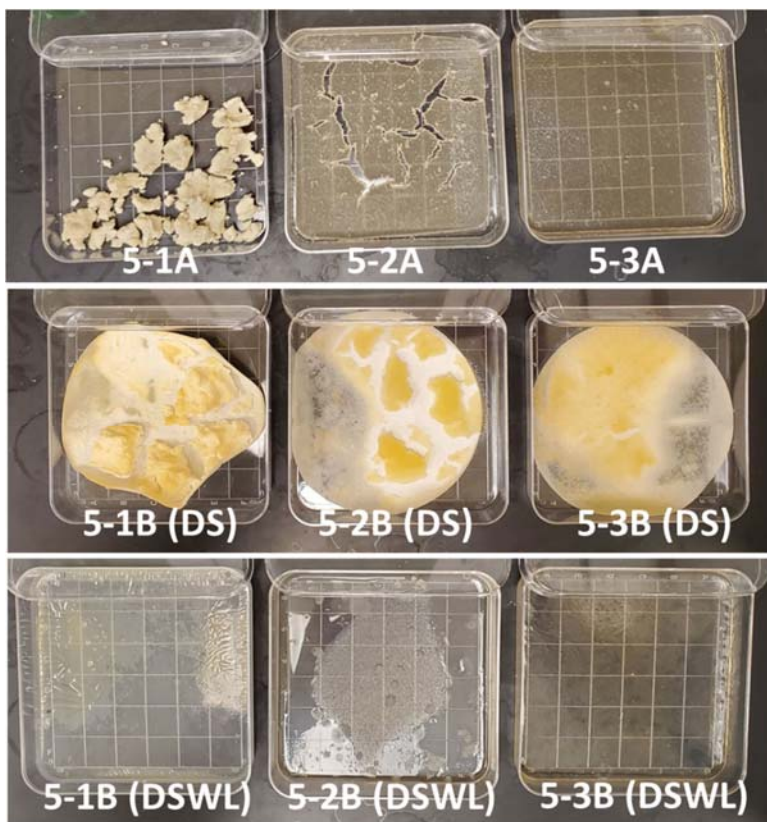
Figure 3-18 Dried solids of (5-1) untreated okara, (5-2) citric-acid treated okara, and (5-3) citric-acid and heat treated okara. Letter "A" denotes unwashed samples, and letter "B" denotes washed samples.

Figure 3-19 Closeup image of sample 5-3B (DS) (washed, solids on filter). A unique sample where the solids on filter paper resembled an elastic membrane, indicating its major composition of soluble polysaccharides.

Soymilk gels were prepared with the dried okara solids ground in a coffee grinder for 1 min (100% wet okara proportionally). The okara-soymilk mixtures were heated at 95 °C for 40 min. Samples were allowed to cool down at room temperature prior to visual analysis.

Soymilk gels with dried untreated okara consist of sample **5-1A** and **5-1B (DS)** where sample **5-1B was** washed, and the remaining solids collected on the filter paper were used to form **5-1B (DS)**. The amount of solids in the washing liquids for **5-1B (DSWL)** was insufficient to form a gel. The visual analysis of the gels prepared with sample **5-1A** and **5-1B (DS)** had coarse appearance with large pores (**Figure 3-20**).

The citric acid treated okara soymilk gels include sample **5-2B (DS)** and **5-3B (DS)**, with an additional heat treatment performed with sample **5-3B**. Sample **5-2B (DS)** was extremely crumbly, had enlarged pores and could easily crumble (**Figure 3-21**), which is indicative of a weak gel behaviour. This observation confirmed previous observation (**Figure 3-11**), where the washed okara sample was more porous than unwashed sample. Sample **5-3B (DS)** on the other hand, was not crumbly but severe water syneresis was observed, showing its poor ability to retain water. Overall, samples **5-2B (DS)** and **5-3B (DS)** both had very weak gel strength in comparison to samples **5-1A** and **5-1B (DS)**. These observations again suggest that the additional heat treatment hydrolyzed the okara structure to a greater extent than using only citric acid.
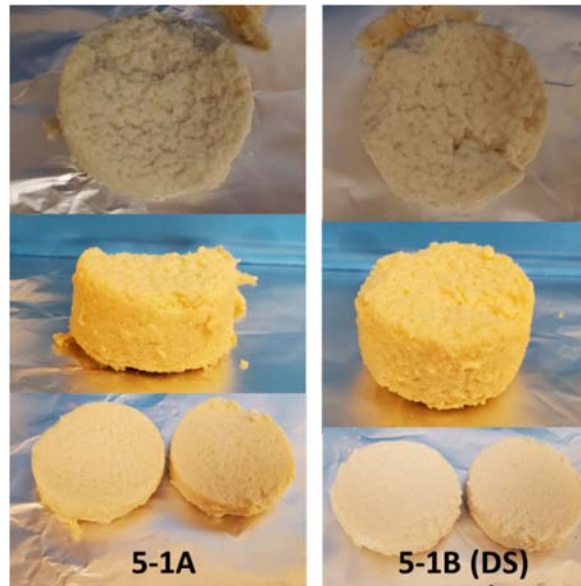
Figure 3-20 Visual observation of samples 5-1A and 5-1B (DS). Both samples used untreated dried okara, except sample 5-1B was washed. Their structure and strength were very similar. The dried washing liquid 5-1B (DSWL) was very small in quantity and thereby cannot be formed into a gel.
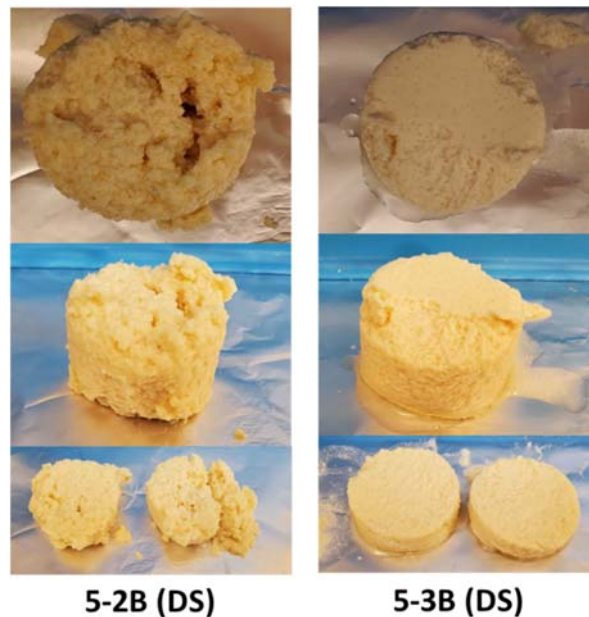
Figure 3-21 Visual observations of samples 5-2B (DS) and 5-3B (DS). Sample 5-2B (DS) was crumbly. Sample 5-3B (DS) had severe water syneresis. Both gels were much weaker in gel strength compared to sample 5-1A and 5-1B (DS).

The soymilk gels prepared with the unwashed, citric acid treated okara, samples *5-2A* and *5-3A,* formed more cohesive gels as compared to *5-2B (DS)* and *5-3B (DS)* (**Figure 3-22**). No water syneresis was observed for samples *5-2A* and *5-3A*, but their gel strength was rather weak. Sample *5-3A* was even softer than sample *5-2A*. This suggests that the higher conversion of insoluble to soluble fibers was prompted by the additional heat treatment, and because soluble fibers possess weaker strength than insoluble fiber, the final gel strength was impeded.
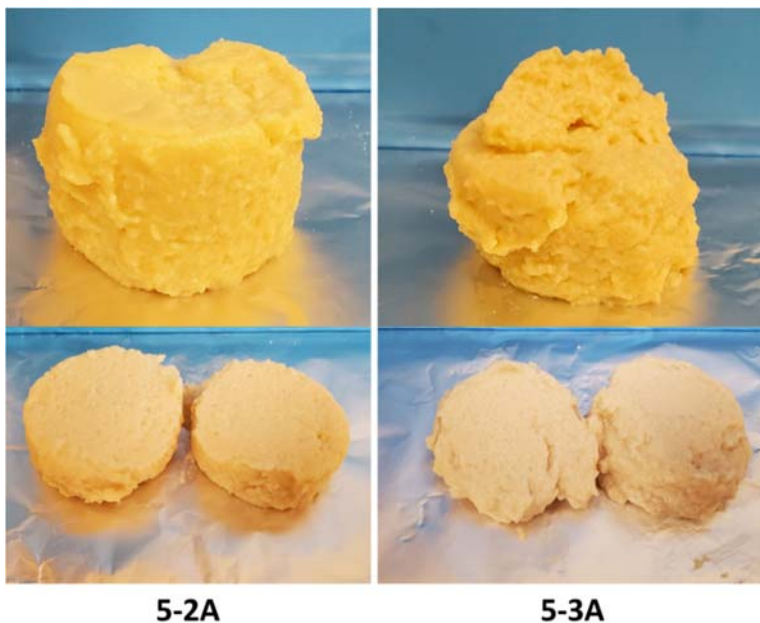
Figure 3-22 Visual observation of samples 5-2A and 5-3A.

The solids remained in the washing liquid (*DSWL*) for samples *5-2B* and *5-3B* were thin and brittle (image not shown). However, before these *DSWL* solids were completely dried, they were very sticky with a glue-like consistency (**Figure 3-18**). The soymilk gels formed with these *DSWL* solids of the citric acid treated okara, *i.e.*, sample *5-2B (DSWL)*, was unexpectedly smooth and cohesive with almost invisible pores (**Figure 3-23**). These observations highlight distinctive differences between the solids recovered on the filter paper (*DS*) and the solids in the washing liquid (*DSWL*), which could be the result of differences in molecular weight of soluble solids of okara upon citric acid hydrolysis. Sample *5-3B (DSWL)* had a weak strength and porous structure and did not form into a cohesive gel. This demonstrates the negative effect of the additional heat treatment.
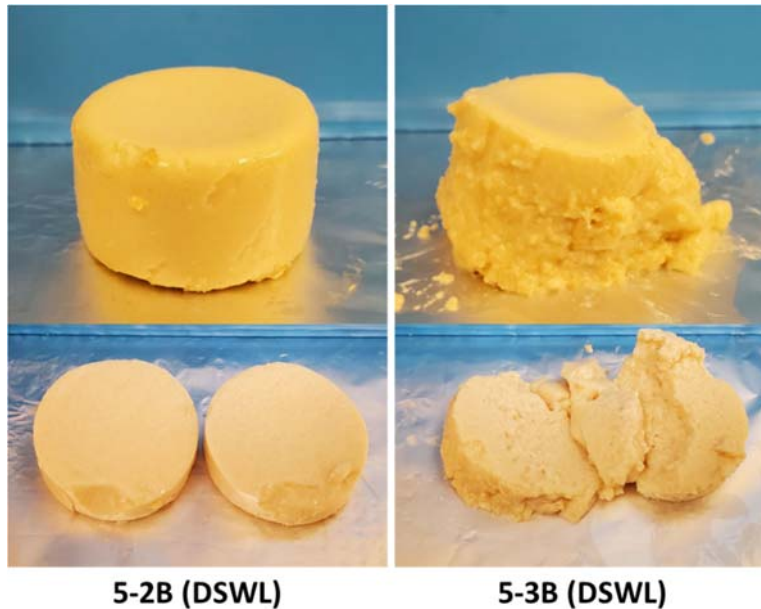
5-2B (DSWL)   5-3B (DSWL)

Figure 3-23 Visual observation of samples 5-2B (DSWL) and 5-3B (DSWL).

3.6 Okara Washing *via* Gravitational Filtration (Part II)

The same experiment conducted in section 3.5 was repeated in order to assess the experimental reproducibility, particularly for the gels prepared with and without the additional heat treatment (section 3.5, sets *5-2* and *5-3*). Minor changes of the experimental conditions were adopted, including the heat treatment of okara and increasing the duration of the additional heat treatment to citric acid treated okara to 2 h.

Four samples were prepared as follows. Set *6-1*: wet okara treated with heat at 100 °C for 1 h. Set **6-2**: wet okara treated with 3:5 w/w citric acid to okara (~10% w/w citric acid). Set **6-3**: wet okara treated with 10% w/w citric acid, then heat-treated at 100 °C for 1 h. Sample **6-4** (only washed): wet okara treated with 10% w/w citric acid, then heat-treated at 100 °C for 2 h. Two conditions were used for sets *1-3* as described previously: without washing (denoted by "*A*") and with washing (denoted by "*B*"). The mass of the four sets of samples is illustrated in **Table 3-2**, and is similar to mass reported for the previous set of experiments (**Table 3-1**). The increased duration of the additional heating (sample *6-4*) did not lead to increased dried solid content in the washing liquid.

Table 3-2 Solids content for three sets of okara samples with and without subsequent washing (replicated experiments).

Sample	Wash	Recorded weights (g)							
		Wet okara used	Water for dispers.	Citric acid added	Total dispers. before drying	Water used for washing	Total washing liquid (WL)	Dried solids on filter (DS)	Dried solids in washing liquid (DSWL)
6-1	A	5	25	-	25.2	-	-	1.3	-
	B	5	25	-	-	20	26.7	0.8	0.4
6-2	A	5	25	3	32.0	-	-	4.4	-
	B	5	25	3	-	20	32.1	1.1	2.6
6-3	A	5	25	3	28.2	-	-	4.5	-
	B	5	25	3	-	20	26.7	2.1	2.1
6-4	B	5	25	3	-	20	17.9	2.3	1.6

A: without washing; B: washing

Soymilk gels prepared with the heat-treated okara (*6-1A*) was stronger and more homogeneous as compared to the soymilk gel with untreated wet okara (100%) (control sample *6-C,* **Figure 3-24**). This suggests that treating okara with only heat is worthwhile for further investigation as a technique to improve gel properties.

Samples *6-2A*, *6-3A*, *6-2B (DSWL)*, *6-3B (DSWL)*, and *6-4B (DSWL)* all formed into gels. Samples *6-2A* and *6-3A* with unwashed okara formed self-standing gels but spread upon hand pressing rather than fracture, which indicated a weak gel behaviour (**Figure 3-25**). In contrast, the soymilk gel prepared with okara treated by citric acid and additional 1-h heating (sample *6-3A*) was stronger by touch than sample *6-2A*.

The soymilk gels prepared with the solids of the washing liquid, *i.e.*, samples *6-2B (DSWL)*, *6-3B (DSWL)*, and *6-4B (DSWL)*, had clear fracture upon hand pressing, suggesting a stronger gel behaviour and there was no significant difference in gel strength and appearance (**Figure 3-26**). The soymilk gel with okara citric acid treatment only, sample *6-2B (DSWL)*, had the highest gel strength by touch, the smallest pore size, and the most homogeneous appearance. The soymilk gel prepared with okara citric acid treatment and additional heat (sample *6-3B, DSWL*) and with the extended 2-h heating duration (sample *6-4B, DSWL*) caused slight decrease in gel strength while an increase in the quantity and size of the pores (**Figure 3-26**). This observation supports

the effect of the additional heat treatment in weakening the gel strength and negatively impact the structure when using the solids from the washing liquid.

When comparing the four treatments, sample **6-2B (DSWL)** was the most homogeneous and sample **6-1A** was more homogeneous than samples **6-3B (DSWL)** and **6-4B (DSWL)**. In terms of gel strength, soymilk gel with citric acid treated okara appeared to be stronger, however, the difference was not significant with hand pressing alone.

The findings in this section suggest that the citric acid treatment with or without the additional heat treatment had significant influence on okara, and the results are reproducible.

Figure 3-24 Physical appearance of control sample (6-C) (100% wet, untreated okara) and sample 6-1A (heat-treated okara). Sample 6-1A was significantly more homogeneous and had higher gel strength.
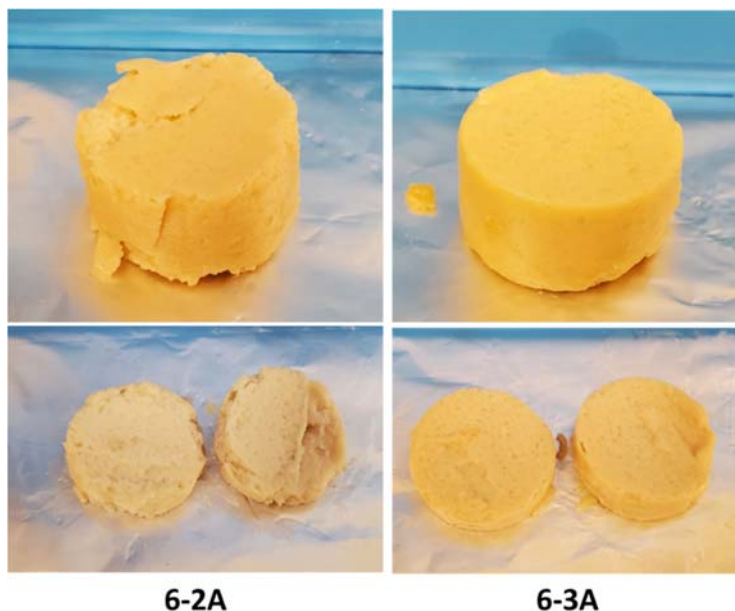
Figure 3-25 Physical appearance of samples 6-2A (citric acid treated okara) and 6-3A (citric acid and heat treated okara). Sample 6-3A was significantly stronger by touch compared to sample 6-2A.
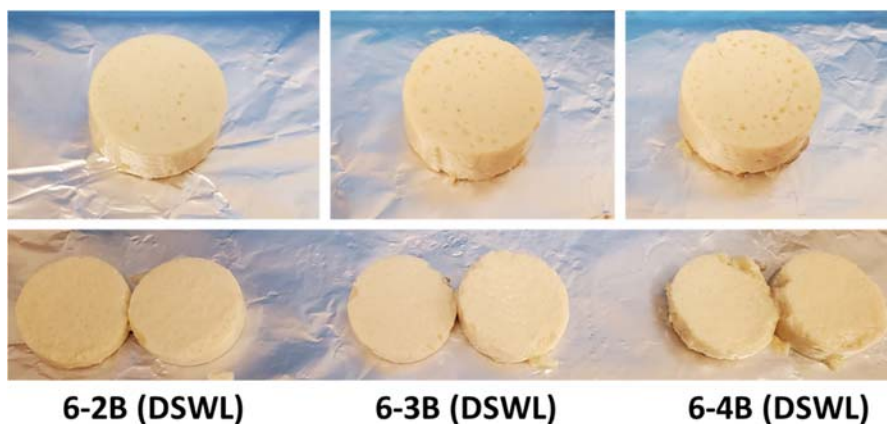
Figure 3-26 Physical appearance of sample 6-2B (DSWL), 6-3B (DSWL), and 6-4B (DSWL). Similar gel structure observed. Sample 6-2B (DSWL) was slightly stronger and more uniform.

3.7 Okara Washing *via* Ultracentrifugation

The recovery of the okara solids present in the washing liquid *via* gravitational filtration was not efficient because samples were gelatinous and viscous in nature. Filtration by gravity was time consuming because of pore blockages on the filtration paper. Other methods for the recovery of

the soluble and insoluble solids from viscous mixtures were considered, and ultracentrifugation was deemed as an efficient separation technique as it offers high centrifugal forces. In this section, the feasibility of ultracentrifugation for the separation of insoluble and soluble fibers upon citric acid treatment of okara is reported.

The okara was treated only with citric acid using the procedure described previously (sections 3.5 and 3.6). Briefly, 10 g wet okara was dispersed in 50 g DI water and mixed for 10 min for an even mixing. Then, 6 g of citric acid was added to the okara dispersed and mixed again for another 30 min. Afterwards, the okara dispersion (12 mL) was transferred into a centrifuge tube (13.2 mL) using a pipette. The dispersion was centrifuged in an ultracentrifuge (Beckman Coulter XPN-100) using the swinging bucket as the rotor. The speed was set to 30,000 rpm for a duration of 30 min. This duration was chosen to account for the acceleration and deceleration time. The temperature was set at 4 °C in case overheating takes place during the high-speed centrifuging process.

Upon centrifugation, a clear 3-phase separation was observed (**Figure 3-27**). The top-most layer was likely consisted of lipids (**Figure 3-27** B & C), which was thin and light and could be removed with a spatula. The middle layer was transparent, having a strong acidic smell, which was likely consisted of water and excess citric acid. While the bottom-most layer was opaque in colour and was most likely composed of the insoluble okara fiber. At the separation between the pellet and the liquid, a thin layer of opaque solids was floating (**Figure 3-27** A). This lighter solid layer may be the smaller molecular weight polysaccharides resulted from acid hydrolysis. However, it was difficult for this lighter solid layer to be separated from the pellet.
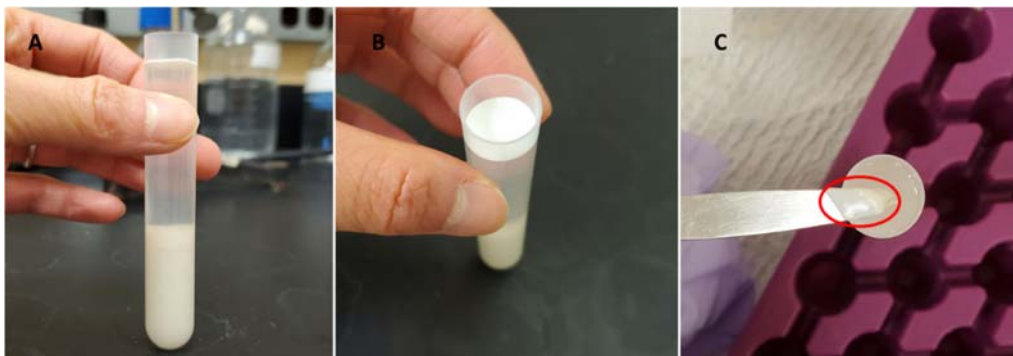
Figure 3-27 Phase separation of citric acid treated okara dispersion upon ultracentrifugation. (A) side view and (B) top view, (C) thin oil layer sitting on top of the centrifuged mixture.

Each layer was collected, placed in a Petri dish and dried under fume hood. The insoluble and soluble components of okara was related to the different layers of the ultracentrifuged okara dispersion. The pellet, representing the insoluble solids, was about 1.6 g, (~57%), and the liquid layer, representing the soluble solids, was about 1.2 g (~43%).

The appearance of the dried solids for each ultracentrifugation layer was similar to the appearance of the corresponding fractions obtained by the gravitational filtration (**Figure 3-28**). The solid in the insoluble fraction was discontinuous and fibrous, which could be comprised of large polysaccharides, such as cellulose, hemicellulose, lignin, that were not readily hydrolyzed by citric acid treatment. The dried solids of the liquid layer were initially sticky and glue-like and became flaky after complete drying (**Figure 3-29**) which resembles the physical appearance of the dried solids from the washing liquid obtained by gravitational filtration.
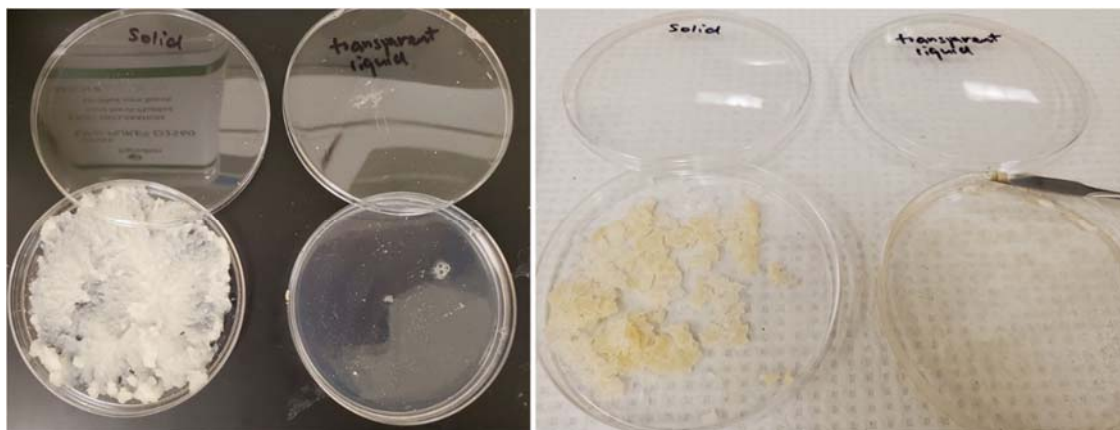
Figure 3-28 Appearance of the various layers obtained during the ultracentrifugation of citric acid treated okara: Before (left) and after (right) drying.

Figure 3-29 Appearance of the dried solids present in the liquid layer generated during the ultracentrifugation of citric acid treated okara. Clear sticky flakes.

3.8 Summary of Results and the Next Steps

Firstly, by reducing the amount of water used for the grinding step of the soybeans (soybean:water = 3.8 w/v), the proximity of proteins was forced to increase to produce a gel-like network without the need to use coagulants. Secondly, it was found that by adding dried okara back to the soymilk, the gel produced was more homogeneous in structure, compared to the one with wet okara. Finally, the preliminary results suggest that citric acid treatment was a suitable method to modify the okara for its improved compatibility with the soy protein matrix. Thereby, in the finalized work, we will adopt the reduced water approach with the use of dried okara. One of the treatments will involve the use of citric acid, accompanied by ultracentrifugation for the extraction of different fractions. We will also consider the heat treatment of okara to examine whether heating has any significant effect on the functional properties of okara and the okara-containing soymilk gels. Lastly, we will investigate the combination treatment of heating and citric acid to evaluate its effect.

4.0 Manuscript 1 Improvement of Compatibility and Homogeneity of Soymilk Gel Containing Okara *via* Citric Acid Modification

4.1 Synopsis

The purpose of this manuscript was to investigate the treatment of soy okara with citric acid to improve its compatibility with the soy protein matrix. The finding unveils the potential in creating high-fiber tofu product in efforts to enhance its nutritional value and minimize waste.

This manuscript was submitted to Food Hydrocolloids and is currently under review.

Improvement of Compatibility and Homogeneity of Soymilk Gel Containing Okara *via* Citric Acid Modification

Overview

The treatment of okara with citric acid, heat, or both combined was investigated to improve the homogeneity and physicochemical properties of soymilk gels containing okara. The thermal stability of okara subjected to heat (95 °C for 1 h), examined by TGA, was similar to untreated okara but reduced when okara was treated with citric acid (3:5 w/w citric acid:okara) with or without subsequent heating. The functional groups of okara, identified by FTIR, remained similar upon okara heat treatment, while the citric acid treatment of okara resulted in a significant increase in esterified carboxyl groups for the insoluble fraction of okara, indicating the presence of esterification between hydroxyl groups of hemicellulose, cellulose, and lignin of okara and carboxylic groups of citric acid or of protein side chains. Okara-containing soymilk gels were prepared and characterized. The Young's modulus was highest for soymilk gels containing citric-acid-modified okara compared to the untreated okara gel and was similar or decreased for gels containing okara subjected to heat treatment. The storage and loss moduli of the soymilk gels were lower for all okara treatments except the combination citric acid heat treatment compared to the gel with untreated okara. Gels containing untreated okara impacted protein aggregation, resulting in a coarse structure. In contrast, gels containing citric-acid-treated okara exhibited a substantially more uniform and continuous protein network. The present study demonstrates the potential of citric acid treatment of okara in creating a homogeneous high-fiber tofu like product in efforts to enhance its nutritional value and minimize processing waste.

Keywords: okara fiber, soymilk gel, citric acid, heat, interaction, microstructure

1. Introduction

Tofu, also known as the soybean curd, has increasingly attracted more consumers especially in recent years due to its plant-based origin, high protein content (~8%), low saturated-fat (~0.7%) and minimal cholesterol content. In conventional tofu production, soybeans, either dehulled or hull-on, are soaked, ground, then filtered to recover and separate the soluble content, soymilk,

from the insoluble residue, okara. The soymilk is gelled to produce pressed or packed tofu [46]. The former involves pressing of the curd to remove excess water, whereas the latter is made without breaking the curd and it typically contains a higher moisture content [46], [95]. The structure of the tofu and the efficiency of protein extraction are affected by the bean to water ratio selected for the grinding step. The typical water to bean ratio is 5-11:1 and 9:1 is considered as the ideal ratio to create the most uniform tofu structure [219]. The conventional tofu production typically involves coagulants to facilitate protein aggregation *via* hydrophobic and electrostatic interactions, as well as hydrogen and disulfide bonds [224].

Okara is the major byproduct of tofu production, averaging about 1.4 kilograms of okara per kilogram of dry soybean, containing ~85% water [6]. It is then burnt or disposed in landfills as waste, or simply used as animal feed [3], [225]. There has been rising interest in incorporating okara into foods because of its high dietary fiber and bioactive constituents, as well as its antioxidant activity [103]. Dry okara contains 40-60% dietary fiber, which are mostly insoluble fibers such as cellulose and hemicellulose, some pectin and lignin [108], 15-30% protein, 8-12% fat and 3% ash [226]. Its composition varies depending on the water used for soaking and pulverization steps, soybean cultivar type, and production methods [104]. Furthermore, okara fibers are irregularly shaped, having cellulose-hemicellulose frames embedded in the amorphous matrices of pectic substances [6].

Recent attention has focused on okara-containing tofu, also referred to as whole soybean curd [4], [5]. Okara tofu is made by either using the whole okara [9], or a fraction of the okara combined with soymilk with subsequent coagulation [5], [119]. Thermal treatment can be used to induce protein coagulation and curd formation where the hydrophobic interior of protein molecules unfolds, leading to self-association or aggregation [227]. Environmental conditions such as pH, ionic strength, and heating conditions can facilitate the formation of stranded-aggregate or particulate-aggregate networks for globular soy proteins [96], [228]. The production of whole soybean curd can be difficult because of the large particle size of the insoluble components of the okara fiber, resulting in the formation of a disordered protein gel structure [4]. Furthermore, the insoluble fibers of okara can reduce the degree of crosslinking between heat-denatured proteins, thereby weakening the texture properties of the curd, creating a

low gel-strength matrix which leads to a coarse gel structure [5], known to be chalky or sandy in texture [7].

Several methods have been investigated to address the disruptive nature of okara fibers in soy protein gels. The particle size of okara fiber can be reduced by physical treatments, such as high-speed shearing [4], high-intensity ultrasound treatment [8], high-pressure homogenization [9] or excessive pulverization [13], [108], [119]. Enzymatic treatments have been investigated including the use of transglutaminase to increase crosslinking of proteins by inducing covalent interactions [5], [10], [11], or cellulase to hydrolyze the cellulose components contained in okara [9], [121], [122]. Combinations of physical and enzymatic treatments have also been considered [12].

Citric acid is an inexpensive food-grade weak acid used in many applications. Because of its unique polycarboxylic structure, it has been used as an ester-bond promoter for wood materials [14]–[16]. To the best of our knowledge, its application has not been adopted for okara materials. It is however strongly hypothesized that both the primary and tertiary carboxylic acid groups of citric acid can act as reactive sites for esterification reactions to take place with hydroxyl groups of the okara fiber [129], [157]. This may enhance okara's compatibility with the food matrix. Moreover, citric acid has been used to hydrolyze insoluble okara fibers producing soluble fibers [156]. The soluble soybean polysaccharides (SSPS) generated upon acid hydrolysis is an anionic substance that contains 18% galacturonic acid and has a pectin-like structure [140], and is often utilized to stabilize acidified milk by preventing excessive protein aggregation [142], [147]. In addition, citric acid may function as a chelator to destabilize calcium-bridge junctures in the pectin constituent of okara to increase the yield of soluble saccharides [155].

The poor interaction between soy protein and insoluble fiber is believed to be the primary reason for the coarse structure and weak strength of okara-containing soymilk gel [123]. Existing methods do not seem to have fully resolved this issue despite efforts to either increase the crosslinking degree of soy proteins or reduce the okara size to compensate for the inferior gel quality [4]. For example, Wei et al. coated okara particles with chitosan and pectin to improve its compatibility with the soymilk gel network [120], however, this approach is complex and may be difficult to adapt in existing operations. Consequently, the objective of this study was to develop a novel and facile approach where citric acid would act as a bond promoter to improve the

compatibility of okara with the soymilk protein matrix to improve the cohesiveness of the soymilk gel with desired strength by thermal coagulation. Heat was also considered as a potential avenue to disrupt the structure of okara or as means to enhance the action of citric acid on okara. The temperature of the thermal treatment of okara and the soymilk coagulation, 95 °C, was selected, which is above the denaturation temperatures of the two major soy protein subunits, β-conglycinin and glycinin.

2   Materials and Methods

2.1   Materials

Soybeans (Nupak, LOT 11741D) were purchased from a local supermarket (Waterloo, ON, Canada). Citric acid anhydrous (CA) was purchased from Fisher Scientific (Fair Lawn, NJ, LOT 144600). Potassium bromide for infrared analysis was obtained from Fisher Chemical (Fisher Chemical P22725, LOT 204922). Rhodamine B was obtained from Sigma Aldrich (India, LOT SLBF0620V).

2.2   Preparation of Soymilk

A mass of 180 g of dry soybeans was fully submerged in filtered water (Brita Faucet Filtration System) at a mass to volume ratio of 1 g to 3 mL and soaked overnight at room temperature. The hydrated soybeans were drained, rinsed, and manually dehulled. Soybeans were dehulled to decrease the difficulty with shearing okara fibers, and to remove most of the pectic substances, which comprise up to 30% of the polysaccharide component in soybean hulls [137]. Then, the soybeans were placed in a high-speed commercial blender (Waring E11524, Dynamic Corp., U.S.) and ground with distilled water (dry soybean:water ratio of 3:8 w/v) on high speed for 2 min for complete pulverization. This low water to bean ratio was selected to promote sufficient hydrophobic interactions between protein molecules in extracted soymilk for adequate gelation without the use of coagulant. The resulting mixture was passed through a cheese cloth bag (Scengclos, Woodridge, IL) to separate the insoluble soybean solids (okara) from the liquid (soymilk). The excess moisture in the okara was removed by manual squeezing. Both the soymilk and okara were weighed. The concentration of okara was in the range of 22-28% okara/soymilk (w/w).

The soymilk was stored at refrigeration temperature in a sealed plastic container until further use. Prepared soymilk was used for the preparation of gels in the later step.

2.3 Okara Treatments

The various okara treatments are illustrated in **Fig. 4-1**. It includes three different treatments, heat, citric acid, and the combination of citric acid and heat.

Both the untreated and treated okara material involved the preparation of an okara dispersion. Specifically, 10 g of okara was dispersed in 50 g of Milli-Q water [107] under magnetic stirring at high speed for 15 min. The untreated okara (*O*) was obtained by transferring the okara dispersion to a glass petri dish with subsequent drying in a forced air oven (Fischer Isotemp 737F) at 60 °C for 16 h or until the mass remained constant. The dried okara was ground in a grinder (Blenderpro) for 30 s to reduce its particle size. The dried okara was stored at room temperature for no longer than one week. The okara with heat treatment (*OH*) was prepared by heating the okara dispersion in a water bath (Thermo Neslab, RTE 111) at 95 °C for 1 h and then left to cool prior to drying in the oven and manipulated as previously described with the untreated okara. The okara with citric acid treatment (*OCA*) was obtained by adding 6 g citric acid to the okara dispersion and mixing under magnetic stirring on high speed at room temperature for 1 h and processed as described with the untreated okara. Note that according to preliminary experiments, a concentration of 3:5 w/w citric acid:okara was suitable in producing a soymilk gel with minimal syneresis. Lastly, the okara treated with a combination of citric acid and heat (*OCAH*) was prepared by mixing the okara dispersion with 6 g of citric acid for 1 h followed by heat treatment at 95 °C for 1 h, then processed as described previously with the untreated okara. The pH of the citric-acid-treated okara dispersion was about 2 (Hydrion pH paper).

2.4 Preparation of Soymilk Gels

The soymilk gels were prepared with the recovered soymilk as-is or mixed with okara. Prior to the heat treatment, three pH measurements of each soymilk mixture were taken using a pH meter (Mettler Toledo, S47 SevenMulti Dual pH and Conductivity Meter). The pH measurements were recorded in triplicates (**Table S. 1** Supplementary).

The soymilk gel with and without okara was obtained by heating at 95 °C for 45 min in water bath. The amount of soymilk used was according to the ratio determined previously after its extraction. When okara was added to the soymilk, magnetic stirring was employed at about 600 rpm for 15 min to ensure adequate distribution of the okara solids. Overmixing was avoided to minimize the amount of air bubbles introduced into the soymilk. The soymilk mixture was placed in a beaker sprayed with a thin layer of oil spray (Pam original, Mississauga, Canada) prior to heating, to prevent the gelled sample from sticking to the beaker wall. The gels were then cooled to room temperature prior to their overnight storage at refrigeration temperature.

Each gel type was prepared in triplicates. **Soymilk gels** were differentiated from okara solids with a letter "**M**" in front to reflect the soymilk content (*e.g.*, *O* refers to untreated okara solids while *MO* refers to soymilk gel prepared with the untreated okara).
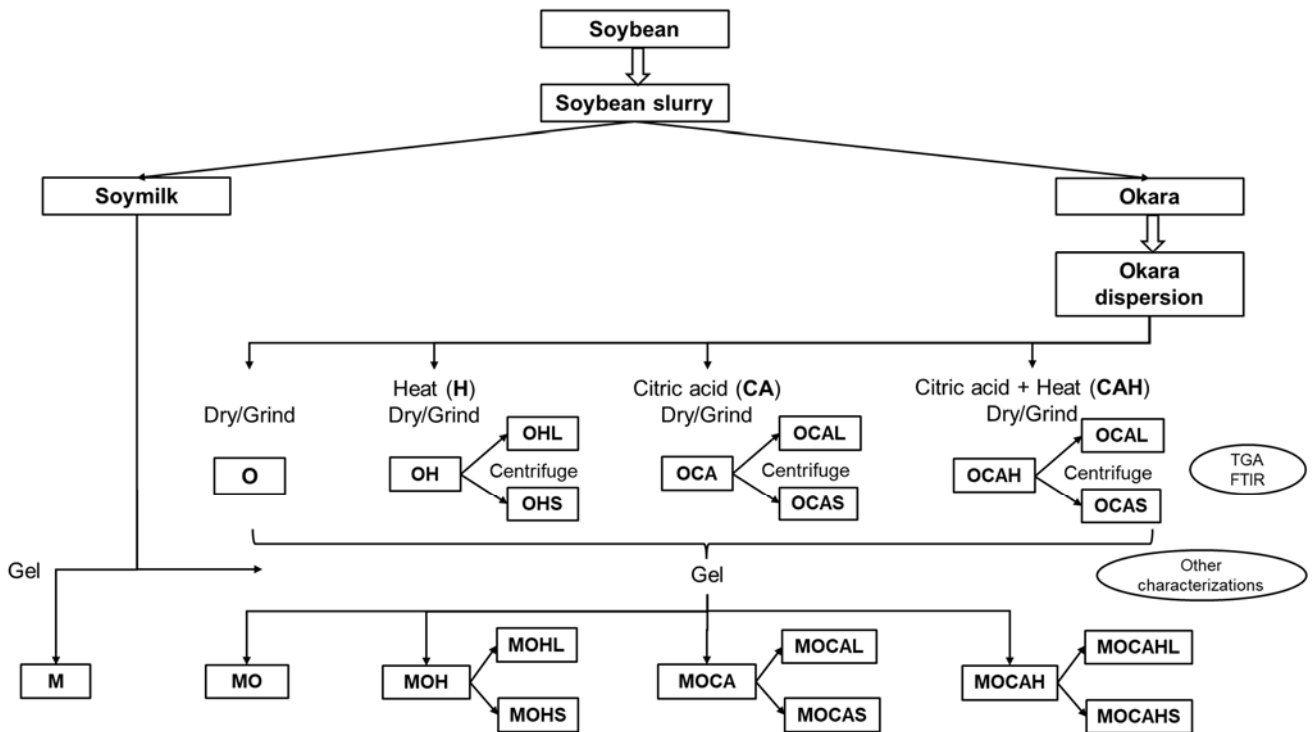
Fig. 4-1 Simplified overall process of gel preparation.

2.5   Quantification of Soluble and Insoluble Okara Solids

The soluble solids were separated from the insoluble solids in the various okara dispersions by ultracentrifugation (Beckman Coulter, Optima XPN100). A fixed angle rotor (Type 45 Ti) was used, and samples were centrifuged at 35,000 rpm (140,000 x g) for 30 min at 4 °C. After

ultracentrifugation, three phases can be clearly identified: a pellet (precipitate), supernatant (liquid fraction) and a thin white lipid layer on top. The liquid phase containing the lipid layer was carefully extracted from the precipitation using a pipette and transferred into two glass petri dishes. The **liquid fraction**, containing the soluble solids, is denoted by "**L**", while the **solid fraction**, containing the insoluble solids, is denoted by "**S**" for all fractionated okara materials.

The mass of the individual fraction of each sample was recorded. The content of the solids was estimated based on an initial mass of 10 g of treated or untreated okara dispersed in 50 g Milli-Q water. Particularly, the okara material with citric acid treatment (*OCA* and *OCAH*) contained an additional 6 g of citric acid. The mass of untreated okara (*O*) and the various treated okara was measured after oven drying and expressed as the mean of three replicates for each type of material. The solid content (%) of each fraction was calculated from the mass of dried solids in the respective fraction divided by the total solid content of the whole okara material prior to ultracentrifugation.

2.6 Thermogravimetric Analysis (TGA)

The thermal stability of soymilk, the various okara materials, and citric acid was obtained by thermogravimetric analysis (TGA, TA Instruments, TGA Q500). For each material type, 15 ± 2 mg of sample was heated from room temperature to 600 °C at 10 °C/min. All tests were carried out in nitrogen with a flow rate of 40 and 60 mL/min for the purge and balance streams, respectively. Variation of residual mass with respect to the change in temperature was generated automatically. Derivative thermogravimetric (DTG) estimation, which represents the rate of weight loss over temperature, was also collected.

2.7 Fourier Transform Infrared Spectroscopy (FTIR)

A mass of 2.05 ± 0.05 mg dried soymilk and treated okara solids was ground with 200 mg KBr using a mortar and pestle, then compressed into pellets *via* a KBr pellet die (MSE Supplies LLC) in a Carver press to 6 metric tons for 5 min. FTIR spectra were collected (Thermo Scientific Nicolet 6700, Waltham, MA, USA) with 32 scans between the wavenumber range of 400 to 4000 cm^{-1} and a resolution of 4 cm^{-1}. A 200 mg KBr pellet served as the background spectrum and was subtracted from the sample spectra. Transmittance was normalized for the ease of comparison.

2.8   Uniaxial Compression of Soymilk Gels

Uniaxial compression test was performed on the cylindrical soymilk gel samples with a mechanical tester (Shimadzu Autograph AGS-X) and a 50-N load cell. Cylindrical-shaped samples, 20 mm diameter and 10 mm height, were cut from the intact gel using a metal corer, immediately taken out from the refrigerator [229]. The central portion of the gel was used for all testing to avoid any skin effects present at the outermost surface [78]. Samples were allowed to equilibrate for 1 h at room temperature prior to testing.

Gel samples at room temperature were compressed uniaxially at 40 mm/min until fracture was visually observed, then manually stopped. Six replicates were prepared for each gel and since three different gels were prepared for a given treatment, a total of 18 replicates was collected for a given treatment type.

The stress-strain curve was used to estimate the true fracture stress and true fracture strain, which is namely, the Hencky stress and strain, as well as Young's modulus.

The true stress ($\sigma(t)$) and true strain (ϵ) were determined according to **Equation 4** and **Equation 5**, respectively, to quantify the change in height and area of the sample [230].

$$\sigma(t) = \frac{F(t)}{A_0} \times \frac{l(t)}{l_0} \qquad\qquad \textbf{Equation 4}$$

$$\epsilon = -\ln\left(\frac{l(t)}{l_0}\right) \qquad\qquad \textbf{Equation 5}$$

Where, l_0 and A_0 are the original height and area of the gel, respectively; $l(t)$ and $F(t)$ are the height and force of the gel at time t, respectively.

The true fracture stress was measured as the maximum point of the stress-strain curve (Guo et al., 2014, Funami, 2011). The MAX function in Excel was used (Microsoft 365, version 2202) to identify the maxima up to a stress when a clear decline was observed. In cases where the decline could not be easily identified, the first derivative was taken to find the slope nearest to zero and the maxima was taken at that point. The true fracture strain was the strain corresponding to the true fracture stress. Young's modulus was the slope of the linear region of the curve located between one and two-thirds of the way to the point of the true fracture stress [231].

2.9   Viscoelastic Properties of Soymilk Gels

Viscoelastic properties of the gels were obtained with the small-amplitude, oscillatory shear test and performed using a rheometer (Thermo Scientific, HAAKE MARS III, USA). A parallel plate geometry (35 mm diameter) with 1 mm gap was employed. Samples were cut from the central portion of the gel using a sharp blade into thin disks with diameter of greater than or equal to 35 mm and around 5 mm in thickness. Gel samples were allowed to equilibrate at room temperature for 1 h after cutting.

Gel samples were loaded into the 10-mm gap space at room temperature. The lift speed was set to 1.25 mm/min when closing the gap to minimize abrupt uniaxial deformation. Samples were then trimmed at a gap space 0.025 mm higher than the measuring position (1 mm), *i.e.,* 1.025 mm. After reaching the measuring position (1 mm), samples were allowed to rest for an additional 10 min to ensure mechanical equilibrium was reached.

The strain sweep test was conducted once for all replicates of each treatment at a strain range between 0.01 – 100% at 1 Hz. The strain at the end of the linear viscoelastic region (LVR) is defined as the strain at which the storage (G') and loss (G'') moduli become dependent on the strain amplitude [195]. This strain can be referred to as yield strain or strain at yielding [194].

The frequency sweep test was conducted in triplicates for all replicates of each treatment at an angular frequency range of 1 – 100 rad/s and 0.1% strain, which was within the LVR of each gel, as determined from their strain sweep test characteristics.

A power law model was used to characterize the angular frequency (ω) dependence on G' and G'' using **Equation 6** and **Equation 7** [195].

$$G' = G'_0 \omega^{n'}$$
<div align="right">**Equation 6**</div>

$$G'' = G''_0 \omega^{n''}$$
<div align="right">**Equation 7**</div>

Where, G'_0 (Pa) and G''_0 (Pa) are storage and viscous moduli at 1 rad/s, respectively. G'_0 is the energy stored and recovered per cycle of sinusoidal shear deformation. The increase in G'_0 indicates that the rigidity of the sample is associated with the formation of an elastic gel structure. G''_0 is the energy dissipated or lost as heat per cycle of sinusoidal strain and indicates the extension of the viscous element in the gel [195]. G'_0 and G''_0 may also be identified as the

resistance to elastic and viscous deformation, respectively [232]. The exponents n' and n''
(dimensionless) denote the influence of angular frequency on both moduli.

Tangent delta (tan δ) is defined as the ratio between the loss modulus (G'') and storage modulus
(G'), as illustrated in **Equation 8**. It quantifies the energy absorption or dispersion of a material.
This ratio is often used to indicate weak or strong gel behaviour.

$$\tan \delta = G''/G'$$ **Equation 8**

2.10 Macrostructure of Soymilk Gels

The appearance of the various soymilk gels was captured with a camera (Samsung Galaxy s10)
at 30 frames per second. The camera was placed on a clamp located 20-cm vertically from the
sample surface and positioned as to be horizontal to the top surface of the gel. The same lighting
was used for all imaging.

All images were cropped to 600 x 578 pixels and converted to binary images using ImageJ
software (version 1.53k, National Institutes of Health, USA). An 8-bit conversion was applied
with grayscale ranging from 0 to 255, while a threshold of 155 was used to characterize the
porosity of the gel. The porosity of the gel as denoted by the black regions was characterized by
its mean cell size (mm^2), cell density (cell/mm^2), and void fraction (%) [120]. Firstly, all images
were calibrated by specifying the actual cross-sectional diameter of a gel in relation to the pixel
size of the image. Then, a particle size analysis was performed. The mean cell size was
automatically generated based on the detection of black regions in the binary image. The cell
density is the ratio of the number of cells to the total cross-sectional area of the gel. The void
fraction is the ratio of the total cell area to the total cross-sectional area of the gel [207].

2.11 Microstructure of Soymilk Gels

The microstructure of the various soymilk gels was examined by confocal laser scanning
microscopy (CLSM, Zeiss LSM 700, AxioObserver) with a Plan-Apochromat 20x/0.8 objective
lens. The soymilk gels were prepared with the addition of Rhodamine B for staining the proteins.
Either 4 g soymilk solution or an okara and soymilk mixture was dyed with 20 µL of 0.2% w/v
Rhodamine B solution, resulting in a final dye concentration of 0.001% w/w [233]. The mixture
was stirred with a magnetic stirrer at 400 rpm for 1 h at room temperature. The container was

covered with parafilm and aluminum foil to prevent moisture loss and light exposure and subsequently stored at fridge temperature overnight. One to two drops of the dyed mixture were placed on concave slides (Eisco, 1''x3'', 1.0-1.2mm), gently pressed down with cover slide (Fisherbrand, 22x22-1.5) and wrapped in aluminum foil. The slide was incubated at 95 $^{\circ}$C for 45 min in a forced air oven (Fischer Isotemp 737F) to replicate previous gelling conditions. The gels were stored at fridge temperature prior to CLSM visualization.

The stained gel samples were imaged with an excitation wavelength of 555 nm and a detection wavelength of 560-800 nm. A pinhole size of 1 airy unit, laser power of 2.0%, and detector gain of 500 were kept for all samples. Resolution of the digital images was 1024 x 1024 pixels. A gamma value of 0.45 was used post processing to enhance image contrast. Images of at least five locations were collected for each sample treatment, and a typical image was presented for each treatment.

2.12 Statistical Analysis

The multiple comparison test, namely, the post-hoc test was used to determine statistical differences between okara treatments using Statistica (version 14.0.0.15, TIBCO software Inc.). Tukey test was used to identify statistical differences between paired means. Means are significantly different if $p \leq 0.05$, and not significantly different if $p \geq 0.05$ [218]. Graphs were constructed using Origin (OriginPro 9.0.0, OriginLab Corp.).

3   Results and Discussion

The influence of heat, citric acid, and the combination citric acid and heat treatments on the structural changes of okara was investigated by examining the properties of okara and of soymilk gels containing okara. Firstly, the solid content, thermal stability measured by TGA, and functional groups identified by FTIR of the okara subjected to the various treatments will be discussed. It is followed by the evaluation of the uniaxial compression and viscoelastic properties as well as the macrostructure and microstructure of the various soymilk gels. A proposed mechanism representing effects of the treatments on the okara structure and resulting soymilk gels will conclude the study.

3.1   Soluble and Insoluble Solids Content of Okara

The changes in the solid content for a given okara treatment can reflect its alterations upon a given treatment. The soluble solids were recovered from the supernatant after the ultracentrifugation of okara. The remaining solids, insoluble solids, were from the pellet. The relative magnitude of soluble and insoluble solids compared to the initial total solids of okara for different treatments will be discussed in this section. This method was selected such that the solid content is based on independent estimation of the soluble and insoluble solids, giving a measure of the loss of solids taking place during the ultracentrifugation. Note that the solids will include citric acid for the okara treatment. Albeit the distribution of citric acid between the soluble and insoluble fractions was not estimated, one can infer that citric acid will be predominantly contained in the soluble fraction based on its solubility.

The heat treatment of okara (**OH**) had a negligible effect on the solubilization of okara (**Table 4-1**), suggesting that heat did not induce a significant conversion of insoluble to soluble okara constituents. In contrast, citric acid treatment of okara (**OCA**) led to a significant increase in soluble solids ($p < 0.05$) while the insoluble solids content was not statistically different ($p > 0.05$) when compared to the heat treatment of okara (**Table 4-1**). It indicates that citric acid may have hydrolyzed larger polysaccharides into smaller and soluble saccharides. The combination citric acid and subsequent heat treatment of okara (**OCAH**) resulted in a significant increase of the soluble solids content (**OCAHL**) and a significant decrease of the insoluble solids content (**OCAHS**) ($p < 0.05$), indicating an extensive conversion of insoluble to soluble solids constituents of okara.

Table 4-1 Solid content of the various okara treatments and fractions (10 g initial mass of okara and 50 g of water). Data presented as average ± standard deviation (n=3). Means in the column of the solid content that do not share a common superscript letter are statistically different.

Okara treatment	Fraction	Mass of citric acid (g)	Mass of aqueous okara dispersion (g)	Mass of dried solids (g)	Solid content (w/w%)
No treatment	Whole (O)	0	59.32 ± 0.19	2.67 ± 0.09	NA

Heat treatment	Whole (OH)	0	57.35 ± 0.41	2.55 ± 0.38	NA
	Soluble (OHL)	0	11.33 ± 1.90	0.19 ± 0.03	7.52 ± 1.24[c]
	Insoluble (OHS)	0	37.97 ± 0.91	1.97 ± 0.06	76.97 ± 2.48[abd]
Citric acid treatment	Whole (OCA)	6	63.45 ± 3.37	8.23 ± 0.38	NA
	Soluble (OCAL)	6	27.26 ± 1.10	2.79 ± 0.19	33.61 ± 2.24[e]
	Insoluble (OCAS)	6	35.30 ± 0.48	5.83 ± 0.58	70.35 ± 6.96[af]
Citric acid and heat treatment	Whole (OCAH)	6	62.09 ± 0.73	8.29 ± 0.30	NA
	Soluble (OCAHL)	6	50.98 ± 0.26	7.19 ± 0.16	86.76 ± 1.90[bg]
	Insoluble (OCAHS)	6	6.17 ± 0.27	1.58 ± 0.09	19.02 ± 1.09[h]

3.2 Thermogravimetric Analysis (TGA)

The thermal degradation of okara can be related to its composition, around 40-60% dietary fiber, cellulose, hemicellulose, and lignin, 15-30% protein and 8-12% lipids, on a dry basis [226], [234]. Concerning the thermal degradation of okara, the first stage, up to 150 °C, is associated with the weight loss caused by the evaporation of water and other volatile constituents [162]. The second stage, 150 to 250 °C, corresponds to the degradation of non-cellulose materials [166]. The third stage, 250 to 380 °C, represents the degradation of some cellulosic components, specifically, the cleavage of their glycosidic linkages [162], [166]. The fourth stage, beyond 380 °C, is associated with the degradation of the amorphous phases of hemicellulose and lignin as well as the crystalline cellulose [166]. The higher the crystallinity of cellulose, the higher its degradation temperature [235]. The formation of char is associated with lignin residue [166], [169]. For the soluble portion of okara, known as the soluble soybean polysaccharides (SSPS), the degradation occurs at around 300 °C [236]. Soy proteins, on the other hand, degrade over a wide temperature range, 255 – 500 °C [163], [164].

The preceding information can be used to understand the thermal degradation profile of soymilk and the various okara materials as illustrated in **Fig. 4-2**. The materials can be classified in three

groups according to their thermal degradation characteristics, namely the rate of mass loss in response to temperature change.

The first group, soymilk (***M***), untreated okara (***O***) and all heat treated okara fractions (***OH, OHL, OHS***), had the highest thermal stability with a relatively linear and small rate of mass loss up to 250 °C followed by a more substantial rate of mass loss up to 380 °C. Both ***M*** and ***O*** had a relatively constant and low rate of thermal degradation over the entire temperature range despite their different composition. The notable difference is that the thermal decomposition of ***M*** started at a lower temperature (~130 °C) and had higher mass loss in the temperature range 150-230 °C as compared to ***O***. These minor differences could be related to the higher contents of protein and volatile constituents of ***M*** compared to ***O***. Additionally, all heat-treated okara materials (***OH, OHL, OHS***) generally demonstrated similar decomposition profiles to ***O***.

The second group had moderate thermal resistance which included the insoluble fraction of the two **CA** treatments, ***OCAS*** and ***OCAHS***. These materials were more heat sensitive than ***M, O*** and all ***OH*** materials but were more heat stable than ***OCA, OCAL, OCAH, OCAHL.*** Their thermal degradation revealed a pronounced mass loss between 200 and 230 °C, followed by a less significant mass loss between 220 and 380 °C (**Table S. 2** Supplementary).

The mass loss of ***OCAS*** and ***OCAHS*** in the temperature range <150 °C and 250-380 °C, was halved in comparison to ***O*** (**Table S. 2** Supplementary), suggesting that some volatile, cellulosic and heat stable materials in the insoluble portion of okara were reduced upon exposure to citric acid. Furthermore, the mass loss of ***OCAS*** and ***OCAHS*** was quite different in the 150-250 °C and 250-280°C temperature range, with ~40% and 24% for ***OCAS*** compared to ~35% and 28 % for ***OCAHS***. This may indicate a larger degree of hemicellulose and cellulose decomposition promoted by the additional heat treatment. Their mass losses in these two temperature ranges were also considerably different than that of the pure citric acid, indicating that the free citric acid was not an important constituent of ***OCAS*** and ***OCAHS.***

The third group of okara materials, whole and soluble fractions of the **CA** and **CAH** treatments of okara, had the highest thermal sensitivity with an elevated rate of mass loss up to 250 °C, followed by a significantly lower rate of mass loss between 250 and 380 °C (**Fig. 4-2**A). A significant portion of these fractions degraded between 150 and 220 °C, ~60% for ***OCAH*** and ***OCAHL*** and ~65% for ***OCA*** and ***OCAL,*** about four-fold higher mass loss as compared to ***O***

(**Table S. 2** Supplementary). It is noted that their thermal degradation profile was fairly similar to that of citric acid with ~90% mass loss between 150 and 250 °C. This indicates that free citric acid was present in these materials and may overlap with the degradation of heat sensitive components of okara that were released upon **CA** treatment. Moreover, a lower residual mass, 11-14 % at 600 °C, was observed for these fractions (**Table S. 2** Supplementary), implying that a lower quantity of lignin was present.
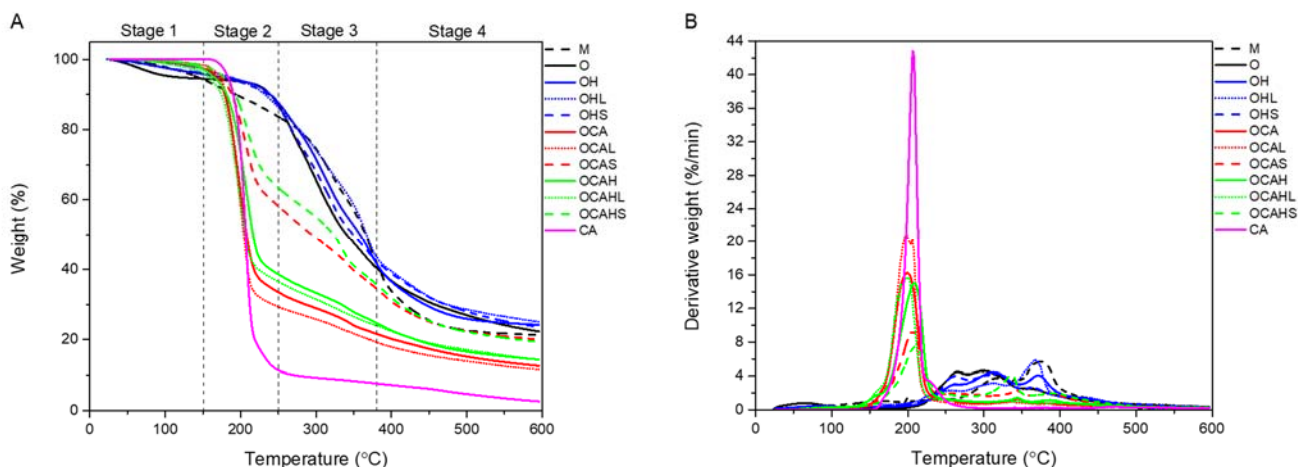
Fig. 4-2 TGA (A) and DTG (B) curves.

3.3 Fourier Transform Infrared Spectroscopy (FTIR)

Infrared spectroscopy provides information on the functional groups of chemical constituents. In the context of soy milk and okara, the bands in the regions of 3650-3100, 3000-2750, 1750-1540, and 1200-950 cm^{-1} will be discussed. The broad band in the region of 3650-3100 cm^{-1} is ascribed to O-H stretching of hydrogen in the hydroxyl group [170]. The bands at ~2920 and ~2854 cm^{-1} are assigned to C-H vibration stretching in polysaccharides [171]. Bands at ~1742 and ~1645 cm^{-1} represent the stretching vibrations of esterified and unesterified carboxyl groups, respectively [172]. The band at ~1645 cm^{-1} can also represent the amide I bond of protein molecules [173], [174]. The band at ~1540 cm^{-1} is ascribed to amide II bond [173], [174]. The region 1200-950 cm^{-1} is the so-called fingerprint region [175], where the location and intensity of the bands differ for each polysaccharide type.

Soymilk (**M**) and untreated okara (**O**) were used for comparison with the various okara treatments and fractions. The FTIR spectrum of **M** reflects its predominant protein content and low carbohydrate content when compared to **O.** This was seen by the increased intensity of bands at 1645 (amide I) and 1540 cm^{-1} (amide II) and the reduced intensity of bands at ~1063 cm^{-1} and ~1170 cm^{-1} [237], which corresponds to the tensile vibration of C-O groups in C-O-H and C-O-C of the aromatic sugar rings in hemicellulose and cellulose [238], [239].

Heat treatment of okara (**OH**) did not induce significant changes in its FTIR spectrum compared to **O** (**Fig. 4-3**A). Minor differences included lower band intensities at 2920, 2854 and 1063 cm^{-1} in the insoluble portion of heat treated okara (**OHS**). This suggests that heat treatment destroyed some C-H bonds of the ring structure of okara fibers, *e.g.*, hemicellulose, cellulose, and lignin. Another difference observed in **OHS** was the decreased band intensity at 1742 cm^{-1}, which indicates reduced esterified carboxyl groups as a result of heat treatment. In contrast, the soluble solids of the heat treated okara (**OHL**) had the lowest band intensity at 1063 cm^{-1} as compared to **OH** and **OHS**, reflecting the limited content of soluble aromatic sugar rings in this fraction.

Significant differences in the FTIR spectra of the citric acid treated okara (**OCA, OCAL, OCAS**) were observed. When examining the FTIR spectrum, one needs to consider their citric acid content and its associated FTIR characteristics. In particular, a single flat band expanding from 1757 to 1677 cm^{-1} corresponds to the carboxyl groups of the pure citric acid (**Fig. 4-3**B). The FTIR spectra of all **CA**-treated okara showed a reduced intensity of the O-H band (3650-3100 cm^{-1}) compared to **O**, which can be ascribed to the decrease of intramolecular hydrogen bonds in hemicellulose and cellulose upon citric acid hydrolysis [240]. Another notable difference observed for all citric acid treated okara was the significant reduction in band intensities at 2920 and 2854 cm^{-1} suggesting lower polysaccharide content in these materials [171], [237] and which was more pronounced for **OCA** and **OCAL** (**Fig. 4-3**B). **OCAS** showed a significant increase in intensity at 1742 cm^{-1} and a drastic decrease in intensity at 1645 cm^{-1} in comparison to **O**, suggesting an increased content of esterified carboxylic groups and a decrease in free carboxylic groups. This finding indicates the occurrence of esterification reactions between the hydroxyl groups of hemicellulose, cellulose, pectin, and/or lignin of the okara fiber and one or more of the carboxylic acid groups of citric acid [128], or with the carboxylic acid side chain of amino acids in the protein (*e.g.*, glutamic and aspartic amino acids) (**Fig. 4-3**). In contrast, the band at ~1742

cm^{-1} became broader while the band at 1645 cm^{-1} was absent for *OCA* and *OCAL* which may be the result of the substantial effect of citric acid in these fractions (**Fig. 4-3**B). Another difference in the absorption bands of *OCA* and *OCAL* was the significantly weaker intensity of the band at 1540 cm^{-1}, ascribed to amide II bond (**Fig. 4-3**B), indicating the limited protein content of these fractions.

Other important differences were observed in the "fingerprint" region, including a significant decrease of the band intensity at ~1070 cm^{-1} associated with hemicellulose or cellulose rings for *OCAS* (**Fig. 4-3**B). This suggests that citric-acid treatment destroyed some ring structures of hemicellulose and cellulose to produce smaller molecular weight saccharides, *e.g.*, oligosaccharides [237], [240]. Similar profiles of the bands at ~1170 and 1070 cm^{-1} were observed in soymilk (*M*) (**Fig. 4-3**B). As soymilk contains small molecular weight saccharides and a relatively low content of high molecular weight polysaccharides [241], one can infer that *OCAS* would possess a similar polysaccharides profile as *M* due to their comparable FTIR spectra. On the other hand, the fingerprint region of *OCAL* and *OCA* resembled that of the pure citric acid (**Fig. 4-3**B), suggesting that citric acid was dominant in these fractions which agrees with the TGA results. *OCAL* and *OCA* had distinct bands located in the region of 1235 – 1045 cm^{-1} that are characteristic of pectin (**Fig. 4-3**B) [242]. Specifically, the bands at 1235, 1143, 1075 and 1045 cm^{-1} are associated with pectic substances and arabinogalactan [243]. As reported previously, the absorption band between 1200 and 1100 cm^{-1} stems from ether (R-O-R) and C-C bond in the ring structure of pectic substances [244].

The additional heating after the citric acid treatment of okara (*OCAH*) had minor effect on the FTIR spectra when compared to the citric acid treatment of okara (*OCA*). Functional groups associated with esterification reactions, bands 1742 and 1645 cm^{-1}, and the presence of pectic substances, *i.e.*, bands in the region 1235-1045 cm^{-1}, were observed in all *OCAH* materials (Fig. B). The O-H band intensity (3650-3000 cm^{-1}) was lower for all **OCAH**-treated okara fractions when compared to *O*. The C-H band of polysaccharides such as cellulose and hemicellulose (2920 and 2854 cm^{-1}) was absent in the soluble fraction (*OCAHL*) indicating that the additional heat treatment intensified the degradation of the okara polysaccharides present in this fraction.
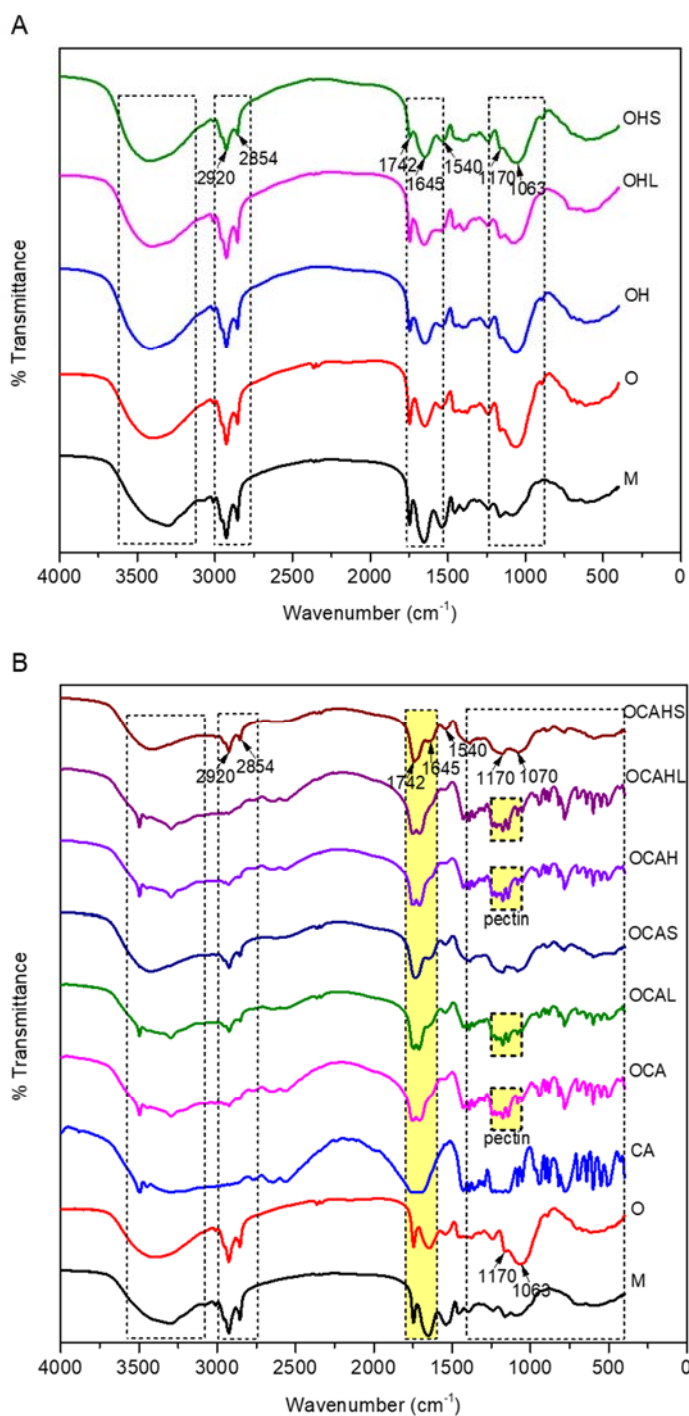
Fig. 4-3 FTIR spectra of heat-treated okara (A), and citric-acid treated, and citric-acid-and-heat-treated okara (B). All graphs were plotted against dried soymilk (M) and untreated okara sample (O) as reference. Pure citric acid (CA) was used as an additional reference for plot B.

3.4   Uniaxial Compression

Large deformation measurements such as uniaxial compression characterize material properties of food gels that can be related to the food eating experience [180], and it is frequently characterized by fracture stress, fracture strain and Young's modulus. Fracture stress is sometimes referred to as gel strength of food products and is associated to "toughness" in relation to texture [32]. Young's modulus, determined by the initial slope of the stress-strain curve, is related to the "firmness" or "hardness" of foods' sensory properties [32]. The strain at fracture, also known as fracture strain, is related to the deformation capacity of the food material [182].

The typical true stress-strain curves of the various soymilk okara gels are presented in **Fig. 4-4**. The stress strain curve for the soymilk gel (***M***) and the soymilk gel with the soluble solids portion of the heat treated okara (***MOHL***) could not be obtained because the self-standing gels were insufficiently strong for the test. In contrast, the soymilk gels with untreated okara, as well as treatments with heat (**H**), citric acid (**CA**) and citric acid and heat (**CAH**), produced self-standing gels that had sufficient strength for the assessment of their mechanical properties.

Most okara-containing soymilk gels and their soluble and insoluble constituents had distinct true stress-strain curves and mechanical properties. The soymilk gel with untreated okara (***MO***) displayed a relatively slow initial increase followed by a more pronounced change of the true stress-strain curve (**Fig. 4-4**A). The ***MO*** gel had fairly high fracture stress, fracture strain and Young's modulus (**Fig. 4-5**), suggesting that the fiber constituents of okara, hemicellulose, cellulose and lignin, imparted strength to the overall soy protein gel network. The ***MO*** gel was selected as a point of comparison to examine the effect of the three okara treatments on the resulting soymilk gel. Overall, the fracture stress of the ***MOHS*** and ***MOCAS*** gels was comparable to the ***MO*** gel. All other gels had lower fracture stress than the ***MO*** gel, indicating lower gel strength. Notably, the ***MOCAHS*** gel had significantly different mechanical properties compared to all the other gels (**Fig. 4-5**B). This gel did not fracture under the experimental conditions employed in this study. However, it was the only gel where water syneresis was observed. It could be related to the poor ability of the large-molecular-weight polysaccharides that remained in this fraction to interact with the water-protein matrix, thereby releasing free water.

The whole heat treated okara soymilk gel (*MOH*) had significantly lower fracture stress and Young's modulus when compared to *MO* gel ($p < 0.05$) (**Fig. 4-5**A,C). On the contrary, gels prepared with the insoluble solids portion of the heat treated okara (*MOHS*) had similar mechanical properties as compared to *MO* ($p > 0.05$) (**Fig. 4-5**). These observations indicate that heat treatment had a negligible effect on the mechanical properties of okara soymilk gels.

The true fracture stress and Young's modulus of the soymilk gel containing the whole citric acid treated okara (*MOCA*) were significantly lower ($p < 0.05$) when compared to *MO* gel (**Fig. 4-5**A,C). The soymilk gels prepared with the soluble solids (*MOCAL*) and the insoluble solids content (*MOCAS*) of the citric acid treated okara displayed a clear and distinct fracture point (**Fig. 4-5**B). In addition, both the *MOCAL* and *MOCAS* gel had markedly lower fracture strain when compared to *MO* ($p < 0.05$) (**Fig. 4-5**B), which is an indication of their low resistance to shape change. The Young's modulus of *MOCAL* significantly increased when compared to *MO* ($p < 0.05$), and the *MOCAS* had the highest value, nearly doubling that of the other gels (**Fig. 4-5**C). This indicates the firmness of *MOCAS*, which could be related to the formation of covalent bonds upon citric acid treatment resulting from the esterification reaction, as seen in its FTIR spectrum.

The true stress-strain curve of the soymilk gel prepared with the whole citric acid and heat treated okara (*MOCAH*) showed similar true stress-strain curve (**Fig. 4-4**B) and comparable mechanical properties as those of *MOCA* ($p > 0.05$) (**Fig. 4-5**). The soymilk gel prepared with the soluble solids (*MOCAHL*) was also characterized by a clear and distinct fracture point (Fig. B). The true fracture stress of the *MOCAHL* was similar to *MOCAL* ($p > 0.05$) (**Fig. 4-5**A), whereas its fracture strain was significantly higher (**Fig. 4-5**B) and its Young's modulus was considerably lower (**Fig. 4-5**C) than the *MOCAL* gel ($p < 0.05$). These changes may reflect the extensive hydrolysis of the okara caused by the heating step following the citric acid treatment as also portrayed in the FTIR profile.

For a given okara treatment, the lowest fracture stress was observed when the soymilk gel was prepared with the whole okara. In contrast, the highest fracture stress was observed for the soymilk gel prepared with the insoluble portion of okara. The fracture stress of soymilk gel prepared with the soluble okara portion was in between that of the whole and insoluble fractions (**Fig. 4-5**A). The weak gel strength of the whole okara soymilk gel may be related to the

competition among its protein, soluble and insoluble constituents for water [245]. It could also be the insoluble portion of okara acting as an inactive filler impacting protein aggregation upon heat denaturation [5], resulting in lower fracture stress of the whole okara gel. When using only the insoluble portion of the okara, it reinforced the matrix because of the high tensile strength of cellulose linked *via* firm hydrogen bonds. For gels prepared with the soluble fraction of the okara, the strength of the network may be related to the presence of pectic substances and the gelling potential of the soluble solids [138].

Fig. 4-4 Typical true stress-strain curve of untreated okara soymilk gel (MO) with MOH & MOHS (A), and MOCA, MOCAL & MOCAS, MOCAH, MOCAHL & MOCAHS (B). All samples fractured up to 65% true strain except for MOCAHS where fracture was undetected.
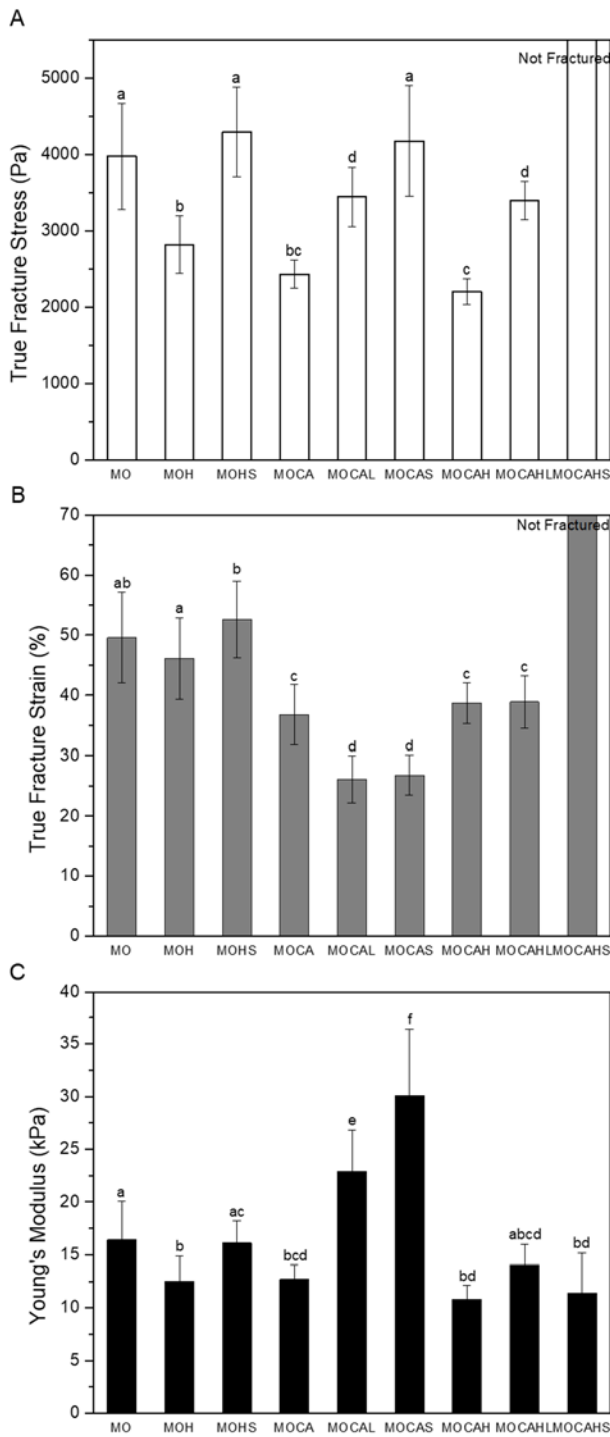
Fig. 4-5 True fracture stress (A), true fracture strain (B), and Young's modulus (C) for all samples. Data expressed in mean ± standard deviation (n=18). Means that do not share a common letter are statistically different.

3.5 Viscoelastic Properties

Rheological measurements provide information on the food material's behaviour under shear stress, generating complementary information on the strength and microstructure of gels [94]. A strong gel has the characteristic of a true gel, and when deformed above a critical value it will rupture rather than flow [246]. Whereas a weak gel possesses characteristics between those of a solution and a strong gel, and it often undergoes a progressive breakdown into smaller clusters as deformation increases [246].

The strain sweep test was firstly employed to determine the linear viscoelastic region (LVR) of the material, and a 0.1% strain was selected such that the strain of all the gels was within the LVR. Initially, all gels experienced a constant storage modulus (G') with a subsequent sudden decrease in G' observed with increasing strain amplitude (**Figure S. 1** Supplementary), which is an indication of the breakage of bonds within the gel network [195]. The yield strain was determined as the strain at which the storage (G') and loss (G'') moduli become dependent on strain amplitude [195]. Low yield strain was observed for the untreated okara soymilk gel (***MO***) and heat-treated okara soymilk gel (***MOH, MOHS***) (**Table 4-2**), indicating that they had less resistance to deformation under shear stress [195]. On the contrary, all the soymilk gels contained citric acid treated okara except for the ***MOCAHS*** gel displayed significantly higher yield strain ($p < 0.05$) (**Table 4-2**), suggesting their increased resistance to shear deformation.

The properties G' and G'' relate to the ability of a material to store energy elastically and dissipate stress through heat, respectively [247]. The tangent delta (tan δ) refers to the viscoelasticity index of a material [247]. The profiles of G', G'' and tan δ as a function of angular frequency of all soymilk gels are illustrated in **Fig. 4-6**. All gels demonstrated a clear gel-like behaviour with G' being significantly higher than G'' (**Fig. 4-6**A,B). This behaviour was confirmed with a tan δ value of less than 1 (**Fig. 4-6**C), indicating that all gels were more solid-like than liquid-like. However, the magnitude of G' was less than 10 times that of G'' for all gels, and thus a weak gel behaviour was suggested [197].

The gels differed according to the magnitude of their G' and G''. These differences will be used to classify the gels in three groups. The first group is the ***MOCAHS*** gel, which had significantly higher G' and G'', in the ranges of 1100 – 2200 kPa and 250 – 470 kPa, respectively, when compared to all the other gels ($p < 0.05$). This was about three-fold higher compared to the

untreated okara soymilk gel (*MO*) (**Fig. 4-6**A,B). Its distinct viscoelastic property aligned with its mechanical behavior where no fracture was detected upon compression, indicating its high gel rigidity [74]. The second group of gels are those gels with moderate G' and G'', in the ranges of 290 – 610 kPa and 60 – 120 kPa, respectively, including the *MO* and *MOHS* gels. Both gels had similar G' and G'' ($p > 0.05$). The third group of gels are those with considerably lower G' and G'', in the ranges of 5 – 95 kPa and 1 – 23 kPa, respectively ($p < 0.05$). The comparison of the viscoelastic properties of the okara soymilk gels prepared in this study to previous studies indicated that even the gels with the lowest G' and G'' (third group) had significantly higher moduli when compared to enzyme-induced okara-tofu of up to 70-fold increase for G' and 160-fold increase for G'' [5], [11]. This points to the high rigidity of the okara soymilk gels prepared in this study. It may mainly be explained by their higher protein content because of the intentionally reduced water quantity used in this study as compared to the conventional tofu production conditions.

Further analysis of the frequency sweep was obtained by fitting the plot of G' and G'' over the angular frequency with the power law equation and determining parameters, G_0', G_0'', n', and n'' (**Equation 6** and **Equation 7**). The fitting was excellent for all gels, with the correlation coefficient, R^2, above 0.99 for G' and 0.95 for G'', except the soymilk gel (*M*) with R^2 around 0.75, notably lower than the other gels ($p < 0.05$) (**Table 4-2**). However, the normal probability plot of the residuals of *M* suggests that the errors were normally distributed (**Figure S. 2** Supplementary).

The parameters G_0' and G_0'', determined as the intercepts of the linear fitting of G' and G'', reflected the profiles of G' and G'' as discussed above (**Table 4-2**). Notably, the G_0' and G_0'' estimates were higher for the soymilk gel prepared with the insoluble solids than those prepared with either the whole fraction or the soluble portion of a given okara treatment. A similar observation was noted with the result of the true fracture stress. This is probably attributed to the insoluble fiber remaining in the insoluble fraction (*e.g.*, cellulose, lignin), which is known to have high mechanical strength, resulting in a gel that is more resistant to deformation [232]. The power law exponents n' and n'', which denote the dependency of G' and G'' on frequency, were similar among gels, 0.12-0.14, and 0.10-0.15, respectively (**Table 4-2**). The soymilk gel (*M*) had the lowest n' and n'' estimates and was statistically different than all other gels, which

113

contradicts with its considerably lower G', alluding to weaker gel behaviour. This may be impacted by its larger experimental error.
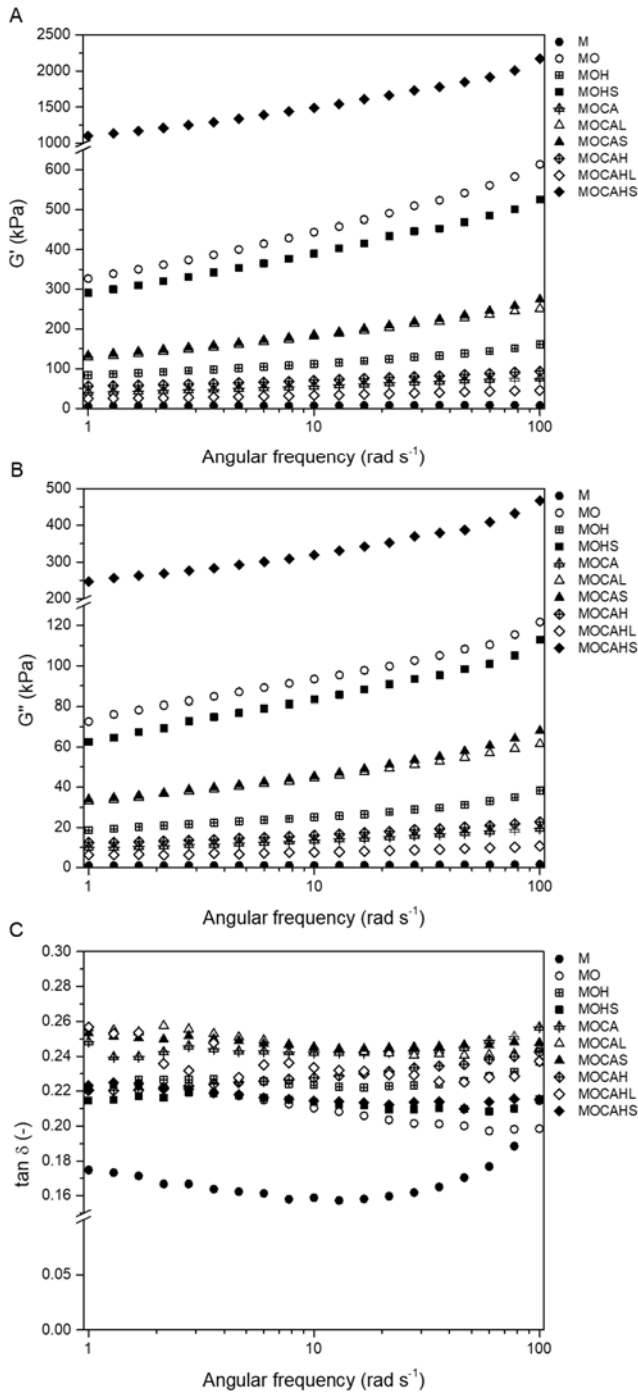

Fig. 4-6 Typical curves of storage modulus, G' (A), loss modulus, G'' (B), and tangent delta (C) over angular frequency.

Table 4-2 Yield strain (n=3) and estimated power law parameters (n=9) of soymilk or okara gels. Results are expressed as mean ± standard deviation. Means in the same column that do not share a common superscript letter are statistically different.

Gel	Yield strain (%)	G_0' x 10^3 (Pa)	n'	R^2	G_0'' x 10^3 (Pa)	n''	R^2
M	8.0 ± 0.2[a]	5.3 ± 1.8[a]	0.08 ± 0.02[a]	0.865 ± 0.118[a]	0.9 ± 0.1[a]	0.09 ± 0.02[a]	0.753 ± 0.213[a]
MO	1.5 ± 0.1[b]	315.1 ± 30.7[b]	0.13 ± 0.01[bce]	0.998 ± 0.002[b]	72.6 ± 6.7[bc]	0.10 ± 0.01[ab]	0.990 ± 0.006[b]
MOH	1.1 ± 0.1[bc]	83.1 ± 21.2[a]	0.12 ± 0.01[b]	0.994 ± 0.008[b]	18.9 ± 4.9[ad]	0.13 ± 0.01[ceh]	0.992 ± 0.007[b]
MOHS	2.9 ± 0.3[c]	295.1 ± 99.7[b]	0.12 ± 0.01[b]	0.995 ± 0.006[b]	63.6 ± 19.8[b]	0.12 ± 0.01[bc]	0.994 ± 0.006[b]
MOCA	6.5 ± 0.7[a]	40.7 ± 10.1[a]	0.14 ± 0.01[bdf]	0.995 ± 0.004[b]	9.4 ± 2.1[ae]	0.15 ± 0.01[d]	0.989 ± 0.006[b]
MOCAL	10.8 ± 1.9[d]	124.2 ± 37.6[a]	0.14 ± 0.01[cdg]	0.994 ± 0.006[b]	31.9 ± 10.2[de]	0.13 ± 0.01[cf]	0.991 ± 0.009[b]
MOCAS	7.3 ± 1.2[a]	125.7 ± 20.1[a]	0.14 ± 0.01[efg]	0.997 ± 0.005[b]	31.7 ± 5.1[de]	0.14 ± 0.01[dhi]	0.994 ± 0.002[b]
MOCAH	6.2 ± 0.4[a]	53.0 ± 14.2[a]	0.13 ± 0.01[bg]	0.996 ± 0.004[b]	11.6 ± 2.6[a]	0.15 ± 0.01[dg]	0.990 ± 0.006[b]
MOCAHL	11.5 ± 1.1[d]	22.1 ± 6.6[a]	0.14 ± 0.01[bg]	0.993 ± 0.006[b]	5.4 ± 1.6[a]	0.12 ± 0.01[bef]	0.951 ± 0.028[b]
MOCAHS	2.4 ± 0.5[bc]	1148.6 ± 240.7[c]	0.14 ± 0.00[bg]	0.994 ± 0.004[b]	245.2 ± 45.8[f]	0.13 ± 0.00[cegi]	0.989 ± 0.007[b]

Note: Data for *MOHL* was not collected due to insufficient quantity of solid collected for the soluble fraction after treatment.

3.6 Macrostructure of Soymilk Gels

The macrostructure of soymilk and okara soymilk gels, examined from their visual appearance, color, homogeneity and void fraction deduced from binary representation of optical images of

the gel surface, are presented in **Fig. 4-7** and **Table 4-3**. The soymilk gel (***M***) and the soymilk gel with untreated okara (***MO***) had the whitest appearance while a yellow hue was observed in all soymilk gels with treated okara (**Fig. 4-7**). The colour difference may reflect the non-enzymatic browning as resulted from the Maillard reaction occurring between some amino acids and non-reducing sugars present in soymilk and okara [121], [149]. The presence of the multiple intermediates and products associated with the Maillard reaction is difficult to locate in the 1600-1200 cm^{-1} region of the FTIR spectra because of the presence of the citric-acid-associated bands [248] (**Fig. 4-7**B).

The homogeneity of the gel surface and the presence of dark regions were quite different according to gel composition. The soymilk gel (***M***) was the most homogeneous without any visible pores (**Fig. 4-7**A, **Table 4-3**). The soymilk gel with untreated okara (***MO***) was somewhat heterogeneous (**Fig. 4-7**B) with visible dark regions (**Table 4-3**). With the heat treatment, whole okara (***MOH***) did not render significant changes to the morphology of the soymilk gel compared to ***MO*** (**Table 4-3**). However, the surface of the soymilk gel with the insoluble solids content of the heat treated okara (***MOHS***) appeared to be more homogeneous, with lower estimated cell size and density as well as void fraction than the ***MO*** (**Fig. 4-7**D and **Table 4-3**).

Moreover, the soymilk gels with citric acid treated okara was considerably more uniform which displayed significant improvements of its homogeneity particularly for gels ***MOCAL*** and ***MOCAS*** when compared to ***MO*** (**Fig. 4-7**F,G). Both ***MOCAL*** and ***MOCAS*** had nearly ten-time lower void fraction when compared to ***MO*** (**Table 4-3**). This suggests that the soluble or insoluble portion of okara generated from the citric acid treatment played an active role, induced positive interactions with the protein network and improved the homogeneity of the soymilk gel. The additional heating step to the citric acid treatment of okara did not induce significant changes to the uniformity of the gel when the whole and the soluble solids of okara were added (***MOCAH, MOCAHL***) in comparison to the corresponding ***MOCA*** gels (**Fig. 4-7**E,F,H,I). However, ***MOCAHS*** was unique in that it had the most heterogeneous structure with large dark regions and increased void fraction (**Fig. 4-7**J, **Table 4-3**). As indicated previously, ***MOCAHS*** showed severe water syneresis. These observations suggest that the insoluble constituents of the citric acid-heat treated okara may act as inactive fillers embedded in the protein gel network,

preventing adequate protein interactions to form a cohesive network, resulting in syneresis and a coarse structure [249].
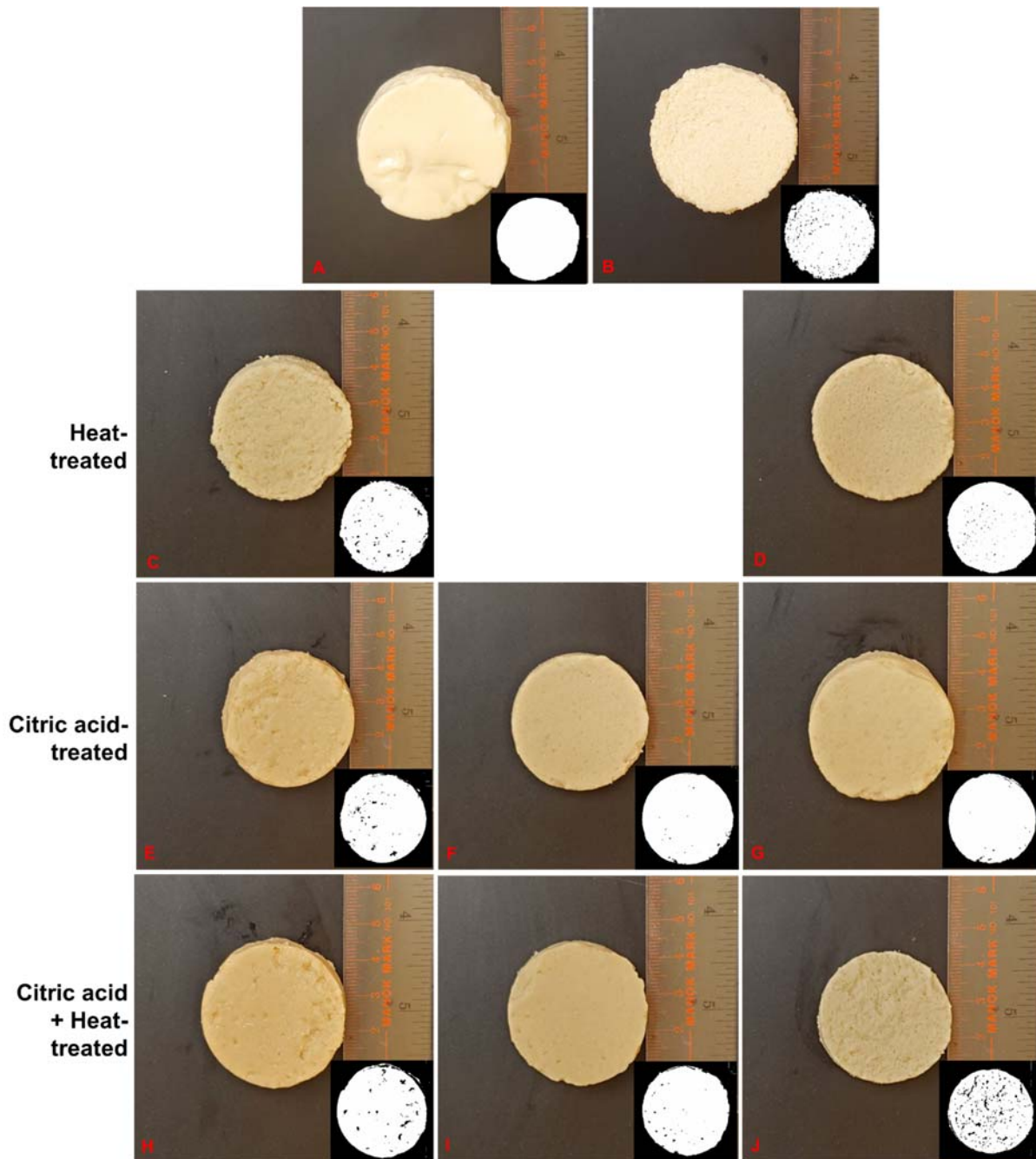

Fig. 4-7 Visual appearance and binary images of the gel cross-sectional area. Row 1: (A) soymilk gel (M); (B) untreated okara soymilk gel (MO). Row 2: heat treated okara soymilk gel: (C) whole (MOH); (D) insoluble solids (MOHS). Row 3: citric acid treated okara soymilk gel: (E) whole (MOCA); (F) soluble solids (MOCAL); (G) insoluble solids (MOCAS). Row 4: citric

acid with heat treated okara soymilk gels: (H) whole (MOCAH); (I) soluble solids (MOCAHL); (J) insoluble solids (MOCAHS).

Table 4-3 Homogeneity of the surface of soymilk and okara soymilk gels as determined by mean cell size, cell density and void fraction based on binary images.

Gel	Mean cell size (mm^2)	Cell density (cell/mm^2)	Void fraction (%)
M	0.03	0.00	0.01
MO	0.10	0.20	1.99
MOH	0.17	0.11	1.90
MOHS	0.07	0.10	0.64
MOCA	0.20	0.08	1.67
MOCAL	0.09	0.04	0.33
MOCAS	0.08	0.03	0.21
MOCAH	0.24	0.07	1.56
MOCAHL	0.15	0.04	0.64
MOCAHS	0.17	0.31	5.35

Note: Data for *MOHL* was not collected due to insufficient quantity of solid collected for the soluble fraction after treatment.

3.7 Microstructure of Soymilk Gels by Confocal Laser Scanning Microscopy (CLSM)

Microstructural analysis provides useful information of a food material that can be related to the mechanical properties, which in turn correlates to its sensory properties [211]. Depending on the types of microstructures, different textural and sensory characteristics may be expected. Generally, microstructure of protein-polysaccharide mixed gels can be classified based on the micrometer length scale into homogeneous and phase-separated structures. Phase-separated microstructure can be further classified into protein-continuous, bicontinuous, and coarse stranded types [211]. Among commonly used imaging techniques, confocal laser scanning microscopy (CLSM) is a non-invasive technique that requires minimum specimen preparation for structural imaging [208].

CLSM images of the various soymilk gels were obtained by staining the soy proteins with Rhodamine B (**Fig. 4-8**). The soymilk gel (*M*) showed a homogeneous structure and a uniform distribution of small protein aggregates (**Fig. 4-8**A), which was also observed *via* visual examination (**Fig. 4-8**A). The incorporation of untreated okara to the soymilk gels (*MO*) affected the homogeneity of the protein distribution as indicated by the appearance of disconnected

118

unstained regions disrupting the continuity of the stained protein regions (**Fig. 4-8**B). These unstained regions were identified as cotyledon cell wall materials [250]. The discontinuity in the protein network caused by the presence of these cotyledon cell wall materials confirms the previous report that soybean fibers reduce the crosslinking degree of heat-denatured proteins, and thus weakens and coarsens the gel structure [5].

The soymilk gel prepared with the heat treated okara still had substantial cotyledon cell wall materials, especially within the whole okara gel (*MOH*) (**Fig. 4-8**C). This suggests that heat treatment had minimal effect on the size of the cotyledon cell wall materials. In contrast, the citric acid treatment of okara (*MOCA, MOCAL, MOCAS*) reduced the quantity and size of the cotyledon cell wall materials, resulting in gels with a notably more uniform protein microstructure (**Fig. 4-8**E,F,G) resembling that of the soymilk gel (*M*). These observations confirm the visual analysis of the homogeneous surface of the citric acid treated okara gels (Fig. E,F,G) and are also supported by the FTIR analysis of okara, consolidating that large-molecular weight polysaccharides were hydrolyzed into smaller saccharides, and thereby significantly improved the incorporation of okara with the remaining gel matrix.

The combination of citric acid and heat treatment produced a soymilk gel where disrupted cotyledon cell wall materials remained visible when using the whole okara (*MOCAH*) (**Fig. 4-8**H). Considerable microstructural changes were observed with the soluble solids (*MOCAHL*), and insoluble solids (*MOCAHS*) compared to the respective citric acid treated okara fractions. Increased number and size of black voids were observed for *MOCAHL* (**Fig. 4-8**I). This agrees with the FTIR analysis where the additional heating notably altered the structure of okara polysaccharides, which may have limited the formation of a uniform protein network. Among all gels, the soymilk gel containing the insoluble solids of the combined heat and citric acid treated okara (*MOCAHS*) had the most significant microstructural changes. Clusters of large protein aggregates were disrupted by large unstained regions (**Fig. 4-8**J), which was likewise observed from the visual appearance of the gel surface (**Fig. 4-8**J). The microstructure of *MOCAHS* represented a coarse stranded gel network [211], [251]. Its coarse network with large cavities may explain the water syneresis that was uniquely observed with *MOCAHS* [201]. Coarse stranded gels typically have multiple fractures, accompanied by the coarsening of the network,

leading to a vague fracture surface [212]. This may explain the absence of compressive fracture associated with ***MOCAHS***.
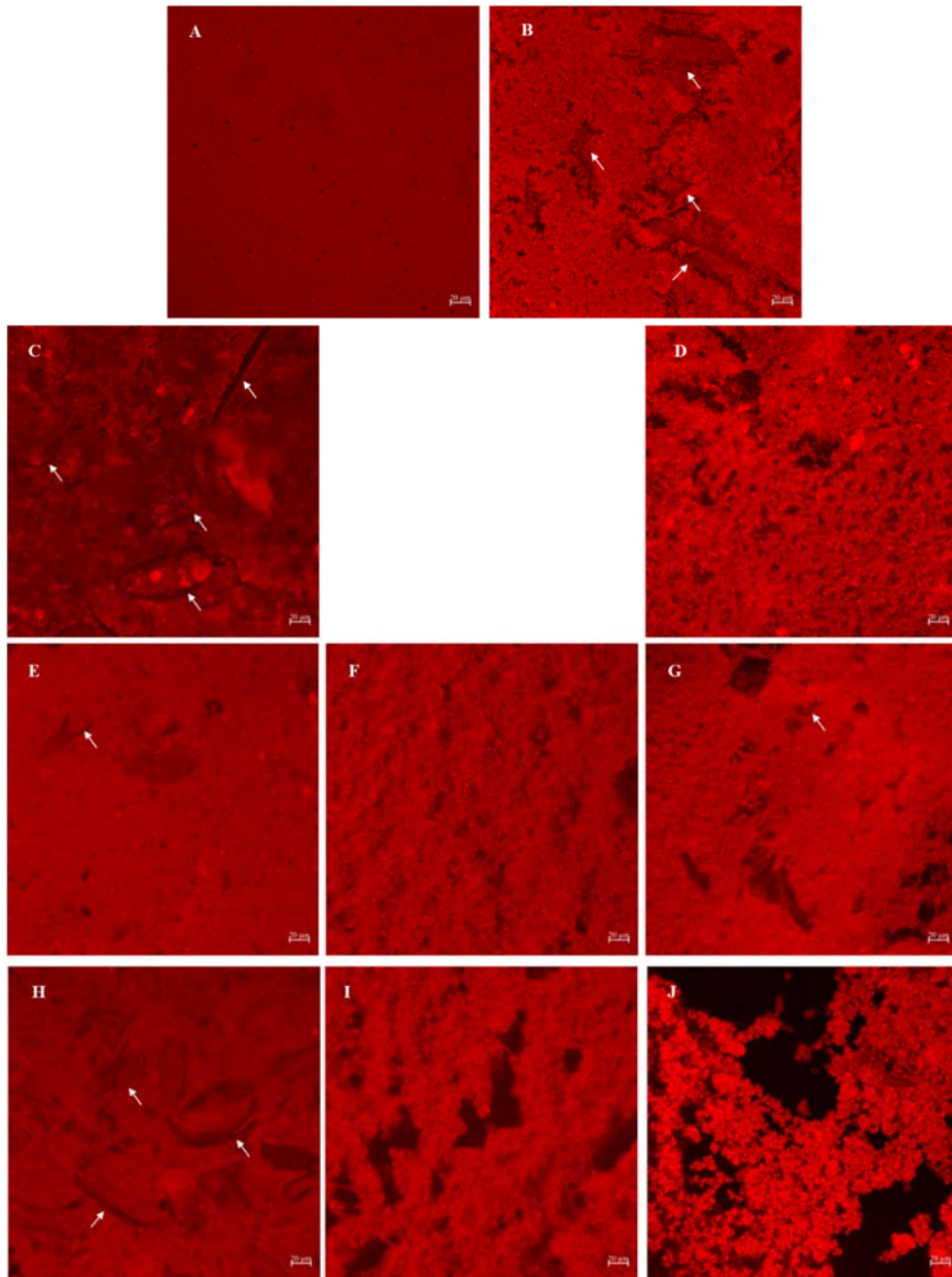

Fig. 4-8 CLSM images: (A) soymilk gel (M); (B) untreated okara soymilk gel (MO); heat treated okara soymilk gels: (C) whole (MOH); (D) insoluble solids (MOHS); citric acid treated okara soymilk gels: (E) whole (MOCA); (F) soluble solids (MOCAL); (G) insoluble solids (MOCAS); citric acid with heat treated okara soymilk gels: (H) whole (MOCAH); (I) soluble solids

(MOCAHL), (J) insoluble solids (MOCAHS). Red regions represent protein-rich areas. White arrows indicate the presence of disrupted okara cell wall. [Refer to the supplementary materials for authors' interpretations of images]

4 Proposed Mechanism

We have developed a hypothetical mechanism based on primarily the TGA and FTIR analyses of okara and the various soymilk okara gels developed and characterized in this study. The visual representation of the proposed mechanism, illustrated in **Fig. 4-9**, describes the modification of okara according to the heat and/or citric acid treatments and integrates the characteristics of the whole okara and its soluble and insoluble constituents. The soluble constituents consist of water-soluble components released from the okara matrix upon ultracentrifugation, and the insoluble constituents represent the water-insoluble components of the soy okara.
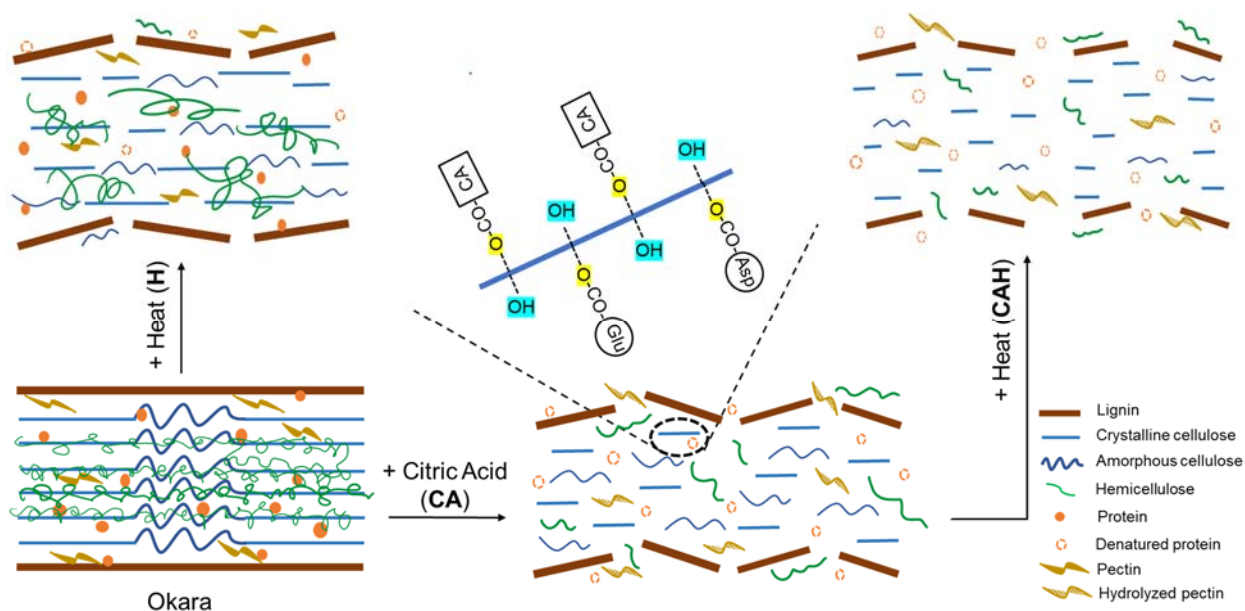

Fig. 4-9 Hypothesized mechanism of heat and citric acid treatments of okara.

Soy okara is complex and contains soluble non-starch components and insoluble dietary fiber from soybean cotyledon [107]. The cell wall of the soybean cotyledon is comprised of polysaccharides that are crosslinked with proteins and lignin [250]. The main constituents of the okara include cellulose, hemicellulose, lignin, pectic substances, and proteins. Cellulose, as the

121

major structural component of the okara, is the core of the matrix. Within the crystalline and amorphous regions of cellulose, strong intra- and intermolecular hydrogen bonds make cellulose highly insoluble while possessing high mechanical strength. Hemicellulose links with cellulose microfibrils *via* hydrogen bonds, and this network forms a strong backbone of plant cell walls [111]. Cellulose-hemicellulose frames are embedded in the amorphous matrices of pectic substances of okara [6]. Lignin can be found on the cell surface and acts as the barrier from the outside environment [111]. Okara contains 15-30% proteins [226] and is distributed throughout the matrix.

Heat treatment (**H**) had minimal effects on okara based on the characteristics investigated in this study. Slightly reduced FTIR band intensities at ~2920 and ~2854 cm^{-1} suggest that heat treatment may have broken some C-H bond of polysaccharides, such as hemicellulose, cellulose, and lignin, reducing them into smaller fragments (**Fig. 4-9**). Since the heat treatment had minimal effects on the properties of okara, the soymilk gel containing the heat treated okara remained coarse in structure and had comparable mechanical properties to the untreated okara soymilk gel (***MO***).

In contrast, the citric acid treatment (**CA**) caused substantial changes to the okara. Citric acid hydrolyzed okara fibers into smaller heat-sensitive saccharides (**Fig. 4-9**). During acid hydrolysis, increased number of hydroxyl groups of hemicellulose, cellulose, lignin, and/or pectin have been exposed as reactive sites for esterification reactions to take place. Moreover, **CA** treatment may have led to the unfolding of soy proteins, exposing their functional groups for the ease of the esterification reactions [252]. It is hypothesized that the soluble portion contains mainly the unreacted citric acid along with small-molecular-weight saccharides and soluble proteins. Conversely, the insoluble fraction is mainly composed of larger polysaccharides that were partially hydrolyzed. The soymilk gel containing **CA**-treated okara reflects the dissimilarities identified by FTIR and TGA, creating markedly different gels. The high mechanical strength of the gels containing the soluble (***MOCAL***) or the insoluble portions (***MOCAS***) of the okara may be explained by the formation of covalent bonds between sugar and protein *via* esterification and/or Maillard reactions, likely compensating for the reduced content of large okara fiber of high strength. Additionally, the ***MOCAL*** and ***MOCAS*** were characterized by a homogeneous and protein-continuous network that may relate to the small molecular-weight

saccharides generated upon acid hydrolysis and their improved incorporation with the remaining gel matrix.

The heating step following the citric acid treatment of okara (**CAH**) induced minor alterations to okara compared to the treatment with only citric acid. Decreased FTIR band intensities associated with the O-H and C-H bonds of okara polysaccharides suggest that more degradation of large-weight polysaccharides occurred due to the additional heating (**Fig. 4-9**). As a result, increased water-soluble constituents and reduced water-insoluble content were noted. The soymilk gel containing the insoluble portion of okara (***MOCAHS***) was unique. It did not fracture during compression, which unveils its high mechanical strength. This could be due to the larger degree of hydrolysis resulting from the additional heating, leaving the insoluble fraction to be predominantly constituted with crystalline polysaccharides that have exceedingly high mechanical strength. However, because of the poor incorporation of these insoluble constituents with the gel matrix, an exceptionally coarse and porous structure was observed along with inferior water holding ability.

5   Conclusions

In this study, the effect of three different treatments of okara, heat, citric acid, and their combination, was investigated with the goal of improving the integration of okara in soymilk gels produced by heat coagulation. The effect of the various okara treatments on its soluble constituents, thermal stability, functional groups and soymilk gel formation was investigated and revealed significant differences. The heat treatment of okara did not induce significant changes to the structural, mechanical, rheological, macrostructural, and microstructural properties of the okara and the okara containing soymilk gels. In contrast, citric acid treatment of okara prompted significant alterations to the structure of the okara fiber. Esterification reactions between the citric-acid-treated okara fiber and protein as well as potential Maillard reaction, could be attributed to a considerably more homogeneous gel matrix and improved compatibility of okara with the protein gel matrix. Citric-acid-treated-okara soymilk gel possessed high fracture stress and Young's modulus. It demonstrated the benefits of modifying okara with citric acid for developing high-fiber tofu products. The combined heat treatment and citric acid treatment (CAH) assisted hydrolysis of insoluble okara fiber to a larger degree compared to the treatment with only citric acid. Substantial heating of okara induced significant changes, especially to the

soymilk gel containing the insoluble portion of the okara. The soymilk gel containing insoluble CAH-treated okara was able to withstand high mechanical stress, but it exhibited an extremely inhomogeneous, coarse stranded type of microstructure with severe water syneresis. Soymilk gels containing the soluble and insoluble okara constituents for all treatments displayed inferior mechanical, rheological, and structural properties as compared to the corresponding okara soluble and insoluble constituents. This supports the benefits of okara fractionation *via* centrifugation. Additionally, treating with citric acid avoids excessive conversion of insoluble to soluble fibers, while offering high utilization of water-insoluble okara. On the contrary, additional heat treatment can cause a drastic decrease in the utilization of insoluble okara solids, thereby limiting the integration of okara fiber in tofu production.

Further studies should examine the citric acid and heat treatment levels to understand the effect of citric acid and to optimize the properties of soymilk gels containing okara.

6   Declaration of Competing Interest

The authors state that there are no competing financial interests or relationships that may have influence on the work reported.

5.0 Manuscript 2 Physicochemical and Nutritional Profiles of Commercial Dairy Cheeses, Tofu, and Plant-Based Cheese Analogues

5.1 Synopsis

The purpose of this manuscript was to establish the baseline profile of commercially available food products including dairy cheeses, plant cheese analogues, and tofu. The finding serves as basis for creating plant-based cheese analogues and may aid in the selection of formulation and processing conditions.

This manuscript was submitted to Journal of Food Engineering and is currently under review.

Physicochemical and Nutritional Profiles of Commercial Dairy Cheeses, Tofu, and Plant-Based Cheese Analogues

Overview

Plant-based cheese analogues have received rising attention due to the associated environmental sustainability and health considerations. However, the development of plant-based cheese with desired attributes is limited because of the lack of characterizations of their properties. In this study, the physicochemical properties of several commercial dairy cheeses, soybean-based products and vegan cheeses were characterized. The commercial mozzarella- and cheddar-style vegan cheeses had exceedingly high mechanical strength and gel rigidity along with excellent water holding capacity (WHC). However, the vegan cheeses were considerably different than pizza or fresh mozzarellas in their properties, but they possessed analogous characteristics to those of paneer. In contrast, tofu products had the lowest mechanical strength of all products with poor WHC. Finally, the carbohydrate and fat components of the products had the most significant correlations with several mechanical and viscoelastic properties ($p < 0.005$). These findings indicate the significant differences between plant-based and dairy cheeses, supporting the need for improvements, such as manipulating their composition.

Keywords: plant-based cheese, tofu, physicochemical, texture, rheology, correlation

1. Introduction

The environmental impact of animal products considerably exceeds that of plant substitute. A plant-based diet has shown to reduce farmland use by 3.1 million-hectare, food's greenhouse gas emission by 6.6 billion metric tons of CO_2-equivalent, acidification and eutrophication effects by 50% and 49%, respectively [24]. The plant-based diet has seen significant growth with $7.4 billion of total sales for 2021 in USA [253] and is often associated with numerous potential health benefits [254].

Plant-based cheese analogues, also known as cheese substitutes or imitation cheeses, experienced a 28% growth in sale from 2019 to 2020 reaching $1.9 billion in USA [25]. They are made by blending various ingredients of plant origin, including carbohydrates, fats, proteins, and gelling

agents, to create a cohesive cheese-like mass [5, 6], contrasting the use of animal milk to produce traditional dairy cheeses. However, the development of cheese analogues with high protein content has been limited by the lack of plant proteins with structure and function similar to casein micelles, the major milk proteins [256]. Hence, most existing commercial plant cheese analogues rely on fat and carbohydrate constituents, and hydrocolloids, resulting in minimal protein content (> 8-fold lower), high carbohydrate content (5-7 times higher) and higher costs, as compared to commercial dairy cheese [257].

The texture attributes of cheese products largely define their quality [258]. Cheeses are viscoelastic materials with textures ranging from soft to hard, and plant-based cheeses are designed to have similar appearance, texture, and flavour as animal-based cheeses [256]. Thus, for plant-based cheese analogues to achieve comparable attributes with dairy cheeses requires a comprehensive mapping of the characteristics of commercial products.

A recent study evaluated the physicochemical and structural properties of commercial plant-based imitation cheese blocks as alternatives to conventional cheddar and processed cheese [257]. Several plant-based cheese analogues illustrated comparable textural and viscoelastic attributes to conventional cheddar cheese [257]. The properties of other types of commercial plant-based cheeses and their comparison to dairy cheese have not been reported in the scientific literature. This leads to the investigation of other types of commercial cheese products, such as high production volume cheeses, *i.e.*, dairy mozzarella and paneer cheese, and compares these products to mozzarella- and cheddar-style vegan cheeses as well as soy protein food products, such as tofu.

Fresh mozzarella, also known as high-moisture mozzarella, is a soft cheese with overlaying layers that form pockets containing liquid of milky appearance [18]. Pizza mozzarella, or low-moisture mozzarella, is a firm or semi-hard cheese generally consumed melted. Paneer, a South-Asian cheese, is made by thermal and acid coagulation without microbial influences [259].

Soy is used extensively as a plant protein source for plant-based cheese substitutes [7, 11], mainly because of its low saturated fat and cholesterol contents [261]. Soy is also used to produce tofu and tempeh, examples of cheese-like products originated from Asia. Tofu production is analogous to that of the selected dairy cheeses, as it is made by heating and salt or

127

acid coagulation and pressed into a solid mass. Tempeh is made from fermented, dehulled, and boiled soybeans to form a compact, white, and cake-forming product [262].

The objective of this study was to compare specific commercial dairy cheese, soy products and plant-based cheese analogues by characterizing their thermal properties, as affected by compositions, and their mechanical, rheological, and WHC properties to obtain texture attributes of the products. The selected commercial products include mozzarella and paneer cheeses, soy tofu, tempeh, and plant-based cheese analogues. Results are complemented with correlation analyses to identify potential associations. The finding will serve as a baseline for creating plant-based cheese analogues and may aid in the selection of formulation and processing conditions.

2. Materials and methods

2.1 Materials and Composition

All commercial products were purchased from local supermarkets in Waterloo, Ontario (Canada). The commercial products are broadly classified into three categories, dairy cheeses, soybean-based products, vegan or plant cheese analogues. The dairy cheeses include fresh mozzarella log (FM), pizza mozzarella (PM), and paneer cheese (P). The soybean-based products include extra firm tofu (EFT), medium firm tofu (MFT), and tempeh (T). The vegan imitation cheeses comprise of mozzarella style block vegan cheese (VM) and medium cheddar style block vegan cheese (VC). The nutritional value and ingredient list provided by the manufacturer for these products are presented in **Table 5-1**.

All characterizations were performed prior to the expiration date based on individual product packaging. Unused samples were wrapped in aluminum foil and stored (4 °C) in airtight Ziplock bags for later use to prevent moisture loss.

Table 5-1 Nutritional composition of commercial products according to the manufacturer ingredient list on wet-weight basis.

Product	Protein (%)	Fat (%)	Carbohydrates (%)	Moisture1 (%)	Ingredient List
Fresh mozzarella (FM)	19.1	19.1	0	61.8	Pasteurized milk, Bacterial culture, Salt, Microbial enzymes, Calcium chloride

Pizza mozzarella (PM)	23.3	26.7	3.3	46.7	Pasteurized milk, Modified milk ingredients, Salt, Bacterial culture, Calcium chloride, Microbial enzyme
Paneer (P)	25.5	21.8	3.6	49.1	Pasteurized milk, Condensed whey, Citric acid
Extra firm tofu (EFT)	16.5	9.4	3.5	70.6	Water, Soybeans (non-GMO), Magnesium chloride, Calcium sulphate
Medium firm tofu (MFT)	8.2	4.7	2.4	84.7	Water, Soybeans (non-GMO), Calcium sulphate, Glucono-delta-lactone
Tempeh (T)	20	9.4	8.2	62.4	Soybeans, Water, Apple cider vinegar, Starter culture (rice, water, rhizopus oligosporus)
Vegan mozzarella (VM)	0	20	22.5	57.5	Water, Refined coconut oil, Modified potato starch, Modified tapioca starch, Sea salt, Natural flavors, Sorbic acid, Carotene
Vegan cheddar (VC)	3.6	21.4	25	50	Oat base (filtered water, gluten-free oat flour), Coconut oil, Modified potato starch, Natural flavours, Salt, Chickpea protein, Chickpea flour, Lactic acid, Annatto (color)

[1] Calculated based on mass balance assuming other constituents are negligible.

2.2 Thermogravimetric Analysis (TGA)

The thermal behaviour of the commercial products was obtained by TGA carried out in a TA Instrument (TGA Q500). In each test, 15 ± 2 mg of the product was heated from room temperature to 600 °C at 10 °C/min. All tests were carried out under nitrogen with a 40 and 60 mL/min flowrate for purge and balance streams, respectively. Variation of the residual mass with respect to temperature was collected automatically. The derivative thermogravimetric (DTG) was constructed and presented as the rate of weight loss over temperature.

2.3 Water Holding Capacity (WHC)

Samples were cut into 20 mm diameter cylinders using a metal corer then weighed (W_t) and placed into 50-mL Falcon centrifuge tubes. Samples were centrifuged in a centrifuge (Eppendorf

5810) at room temperature for 20 min at three different centrifugal forces, *i.e.*, 4,062 x g, 8,119 x g, and 12,074 x g.

After centrifugation, two methods were followed to measure the weight of released water (W_r). In the first method, where there was significant amount of water released from centrifugation, the released water was decanted into a pre-tared container. The water remaining on the surface of the centrifuge tube wall was then absorbed using a pre-tared Kimwipe. The total weight of the decanted water and the absorbed water on Kimwipe was denoted as W_r. The second method was employed when the released water was not substantial to be decanted. The initial weight of the empty centrifuge tube was measured. After centrifugation, the sample was carefully removed using a tweezer and dabbed on a pre-tared Kimwipe. The empty centrifuge tube that had moisture on the wall was weighed again. Hence, in the second method, W_r is the total weight of the absorbed water on Kimwipe and the difference of the weight of the empty tube before and after centrifugation.

The water holding capacity was calculated according to **Equation 9**.

$$WHC\ (\%) = 100\% \times \frac{W_t - W_r}{W_t} \qquad \textbf{Equation 9}$$

Where, W_t is the initial sample weight (g), and W_r is the weight of the released water (g), calculated accordingly to the first or second method.

If the measured WHC of a sample was nearly 100% at the highest centrifugal force (12,074 x g), then the WHC was not measured at lower centrifugal forces and was assumed to be 100%.

2.4 Uniaxial Compression

Uniaxial compression was performed using a mechanical tester (Shimadzu Autograph AGS-X) with 50 N and 500 N load cells. A cylindrical sample, 20 mm diameter and 10 mm height, was cut from the main product immediately after taken out of a fridge using a metal corer [229]. The central portion of the sample was used to avoid the skin effect formed on the outmost layer of the product [78]. Samples were allowed to equilibrate at room temperature for 1 h prior to measurement. The samples were compressed at 40 mm/min uniaxially until fracture was visually observed. All tests were conducted at room temperature. Initial measurements were obtained with a 500 N cell as load. Measurements were completed for seven replicates when fracture was

clearly observed. If no clear fracture was observed, an indication of the high softness of the sample, a 50 N load cell was employed and shown to be sufficiently sensitive for the detection of the fracture with the testing of seven replicates.

The Hencky stress and strain, also known as the true stress ($\sigma(t)$) and true strain (ϵ), were determined according to **Equation 10** and **Equation 11**, respectively [230].

$$\sigma(t) = \frac{F(t)}{A_0} \times \frac{l(t)}{l_0}$$ **Equation 10**

$$\epsilon = -\ln\left(\frac{l(t)}{l_0}\right)$$ **Equation 11**

Where, l_0 and A_0 are the original height and area of the sample, respectively; $l(t)$ and $F(t)$ are the height and force at time t, respectively.

True fracture stress was measured as the maximum point of the stress-strain curve [182]. The MAX function in Excel (Microsoft 365, version 2202) was used to identify the maxima up to a strain where a clear decline in stress was observed. True fracture strain was the strain corresponding to the maximum point of the true stress-strain curve. Young's modulus was determined in the linear region of the true stress-strain curve located between one and two-thirds of the way to the point of maximum true stress [231].

2.5 Viscoelastic Measurements

The small amplitude oscillatory shear test was performed using a rheometer (Thermo Scientific HAAKE MARS III) with 35 mm in diameter and 1 mm gap parallel plates. Samples were cut from the central portion of the original product into thin disk or squares that have a diameter or length greater or equal to 35 mm, and around 1.5 mm in thickness using a cheese slicer with metal wire. Samples were allowed to equilibrate at room temperature for 1 h after cutting.

Samples were loaded initially at room temperature into a 4 mm gap space. The lift speed was set to 1.25 mm/min when closing the gap to minimize abrupt uniaxial deformation. Samples were then trimmed at a gap space 0.025 mm higher than the measuring position of 1 mm to optimize the filling. After reaching the measuring position of 1 mm, samples were allowed to rest for an additional 10 min to ensure that mechanical equilibrium was reached.

The strain sweep test was conducted once for each product type with a strain range of 0.01 – 100% at 1 Hz. Seven repetitions for the acquisition of each data point were employed to improve data accuracy. The yield strain or the strain at the end of the linear viscoelastic region (LVR) is defined as the applied strain at which irreversible plastic deformation is first observed across the specimen [263].

The frequency sweep test was conducted in triplicates for each product at an angular frequency range of 1 – 100 rad/s for 0.1% strain, which was within the LVR for all samples as determined from the strain sweep test. Twenty-five repetitions were adopted for the acquisition of each data point.

A power law model was used to characterize the angular frequency (ω) dependence on the dynamic moduli, G' and G'' using **Equation 12** and **Equation 13** [195].

$$G' = G_0'\omega^{n'} \hspace{4cm} \textbf{Equation 12}$$

$$G'' = G_0''\omega^{n''} \hspace{4cm} \textbf{Equation 13}$$

Where, G_0' (Pa) and G_0'' (Pa) are storage and viscous moduli at 1 rad/s, respectively. G_0' is the energy stored and recovered per cycle of sinusoidal shear deformation. The increase in G_0' indicates rigidity of the material associated with the formation of an elastic gel structure. G_0'' is the energy dissipated or lost as heat per cycle of sinusoidal strain and indicates the extension of the viscous element in the material [195]. The exponents n' and n'' (dimensionless) denote the influence of ω on each modulus.

The tangent delta (tan δ) is defined as the ratio between the loss modulus (G'') and storage modulus (G'), as illustrated in **Equation 14**. It quantifies the energy absorption or dissipation of a material.

$$\tan \delta = G''/G' \hspace{4cm} \textbf{Equation 14}$$

2.6 Statistical Analyses and Correlation

The statistical significance of the experimental results was examined using by one-way ANOVA with the Statistica package program (version 14.0.0.15, TIBCO software Inc.). The Tukey test was used as a multiple comparison test for comparing the statistical difference between paired

means. Means are significantly different if $p \leq 0.05$, and not significant different if $p > 0.05$ [218]. Graphs were constructed in Origin (OriginPro 9.0.0, OriginLab Corp.).

A correlation matrix based on the Pearson correlation coefficient between two sets of data was created using the Statistica software (version 14.0.0.15, TIBCO software Inc.). The sets of data included WHC, mechanical, rheological, and composition of the six commercial samples (FM, P, EFT, MFT, VM and VC).

3. Results and Discussion

3.1 Thermogravimetric Analysis (TGA)

The thermal stability of the commercial products investigated reflects their various and distinct constituents (**Table 5-1**). All products degraded in multiple stages, as presented in **Fig. 5-1**A, with the major decomposition peaks displayed in their DTG (**Fig. 5-1**B).

The TGA profiles were divided into four stages. The first stage up to 150 ℃ is associated with the weight loss caused by the evaporation of water and other volatile materials [162]. The second stage from 150 to 240 ℃ can be associated to the degradation of heat-sensitive components, which could involve smaller-molecular weight saccharides. The third stage, from 240 to 400 ℃, corresponds to the degradation of backbone peptide bonds of proteins in protein-rich materials [23, 24], *e.g.*, dairy cheeses and tofu, or the degradation of polysaccharides such as starch [165] as largely present in the vegan cheeses. The last stage, from 400 to 600 °C, refers to the decomposition of heat-stable constituents.

The thermal degradation profile of the selected commercial products was similar for most products except tempeh and vegan cheddar (**Fig. 5-1**). The dairy cheeses (FM, PM, P) and the tofu products (EFT, MFT) had similar thermal decomposition profiles with minimal mass loss occurring in the first two stages and most weight loss taking place during the third stage (**Fig. 5-1**A). The three dairy cheeses had a major degradation peak at around 330 °C at a rate of ~8 %/min, which was associated with the decomposition of milk protein and fat [264]. Although pizza mozzarella had the lowest moisture content, its weight loss below 150 °C was double that of the dairy cheeses (**Table S. 6** Supplementary), and this could be associated with the presence of volatile constituents. The medium firm and extra firm tofu products had a single decomposition peak at 328 and 362 °C, respectively, at a rate of about 5.5 %/min (**Table S. 6**

Supplementary), which may relate to the protein constituent [163]. In contrast, tempeh had a significant weight loss during the first stage (~23%), followed by a more gradual weight loss in the second stage, and a more rapid weight loss during the third stage (**Fig. 5-1**A). The significant mass loss below 150 °C may reflect the volatile components generated from the fermentation of soybeans in tempeh preparation [265]. The vegan cheddar (VC) had a unique and distinct thermal degradation profile compared to all other products with about 43 % weight loss in the first stage, negligible weight loss in the second stage and a more gradual weight loss in the third stage. This is unexpected since the major ingredients of VC and VM products are similar (**Table 5-1**). This difference might be related to the variations in the processing of the ingredients.
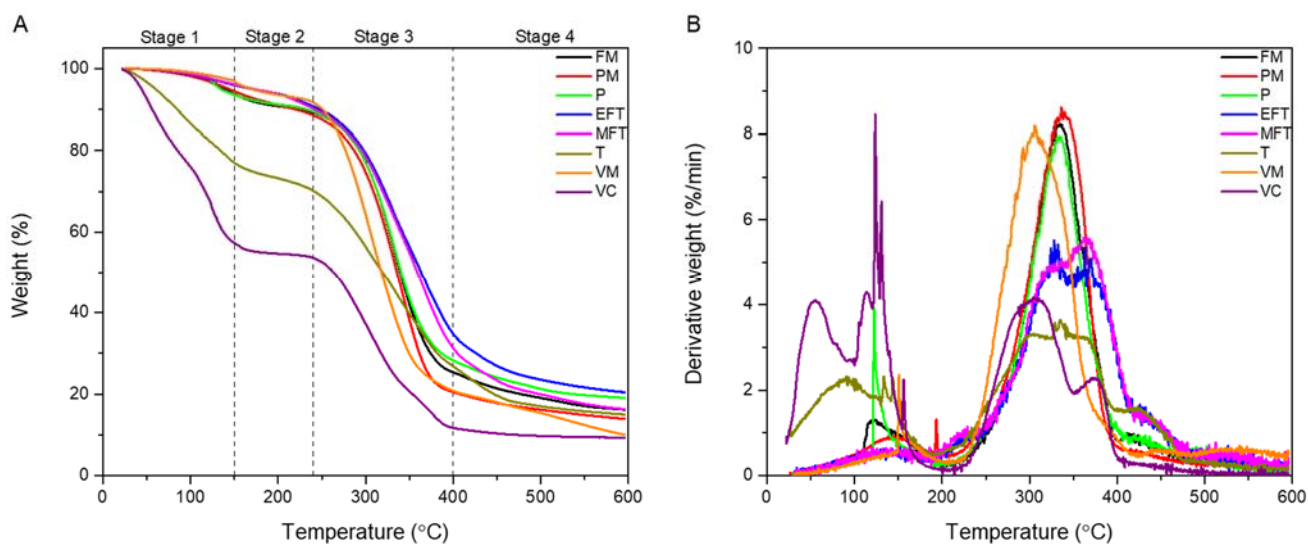
Fig. 5-1 TGA (A) and DTG (B) graphs of commercial products. Abbreviations: FM, fresh mozzarella; PM, pizza mozzarella; P, paneer; EFT, extra firm tofu; MFT, medium firm tofu; T, tempeh; VM, vegan mozzarella; VC, vegan cheddar.

3.2 Water Holding Capacity (WHC)

The water holding capacity (WHC) of a gel is considered an indicator of its stability, syneresis, microbial safety, and functional properties, such as strength and microstructure [266]. It also represents the ability of a material to immobilize water by capillary effects within the matrix [200]. Materials with a coarse structure and large pores tend to bind water to a lower extent because of low capillary forces [201]. WHC is generally estimated by centrifugation at a

predetermined g-force and time [267]. The parameters for centrifugation in the literature appear to be selected arbitrarily. As these conditions will impact the water movement, the WHC was measured for different centrifugal forces while keeping the duration of the centrifugation constant.

The WHC of the commercial products can be organized into two groups (**Table 5-2**). The first group of products has a WHC of nearly 100% at the highest centrifugal force, *i.e.*, the two vegan cheeses and paneer. The WHC was not estimated at lower centrifugal forces for these products. The vegan cheeses contain starch which is known for its ability to swell and immobilize water due to gelatinization [232]. The high WHC of paneer may be attributed to its compact protein matrix that was exceptional in immobilizing water [28, 29]. The second group consists of those products with a significantly lower WHC at the highest centrifugal force, including fresh mozzarella (FM) and the two tofu products. These products had poorer ability to retain water in their matrices. The extra firm tofu had slightly higher WHC than medium firm tofu for a given centrifugal force, which may be related to its more compact structure as well as the use of magnesium chloride as the coagulant instead of glucono-δ-lactone (GDL) (**Table 5-1**) since the salt-induced tofu gel tends to have lower syneresis than acid-induced gel [74]. The WHC characteristics of the tofu and dairy cheese may reflect the different surface hydrophilicity of their respective proteins (β-conglycinin, glycinin and casein), thereby creating distinct gel matrices [6, 33].

The WHC estimates can be quite sensitive to centrifugal force conditions (**Table 5-2**). The WHC estimates at the lowest centrifugal force, *i.e.*, 4,062 x g was significantly different for all three products when compared to the estimates at the two higher centrifugal forces ($p < 0.05$) while the WHC estimates at the two higher centrifugal forces, *i.e.*, 8,119 and 12,074 x g were not statistically different ($p > 0.05$). Hence, care should be taken when selecting centrifugation conditions to assess WHC.

Table 5-2 Water holding capacity (WHC) of commercial products as centrifuged at different centrifugal forces for 20 min. Values expressed as means of 3 replicates ± standard deviation. Means in the same column (indicated by the first letter) or row (indicated by the second letter) that do not share a common superscript letter are significantly different. Pizza mozzarella and tempeh were not evaluated. Abbreviations can be referred to **Fig. 5-1**.

Products	Water Holding Capacity (WHC) (%)		
	Centrifugal force (x g)		
	4,062	8,119	12,074
FM	87.9 ± 1.45^{ai}	78.6 ± 2.19^{cj}	72.6 ± 2.66^{dj}
P	NM[1]	NM[1]	99.5 ± 0.20^{e}
EFT	88.4 ± 0.53^{ak}	82.6 ± 2.81^{cl}	78.3 ± 3.47^{fl}
MFT	84.6 ± 0.40^{bm}	75.0 ± 4.99^{cn}	68.8 ± 1.00^{dn}
VM	NM[1]	NM[1]	99.9 ± 0.07^{e}
VC	NM[1]	NM[1]	99.9 ± 0.04^{e}

[1]Not measured.

3.3 Mechanical Properties of Commercial Products

Uniaxial compression provides information related to the textural attributes of soft foods [180]. Fracture stress, measured as the maxima of a stress-strain curve [182], is often referred to as gel strength [32]. Fracture strain is associated with the deformation capacity of a food material [182] and the Young's modulus is related to the sensory firmness of food [32].

Tempeh was crumbly and heterogeneous such that a representative sample could not be prepared. Two different test loads, 50 N and 500 N, were used to cover the wide range of textures. The former load was used for fresh mozzarella (FM) and medium firm tofu (MFT), while the latter was used for all the other products because of their higher stiffness. All products fractured up to a true strain value of 2. Typical true stress and strain curve of the various products is illustrated in **Fig. 5-2** where different fracture behaviors were observed.

The two vegan cheeses displayed clear and sharp fracture at significantly higher stress than the other products (**Fig. 5-2**), suggesting that the two vegan cheeses possessed high gel strength [32]. Also, the pizza mozzarella (PM), panner (P) and extra firm tofu (EFT) displayed somewhat clear fracture with higher fracture stresses than MFT and FM, but lower than the two vegan cheeses. In contrast, the MFT and the FM displayed vague fracture points reflecting their low stress and weaker gel strength.

The mechanical properties, presented in **Fig. 5-3**, will be discussed according to product types. The three dairy cheeses displayed significantly different true fracture stress, true fracture strain, and Young's modulus ($p < 0.05$). PM had higher true fracture stress and Young's modulus, but lower fracture strain than the other two dairy cheeses. This suggests that PM was firmer in

texture [32] while being less resistant to deformation [182]. In contrast, FM possessed the lowest fracture stress and Young's modulus but the highest fracture strain among all products, pointing to its weak strength but having excellent resistance to deformation, which might be related to its high springiness (visual observation). The distinct mechanical properties of PM and FM could be related to the differences in their preparation and in the desired mode of consumption, *i.e.*, consumed heated or fresh. Paneer, on the other hand, demonstrated mechanical properties that were in between the two mozzarella cheeses. The EFT and MFT had relatively low fracture stress and Young's modulus but high fracture strain. The inferior mechanical properties of tofu and FM agrees with the poor WHC (**Table 5-2**). EFT had about two-fold higher fracture stress and Young's modulus than the MFT, and thus EFT was a firmer and stronger gel [32] possibly because of its lower moisture content resulting from more intense pressing steps and different coagulation conditions. Lastly, the fracture stress and Young's modulus of the two vegan cheeses were at least 1.5 times higher than all the other products. Vegan cheddar (VC) had significantly higher Young's modulus than the vegan mozzarella (VM) ($p < 0.05$), which alludes to the firmer characteristic often associated with conventional cheddar cheese.

The mechanical properties of the VM were the closest to those of PM, supporting the manufacturing goal in imitating the texture of pizza-mozzarella type of cheeses. The fracture strain and Young's modulus of paneer were similar to those of EFT ($p > 0.05$) such that EFT may be an acceptable plant-based substitute based on texture attributes. The MFT may be considered an appropriate substitute for FM in terms of texture, as they exhibit comparable firmness, *i.e.*, fracture stress and Young's modulus ($p > 0.05$).
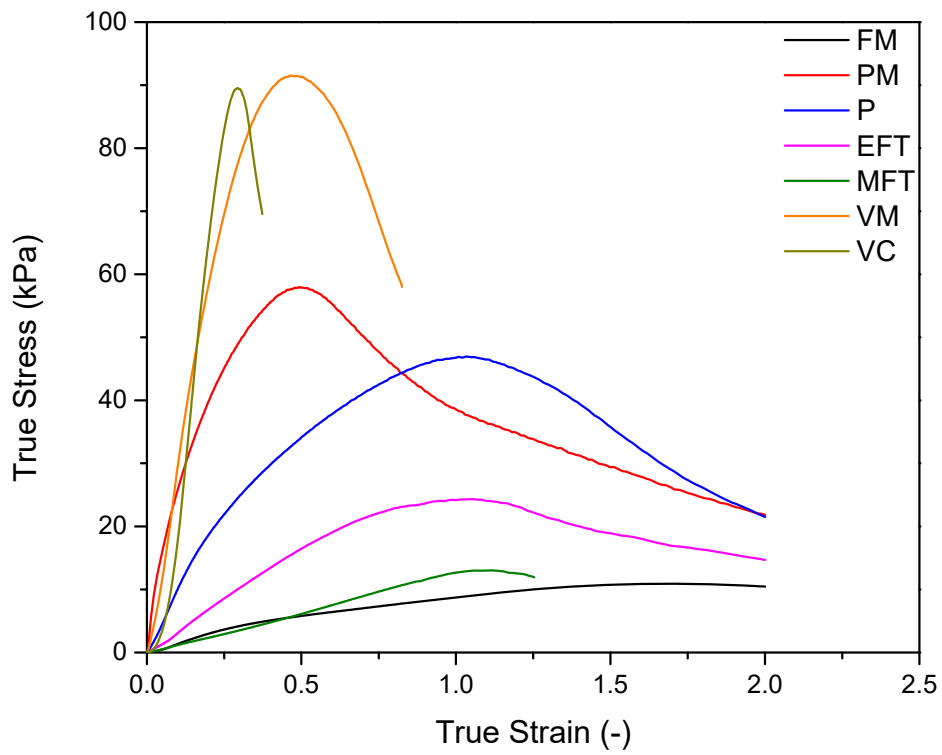
Fig. 5-2. Typical true stress-strain curves of commercial dairy cheese, tofu and vegan cheese products. Abbreviations can be referred to **Fig. 5-1**.
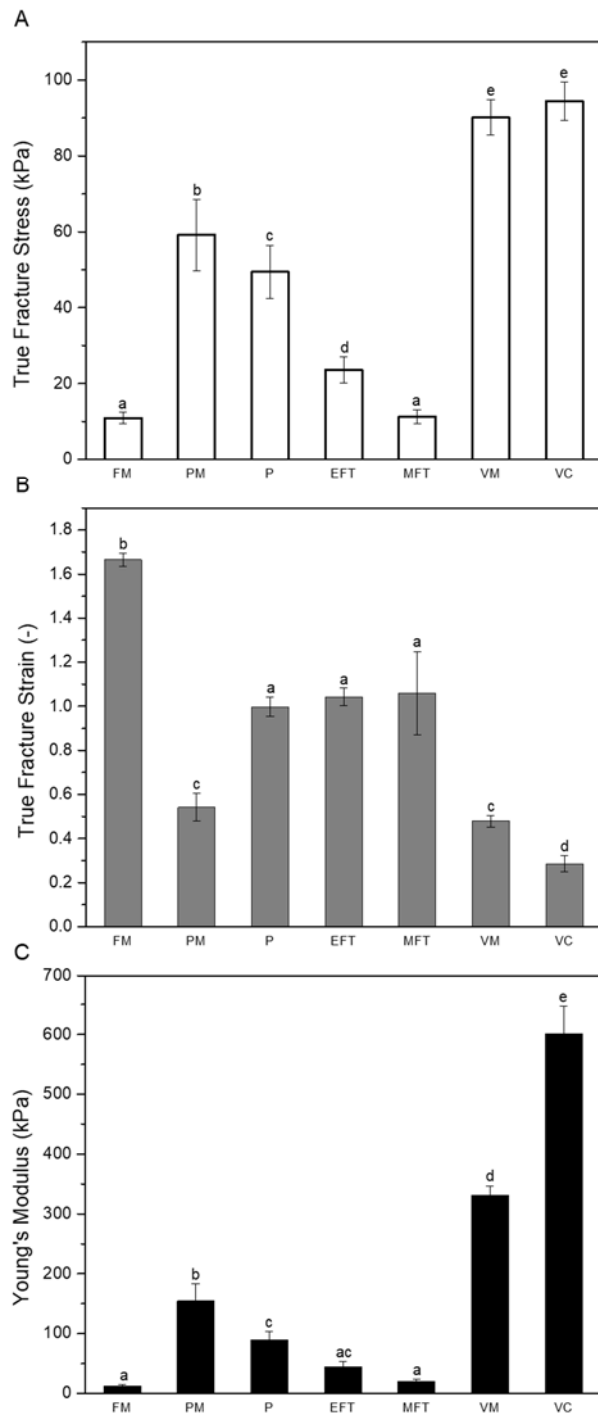
Fig. 5-3. True fracture stress (A), true fracture strain (B), and Young's modulus (C) of commercial products. Data expressed in mean ± standard deviation (n=7). Means that do not share a common letter are statistically different. Abbreviations can be referred to **Fig. 5-1**.

3.4 Viscoelastic Properties of Commercial Products

Shearing is an important motion in food breakdown during consumption. The behavior of food materials under shearing can be obtained from their rheological characteristics together with information on the strength and microstructure of gel materials [94].

The linear viscoelastic region (LVR) of the products, obtained from strain sweep tests, indicates an initial constant storage modulus (G') followed by a sudden decrease in G' with increasing strain (**Figure S. 6** Supplementary), which implies the breakdown of bonds within the gel network [195]. The end-of-LVR strain or yield strain, the strain at which the storage (G') and loss (G'') moduli change with strain amplitude [195], was lower for dairy and vegan cheeses but higher for tofu products (**Figure S. 6** Supplementary). This suggests that dairy and vegan cheeses had lower resistance to shear, whereas tofu products were the opposite [195].

Based on the LVR profile, a 0.1% strain was selected to conduct frequency sweep tests such that all products were well within the LVR. The typical storage modulus, G', loss modulus, G'', and tan δ of the products as a function of angular frequency is presented in **Fig. 5-4**. G' and G'' are related to the capacity of a material to store energy elastically and dissipate stress through heat, respectively [247]. All products demonstrated clear gel-like behaviour with significantly higher G' than G'' (**Fig. 5-4**). When the magnitude of G' is less than ten times higher than G'', a weak gel behaviour is suggested [197], and it was observed for the dairy cheese and tofu products but not for the two vegan cheeses. These findings consolidated the uniaxial compression observations, where clear rupture was observed for the vegan cheese confirming their strong gel behaviour. In contrast, a weak gel-like behaviour was noted for the other products [246], where they mostly underwent progressive breakdown.

The magnitude of G' and G'' varied significantly among products (**Fig. 5-4**). The VC had the highest G', around 1000 kPa, while MFT and PM had the lowest G', around 100 kPa (**Fig. 5-4**A). VM and paneer had relatively high G', in the range of 600-1000 kPa while EFT and FM had lower G', in the range of 300-500 kPa. The magnitude of G'' according to product type differed from the magnitude of G'. Paneer had the highest G'' values, whereas the two vegan cheeses had lower G'' (**Fig. 5-4**B).

The relative variation between G' and G" was captured by the tan δ estimates, the ratio between G'' and G', referred to as the index of a material's viscoelasticity [247]. All products were characterized by tan δ < 1 (**Fig. 5-4**C), an indication of a more solid-like behaviour [269]. Furthermore, as noted by a tan δ > 0.1, all products except the two vegan cheeses possessed a weak gel behaviour [38, 41], aligning with the results of the G' and G'' magnitudes. The tan δ estimates clustered according to product types. Dairy cheeses had the highest tan δ, followed by the tofu products and vegan cheeses. This suggests that the dairy cheeses had the weakest gel behaviour while vegan cheeses possessed the strongest gel behaviour.
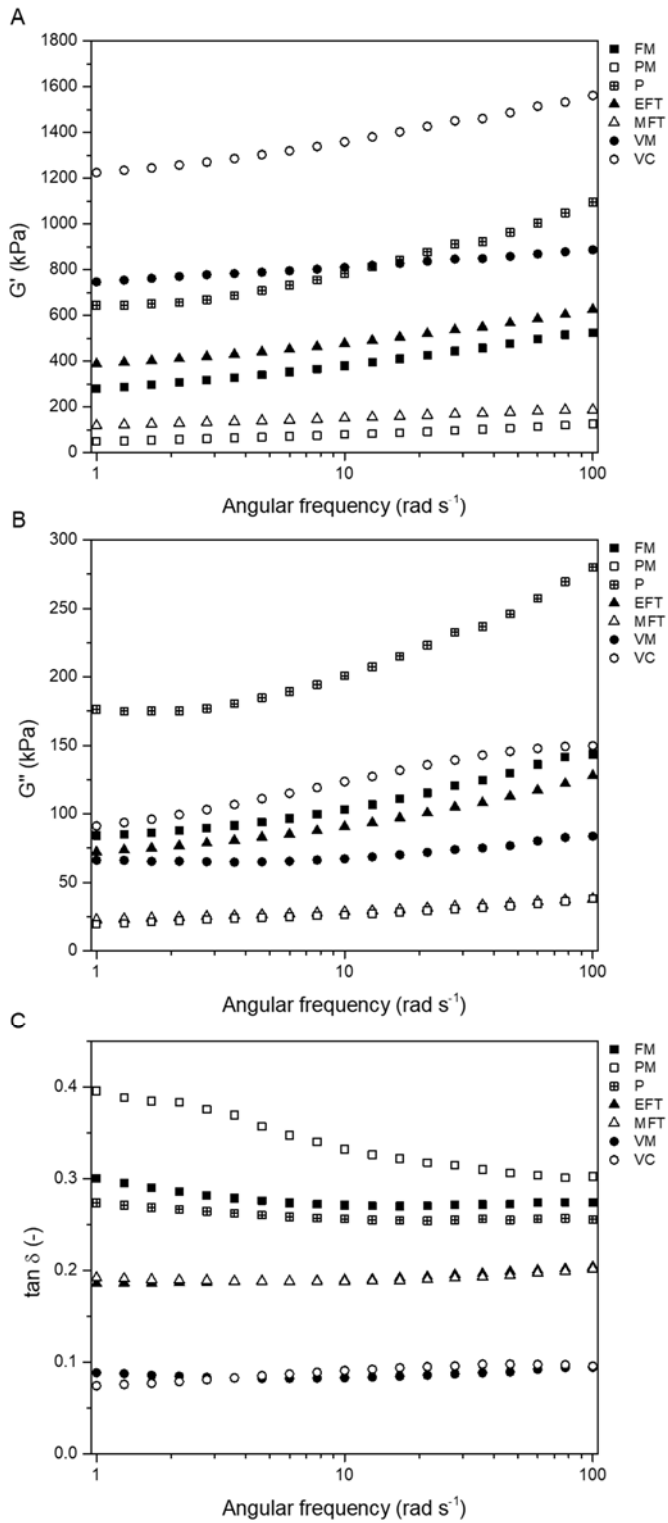
Fig. 5-4. Typical storage modulus, G' (A), loss modulus, G'' (B), and tan δ (C) of commercial products as a function of angular frequency (rad s^{-1}). Abbreviations can be referred to **Fig. 5-1**.

The power-law parameters, G_0', G_0'', n', and n'' as determined by linear regression according to **Equation 12** and **Equation 13** are summarized in **Table S. 7** Supplementary. A higher G_0' usually relates to denser gel network accounting for higher rigidity of the gel structure and vice versa [195]. The result of G_0' and G_0'' confirmed the previous observation of gel behaviour, with VC and PM possessing the highest and lowest values, respectively. The parameters n' and n'' represent the dependency of G' and G'' on angular frequency, and higher values suggest a stronger influence of frequency, reflecting a weak gel behaviour [20, 38]. The finding of n' and n'' values once again supported the preceding results.

In summary, the viscoelastic properties of the vegan cheeses did not replicate those of dairy cheeses where the vegan cheeses possessed strong gel behaviour as indicated by the tan δ and the power law parameters.

3.5 Correlations between Product Characteristics

The presence of linear correlations between the characteristics of the commercial products was examined. Pearson correlation coefficients, representing the ratio between the covariance of two variables and the product of their standard deviation, were assessed as a preliminary screening for linear relationships between any two variables. The Pearson correlation matrix of the characterized properties of FM, P, EFT, MFT, VM, and VC is presented in **Table 5-3** for three significance levels.

A positive correlation with the highest significance level ($p < 0.005$) was identified between fracture stress and carbohydrate content, indicating that increasing the carbohydrate content leads to a stronger food material. The negative correlations with the highest significance level were between yield strain and fat content, n' and carbohydrate content, and moisture and fat content. This suggests that a lower fat content is correlated with a material that is more resistant to shear deformation. These findings alluded to the important role of major food constituents in creating a product with specific mechanical and viscoelastic characteristics.

A positive correlation with a moderate significance level ($p < 0.01$) was noted between the mechanical property estimated under compression, fracture strain, and the viscoelastic property estimated under shear conditions, n'. A positive correlation revealed at a low significance level ($p < 0.05$) was found between fracture stress and the carbohydrate content. Whereas negative

143

correlations ($p < 0.05$) were associated with materials' composition, between yield strain and fat, n' and carbohydrate content, and fat and moisture.

In brief, commercial food products investigated in this study that have excellent capacity to immobilize water are likely to have higher strength and rigidity. The negative correlation observed between the true fracture stress and true fracture strain indicates that products with higher strength tend to fracture at a lower strain and vice versa. Materials possessing at high strength tend to display distinct fracture points. Conversely, softer materials tend to experience slower and progressive breakdown [246], which may explain the higher identified fracture strain. The positive correlations between G_0' and the fracture stress and Young's modulus indicate that material with high rigidity is also likely to possess high strength and firmness.

Table 5-3 Correlation matrix of WHC, mechanical, rheological, and compositional properties of six commercial products (n=6).

	WHC	Frac. stress	Frac. strain	Young's modulus	Yield strain	G_0'	n'	G_0''	n''	Protein	Fat	Carb	Moisture
WHC	1	**0.910***	-0.750	0.563	-0.637	**0.871***	-0.659	0.517	-0.524	-0.228	0.771	0.740	**-0.826***
Frac. stress		1	**-0.898***	0.716	-0.521	**0.903***	**-0.887***	0.144	-0.577	-0.594	0.650	**0.952***	-0.671
Frac. strain			1	-0.718	0.097	-0.788	**0.936***	0.082	0.440	0.708	-0.270	**-0.911***	0.338
Young's modulus				1	-0.256	**0.884***	-0.611	0.084	0.126	-0.450	0.438	0.754	-0.511
Yield strain					1	-0.541	0.152	-0.567	0.398	-0.089	**-0.969***	-0.363	**0.896***
G_0'						1	-0.695	0.362	-0.200	-0.344	0.716	**0.829***	-0.792
n'							1	0.287	0.613	**0.850***	-0.265	**-0.957***	0.280
G_0''								1	0.128	0.705	0.639	-0.147	-0.729
n''									1	0.505	-0.339	-0.539	0.244
Protein										1	0.057	-0.792	-0.122
Fat											1	0.478	**-0.974***
Carb												1	-0.478
Moisture													1

*Significant at $p < 0.05$ (two-tailed test).

**Significant at $p < 0.01$ (two-tailed test).

***Significant at $p < 0.005$ (two-tailed test).

3.6 Profiles of Commercial Products

A profile for each commercial product was created from a representative and quantifiable measure of the properties assessed in this study. The residual mass at the end of the second stage, *i.e.*, 240 °C, was selected to represent the thermal stability of the product. The fracture stress was selected as a measure of the gel strength. The storage modulus, G_0', estimated from the power law representation, was selected to represent the gel rigidity. The WHC was selected to represent water immobilization. A common scale across all selected properties was obtained by normalizing data with a scale from one, lowest value, to five, highest value. A visual representation of the profile, given as a radar graph, illustrates a unique product profile (**Fig. 5-5**).

The profile of the three dairy cheeses was fairly different from each other, reflecting their distinct composition and processing characteristics. The FM and PM had substantially distinct fracture stress, with PM being mechanically stronger. This could be due to the differences in their moisture content as well as their processing. Pizza mozzarella is often stretched extensively and lightly aged. The two mozzarella products have low gel rigidity (indicated by G_0') while possessing excellent thermal stability. In contrast, paneer possesses high thermal stability and excellent WHC with good gel strength and rigidity.

The profile of the two tofu products was similar, with most properties occupying the lower scale. MFT had lower WHC, strength and rigidity compared to extra firm tofu. The profile of the two tofu products was close to the profile of FM, emphasizing the soft texture of FM.

The profile of the two vegan cheeses is located close to the top of the scale for all properties except for thermal stability. This could be attributed to the high carbohydrate content of these cheeses, as starch often imparts substantial mechanical strength to the network while enhancing the ability of water retention [270]. The profile of the VM was considerably different from that of PM but similar to paneer. The VC had the lowest thermal stability and was far from the other commercial products' properties.
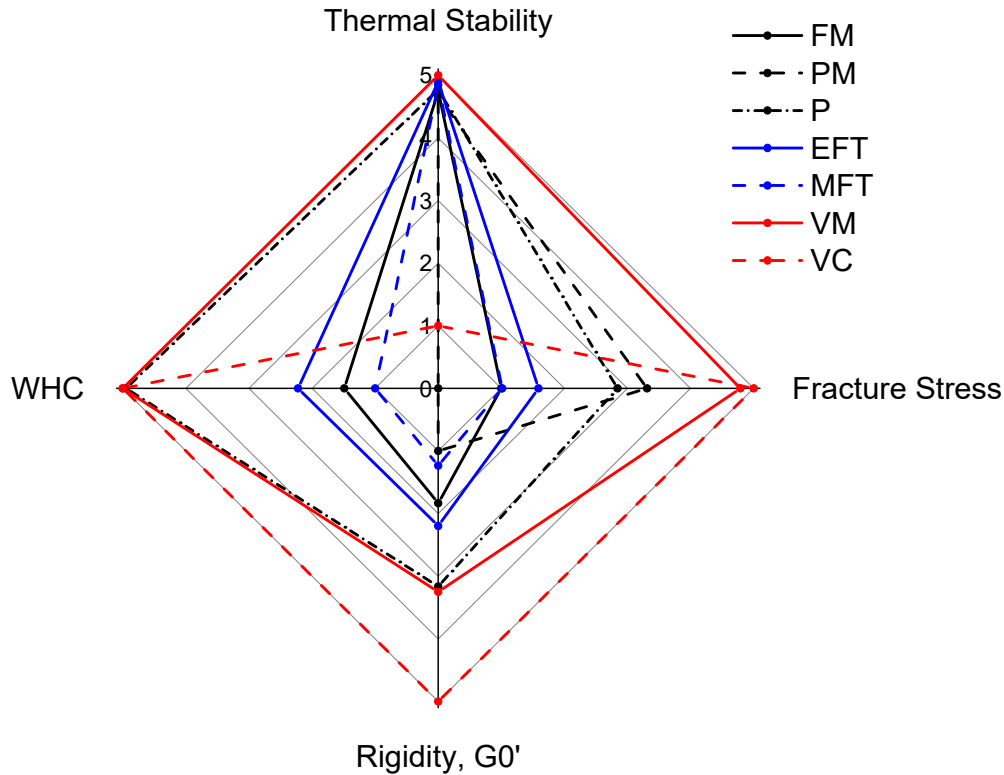
Fig. 5-5. Thermal stability, fracture stress, gel rigidity (G_0'), and WHC of commercial products. Results normalized to a scale of 1-5 (1 = low value and 5 = high value). Abbreviations can be referred to **Fig. 5-1**.

4. Conclusions and Recommendations

This study presents the mapping of the physicochemical properties of three groups of commercial products, *i.e.*, dairy cheeses, tofu products, and vegan cheeses. The vegan cheddar and mozzarella cheese analogues had high mechanical strength and gel rigidity with minimum water exudation, potentially related to the substantial use of starch. The pizza and vegan mozzarella were unexpectedly different. The vegan mozzarella, however, shared similarities with paneer. The tofu products were significantly different from the other products, characterized by weaker strength and poorer WHC. These results suggest that there remains space for improvement of plant-based cheeses, especially concerning their textural and nutritional attributes.

Several significant linear correlations were observed among the measured properties as also confirmed by the normal distribution of residuals (**Figure S. 7** Supplementary). The carbohydrate content of the selected commercial products was positively correlated to the true fracture stress while negatively associated with the viscoelastic power law parameter, n' ($p < 0.005$). The fat constituent was negatively related to the yield strain ($p < 0.005$). These results may explain the extensive use of starch and oil in creating vegan cheese analogues with desired texture.

Future work could involve the expansion of present baseline profiles by investigating the morphology of products as well as conducting extensive sensory and flavor assessments.

5. Declaration of Competing Interest

The authors state that there are no competing financial interests or relationships that may have influence on the work reported.

6.0 Comparison of Okara-containing Soymilk Gels with Commercial Tofu

In this section, the okara-containing soymilk gels are compared with commercial tofu products because of their closest resemblance in terms of composition and preparation. The comparison is based on the mechanical and viscoelastic properties of these products.

The mechanical properties of the okara-containing soymilk gels and commercial tofu products, summarized in **Table 6-1**, indicate that regardless of the different treatments, the whole soybean gels have significantly lower true fracture stress, about 5-10 times, compared to commercial extra firm tofu and about 3-5 times lower when compared to commercial medium firm tofu. This suggests that the okara soymilk gels are much weaker in gel strength. It is likely because of the differences in the preparation method. Commercial tofu typically follows the conventional method where soybeans are ground in higher volumes of water, *e.g.*, soybean to water ratio is 1:5-11 [219], followed by coagulant addition to produce curds, which is pressed under loads to remove excess water. In contrast, the soymilk okara gels were prepared with a much lower soybean to water ratio, *i.e.*, 3:8 w/v dried soybeans to water, in order to facilitate protein aggregation without the use of coagulants and in the absence of the pressing step. All these distinctions of their formulation and processing could be the causes of the significant difference observed concerning the true fracture stress. However, further investigation is needed to identify the exact cause. Lastly, the fracture stress was not influenced by different okara treatments to a large degree, as the range of variation was relatively narrow.

In contrast, the true fracture strain of the okara soymilk gels was slightly lower than those of the commercial tofu, which could be within the experimental errors (**Table 6-1**). On the other hand, the Young's modulus of the okara soymilk gels fell in between of the commercial medium firm and extra firm tofu. This shows that the okara-containing soymilk gels had similar firmness to these two types of commercial tofu [32]. Therefore, the okara-containing soymilk gels generally had comparable mechanical properties to those of the commercial firm tofu despite differences in their formulation and processing. Albeit the processing technique of the okara containing soymilk gels could be altered to enhance the fracture stress of the okara-containing soymilk gels.

Table 6-1 True fracture stress, true fracture strain and Young's modulus of the okara containing soymilk gels and commercial tofu products investigated in this study.

Sample	True fracture stress (kPa)	True fracture strain (%)	Young's modulus (kPa)
Okara-containing soymilk gels	2.2 – 4.3	26.1 – 52.6	10.8 – 30.1
Commercial extra firm tofu	23.2	64.7	44.8
Commercial medium firm tofu	11.2	64.8	20.4

The viscoelastic properties of the okara containing soymilk gels and the extra firm and medium firm commercial tofu are presented in **Table 6-2**. The yield strain, the strain at the end of linear viscoelastic region (LVR) of the strain sweep test, of the okara-containing soymilk gels covers a wide range and comparable to the two commercial tofu products. This indicates that the okara-containing soymilk had comparable deformation resistance to shear stress as compared to the commercial tofu. Similarly, the estimated G_0' of the okara-containing tofu gels spans a wide range. When examining specific okara treatment, the estimated G_0' of the soymilk gel containing untreated okara (***MO***) was around 315 kPa, which is the closest to the commercial extra firm tofu. This shows that the soymilk gel containing untreated okara shared similar gel rigidity as commercial extra firm tofu. On the other hand, the soymilk gels containing soluble (***MOCAL***) and insoluble portions (***MOCAS***) of citric-acid-treated okara had G_0' estimates about 124 and 126 kPa, respectively, which are the closest to the commercial medium firm tofu. This suggests that ***MOCAL*** and ***MOCAS*** were similar in gel rigidity as the medium firm tofu. Similar observations were noted for G_0'' estimates. The n' and n'' estimates of all the okara-containing soymilk gels were similar to the two commercial tofu, alluding to their comparable gel behaviour. As a comparison, the viscoelastic properties of the okara tofu gels resembled those of the commercial tofu, unveiling their comparable gel behaviour under shear stress.

Table 6-2 Yield strain and power law estimates of the okara-containing soymilk gels and commercial tofu products.

Sample	Yield strain (%)	G_0' x 10^3 (Pa)	n'	G_0'' x 10^3 (Pa)	n''
Okara-containing soymilk gels	1.1 – 11.5	40.7 – 1148.6	0.12 – 0.14	5.4 – 245.2	0.10 – 0.15
Commercial extra firm tofu	6.3	378.1	0.10	69.8	0.12
Commercial medium firm tofu	7.7	115.5	0.11	21.7	0.12

7.0   Conclusions and Recommendations

The first portion of this work focused on the preparation of whole soybean tofu gel, containing okara and soymilk. Okara and soymilk were obtained by soaking soybeans with a relatively low soybean to water ratio. Soymilk gels were prepared *via* thermal treatment in the absence of coagulants. The work focuses on the compatibility between okara and the soy protein network by investigating the potential of thermal and citric acid treatments and the combined treatment of okara to improve the quality of the okara-containing soymilk gels. The heat treatment of okara did not initiate significant modification to the structural, mechanical, and rheological properties of okara soymilk gels. Conversely, the citric acid treatment of okara altered its structure considerably through esterification and possibly Maillard reactions. The significant changes in citric acid treated okara led to high mechanical strength and homogeneous structure of okara-containing soymilk gels. The results illustrate the benefit of modifying okara with citric acid to develop high-fiber tofu. Finally, the combination of citric acid and heat treatment of okara promoted larger degree of acid hydrolysis but resulted in okara-containing soymilk gels exhibiting extremely heterogeneous structure with severe water syneresis.

The second portion of this work focused on the characterization of the thermal, mechanical, rheological properties and water holding capacity (WHC) of selected commercial products to establish the baseline profile for the future production of cheese analogue materials. The three groups of commercial products included dairy cheeses, soybean-based products, and two vegan cheeses, with a wide spectrum of production conditions and properties. The vegan mozzarella had very little resemblance to the pizza mozzarella but had similar thermal stability, gel strength, gel rigidity, and WHC to paneer cheese. The tofu products, on the other hand, were significantly different than the vegan and dairy cheeses. They possessed much weaker mechanical strength, gel rigidity and poor WHC.

Although the okara-containing soymilk tofu gel and the commercial tofu were distinct in their production and composition, the okara-containing soymilk gel had comparable firmness and gel rigidity to the commercial tofu. Conversely, the comparatively lower true fracture stress of the okara-containing soymilk gel may point to the use of a low water concentration in the soybean grinding step as well as the absence of coagulant for gelation.

The commercial vegan cheeses are largely composed of starches and oil, which provided inferior nutritional content compared to the dairy cheeses. Therefore, there remains space for improvement in both textural and nutritional aspects of plant-based cheeses.

Future studies could focus on the citric acid content and heat treatments to optimize the properties of okara-containing soymilk tofu gels. Furthermore, sensory evaluations of the okara soymilk gels may be performed. Additionally, the investigation of the microstructure of the commercial products could assist with the understanding of their network structures and the development of soybean-derived cheese analogues.

Letters of Copyright Permissions

Figure 8-1 Copyright permission from Copyright Clearance Center for reusing figures, tables, data from references.

References

[1]   R. Farahmandfar, M. M. Tehrani, S. M. A. Razavi, and M. B. H. Najafi, "Effect of trisodium citrate concentration and soy cheese on meltability of pizza cheese," *Int J Food Prop*, vol. 14, no. 4, pp. 697–707, 2011, doi: 10.1080/10942910903367621.

[2]   J. Medic, C. Atkinson, and C. R. Hurburgh, "Current knowledge in soybean composition," *JAOCS, Journal of the American Oil Chemists' Society*, vol. 91, no. 3, pp. 363–384, 2014, doi: 10.1007/s11746-013-2407-9.

[3]   D. K. O'Toole, "Characteristics and use of okara, the soybean residue from soy milk production - A review," *J Agric Food Chem*, vol. 47, no. 2, pp. 363–371, 1999, doi: 10.1021/jf980754l.

[4]   C. Wang *et al.*, "Incorporation of High-Speed Shearing in the Fabrication of Whole Soybean Curd: Effects on Aggregation Behaviors and Microstructures," *Food Bioproc Tech*, vol. 13, no. 4, pp. 611–624, 2020, doi: 10.1007/s11947-020-02417-w.

[5]   M. Zhang, P. Wang, M. Zou, R. Yang, M. Tian, and Z. Gu, "Microbial transglutaminase-modified protein network and its importance in enhancing the quality of high-fiber tofu with okara," *Food Chem*, vol. 289, no. March, pp. 169–176, 2019, doi: 10.1016/j.foodchem.2019.03.038.

[6]   H. Yoshii, T. Furuta, H. Maeda, and H. Mori, "Hydrolysis Kinetics of Okara and Characterization of Its Water-Soluble Polysaccharides," *Biosci Biotechnol Biochem*, vol. 60, no. 9, pp. 1406–1409, 1995, [Online]. Available: http://www.mendeley.com/research/geology-volcanic-history-eruptive-style-yakedake-volcano-group-central-japan/

[7]   M. Tangyu, J. Muller, C. J. Bolten, and C. Wittmann, "Fermentation of plant-based milk alternatives for improved flavour and nutritional value," *Appl Microbiol Biotechnol*, vol. 103, no. 23–24, pp. 9263–9275, 2019, doi: 10.1007/s00253-019-10175-9.

[8]   X. Fan *et al.*, "Mechanism of change of the physicochemical characteristics, gelation process, water state, and microstructure of okara tofu analogues induced by high-intensity ultrasound treatment," *Food Hydrocoll*, vol. 111, no. February 2020, p. 106241, 2021, doi: 10.1016/j.foodhyd.2020.106241.

[9]   Y. Yang, Z. Ji, C. Wu, Y. Y. Ding, and Z. Gu, "Effect of the heating process on the physicochemical characteristics and nutritional properties of whole cotyledon soymilk and tofu," *RSC Adv*, vol. 10, no. 67, pp. 40625–40636, 2020, doi: 10.1039/d0ra07911a.

[10]   C. Wang, J. Li, S. Zhou, J. Zhou, and Q. Lan, "Application of transglutaminase for quality improvement of whole soybean curd," *J Food Sci Technol*, vol. 56, no. 1, pp. 233–244, 2019, doi: 10.1007/s13197-018-3480-8.

[11] W. Yan, Y. Kun, X. Yang, G. Li, and D. Xianfeng, "Physicochemical properties of soya bean protein gel prepared by microbial transglutaminase in the presence of okara," *Int J Food Sci Technol*, vol. 50, no. 11, pp. 2402–2410, 2015, doi: 10.1111/ijfs.12906.

[12] Q. Zhang *et al.*, "Fabrication of whole soybean curd using three soymilk preparation techniques," *Lwt*, vol. 104, no. October 2018, pp. 91–99, 2019, doi: 10.1016/j.lwt.2019.01.042.

[13] I. Ullah, Y. Hu, J. You, T. Yin, S. Xiong, and Z. Din, "Influence of okara dietary fiber with varying particle sizes on gelling properties, water state and microstructure of tofu gel," *Food Hydrocoll*, vol. 89, pp. 512–522, 2019, doi: 10.1016/j.foodhyd.2018.11.006.

[14] C. del Menezzi, S. Amirou, A. Pizzi, X. Xi, and L. Delmotte, "Reactions with wood carbohydrates and lignin of citric acid as a bond promoter of wood veneer panels," *Polymers (Basel)*, vol. 10, no. 8, 2018, doi: 10.3390/polym10080833.

[15] X. Feng, Z. Xiao, S. Sui, Q. Wang, and Y. Xie, "Esterification of wood with citric acid: The catalytic effects of sodium hypophosphite (SHP)," *Holzforschung*, vol. 68, no. 4, pp. 427–433, 2014, doi: 10.1515/hf-2013-0122.

[16] H. Shao, H. Sun, B. Yang, H. Zhang, and Y. Hu, "Facile and green preparation of hemicellulose-based film with elevated hydrophobicity: Via cross-linking with citric acid," *RSC Adv*, vol. 9, no. 5, pp. 2395–2401, 2019, doi: 10.1039/c8ra09937e.

[17] P. F. Fox and P. L. H. McSweeney, "Introduction," in *Cheese: chemistry, physics & microbiology*, 2017, pp. 5–21.

[18] "Standard for Mozzarella (CXS 262-2006)," 2019. doi: 10.4324/9781315853178.

[19] P. S. Kindstedt, "Mozzarella and Pizza Cheese," in *Cheese: Chemistry, Physics and Microbiology*, Burlington, 1999, pp. 337–362. doi: 10.1007/978-1-4615-2800-5_12.

[20] P. L. H. McSweeney, G. Ottogalli, and P. F. Fox, "Diversity and Classification of Cheese Varieties: An Overview," *Cheese: Chemistry, Physics and Microbiology: Fourth Edition*, vol. 1, pp. 781–808, 2017, doi: 10.1016/B978-0-12-417012-4.00031-4.

[21] G. Singh, A. Kumar, B. K. Kumbhar, and B. N. Dar, "Optimization of processing parameters and ingredients for development of low-fat fibre-supplemented paneer," *J Food Sci Technol*, vol. 52, no. 2, pp. 709–719, 2015, doi: 10.1007/s13197-013-1049-0.

[22] S. Kumar, D. C. Rai, K. Niranjan, and Z. F. Bhat, "Paneer - An Indian soft cheese variant: A review," *J Food Sci Technol*, vol. 51, no. 5, pp. 821–831, 2014, doi: 10.1007/s13197-011-0567-x.

[23] R. Shah, A. H. Jana, K. D. Aparnathi, and P. S. Prajapati, "Process standardization for rennet casein based Mozzarella cheese analogue," *J Food Sci Technol*, vol. 47, no. 5, pp. 574–578, 2010, doi: 10.1007/s13197-010-0104-3.

[24] J. Poore and T. Nemecek, "Reducing food's environmental impacts through producers and consumers," *Science (1979)*, vol. 360, no. 6392, pp. 987–992, 2018, doi: 10.1126/science.aaq0216.

[25] Good Food Institute, "State of the industry report: Plant-based meat, eggs, and dairy," 2021.

[26] H. P. Bachmann, "Cheese analogues: A review," *Int Dairy J*, vol. 11, no. 4–7, pp. 505–515, 2001, doi: 10.1016/S0958-6946(01)00073-5.

[27] R. Farahmandfar, M. Mazaheri Tehrani, S. M. A. Razavi, and M. B. Habibi Najafi, "Effect of soy cheese and trisodium citrate on pizza cheese," *International Journal of Food Engineering*, vol. 6, no. 5, 2010, doi: 10.2202/1556-3758.1777.

[28] C. S. T. Yang and M. v. Taranto, "Textural Properties of Mozzarella Cheese Analogs Manufactured from Soybeans," *J Food Sci*, vol. 47, no. 3, pp. 906–910, 1982, doi: 10.1111/j.1365-2621.1982.tb12742.x.

[29] C. S. T. Yang, M. v. Taranto, and M. Cheryan, "Optimization of Textural and Morphological Properties of a Soy-Gelatin Mozzarella Cheese Analog," *J Food Process Preserv*, vol. 7, no. 1, pp. 41–64, 1983, doi: 10.1111/j.1745-4549.1983.tb00662.x.

[30] C. S. T. Yang and M. Cheryan, "Rheological Properties of a Progel Formed From a Soy-Gelatin Mozzarella Cheese Analog," *J Texture Stud*, vol. 14, no. 2, pp. 125–142, 1983, doi: 10.1111/j.1745-4603.1983.tb00339.x.

[31] S. S. Schiffman, G. Musante, and J. Conger, "Application of multidimensional scaling to ratings of foods for obese and normal weight individuals," *Physiol Behav*, vol. 21, no. 3, pp. 417–422, 1978, doi: 10.1016/0031-9384(78)90102-6.

[32] T. Funami, "Next target for food hydrocolloid studies: Texture design of foods using hydrocolloid technology," *Food Hydrocoll*, vol. 25, no. 8, pp. 1904–1914, 2011, doi: 10.1016/j.foodhyd.2011.03.010.

[33] M. Stieger and F. van de Velde, "Microstructure, texture and oral processing: New ways to reduce sugar and salt in foods," *Curr Opin Colloid Interface Sci*, vol. 18, no. 4, pp. 334–348, 2013, doi: 10.1016/j.cocis.2013.04.007.

[34] K. Kohyama, "Oral sensing of food properties," *J Texture Stud*, vol. 46, no. 3, pp. 138–151, 2015, doi: 10.1111/jtxs.12099.

[35] L. M. Duizer, B. James, V. K. Corrigan, J. Feng, D. I. Hedderley, and F. R. Harker, "Use of a panel knowledgeable in material science to study sensory perception of texture," *J Texture Stud*, vol. 42, no. 4, pp. 309–318, 2011, doi: 10.1111/j.1745-4603.2010.00279.x.

[36] J. Ahmed, P. Ptaszek, and S. Basu, *Advances in Food Rheology*. 2016.

[37] A. Redondo-Cuenca, M. J. Villanueva-Suárez, M. D. Rodríguez-Sevilla, and I. Mateos-Aparicio, "Chemical composition and dietary fibre of yellow and green commercial

soybeans (Glycine max)," *Food Chem*, vol. 101, no. 3, pp. 1216–1222, 2007, doi: 10.1016/j.foodchem.2006.03.025.

[38]   N. Catsimpoolas and C. Ekenstam, "Isolation of alpha, beta, and gamma conglycinins," *Arch Biochem Biophys*, vol. 129, no. 2, pp. 490–497, 1969, doi: 10.1016/0003-9861(69)90206-9.

[39]   W. J. Wolf, "Soybean Proteins: Their Functional, Chemical, and Physical Properties," *J Agric Food Chem*, vol. 18, no. 6, pp. 969–976, 1970, doi: 10.1021/jf60172a025.

[40]   A. Singh, M. Meena, D. Kumar, A. K. Dubey, and M. I. Hassan, "Structural and Functional Analysis of Various Globulin Proteins from Soy Seed," *Crit Rev Food Sci Nutr*, vol. 55, no. 11, pp. 1491–1502, 2015, doi: 10.1080/10408398.2012.700340.

[41]   W. J. Wolf and T. C. Nelsen, "Partial purification and characterization of the 15S globulin of soybeans, a dimer of glycinin," *J Agric Food Chem*, vol. 44, no. 3, pp. 785–791, 1996, doi: 10.1021/jf940493p.

[42]   K. Deng, Y. Huang, and Y. Hua, "Isolation of glycinin (11S) from lipid-reduced soybean flour: Effect of processing conditions on yields and purity," *Molecules*, vol. 17, no. 3, pp. 2968–2979, 2012, doi: 10.3390/molecules17032968.

[43]   M. Adachi *et al.*, "Crystal structure of soybean 11S globulin: Glycinin A3B4 homohexamer," *Proc Natl Acad Sci U S A*, vol. 100, no. 12, pp. 7395–7400, 2003, doi: 10.1073/pnas.0832158100.

[44]   E. G. Hammond, L. A. Johnson, and P. A. Murphy, "Soybean: Grading and Marketing," 2016.

[45]   V. H. Thanh and K. Shibasaki, "Major Proteins of Soybean Seeds. Reconstitution of β-Conglycinin from Its Subunits," *J Agric Food Chem*, vol. 26, no. 3, pp. 695–698, 1978, doi: 10.1021/jf60217a027.

[46]   Q. Zhang and W. Qin, *Tofu and soy products: The effect of structure on their physicochemical properties*, vol. 3. Elsevier, 2018. doi: 10.1016/B978-0-08-100596-5.21700-9.

[47]   T. Ono, M. R. Choi, A. Ikeda, and S. Odagigi, "Changes in the Composition and Size Distribution of Soymilk Protein Particles by Heating," *Agric Biol Chem*, vol. 55, no. 9, pp. 2291–2297, 1991, doi: 10.1271/bbb1961.55.2291.

[48]   X. S. Sun, D. Wang, L. Zhang, X. Mo, L. Zhu, and D. Bolye, "Morphology and phase separation of hydrophobic clusters of soy globular protein polymers," *Macromol Biosci*, vol. 8, no. 4, pp. 295–303, 2008, doi: 10.1002/mabi.200700235.

[49]   B. J. H. Kuipers and H. Gruppen, "Identification of strong aggregating regions in soy glycinin upon enzymatic hydrolysis," *J Agric Food Chem*, vol. 56, no. 10, pp. 3818–3827, 2008, doi: 10.1021/jf703781j.

158

[50]   Y. Chen and T. Ono, "Simple extraction method of non-allergenic intact soybean oil bodies that are thermally stable in an aqueous medium," *J Agric Food Chem*, vol. 58, no. 12, pp. 7402–7407, 2010, doi: 10.1021/jf1006159.

[51]   X. Zhao *et al.*, "Analysis of the amino acids of soy globulins by AOT reverse micelles and aqueous buffer," *Appl Biochem Biotechnol*, vol. 165, no. 3–4, pp. 802–813, 2011, doi: 10.1007/s12010-011-9298-8.

[52]   J. E. Kinsella, "Functional properties of soy proteins," *J Am Oil Chem Soc*, vol. 56, no. 3, pp. 242–258, 1979, doi: 10.1007/BF02671468.

[53]   G. O. Phillips and P. A. Williams, "Chapter 1: Introduction to food proteins," in *Handbook of Food Proteins*, 2011, pp. 1–12. doi: 10.1016/B978-1-84569-758-7.50001-0.

[54]   D. J. McClements, "Protein-stabilized emulsions," *Curr Opin Colloid Interface Sci*, vol. 9, no. 5, pp. 305–313, 2004, doi: 10.1016/j.cocis.2004.09.003.

[55]   H. Shan *et al.*, "Gelation property of alcohol-extracted soy protein isolate and effects of various reagents on the firmness of heat-induced gels," *Int J Food Prop*, vol. 18, no. 3, pp. 627–637, 2015, doi: 10.1080/10942912.2013.850508.

[56]   H. Zhao, W. Li, F. Qin, and J. Chen, "Calcium sulphate-induced soya bean protein tofu-type gels: influence of denaturation and particle size," *Int J Food Sci Technol*, vol. 51, no. 3, pp. 731–741, 2016, doi: 10.1111/ijfs.13010.

[57]   J. Wang *et al.*, "Concentration-dependent improvement of gelling ability of soy proteins by preheating or ultrasound treatment," *Lwt*, vol. 134, no. August, p. 110170, 2020, doi: 10.1016/j.lwt.2020.110170.

[58]   D. Syah, A. B. Sitanggang, R. F. Faradilla, V. Trisna, Y. Karsono, and D. A. Septianita, "The influences of coagulation conditions and storage proteins on the textural properties of soy-curd (tofu)," *CYTA - Journal of Food*, vol. 13, no. 2, pp. 259–263, 2015, doi: 10.1080/19476337.2014.948071.

[59]   T. Fujii, "Coagulation and rheological behaviors of soy milk colloidal dispersions," *Biosci Biotechnol Biochem*, vol. 81, no. 4, pp. 680–686, 2017, doi: 10.1080/09168451.2017.1282810.

[60]   T. E. Clemente and E. B. Cahoon, "Soybean oil: Genetic approaches for modification of functionality and total content," *Plant Physiol*, vol. 151, no. 3, pp. 1030–1040, 2009, doi: 10.1104/pp.109.146282.

[61]   S. T. Guo, T. Ono, and M. Mikami, "Interaction between Protein and Lipid in Soybean Milk at Elevated Temperature," *J Agric Food Chem*, vol. 45, no. 12, pp. 4601–4605, 1997, doi: 10.1021/jf970417x.

[62]   S. T. Guo, C. Tsukamoto, K. Takahasi, K. Yagasaki, Q. X. Nan, and T. Ono, "Incorporation of soymilk lipid into soy protein coagulum by the addition of calcium

chloride," *J Food Sci*, vol. 67, no. 9, pp. 3215–3219, 2002, doi: 10.1111/j.1365-2621.2002.tb09568.x.

[63]   X. Peng, C. Ren, and S. Guo, "Particle formation and gelation of soymilk: Effect of heat," *Trends Food Sci Technol*, vol. 54, pp. 138–147, 2016, doi: 10.1016/j.tifs.2016.06.005.

[64]   M. Choct, Y. Dersjant-Li, J. McLeish, and M. Peisker, "Soy oligosaccharides and soluble non-starch polysaccharides: A review of digestion, nutritive and anti-nutritive effects in pigs and poultry," *Asian-Australas J Anim Sci*, vol. 23, no. 10, pp. 1386–1398, 2010, doi: 10.5713/ajas.2010.90222.

[65]   C. Wu, W. B. Navicha, Y. Hua, Y. Chen, X. Kong, and C. Zhang, "Effects of removal of non-network protein on the rheological properties of heat-induced soy protein gels," *Lwt*, vol. 95, no. September 2017, pp. 193–199, 2018, doi: 10.1016/j.lwt.2018.04.077.

[66]   C. Wu, Y. Hua, Y. Chen, X. Kong, and C. Zhang, "Release behavior of non-network proteins and its relationship to the structure of heat-induced soy protein gels," *J Agric Food Chem*, vol. 63, no. 16, pp. 4211–4219, 2015, doi: 10.1021/acs.jafc.5b00132.

[67]   C. Wu, Y. Hua, Y. Chen, X. Kong, and C. Zhang, "Effect of temperature, ionic strength and 11S ratio on the rheological properties of heat-induced soy protein gels in relation to network proteins content and aggregates size," *Food Hydrocoll*, vol. 66, pp. 389–395, 2017, doi: 10.1016/j.foodhyd.2016.12.007.

[68]   L. J. Campbell, X. Gu, S. J. Dewar, and S. R. Euston, "Effects of heat treatment and glucono-δ-lactone-induced acidification on characteristics of soy protein isolate," *Food Hydrocoll*, vol. 23, no. 2, pp. 344–351, 2009, doi: 10.1016/j.foodhyd.2008.03.004.

[69]   N. Chen, M. Zhao, C. Chassenieux, and T. Nicolai, "The effect of adding NaCl on thermal aggregation and gelation of soy protein isolate," *Food Hydrocoll*, vol. 70, pp. 88–95, 2017, doi: 10.1016/j.foodhyd.2017.03.024.

[70]   H. N. Xu, Y. Liu, and L. Zhang, "Salting-out and salting-in: Competitive effects of salt on the aggregation behavior of soy protein particles and their emulsifying properties," *Soft Matter*, vol. 11, no. 29, pp. 5926–5932, 2015, doi: 10.1039/c5sm00954e.

[71]   K. Kohyama, Y. Sano, and E. Doi, "Rheological Characteristics and Gelation Mechanism of Tofu (Soybean Curd)," *J Agric Food Chem*, vol. 43, no. 7, pp. 1808–1812, 1995, doi: 10.1021/jf00055a011.

[72]   X. T. He, D. B. Yuan, J. M. Wang, and X. Q. Yang, "Thermal aggregation behaviour of soy protein: Characteristics of different polypeptides and sub-units," *J Sci Food Agric*, vol. 96, no. 4, pp. 1121–1131, 2016, doi: 10.1002/jsfa.7184.

[73]   Q. Zhang *et al.*, "Research progress in tofu processing: From raw materials to processing conditions," *Crit Rev Food Sci Nutr*, vol. 58, no. 9, pp. 1448–1467, 2018, doi: 10.1080/10408398.2016.1263823.

[74] N. Murekatete, Y. Hua, M. V. M. Chamba, O. Djakpo, and C. Zhang, "Gelation Behavior and Rheological Properties of Salt- or Acid-Induced Soy Proteins Soft Tofu-Type Gels," *J Texture Stud*, vol. 45, no. 1, pp. 62–73, 2014, doi: 10.1111/jtxs.12052.

[75] S. Li Tay, H. Yao Tan, and C. Perera, "The Coagulating Effects of Cations and Anions on Soy Protein," *Int J Food Prop*, vol. 9, no. 2, pp. 317–323, 2006, doi: 10.1080/10942910600596340.

[76] C. Kuraishi, K. Yamazaki, and Y. Susa, "Transglutaminase: Its utilization in the food industry," *Food Reviews International*, vol. 17, no. 2, pp. 221–246, 2001, doi: 10.1081/FRI-100001258.

[77] J. Li, Y. Cheng, E. Tatsumi, M. Saito, and L. Yin, "The use of W/O/W controlled-release coagulants to improve the quality of bittern-solidified tofu," *Food Hydrocoll*, vol. 35, pp. 627–635, 2014, doi: 10.1016/j.foodhyd.2013.08.002.

[78] M. P. Prabhakaran, C. O. Perera, and S. Valiyaveettil, "Effect of different coagulants on the isoflavone levels and physical properties of prepared firm tofu," *Food Chem*, vol. 99, no. 3, pp. 492–499, 2006, doi: 10.1016/j.foodchem.2005.08.011.

[79] R. Wang, X. Jin, S. Su, Y. Lu, and S. Guo, "Soymilk gelation: The determinant roles of incubation time and gelation rate," *Food Hydrocoll*, vol. 97, no. September 2018, p. 105230, 2019, doi: 10.1016/j.foodhyd.2019.105230.

[80] K. Toda, T. Ono, K. Kitamura, M. Hajika, K. Takahashi, and Y. Nakamura, "Seed protein content and consistency of tofu prepared with different magnesium chloride concentrations in six Japanese soybean varieties," *Breed Sci*, vol. 53, no. 3, pp. 217–223, 2003, doi: 10.1270/jsbbs.53.217.

[81] Y. Onodera, T. Ono, K. Nakasato, and K. Toda, "Homogeneity and microstructure of tofu depends on 11S/7S globulin ratio in soymilk and coagulant concentration," *Food Sci Technol Res*, vol. 15, no. 3, pp. 265–274, 2009, doi: 10.3136/fstr.15.265.

[82] X. Wang, K. Luo, S. Liu, B. Adhikari, and J. Chen, "Improvement of gelation properties of soy protein isolate emulsion induced by calcium cooperated with magnesium," *J Food Eng*, vol. 244, no. July 2018, pp. 32–39, 2019, doi: 10.1016/j.jfoodeng.2018.09.025.

[83] K. H. Joo and G. A. Cavender, "Investigation of tofu products coagulated with trimagnesium citrate as a novel alternative to nigari and gypsum: Comparison of physical properties and consumer preference," *Lwt*, vol. 118, no. November 2019, p. 108819, 2020, doi: 10.1016/j.lwt.2019.108819.

[84] Y. guo Shi *et al.*, "Influence of four different coagulants on the physicochemical properties, textural characteristics and flavour of tofu," *Int J Food Sci Technol*, vol. 55, no. 3, pp. 1218–1229, 2020, doi: 10.1111/ijfs.14357.

[85] V. A. Obatolu, "Effect of different coagulants on yield and quality of tofu from soymilk," *European Food Research and Technology*, vol. 226, no. 3, pp. 467–472, 2008, doi: 10.1007/s00217-006-0558-8.

[86] J. M. DeMan, L. DeMan, and S. Gupta, "Texture and microestructure of soybean curd (tofu) as affected by different coagulants," *Foods Microstructure*, vol. 5, no. 1, pp. 83–89, 1986.

[87] I. Challen and R. Moorhouse, "Chapter 8 Hydrocolloids in Restructured Foods," in *Hydrocolloids in food processing*, 2011, pp. 165–214.

[88] T. Nagano, H. Mori, and K. Nishinari, "Rheological properties and conformational states of β-conglycinin gels at acidic pH," *Biopolymers*, vol. 34, no. 2, pp. 293–298, 1994, doi: 10.1002/bip.360340215.

[89] T. S. Li, "Functional and Structural Properties of Molecular Soy Protein Fractions," 2005.

[90] J. Zhu *et al.*, "Effect of microbial transglutaminase cross-linking on the quality characteristics and potential allergenicity of tofu," *Food Funct*, vol. 10, no. 9, pp. 5485–5497, 2019, doi: 10.1039/c9fo01118h.

[91] C. H. Tang, H. Wu, H. P. Yu, L. Li, Z. Chen, and X. Q. Yang, "Coagulation and gelation of soy protein isolates induced by microbial transglutaminase," *J Food Biochem*, vol. 30, no. 1, pp. 35–55, 2006, doi: 10.1111/j.1745-4514.2005.00049.x.

[92] K. Nishinari, Y. Fang, S. Guo, and G. O. Phillips, "Soy proteins: A review on composition, aggregation and emulsification," *Food Hydrocoll*, vol. 39, pp. 301–318, 2014, doi: 10.1016/j.foodhyd.2014.01.013.

[93] C. H. Tang, L. Li, J. L. Wang, and X. Q. Yang, "Formation and rheological properties of 'cold-set' tofu induced by microbial transglutaminase," *LWT - Food Science and Technology*, vol. 40, no. 4, pp. 579–586, 2007, doi: 10.1016/j.lwt.2006.03.001.

[94] X. Wang *et al.*, "Textural and Rheological Properties of Soy Protein Isolate Tofu-Type Emulsion Gels: Influence of Soybean Variety and Coagulant Type," *Food Biophys*, vol. 13, no. 3, pp. 324–332, 2018, doi: 10.1007/s11483-018-9538-3.

[95] Z. S. Liu and S. K. C. Chang, "Effect of soy milk characteristics and cooking conditions on coagulant requirements for making filled tofu," *J Agric Food Chem*, vol. 52, no. 11, pp. 3405–3411, 2004, doi: 10.1021/jf035139i.

[96] A. M. Nik, M. Alexander, V. Poysa, L. Woodrow, and M. Corredig, "Effect of Soy Protein Subunit Composition on the Rheological Properties of Soymilk during Acidification," *Food Biophys*, vol. 6, no. 1, pp. 26–36, 2011, doi: 10.1007/s11483-010-9172-1.

[97] T. Nagano and M. Tokita, "Viscoelastic properties and microstructures of 11S globulin and soybean protein isolate gels: Magnesium chloride-induced gels," *Food Hydrocoll*, vol. 25, no. 7, pp. 1647–1654, 2011, doi: 10.1016/j.foodhyd.2011.03.001.

[98]   A. H. Clark, G. M. Kavanagh, and S. B. Ross-Murphy, "Globular protein gelation- Theory and experiment," *Food Hydrocoll*, vol. 15, no. 4–6, pp. 383–400, 2001, doi: 10.1016/S0268-005X(01)00042-X.

[99]   M. C. Puppo and M. C. Añón, "Structural Properties of Heat-Induced Soy Protein Gels As Affected by Ionic Strength and pH," *J Agric Food Chem*, vol. 46, no. 9, pp. 3583–3589, 1998, doi: 10.1021/jf980006w.

[100] E. J. Noh, S. Y. Park, J. I. Pak, S. T. Hong, and S. E. Yun, "Coagulation of soymilk and quality of tofu as affected by freeze treatment of soybeans," *Food Chem*, vol. 91, no. 4, pp. 715–721, 2005, doi: 10.1016/j.foodchem.2004.06.050.

[101] C. Tang, "Effect of thermal pretreatment of raw soymilk on the gel strength and microstructure of tofu induced by microbial transglutaminase," *LWT*, vol. 40, pp. 1403–1409, 2007, doi: 10.1016/j.lwt.2006.09.006.

[102] F. J. Kao, N. W. Su, and M. H. Lee, "Development and quality of tofu analogue prepared from whole soybeans," in *ACS Symposium Series*, vol. 1059, American Chemical Society, 2010, pp. 277–291. doi: 10.1021/bk-2010-1059.ch018.

[103] I. Mateos-Aparicio, A. Redondo-Cuenca, and M. J. Villanueva-Suárez, "Isolation and characterisation of cell wall polysaccharides from legume by-products: Okara (soymilk residue), pea pod and broad bean pod," *Food Chem*, vol. 122, no. 1, pp. 339–345, 2010, doi: 10.1016/j.foodchem.2010.02.042.

[104] B. Li, M. Qiao, and F. Lu, "Composition, Nutrition, and Utilization of Okara (Soybean Residue)," *Food Reviews International*, vol. 28, no. 3, pp. 231–252, 2012, doi: 10.1080/87559129.2011.595023.

[105] V. R. G. de Figueiredo, F. Yamashita, A. L. L. Vanzela, E. I. Ida, and L. E. Kurozawa, "Action of multi-enzyme complex on protein extraction to obtain a protein concentrate from okara," *J Food Sci Technol*, vol. 55, no. 4, pp. 1508–1517, 2018, doi: 10.1007/s13197-018-3067-4.

[106] X. Tao *et al.*, "Effects of pretreatments on the structure and functional properties of okara protein," *Food Hydrocoll*, vol. 90, no. August 2018, pp. 394–402, 2019, doi: 10.1016/j.foodhyd.2018.12.028.

[107] S. Plazzotta, M. Moretton, S. Calligaris, and L. Manzocco, "Physical, chemical, and techno-functional properties of soy okara powders obtained by high pressure homogenization and alkaline-acid recovery," *Food and Bioproducts Processing*, vol. 128, pp. 95–101, 2021, doi: 10.1016/j.fbp.2021.04.017.

[108] Y. Arai, K. Nishinari, and T. Nagano, "Developing Soybean Protein Gel-Based Foods from Okara Using the Wet-Type Grinder Method," *Foods*, vol. 10, no. 2, p. 348, 2021, doi: 10.3390/foods10020348.

[109] C. Wang *et al.*, "High-speed shearing of soybean flour suspension disintegrates the component cell layers and modifies the hydration properties of okara fibers," *Lwt*, vol. 116, no. August, 2019, doi: 10.1016/j.lwt.2019.108505.

[110] Z. Anwar, M. Gulfraz, and M. Irshad, "Agro-industrial lignocellulosic biomass a key to unlock the future bio-energy: A brief review," *J Radiat Res Appl Sci*, vol. 7, no. 2, pp. 163–173, 2014, doi: 10.1016/j.jrras.2014.02.003.

[111] N. Mosier *et al.*, "Features of promising technologies for pretreatment of lignocellulosic biomass," *Bioresour Technol*, vol. 96, no. 6, pp. 673–686, 2005, doi: 10.1016/j.biortech.2004.06.025.

[112] A. Zoghlami and G. Paës, "Lignocellulosic Biomass: Understanding Recalcitrance and Predicting Hydrolysis," *Front Chem*, vol. 7, no. December, 2019, doi: 10.3389/fchem.2019.00874.

[113] F. H. Isikgor and C. R. Becer, "Lignocellulosic biomass: a sustainable platform for the production of bio-based chemicals and polymers," *Polym Chem*, vol. 6, no. 25, pp. 4497–4559, 2015, doi: 10.1039/c5py00263j.

[114] M. Kugimiya, "Maceration of dietary fibers of okara by successive treatments with acid and alkali," *Nippon Shokuhin Kogyo Gakkaishi*, vol. 42, no. 4, pp. 273–278, 1995.

[115] K. A. Campbell *et al.*, "Advances in aqueous extraction processing of soybeans," *JAOCS, Journal of the American Oil Chemists' Society*, vol. 88, no. 4, pp. 449–465, 2011, doi: 10.1007/s11746-010-1724-5.

[116] K. E. Preece, N. Hooshyar, and N. J. Zuidam, "Whole soybean protein extraction processes: A review," *Innovative Food Science and Emerging Technologies*, vol. 43, no. July, pp. 163–172, 2017, doi: 10.1016/j.ifset.2017.07.024.

[117] C. J. Houtman, P. Kitin, J. C. D. Houtman, K. E. Hammel, and C. G. Hunt, "Acridine orange indicates early oxidation of wood cell walls by fungi," *PLoS One*, vol. 11, no. 7, pp. 1–19, 2016, doi: 10.1371/journal.pone.0159715.

[118] K. E. Preece, E. Drost, N. Hooshyar, A. Krijgsman, P. W. Cox, and N. J. Zuidam, "Confocal imaging to reveal the microstructure of soybean processing materials," *J Food Eng*, vol. 147, pp. 8–13, 2015, doi: 10.1016/j.jfoodeng.2014.09.022.

[119] Q. Lan *et al.*, "Influence of okara with varying particle sizes on the gelling, rheological, and microstructural properties of glucono-δ-lactone-induced tofu," *J Food Sci Technol*, 2020, doi: 10.1007/s13197-020-04563-7.

[120] F. Wei, F. Ye, S. Li, L. Wang, J. Li, and G. Zhao, "Layer-by-layer coating of chitosan/pectin effectively improves the hydration capacity, water suspendability and tofu gel compatibility of okara powder," *Food Hydrocoll*, vol. 77, pp. 465–473, 2018, doi: 10.1016/j.foodhyd.2017.10.024.

[121] S. Huang, Y. He, Y. Zou, and Z. Liu, "Modification of insoluble dietary fibres in soya bean okara and their physicochemical properties," *Int J Food Sci Technol*, vol. 50, no. 12, pp. 2606–2613, 2015, doi: 10.1111/ijfs.12929.

[122] Q. Wang, P. Shen, and B. Chen, "Ultracentrifugal milling and steam heating pretreatment improves structural characteristics, functional properties, and in vitro binding capacity of cellulase modified soy okara residues," *Food Chem*, vol. 384, no. February, p. 132526, 2022, doi: 10.1016/j.foodchem.2022.132526.

[123] Y. Xiao *et al.*, "Gel properties and formation mechanism of soy protein isolate gels improved by wheat bran cellulose," *Food Chem*, vol. 324, no. November 2019, p. 126876, 2020, doi: 10.1016/j.foodchem.2020.126876.

[124] G. Beck, "Leachability and decay resistance of wood polyesterified with sorbitol and citric acid," *Forests*, vol. 11, no. 6, pp. 1–17, 2020, doi: 10.3390/f11060650.

[125] J. Miklečić and V. Jirouš-Rajković, "Accelerated weathering of coated and uncoated beech wood modified with citric acid," *Drvna Industrija*, vol. 62, no. 4, pp. 277–282, 2011, doi: 10.5552/drind.2011.1116.

[126] L. An *et al.*, "Efficient and green approach for the esterification of lignin with oleic acid using surfactant-combined microreactors in water," *Bioresources*, vol. 15, no. 1, pp. 89–104, 2020, doi: 10.15376/biores.15.1.89-104.

[127] D. Ando and K. Umemura, "Bond structures between wood components and citric acid in wood-based molding," *Polymers (Basel)*, vol. 13, no. 1, pp. 1–9, 2021, doi: 10.3390/polym13010058.

[128] X. Cui, A. Ozaki, T. A. Asoh, and H. Uyama, "Cellulose modified by citric acid reinforced Poly(lactic acid) resin as fillers," *Polym Degrad Stab*, vol. 175, 2020, doi: 10.1016/j.polymdegradstab.2020.109118.

[129] X. Cui, T. Honda, T. A. Asoh, and H. Uyama, "Cellulose modified by citric acid reinforced polypropylene resin as fillers," *Carbohydr Polym*, vol. 230, no. October 2019, 2020, doi: 10.1016/j.carbpol.2019.115662.

[130] L. Chen, J. Y. Zhu, C. Baez, P. Kitin, and T. Elder, "Highly thermal-stable and functional cellulose nanocrystals and nanofibrils produced using fully recyclable organic acids," *Green Chemistry*, vol. 18, no. 13, pp. 3835–3843, 2016, doi: 10.1039/c6gc00687f.

[131] M. Cheng, Z. Qin, Y. Chen, J. Liu, and Z. Ren, "Facile one-step extraction and oxidative carboxylation of cellulose nanocrystals through hydrothermal reaction by using mixed inorganic acids," *Cellulose*, vol. 24, no. 8, pp. 3243–3254, 2017, doi: 10.1007/s10570-017-1339-1.

[132] S. S. Lal and S. T. Mhaske, *Old corrugated box (OCB)-based cellulose nanofiber-reinforced and citric acid-cross-linked TSP–guar gum composite film*, vol. 78, no. 2. Springer Berlin Heidelberg, 2021. doi: 10.1007/s00289-020-03138-y.

[133] W. Ma, S. Rokayya, L. Xu, X. Sui, L. Jiang, and Y. Li, "Physical-Chemical Properties of Edible Film Made from Soybean Residue and Citric Acid," *J Chem*, vol. 2018, 2018, doi: 10.1155/2018/4026831.

[134] D. M. de Carvalho and J. L. Colodette, "Comparative study of acid hydrolysis of lignin and polysaccharides in biomasses," *Bioresources*, vol. 12, no. 4, pp. 6907–6923, 2017, doi: 10.15376/biores.12.4.6907-6923.

[135] S. Hiltunen and H. Sirén, "Analysis of monosaccharides and oligosaccharides in the pulp and paper industry by use of capillary zone electrophoresis: A review," *Anal Bioanal Chem*, vol. 405, no. 17, pp. 5773–5784, 2013, doi: 10.1007/s00216-013-7031-x.

[136] M. C. Porfiri, J. Vaccaro, C. A. Stortz, D. A. Navarro, J. R. Wagner, and D. M. Cabezas, "Insoluble soybean polysaccharides: Obtaining and evaluation of their O/W emulsifying properties," *Food Hydrocoll*, vol. 73, pp. 262–273, 2017, doi: 10.1016/j.foodhyd.2017.06.034.

[137] A. C. Colletti, J. F. Delgado, D. M. Cabezas, J. R. Wagner, and M. C. Porfiri, "Soybean Hull Insoluble Polysaccharides: Improvements of Its Physicochemical Properties Through High Pressure Homogenization," *Food Biophys*, vol. 15, no. 2, pp. 173–187, 2020, doi: 10.1007/s11483-019-09613-y.

[138] H. Furuta and H. Maeda, "Rheological properties of water-soluble soybean polysaccharides extracted under weak acidic condition," *Food Hydrocoll*, vol. 13, no. 3, pp. 267–274, 1999, doi: 10.1016/S0268-005X(99)00009-0.

[139] A. Nakamura, H. Furuta, H. Maeda, Y. Nagamatsu, and A. Yoshimoto, "Analysis of structural components and molecular construction of soybean soluble polysaccharides by stepwise enzymatic degradation," *Biosci Biotechnol Biochem*, vol. 65, no. 10, pp. 2249–2258, 2001, [Online]. Available: https://www.researchgate.net/publication/269107473_What_is_governance/link/548173090cf22525dcb61443/download%0Ahttp://www.econ.upf.edu/~reynal/Civil wars_12December2010.pdf%0Ahttps://think-asia.org/handle/11540/8282%0Ahttps://www.jstor.org/stable/41857625

[140] J. Li, S. Matsumoto, A. Nakamura, H. Maeda, and Y. Matsumura, "Characterization and functional properties of sub-fractions of soluble soybean polysaccharides," *Biosci Biotechnol Biochem*, vol. 73, no. 12, pp. 2568–2575, 2009, doi: 10.1271/bbb.70799.

[141] Q. Zhao *et al.*, "Interactions between soluble soybean polysaccharide and starch during the gelatinization and retrogradation: Effects of selected starch varieties," *Food Hydrocoll*, vol. 118, no. December 2020, p. 106765, 2021, doi: 10.1016/j.foodhyd.2021.106765.

[142] Y. Cai, B. Cai, and S. Ikeda, "Stabilization of milk proteins in acidic conditions by pectic polysaccharides extracted from soy flour," *J Dairy Sci*, vol. 100, no. 10, pp. 7793–7801, 2017, doi: 10.3168/jds.2016-12190.

[143] A. Nakamura, N. Fujii, J. Tobe, N. Adachi, and M. Hirotsuka, "Characterization and functional properties of soybean high-molecular-mass polysaccharide complex," *Food Hydrocoll*, vol. 29, no. 1, pp. 75–84, 2012, doi: 10.1016/j.foodhyd.2012.01.018.

[144] D. Salarbashi, M. Tafaghodi, B. S. F. Bazzaz, and B. Jafari, "Characterization of soluble soybean (SSPS) polysaccharide and development of eco-friendly SSPS/TiO2 nanoparticle bionanocomposites," *Int J Biol Macromol*, vol. 112, pp. 852–861, 2018, doi: 10.1016/j.ijbiomac.2018.01.182.

[145] H. Maeda and A. Nakamura, "Soluble soybean polysaccharide," in *Handbook of Hydrocolloids*, Elsevier, 2009, pp. 693–709. doi: 10.1533/9781845695873.693.

[146] M. Nakauma *et al.*, "Comparison of sugar beet pectin, soybean soluble polysaccharide, and gum arabic as food emulsifiers. 1. Effect of concentration, pH, and salts on the emulsifying properties," *Food Hydrocoll*, vol. 22, no. 7, pp. 1254–1267, 2008, doi: 10.1016/j.foodhyd.2007.09.004.

[147] Y. Guo, Y. Wei, Z. Cai, B. Hou, and H. Zhang, "Stability of acidified milk drinks induced by various polysaccharide stabilizers: A review," *Food Hydrocoll*, vol. 118, no. April, p. 106814, 2021, doi: 10.1016/j.foodhyd.2021.106814.

[148] M. Yousefi and S. M. Jafari, "Recent advances in application of different hydrocolloids in dairy products to improve their techno-functional properties," *Trends Food Sci Technol*, vol. 88, no. October 2018, pp. 468–483, 2019, doi: 10.1016/j.tifs.2019.04.015.

[149] Q. Lan *et al.*, "Effect of soybean soluble polysaccharide on the formation of glucono-δ-lactone-induced soybean protein isolate gel," *Polymers (Basel)*, vol. 11, no. 12, 2019, doi: 10.3390/polym11121997.

[150] B. Chen *et al.*, "Improvements in physicochemical and emulsifying properties of insoluble soybean fiber by physical-chemical treatments," *Food Hydrocoll*, vol. 93, no. July 2018, pp. 167–175, 2019, doi: 10.1016/j.foodhyd.2019.01.058.

[151] L. Huang *et al.*, "Stability of emulsion stabilized by low-concentration soybean protein isolate: Effects of insoluble soybean fiber," *Food Hydrocoll*, vol. 97, no. July, p. 105232, 2019, doi: 10.1016/j.foodhyd.2019.105232.

[152] H. Shi *et al.*, "Two-step hydrolysis method for monosaccharide composition analysis of natural polysaccharides rich in uronic acids," *Food Hydrocoll*, vol. 101, no. November 2019, p. 105524, 2020, doi: 10.1016/j.foodhyd.2019.105524.

[153] K. K. Valladares-Diestra, L. Porto de Souza Vandenberghe, L. A. Zevallos Torres, A. Zandoná Filho, A. Lorenci Woiciechowski, and C. Ricardo Soccol, "Citric acid assisted hydrothermal pretreatment for the extraction of pectin and xylooligosaccharides production from cocoa pod husks," *Bioresour Technol*, vol. 343, no. September 2021, 2022, doi: 10.1016/j.biortech.2021.126074.

[154] Desniorita, N. Nazir, Novelina, K. Sayuti, and Jasril, "Application of Pectin Extracted from Cocoa Pod in the Production of Edible Film," *IOP Conf Ser Earth Environ Sci*, vol. 347, no. 1, 2019, doi: 10.1088/1755-1315/347/1/012060.

[155] S. M. M. Islam, A. A. Loman, and L. K. Ju, "High monomeric sugar yields from enzymatic hydrolysis of soybean meal and effects of mild heat pretreatments with chelators," *Bioresour Technol*, vol. 256, no. December 2017, pp. 438–445, 2018, doi: 10.1016/j.biortech.2018.02.054.

[156] M. G. Gomes *et al.*, "Pretreated Sugarcane Bagasse with Citric Acid Applied in Enzymatic Hydrolysis," *Industrial Biotechnology*, vol. 16, no. 2, pp. 117–124, 2020, doi: 10.1089/ind.2019.0039.

[157] B. A. J. Noordover, R. Duchateau, R. A. T. M. van Benthem, W. Ming, and C. E. Koning, "Enhancing the functionality of biobased polyester coating resins through modification with citric acid," *Biomacromolecules*, vol. 8, no. 12, pp. 3860–3870, 2007, doi: 10.1021/bm700775e.

[158] B. N. Ferdousi, M. M. Islam, T. Okajima, and T. Ohsaka, "Exploring pKa of peroxycitric acid coexisting with citric acid in aqueous solution with voltmmetric, potentiometic and chromatographic approaches," *Int J Electrochem Sci*, vol. 11, no. 7, pp. 6215–6228, 2016, doi: 10.20964/2016.07.30.

[159] N. K. Garrity, W. J. Grigsby, J. Jin, and N. R. Edmonds, "Rheological behaviors exhibited by soy protein systems under dynamic aqueous environments," *J Appl Polym Sci*, vol. 134, no. 46, pp. 1–7, 2017, doi: 10.1002/app.45513.

[160] J. S. Henao Ossa, J. R. Wagner, and G. G. Palazolo, "Influence of chemical composition and structural properties on the surface behavior and foam properties of tofu-whey concentrates in acid medium," *Food Research International*, vol. 128, no. October 2019, p. 108772, 2020, doi: 10.1016/j.foodres.2019.108772.

[161] Y. Xu, Y. Tao, and S. Shivkumar, "Effect of freeze-thaw treatment on the structure and texture of soft and firm tofu," *J Food Eng*, vol. 190, pp. 116–122, 2016, doi: 10.1016/j.jfoodeng.2016.06.022.

[162] J. Baruah, R. C. Deka, and E. Kalita, "Greener production of microcrystalline cellulose (MCC) from Saccharum spontaneum (Kans grass): Statistical optimization," *Int J Biol Macromol*, vol. 154, pp. 672–682, 2020, doi: 10.1016/j.ijbiomac.2020.03.158.

[163] Y. Xu *et al.*, "Nacre-inspired construction of soft–hard double network structure to prepare strong, tough, and water-resistant soy protein adhesive," *J Appl Polym Sci*, vol. 139, no. 21, pp. 1–13, 2022, doi: 10.1002/app.52202.

[164] Y. Zhang *et al.*, "Preparation and characterization of a soy protein-based high-performance adhesive with a hyperbranched cross-linked structure," *Chemical Engineering Journal*, vol. 354, no. August, pp. 1032–1041, 2018, doi: 10.1016/j.cej.2018.08.072.

[165] S. M. Amaraweera *et al.*, "Preparation and characterization of biodegradable cassava starch thin films for potential food packaging applications," *Cellulose*, vol. 28, no. 16, pp. 10531–10548, 2021, doi: 10.1007/s10570-021-04199-6.

[166] A. Sonia and K. Priya Dasan, "Chemical, morphology and thermal evaluation of cellulose microfibers obtained from Hibiscus sabdariffa," *Carbohydr Polym*, vol. 92, no. 1, pp. 668–674, 2013, doi: 10.1016/j.carbpol.2012.09.015.

[167] H. S. Hafid, F. N. Omar, J. Zhu, and M. Wakisaka, "Enhanced crystallinity and thermal properties of cellulose from rice husk using acid hydrolysis treatment," *Carbohydr Polym*, vol. 260, no. October 2020, p. 117789, 2021, doi: 10.1016/j.carbpol.2021.117789.

[168] H. Chen, "Characteristics of lignocellulose conversion technologies," in *Lignocellulose Biorefinery Engineering: Principles and Applications*, no. 1, 2015, pp. 87–124.

[169] M. S. Jahan, A. Saeed, Z. He, and Y. Ni, "Jute as raw material for the preparation of microcrystalline cellulose," *Cellulose*, vol. 18, no. 2, pp. 451–459, 2011, doi: 10.1007/s10570-010-9481-z.

[170] I. Ullah, T. Yin, S. Xiong, J. Zhang, Z. ud Din, and M. Zhang, "Structural characteristics and physicochemical properties of okara (soybean residue) insoluble dietary fiber modified by high-energy wet media milling," *LWT - Food Science and Technology*, vol. 82, pp. 15–22, 2017, doi: 10.1016/j.lwt.2017.04.014.

[171] X. Yan, R. Ye, and Y. Chen, "Blasting extrusion processing: The increase of soluble dietary fiber content and extraction of soluble-fiber polysaccharides from wheat bran," *Food Chem*, vol. 180, pp. 106–115, 2015, doi: 10.1016/j.foodchem.2015.01.127.

[172] S. Ahmadi *et al.*, "Increasing RG-I content and lipase inhibitory activity of pectic polysaccharides extracted from goji berry and raspberry by high-pressure processing," *Food Hydrocoll*, vol. 126, no. November 2021, p. 107477, 2022, doi: 10.1016/j.foodhyd.2021.107477.

[173] R. M. Khoder *et al.*, "Effects of nano fish bone on gelling properties of tofu gel coagulated by citric acid," *Food Chem*, vol. 332, no. January, p. 127401, 2020, doi: 10.1016/j.foodchem.2020.127401.

[174] I. Mateos-Aparicio, C. Mateos-Peinado, A. Jiménez-Escrig, and P. Rupérez, "Multifunctional antioxidant activity of polysaccharide fractions from the soybean byproduct okara," *Carbohydr Polym*, vol. 82, no. 2, pp. 245–250, 2010, doi: 10.1016/j.carbpol.2010.04.020.

[175] M. A. Coimbra, A. Barros, M. Barros, D. N. Rutledge, and I. Delgadillo, "Multivariate analysis of uronic acid and neutral sugars in whole pectic samples by FT-IR spectroscopy," *Carbohydr Polym*, vol. 37, no. 3, pp. 241–248, 1998, doi: 10.1016/S0144-8617(98)00066-6.

[176] H. S. Joyner (Melito), "Explaining food texture through rheology," *Curr Opin Food Sci*, vol. 21, pp. 7–14, 2018, doi: 10.1016/j.cofs.2018.04.003.

[177] A. A. Anton and F. B. Luciano, "Instrumental texture evaluation of extruded snack foods: A review," *Ciencia y Tecnologia Alimentaria*, vol. 5, no. 4, pp. 245–251, 2007, doi: 10.1080/11358120709487697.

[178] M. Devezeaux de Lavergne, F. van de Velde, and M. Stieger, "Bolus matters: the influence of food oral breakdown on dynamic texture perception," *Food Funct*, vol. 8, no. 2, pp. 464–480, 2017, doi: 10.1039/c6fo01005a.

[179] J. Chen, "Food oral processing-A review," *Food Hydrocoll*, vol. 23, no. 1, pp. 1–25, 2009, doi: 10.1016/j.foodhyd.2007.11.013.

[180] L. Day and M. Golding, *Food structure, rheology, and texture*, vol. 3. Elsevier, 2018. doi: 10.1016/B978-0-08-100596-5.03412-0.

[181] K. Kohyama, Z. Gao, T. Watanabe, S. Ishihara, S. Nakao, and T. Funami, "Relationships Between Mechanical Properties Obtained from Compression Test and Electromyography Variables During Natural Oral Processing of Gellan Gum Gels," *J Texture Stud*, vol. 48, no. 1, pp. 66–75, 2017, doi: 10.1111/jtxs.12211.

[182] J. Guo *et al.*, "Fabrication of edible gellan gum/soy protein ionic-covalent entanglement gels with diverse mechanical and oral processing properties," *Food Research International*, vol. 62, pp. 917–925, 2014, doi: 10.1016/j.foodres.2014.05.014.

[183] J. J. Hou *et al.*, "Edible double-network gels based on soy protein and sugar beet pectin with hierarchical microstructure," *Food Hydrocoll*, vol. 50, pp. 94–101, 2015, doi: 10.1016/j.foodhyd.2015.04.012.

[184] J. J. Hou, X. Q. Yang, S. R. Fu, M. P. Wang, and F. Xiao, "Preparation of double-network tofu with mechanical and sensory toughness," *Int J Food Sci Technol*, vol. 51, no. 4, pp. 962–969, 2016, doi: 10.1111/ijfs.13043.

[185] C. Deng, Y. Liu, J. Li, M. P. Yadav, and L. Yin, "Diverse rheological properties, mechanical characteristics and microstructures of corn fiber gum/soy protein isolate hydrogels prepared by laccase and heat treatment," *Food Hydrocoll*, vol. 76, pp. 113–122, 2018, doi: 10.1016/j.foodhyd.2017.01.012.

[186] C. S. F. Picone, K. P. Takeuchi, and R. L. Cunha, "Heat-Induced Whey Protein Gels: Effects of pH and the Addition of Sodium Caseinate," *Food Biophys*, vol. 6, no. 1, pp. 77–83, 2011, doi: 10.1007/s11483-010-9177-9.

[187] W. Yan, L. Yin, J. Li, M. P. Yadav, and X. Jia, "Development of Corn Fiber Gum–Soybean Protein Isolate Double Network Hydrogels Through Synergistic Gelation," *Food Bioproc Tech*, vol. 13, no. 3, pp. 511–521, 2020, doi: 10.1007/s11947-020-02412-1.

[188] M. S. Rahman and A. I. Al-Mahrouqi, "Instrumental texture profile analysis of gelatin gel extracted from grouper skin and commercial (bovine and porcine) gelatin gels," *Int J Food Sci Nutr*, vol. 60, no. SUPPL. 7, pp. 229–242, 2009, doi: 10.1080/09637480902984414.

[189] V. A. Jideani, "Instrumental and sensory textural properties of fura," *Int J Food Prop*, vol. 5, no. 2, pp. 367–377, 2002, doi: 10.1081/JFP-120005792.

[190] J. R. Stokes, M. W. Boehm, and S. K. Baier, "Oral processing, texture and mouthfeel: From rheology to tribology and beyond," *Curr Opin Colloid Interface Sci*, vol. 18, no. 4, pp. 349–359, 2013, doi: 10.1016/j.cocis.2013.04.010.

[191] S. Yuan and S. K. C. Chang, "Standardization of physical parameters for Instron texture analysis for tofu quality evaluation," *ACS Symposium Series*, vol. 1059, pp. 231–248, 2010, doi: 10.1021/bk-2010-1059.ch015.

[192] M. Peleg, "The instrumental texture profile analysis revisited," *J Texture Stud*, vol. 50, no. 5, pp. 362–368, 2019, doi: 10.1111/jtxs.12392.

[193] K. Muthukumarappan and G. J. Swamy, "Product Specific Studies in Rheology," in *Advances in Food Rheology and Its Applications*, Woodhead Publishing Series in Food Science, 2017, pp. 245–275.

[194] M. Brighenti, S. Govindasamy-Lucey, J. J. Jaeggi, M. E. Johnson, and J. A. Lucey, "Behavior of stabilizers in acidified solutions and their effect on the textural, rheological, and sensory properties of cream cheese," *J Dairy Sci*, vol. 103, no. 3, pp. 2065–2076, 2020, doi: 10.3168/jds.2019-17487.

[195] N. Murekatete, Z. Caimeng, H. Joseph, K. Eric, and H. Yufei, "Soybean Oil Volume Fraction Effects on the Rheology Characteristics and Gelation Behavior of Glucono-δ-Lactone and Calcium Sulfate-Induced Tofu Gels," *J Texture Stud*, vol. 47, no. 2, pp. 112–130, 2016, doi: 10.1111/jtxs.12166.

[196] Y. H. Chang, S. Y. Shiau, F. B. Chen, and F. R. Lin, "Effect of microbial transglutaminase on the rheological and textural characteristics of black soybean packed tofu coagulating with Agar," *LWT - Food Science and Technology*, vol. 44, no. 4, pp. 1107–1112, 2011, doi: 10.1016/j.lwt.2010.10.020.

[197] S. Ikeda and K. Nishinari, "'Weak gel'-type rheological properties of aqueous dispersions of nonaggregated κ-carrageenan helices," *J Agric Food Chem*, vol. 49, no. 9, pp. 4436–4441, 2001, doi: 10.1021/jf0103065.

[198] E. W. Vaclavik, Vickie, Christian, "Chapter 2: Water," in *Essentials of Food Science*, 1998, pp. 21–32.

[199] W. Kneifel, P. Paquin, T. Abert, and J. P. Richard, "Water-Holding Capacity of Proteins with Special Regard to Milk Proteins and Methodological Aspects—A Review," *J Dairy Sci*, vol. 74, no. 7, pp. 2027–2041, 1991, doi: 10.3168/jds.S0022-0302(91)78373-2.

[200] M. Wu, Y. L. Xiong, J. Chen, X. Tang, and G. Zhou, "Rheological and microstructural properties of porcine myofibrillar protein-lipid emulsion composite gels," *J Food Sci*, vol. 74, no. 4, pp. 207–217, 2009, doi: 10.1111/j.1750-3841.2009.01140.x.

[201] V. L. Sok Line, G. E. Remondetto, and M. Subirade, "Cold gelation of β-lactoglobulin oil-in-water emulsions," *Food Hydrocoll*, vol. 19, no. 2, pp. 269–278, 2005, doi: 10.1016/j.foodhyd.2004.06.004.

[202] L. A. S. Aljawad and J. A. A. Bowers, "Water-Binding Capacity of Ground Lamb-Soy Mixtures with Different Levels of Water and Salt and Internal End-Point Temperatures," *J Food Sci*, vol. 53, no. 2, pp. 376–378, 1988, doi: 10.1111/j.1365-2621.1988.tb07709.x.

[203] A. N. A. Aryee, D. Agyei, and C. C. Udenigwe, "Impact of processing on the chemistry and functionality of food proteins," *Proteins in Food Processing: Second Edition*, pp. 27–45, 2018, doi: 10.1016/B978-0-08-100722-8.00003-6.

[204] K. O. Honikel and R. Hamm, "Measurement of water-holding capacity and juiciness," *Quality Attributes and their Measurement in Meat, Poultry and Fish Products*, pp. 125–161, 1994, doi: 10.1007/978-1-4615-2167-9_5.

[205] F. H. Cao *et al.*, "Effects of organic acid coagulants on the physical properties of and chemical interactions in tofu," *LWT - Food Science and Technology*, vol. 85, pp. 58–65, 2017, doi: 10.1016/j.lwt.2017.07.005.

[206] H. Zhao, B. Yu, Y. Hemar, J. Chen, and B. Cui, "Improvement of calcium sulfate-induced gelation of soy protein via incorporation of soy oil before and after thermal denaturation," *Lwt*, vol. 117, no. June 2019, p. 108690, 2020, doi: 10.1016/j.lwt.2019.108690.

[207] I. A. Rubel, E. E. Pérez, G. D. Manrique, and D. B. Genovese, "Fibre enrichment of wheat bread with Jerusalem artichoke inulin: Effect on dough rheology and bread quality," *Food Structure*, vol. 3, pp. 21–29, 2015, doi: 10.1016/j.foostr.2014.11.001.

[208] M. Ferrando and W. E. L. Spiess, "Review : Confocal scanning laser microscopy . A powerful tool in food science Revision : Microscop & iacute ; a l & aacute ; ser confocal de barrido . Una potente," *Food Science and Technology International*, vol. 6, no. 4, pp. 267–284, 2000.

[209] T. Zimmermann, J. Marrison, K. Hogg, and P. O'Toole, *Clearing Up the Signal: Spectral Imaging and Linear Unmixing in Fluorescence Microscopy. Confocal Microscopy Methods in Molecular Biology*. 2014. [Online]. Available: http://dx.doi.org/10.1007/978-1-60761-847-8_5

[210] A. Canette and R. Briandet, "Microscopy: Confocal Laser Scanning Microscopy," *Encyclopedia of Food Microbiology: Second Edition*, pp. 676–683, 2014, doi: 10.1016/B978-0-12-384730-0.00214-7.

[211] L. van den Berg, T. van Vliet, E. van der Linden, M. A. J. S. van Boekel, and F. van de Velde, "Physical properties giving the sensory perception of whey proteins/polysaccharide gels," *Food Biophys*, vol. 3, no. 2, pp. 198–206, 2008, doi: 10.1007/s11483-008-9084-5.

[212] L. van den Berg, T. van Vliet, E. van der Linden, M. A. J. S. van Boekel, and F. van de Velde, "Breakdown properties and sensory perception of whey proteins/polysaccharide mixed gels as a function of microstructure," *Food Hydrocoll*, vol. 21, no. 5–6, pp. 961–976, 2007, doi: 10.1016/j.foodhyd.2006.08.017.

[213] Y. Feng, W. Liu, R. Mercadé-Prieto, and X. D. Chen, "Dye-protein interactions between Rhodamine B and whey proteins that affect the photoproperties of the dye," *J Photochem Photobiol A Chem*, vol. 408, no. October 2020, 2021, doi: 10.1016/j.jphotochem.2020.113092.

[214] S. Yan, F. Xie, S. Zhang, L. Jiang, B. Qi, and Y. Li, "Effects of soybean protein isolate − polyphenol conjugate formation on the protein structure and emulsifying properties: Protein − polyphenol emulsification performance in the presence of chitosan," *Colloids Surf A Physicochem Eng Asp*, vol. 609, no. June 2020, p. 125641, 2021, doi: 10.1016/j.colsurfa.2020.125641.

[215] Y. Y. Chang, D. Li, L. J. Wang, C. H. Bi, and B. Adhikari, "Effect of gums on the rheological characteristics and microstructure of acid-induced SPI-gum mixed gels," *Carbohydr Polym*, vol. 108, no. 1, pp. 183–191, 2014, doi: 10.1016/j.carbpol.2014.02.089.

[216] C. H. Bi, D. Li, L. J. Wang, and B. Adhikari, "Viscoelastic properties and fractal analysis of acid-induced SPI gels at different ionic strength," *Carbohydr Polym*, vol. 92, no. 1, pp. 98–105, 2013, doi: 10.1016/j.carbpol.2012.08.081.

[217] S. Lee and D. K. Lee, "What is the proper way to apply the multiple comparison test?," *Korean J Anesthesiol*, vol. 71, no. 5, pp. 353–360, 2018, doi: 10.4097/kja.d.18.00242.

[218] E. Sulejmani, O. S. Boran, T. Huppertz, and A. A. Hayaloglu, "Rheology, microstructure and sensory properties of low-fat milk jam: Influence of inulin type, sucrose content, sodium bicarbonate and calcium chloride," *Int Dairy J*, vol. 123, p. 105162, 2021, doi: 10.1016/j.idairyj.2021.105162.

[219] F. J. Kao, N. W. Su, and M. H. Lee, "Effect of Water-to-Bean Ratio on the Contents and Compositions of Isoflavones in Tofu," *J Agric Food Chem*, vol. 52, no. 8, pp. 2277–2281, 2004, doi: 10.1021/jf035410w.

[220] C. Wu, W. Ma, and Y. Hua, "The relationship between breaking force and hydrophobic interactions or disulfide bonds involved in heat-induced soy protein gels as affected by heating time and temperature," *Int J Food Sci Technol*, vol. 54, no. 1, pp. 231–239, 2019, doi: 10.1111/ijfs.13931.

[221] H. Bader Ul Ain *et al.*, "Comparative study of chemical treatments in combination with extrusion for the partial conversion of wheat and sorghum insoluble fiber into soluble," *Food Sci Nutr*, vol. 7, no. 6, pp. 2059–2067, 2019, doi: 10.1002/fsn3.1041.

[222] S. Huang, R. Tao, A. Ismail, and Y. Wang, "Cellulose nanocrystals derived from textile waste through acid hydrolysis and oxidation as reinforcing agent of soy protein film," *Polymers (Basel)*, vol. 12, no. 4, 2020, doi: 10.3390/POLYM12040958.

[223] W. Hou, L. Yang, F. Yin, Y. Mo, R. Liao, and Y. Yuan, "Preparation of a Novel Cellulose Insulation with Network Structure by Citric Acid Crosslinking," *IEEE Transactions on Dielectrics and Electrical Insulation*, vol. 28, no. 4, pp. 1171–1180, 2021, doi: 10.1109/TDEI.2021.009522.

[224] S. M. Loveday, "Food Proteins: Technological, Nutritional, and Sustainability Attributes of Traditional and Emerging Proteins," *Annu Rev Food Sci Technol*, vol. 10, no. 1, pp. 311–339, 2019, doi: 10.1146/annurev-food-032818-121128.

[225] M. M. Rahman, K. Mat, G. Ishigaki, and R. Akashi, "A review of okara (soybean curd residue) utilization as animal feed: Nutritive value and animal performance aspects," *Anim Sci J*, vol. 92, no. 1, p. e13594, 2021, doi: 10.1111/asj.13594.

[226] W. C. Vong and S. Q. Liu, "Biovalorisation of okara (soybean residue) for food and nutrition," *Trends Food Sci Technol*, vol. 52, pp. 139–147, 2016, doi: 10.1016/j.tifs.2016.04.011.

[227] H. H. Liu and M. I. Kuo, "Effect of microwave heating on the viscoelastic property and microstructure of soy protein isolate gel," *J Texture Stud*, vol. 42, no. 1, pp. 1–9, 2011, doi: 10.1111/j.1745-4603.2010.00262.x.

[228] Z. S. Liu, S. K. C. Chang, L. te Li, and E. Tatsumi, "Effect of selective thermal denaturation of soybean proteins on soymilk viscosity and tofu's physical properties," *Food Research International*, vol. 37, no. 8, pp. 815–822, 2004, doi: 10.1016/j.foodres.2004.04.004.

[229] S. Matsuyama, M. Nakauma, T. Funami, K. Hori, and T. Ono, "Human physiological responses during swallowing of gel-type foods and its correlation with textural perception," *Food Hydrocoll*, vol. 111, no. September 2020, p. 106353, 2021, doi: 10.1016/j.foodhyd.2020.106353.

[230] V. D. Truong and C. R. Daubert, "Comparative study of large strain methods for assessing failure characteristics of selected food gels," *J Texture Stud*, vol. 31, no. 3, pp. 335–353, 2000, doi: 10.1111/j.1745-4603.2000.tb00294.x.

[231] W. Canet, M. D. Alvarez, and M. J. Gil, "Fracture behaviour of potato samples (cv. Desiree) under uniaxial compression," *J Food Eng*, vol. 82, no. 4, pp. 427–435, 2007, doi: 10.1016/j.jfoodeng.2007.02.054.

[232] L. Campo and C. Tovar, "Influence of the starch content in the viscoelastic properties of surimi gels," *J Food Eng*, vol. 84, no. 1, pp. 140–147, 2008, doi: 10.1016/j.jfoodeng.2007.05.011.

[233] W. N. Ainis, C. Ersch, C. Farinet, Q. Yang, Z. J. Glover, and R. Ipsen, "Rheological and water holding alterations in mixed gels prepared from whey proteins and rapeseed proteins," *Food Hydrocoll*, vol. 87, no. January 2018, pp. 723–733, 2019, doi: 10.1016/j.foodhyd.2018.08.023.

[234] L. Jankowiak, D. M. Sevillano, R. M. Boom, M. Ottens, E. Zondervan, and A. J. van der Goot, "A process synthesis approach for isolation of isoflavones from okara," *Ind Eng Chem Res*, vol. 54, no. 2, pp. 691–699, 2015, doi: 10.1021/ie5038962.

[235] S. Ouajai and R. A. Shanks, "Morphology and structure of hemp fibre after bioscouring," *Macromol Biosci*, vol. 5, no. 2, pp. 124–134, 2005, doi: 10.1002/mabi.200400151.

[236] Y. Zhang *et al.*, "Preparation and characterization of a soy protein-based high-performance adhesive with a hyperbranched cross-linked structure," *Chemical Engineering Journal*, vol. 354, no. June, pp. 1032–1041, 2018, doi: 10.1016/j.cej.2018.08.072.

[237] X. Fan *et al.*, "Effects of ultrasound-assisted enzyme hydrolysis on the microstructure and physicochemical properties of okara fibers," *Ultrason Sonochem*, vol. 69, no. July, 2020, doi: 10.1016/j.ultsonch.2020.105247.

[238] J. Chu, H. Zhao, Z. Lu, F. Lu, X. Bie, and C. Zhang, "Improved physicochemical and functional properties of dietary fiber from millet bran fermented by Bacillus natto," *Food Chem*, vol. 294, no. 1, pp. 79–86, 2019, doi: 10.1016/j.foodchem.2019.05.035.

[239] C. Sun, X. Wu, X. Chen, X. Li, Z. Zheng, and S. Jiang, "Production and characterization of okara dietary fiber produced by fermentation with Monascus anka," *Food Chem*, vol. 316, no. September 2019, p. 126243, 2020, doi: 10.1016/j.foodchem.2020.126243.

[240] Y. Wen, M. Niu, B. Zhang, S. Zhao, and S. Xiong, "Structural characteristics and functional properties of rice bran dietary fiber modified by enzymatic and enzyme-micronization treatments," *LWT - Food Science and Technology*, vol. 75, pp. 344–351, 2017, doi: 10.1016/j.lwt.2016.09.012.

[241] B. De, A. Shrivastav, T. Das, and T. K. Goswami, "Physicochemical and nutritional assessment of soy milk and soymilk products and comparative evaluation of their effects on blood gluco-lipid profile," *Applied Food Research*, vol. 2, no. 2, p. 100146, 2022, doi: 10.1016/j.afres.2022.100146.

[242] Z. Košťálová and Z. Hromádková, "Structural characterisation of polysaccharides from roasted hazelnut skins," *Food Chem*, vol. 286, no. September 2018, pp. 179–184, 2019, doi: 10.1016/j.foodchem.2019.01.203.

[243] M. Szymanska-Chargot and A. Zdunek, "Use of FT-IR Spectra and PCA to the Bulk Characterization of Cell Wall Residues of Fruits and Vegetables Along a Fraction Process," *Food Biophys*, vol. 8, no. 1, pp. 29–42, 2013, doi: 10.1007/s11483-012-9279-7.

[244] M. A. Monsoor, U. the Kalapathy, and A. Proctor, "Determination of polygalacturonic acid content in pectin extracts by diffuse reflectance Fourier transform infrared spectroscopy," *Food Chem*, vol. 74, no. 2, pp. 233–238, 2001, doi: 10.1016/S0308-8146(01)00100-5.

[245] Z. Lyu, G. Sala, and E. Scholten, "Water distribution in maize starch-pea protein gels as determined by a novel confocal laser scanning microscopy image analysis method and its effect on structural and mechanical properties of composite gels," *Food Hydrocoll*, vol. 133, no. July, p. 107942, 2022, doi: 10.1016/j.foodhyd.2022.107942.

[246] I. Rosalina and M. Bhattacharya, "Dynamic rheological measurements and analysis of starch gels," *Carbohydr Polym*, vol. 48, no. 2, pp. 191–202, 2002, doi: 10.1016/S0144-8617(01)00235-1.

[247] J. S. Mounsey and E. D. O'Riordan, "Characteristics of Imitation Cheese Containing Native Starches," *Sensory and Nutritive Qualities of Food Characteristics*, vol. 66, no. 4, pp. 586–591, 2001.

[248] A. G. Hardie, J. J. Dynes, L. M. Kozak, and P. M. Huang, "Biomolecule-induced carbonate genesis in abiotic formation of humic substances in nature," *Can J Soil Sci*, vol. 89, no. 4, pp. 445–453, 2009, doi: 10.4141/cjss08074.

[249] X. Jin, R. Qu, Y. Wang, D. Li, and L. Wang, "Effect and Mechanism of Acid-Induced Soy Protein Isolate Gels as Influenced by Cellulose Nanocrystals and Microcrystalline Cellulose," *Foods*, vol. 11, no. 3, 2022, doi: 10.3390/foods11030461.

[250] K. E. Preece, N. Hooshyar, A. J. Krijgsman, P. J. Fryer, and N. J. Zuidam, "Intensification of protein extraction from soybean processing materials using hydrodynamic cavitation," *Innovative Food Science and Emerging Technologies*, vol. 41, pp. 47–55, 2017, doi: 10.1016/j.ifset.2017.01.002.

[251] V. Urbonaite *et al.*, "Relation between gel stiffness and water holding for coarse and fine-stranded protein gels," *Food Hydrocoll*, vol. 56, pp. 334–343, 2016, doi: 10.1016/j.foodhyd.2015.12.011.

[252] Y. Cai *et al.*, "Adjustment of the structural and functional properties of okara protein by acid precipitation," *Food Biosci*, vol. 37, no. May, p. 100677, 2020, doi: 10.1016/j.fbio.2020.100677.

[253] Good Food Institute, "2021 State of the industry report: Plant-based meat, seafood, eggs, and dairy," 2022.

[254] H. Kim, L. E. Caulfield, V. Garcia-Larsen, L. M. Steffen, J. Coresh, and C. M. Rebholz, "Plant-Based Diets Are Associated With a Lower Risk of Incident Cardiovascular Disease, Cardiovascular Disease Mortality, and All-Cause Mortality in a General Population of Middle-Aged Adults," *J Am Heart Assoc*, vol. 8, no. 16, 2019, doi: 10.1161/JAHA.119.012865.

[255] N. Noronha, E. D. O'Riordan, and M. O'Sullivan, "Influence of processing parameters on the texture and microstructure of imitation cheese," *European Food Research and Technology*, vol. 226, no. 3, pp. 385–393, 2008, doi: 10.1007/s00217-006-0549-9.

[256] L. Grossmann and D. J. McClements, "The science of plant-based foods: Approaches to create nutritious and sustainable plant-based cheese analogs," *Trends Food Sci Technol*, vol. 118, no. PA, pp. 207–229, 2021, doi: 10.1016/j.tifs.2021.10.004.

[257] N. Grasso, Y. H. Roos, S. v. Crowley, E. K. Arendt, and J. A. O'Mahony, "Composition and physicochemical properties of commercial plant-based block-style products as alternatives to cheese," *Future Foods*, vol. 4, no. May, p. 100048, 2021, doi: 10.1016/j.fufo.2021.100048.

[258] C. D. Everard, D. J. O'Callaghan, T. v. Howard, C. P. O'Donnell, E. M. Sheehan, and C. M. Delahunty, "Relationships between sensory and rheological measurements of texture in maturing commercial Cheddar cheese over a range of moisture and pH at the point of manufacture," *J Texture Stud*, vol. 37, no. 4, pp. 361–382, 2006, doi: 10.1111/j.1745-4603.2006.00057.x.

[259] S. Kapoor, M. P. Singh, H. Vatankhah, G. K. Deshwal, and H. S. Ramaswamy, "Production and quality improvement of Indian cottage cheese (Paneer) using high pressure processing," *Innovative Food Science and Emerging Technologies*, vol. 72, no. September 2020, p. 102746, 2021, doi: 10.1016/j.ifset.2021.102746.

[260] E. C. Short, A. J. Kinchla, and A. A. Nolden, "Plant-based cheeses: A systematic review of sensory evaluation studies and strategies to increase consumer acceptance," *Foods*, vol. 10, no. 4, 2021, doi: 10.3390/foods10040725.

[261] C. Chatterjee, S. Gleddie, and C.-W. Xiao, "Soybean Bioactive Peptides and Their Functional Properties," *Nutrients*, vol. 10, no. 9, p. 1211, 2018, doi: 10.3390/nu10091211.

[262] A. D. Ahnan-Winarno, L. Cordeiro, F. G. Winarno, J. Gibbons, and H. Xiao, "Tempeh: A semicentennial review on its health benefits, fermentation, safety, processing, sustainability, and affordability," *Compr Rev Food Sci Food Saf*, vol. 20, no. 2, pp. 1717–1767, 2021, doi: 10.1111/1541-4337.12710.

[263] T. Chen, "Rheological Techniques for Yield Stress Analysis," 2000. [Online]. Available: http://www.tainstruments.com/pdf/literature/RH025.pdf

[264] K. Dolatowska-Żebrowska, E. Ostrowska-Ligęza, M. Wirkowska-Wojdyła, J. Bryś, and A. Górska, "Characterization of thermal properties of goat milk fat and goat milk chocolate by using DSC, PDSC and TGA methods," *J Therm Anal Calorim*, vol. 138, no. 4, pp. 2769–2779, 2019, doi: 10.1007/s10973-019-08181-0.

[265] X. Mei Feng, T. Ostenfeld Larsen, and J. Schnürer, "Production of volatile compounds by Rhizopus oligosporus during soybean and barley tempeh fermentation," *Int J Food Microbiol*, vol. 113, no. 2, pp. 133–141, 2007, doi: 10.1016/j.ijfoodmicro.2006.06.025.

[266] C. G. Kees de Kruif, S. G. Anema, C. Zhu, P. Havea, and C. Coker, "Water holding capacity and swelling of casein hydrogels," *Food Hydrocoll*, vol. 44, pp. 372–379, 2015, doi: 10.1016/j.foodhyd.2014.10.007.

[267] V. Urbonaite, H. H. J. de Jongh, E. van der Linden, and L. Pouvreau, "Origin of water loss from soy protein gels," *J Agric Food Chem*, vol. 62, no. 30, pp. 7550–7558, 2014, doi: 10.1021/jf501728t.

[268] M. Chen *et al.*, "Study on the emulsifying stability and interfacial adsorption of pea proteins," *Food Hydrocoll*, vol. 88, no. August 2018, pp. 247–255, 2019, doi: 10.1016/j.foodhyd.2018.09.003.

[269] H. Murata, "Polymerization: Rheology - Theory and Application to Biomaterials (Chapter 17)," in *Polymerization*, 2012, pp. 403–425. [Online]. Available: http://www.intechopen.com/books/polymerization/rheology-theory-and-application-to-biomaterials

[270] M. Du, W. Lu, Y. Zhang, A. Mata, and Y. Fang, "Natural polymer-sourced interpenetrating network hydrogels: Fabrication, properties, mechanism and food applications," *Trends Food Sci Technol*, vol. 116, no. June, pp. 342–356, 2021, doi: 10.1016/j.tifs.2021.07.031.

[271] L. Ong, R. R. Dagastine, S. E. Kentish, and S. L. Gras, "Microstructure of milk gel and cheese curd observed using cryo scanning electron microscopy and confocal microscopy," *LWT - Food Science and Technology*, vol. 44, no. 5, pp. 1291–1302, 2011, doi: 10.1016/j.lwt.2010.12.026.

[272] B. Li, W. Yang, Y. Nie, F. Kang, H. D. Goff, and S. W. Cui, "Effect of steam explosion on dietary fiber, polysaccharide, protein and physicochemical properties of okara," *Food Hydrocoll*, vol. 94, no. December 2018, pp. 48–56, 2019, doi: 10.1016/j.foodhyd.2019.02.042.

[273] D. Lin *et al.*, "Effects of microbial fermentation and microwave treatment on the composition, structural characteristics, and functional properties of modified okara dietary fiber," *Lwt*, vol. 123, no. January, 2020, doi: 10.1016/j.lwt.2020.109059.

Appendices

Appendix A Okara Manuscript

Supporting Information

Table and Figure

Table S. 1 pH values of soymilk gel and untreated or treated okara soymilk gels. Results are expressed as mean ± standard deviation (n=3).

Sample	pH
M	6.55 ± 0.02
MO	6.54 ± 0.01
MOH	6.66 ± 0.01
MOHS	6.56 ± 0.00
MOCA	2.63 ± 0.01
MOCAL	2.82 ± 0.01
MOCAS	2.92 ± 0.01
MOCAH	2.59 ± 0.01
MOCAHL	2.61 ± 0.01
MOCAHS	4.22 ± 0.04

Note: pH value for MOHL was not collected due to the insufficient quantity of solid collected for the soluble fraction after treatment.

Table S. 2 Thermal degradation properties of soymilk and okara materials.

Material	Degradation peak (°C (decomposition rate, %/min))			Mass loss (wt%)				Mass at 600 °C (wt%)
	Peak #1	Peak #2	Peak #3	< 150 °C	150-250 °C	250-380 °C	380-600 °C	
M	**377 (5.7)**	-	-	5.7	10.6	41.6	20.8	21.3
O	**291 (4.5)**	-	-	5.5	7.5	46.5	18.1	22.3
OH	258 (2.9)	**312 (4.4)**	372 (4.1)	4.2	8.1	46.0	17.5	24.2
OHL	253 (2.3)	312 (3.2)	**368 (5.9)**	2.7	10.9	42.8	18.5	25.1
OHS	259 (4.0)	**323 (4.4)**	366 (2.6)	4.0	9.2	44.4	18.9	23.6
OCA	**199 (16.3)**	345 (1.3)	-	2.5	64.0	11.8	9.1	12.6
OCAL	**198 (20.9)**	-	-	1.6	69.0	10.0	7.8	11.5
OCAS	**207 (9.4)**	344 (2.3)	-	2.4	39.4	23.7	14.5	20.0
OCAH	**209 (15.0)**	344 (1.4)	-	2.8	58.7	13.8	10.4	14.3
OCAHL	**198 (15.7)**	-	-	3.8	59.7	12.5	9.7	14.2
OCAHS	**210 (7.5)**	337 (4.3)	392 (2.0)	2.0	34.6	27.7	16.4	19.4
CA	**207 (42.8)**	-	-	0	88.7	3.7	5.1	2.5

The major peak for each sample is **bolded**.
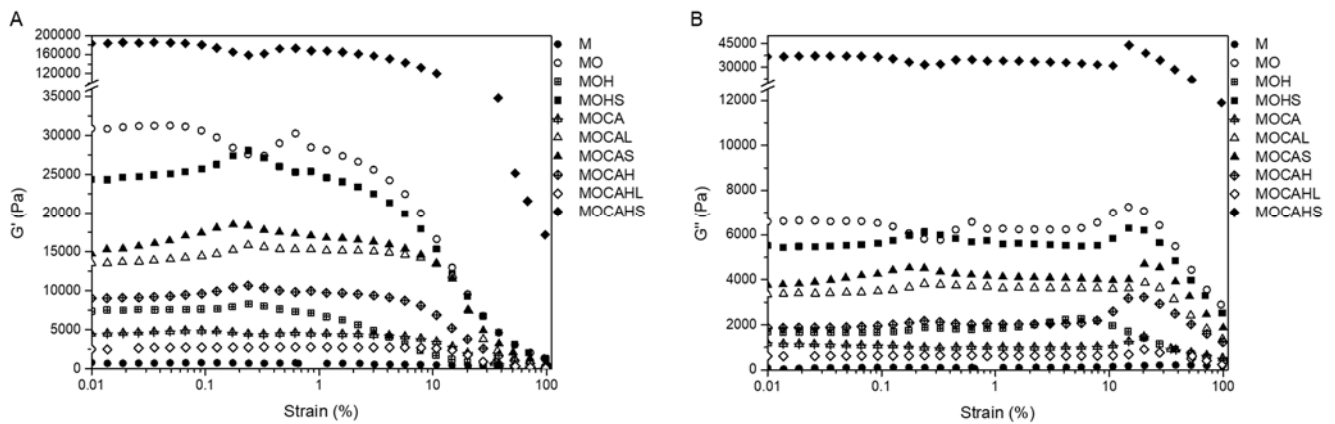
Figure S. 1 Typical curves of storage modulus, G' (A) and loss modulus, G'' (B) over strain.
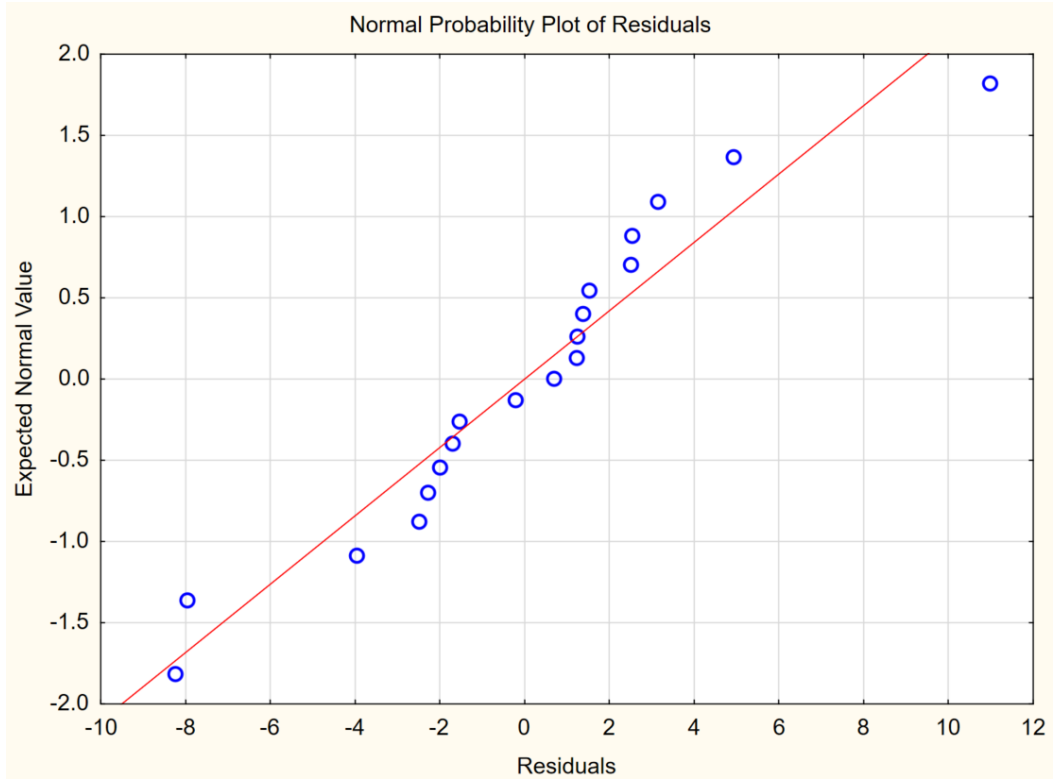
Figure S. 2 Normal probability plot of residuals of sample *M*.

Preece et al. reported the CLSM images of aqueous dispersion of whole dehulled soybean [250]. Their system is analogous to our system where all the constituents of soybeans were present. In their study, the unstained and stranded regions were identified to be the cotyledon cell wall materials, which are the empty cotyledon cell walls from which the contents had been extracted [250].

Concerning the composition of soybeans, beside the okara fiber, proteins and lipids were the main constituents. The proteins were stained by Rhodamine B (shown in red) in the CLSM images. Oil droplets on the other hand, should exhibit a circular shape, and they tend to be evenly embedded in the protein matrix as seen by CLSM images [271]. Thereby, the only possibility to explain the strand-like unstained regions would be the okara fibers, which was indicated by the white arrows in the CLSM images. Specifically, these are the empty cotyledon cell walls from which the contents had been extracted [250].

On the other hand, the irregularly shaped black cavities or voids are most likely the pores or air bubbles in the gel structure.
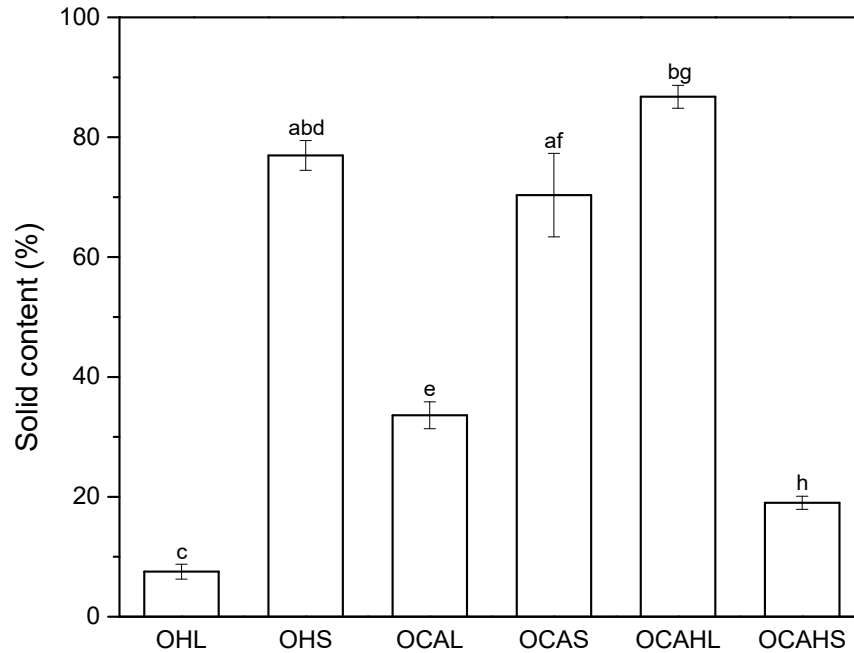
Figure S. 3 Solid content (%) of soluble (denoted as "L") and insoluble (denoted as "S") fractions with various okara treatments. Means that do not share a common letter are statistically different.

Table S. 3 True fracture stress, true fracture strain and Young's modulus of soymilk gel and untreated or treated okara soymilk gels. Results are expressed as mean ± standard deviation (n=18). Means in the same column that do not share a common superscript letter are statistically different.

Gel	True Fracture stress (kPa)	True Fracture strain (%)	Young's modulus (kPa)
MO	3.97 ± 0.70^a	49.6 ± 7.5^{ab}	16.4 ± 3.7^a
MOH	2.82 ± 0.37^b	46.1 ± 6.7^a	12.5 ± 2.4^b
MOHS	4.30 ± 0.59^a	52.6 ± 6.4^b	16.1 ± 2.1^{ac}
MOCA	2.44 ± 0.18^{bc}	36.8 ± 5.0^c	12.7 ± 1.4^{bcd}
MOCAL	3.44 ± 0.39^d	26.1 ± 3.9^d	22.9 ± 3.9^e
MOCAS	4.18 ± 0.73^a	26.8 ± 3.3^d	30.1 ± 6.3^f
MOCAH	2.21 ± 0.17^c	38.7 ± 3.4^c	10.8 ± 1.3^{bd}
MOCAHL	3.40 ± 0.25^d	38.9 ± 4.4^c	14.1 ± 1.9^{abcd}
MOCAHS	No fracture detected		11.4 ± 3.8^{bd}

Note: Data for M and MOHL were not collected, due to the lack of gel strength and insufficient quantity of solid collected for the soluble fraction after treatment, respectively.

Result Comparison with Existing Publications

Table S. 4 Summary of existing publications of treated okara fibers in solid form.

Objective	Source of Major Ingredient(s)	Okara Treatment Method(s)	Treatment Process	Okara Properties		Treated Soy Okara Sample Properties	Reference
				FTIR		Microstructure	
Examine effect of ultrasound powers on okara fiber structural and physicochemical properties	Commercial okara	Ultrasound treatment at power intensities of 0, 44, 127, 190, 255, and 318 W/cm^2	Okara was firstly ground with high-speed grinder to reduce particle size to 80-100 um, then dispersed in DI water for treatment with ultrasound	Decrease in bands 1157 and 1023 cm^{-1} as ultrasound power intensity increases, indicating the decomposition of okara fibers into oligosaccharides		Okara surface was smooth without ultrasound treatment; with ultrasound treatment, okara fibers became broken and flaky forming irregular block-like structure that was tightly packed (SEM)	[237]
Improve functionalities of okara by enzymatic, chemical or physical modifications	Dried commercial okara, combined with phosphate buffer (PB) and NaOH, treated with	Cellulase treatment; Chemical treatment (0.1-0.9 Na$_2$HPO$_4$); Physical treatment (high-pressure homogenizer)	Cellulase treatment: dried IDF dispersed in PB with cellulase; Chemical treatment: dried IDF treated with Na$_2$HPO$_4$;	Band at 1680 cm^{-1} became more prominent, indicating modified okara fibers were oxidized, which may be caused by the disruption	-		[121]

	trypsase, then centrifuged to collect supernatant as insoluble dietary fiber (IDF)		Physical treatment: dried IDF suspended acetic acid buffer then homogenized in high-pressure homogenizer, then treated with cellulase; supernatant was collected after centrifugation and freeze-dried for all treatments	of bonds of IDF into small fractions and were more prone to oxidization		
Effect of steam explosion on okara properties	Commercial wet okara	Steam explosion	Okara powder treated with steam explosion then dried and ground to sieve through 40-80 mesh sieves	-	Okara destroyed into small fragments with loose sheet structure upon steam explosion (SEM)	[272]
Effect of microbial fermentation and microwave treatment on functional properties of okara	Commercial okara	Fermentation treatment and microwave treatment	Fermentation treatment (FDF): okara fibers were fermented at 30 °C for 2 days; Microwave treatment (MDF): okara fibers were diluted in 3% citric acid and microwaved at 600 W for 2.5 min; all treated samples were freeze-dried and crushed through 0.25 mm mesh sieves	Change of functional groups in cellulose and hemicellulose were noted for microwave treatment, whereas changes in fermented okara fiber was not obvious	Unfermented okara fibers were massive with wrinkled surface, whereas fermented okara had much looser surface and particles were more dispersed; microwaved okara fibers had porous and loose structure, possibly due to cellular ruptures caused by microwave energy (SEM)	[273]
Examine okara properties obtained by high pressure homogenization and alkaline-acid recovery	Commercial fresh okara	High pressure homogenization and alkaline-acid recovery	Okara-water dispersion was homogenized first with a high-speed blender then treated with a high-pressure homogenizer (HPH); okara was then submitted to alkaline-acid recovery adjusting pH to 12 with NaOH, then acidifying the supernatant to pH 4.2 with HCl; centrifuged to obtain	Samples subjected to highest homogenization pressure (HPH) showed the most significant peaks associated to lipids; HPH favours the release of intracellular components other than proteins	-	[107]

			precipitate to be freeze-dried			
Examine O/W emulsifying properties of insoluble soybean polysaccharides	Commercial defatted solvent-free soy flour (DSF)	High pressure valve homogenization or high intensity ultrasonic homogenization	DSF subjected to alkaline treatment (pH 9) with NaOH; residue was centrifuged then subjected to acid treatment (pH 3.5) with HCl; then treated with high pressure homogenization or ultrasonic homogenization	Increase in band intensities associated with protein and carbohydrate for homogenized insoluble soybean polysaccharide (ISPS) samples	-	[136]
Effect of centrifugal milling and steam heating pre-treatment on cellulase modified soy okara residues	Fresh soy okara prepared with a pilot-scale soymilk and tofu equipment, then dried in a conveyor oven	Ultracentrifugal milling, Steam heating, Enzymatic hydrolysis (including cellulase, xylanase, and multienzyme complex)	Ultracentrifugal milling: dried okara milled in an ultracentrifugal mill through 250-1000 um sieve; Steam heating: raw or milled okara subjected to steam heating via autoclave; Enzymatic hydrolysis: citric acid buffer (pH 5.5) containing enzyme was added to steam preheated okara samples to incubate and centrifuged; pellet was washed and freeze-dried	Band associated with oligosaccharides (1035 cm^{-1}) increased by different treatments, suggesting the decomposition of insoluble fiber into small molecular weight substances such as oligosaccharides	Modified okara residues (740 um) displayed clear honeycomb-like structure with compact texture and smooth surface (SEM); okara treated with ultracentrifugal milling (390 um), had flaky and stacked structure; as okara size decreased further (147 um), honeycomb-structure was no longer observed (SEM)	[122]

Table S. 5 Summary of existing publications of treated okara incorporated into soymilk for the formation of tofu analogue gels induced by heat and use of coagulant.

Objective	Source of Major Ingredient(s)	Okara Treatment Method(s)	Treatment Process	Gel Preparation	Treated Soy Okara Sample Properties			Reference
					Mechanical	Viscoelastic	Microstructure	
Produce nanocellulose from okara and gel with SPI	Commercial defatted okara and SPI	Wet-type grinding	2 wt% okara pulverized with Supermasscolloider	6% SPI homogenized with wet ground okara, gelled with $MgCl_2$ and NaCl, heated at 80 °C for 30 min	Breaking Stress: 220-500 Pa; Breaking Strain: 38-41%	-	-	[108]
Effect of high-intensity ultrasound treatment on properties of okara tofu	Commercial okara and SPI	High-intensity ultrasound treatment at 500, 600, 700, and 800 W for 20 min	Okara ground in high-speed grinder then mixed with SPI-water suspension; treated with ultrasound at 25 °C	1% w/v GDL added to treated okara-SPI suspension, heated at 80 °C then cooled	Hardness: 306-657 g (trigger force = 5 g)	G_0': 103-124 Pa; G_0'': 53-95 Pa	Ultrasound-treated okara broken into flaky pieces embedded irregularly in network with non-uniform pores (SEM)	[8]
Effect of soybean soluble polysaccharides (SSPS) on GDL-induced SPI gel	Commercial SSPS and SPI	-	-	10% w/v SPI mixed with 0-15% w/w SSPS and heated at 75 °C then 90 °C for 10 min; GDL was added and incubated at 85 °C and cooled	Gel strength: 40-64 g	-	SSPS retarded the formation of SPI gels, resulting in a loose microstructure with larger pore sizes (SEM)	[149]
Effect of okara particle size on properties of GDL-induced tofu	Soybean seeds	Okara was prepared from soybean seeds by grinding soaked seeds followed by drying	Dried okara was micronized by an ultra-micro pulverizer and sieved through 40-200 meshes to obtain particle sizes of 250-380 um, 150-180 um,	Okara combined with soymilk and heated at 75 °C then 90 °C for 10 min; 0.3% GDL was	Gel strength: 63-86 g	-	Gels with large-sized okara (250-380 um) had loose and non-uniform structure whereas the one with small	[119]

			120-150 um, and < 75 um	added and incubated at 85 °C and cooled			okara (< 75 um) showed more compact structure (SEM)	
Effect of okara particle size on okara-tofu gels	Commercial fresh okara and soybean seeds	Pulverization and/or high-energy wet milling	Fresh okara was dried and defatted then treated 1M NaOH and later 1M HCl; dried okara was coarse milled with a pulverizer then sieved to pore sizes < 120 um (MDF, 110 um); some were further ground with a high-energy wet mill (NDF, 370 nm)	Soaked soybeans were ground to extract soymilk; suspensions of MDF and NDF were homogenized and mixed with soymilk at ratio of 0-50 % (v/v); dispersion was heated to 95 °C with the addition of 0.02 M $MgCl_2$ followed by incubation at 80 °C to form gel that was later molded under atmospheric pressure	Hardness: 558-1070 g (MDF-added tofu); 244-1084 g (NDF-added tofu)	-	Addition of some MDF (<20%) did not alter the continuous phase but irregularly distributed fragments were observed; With MDF increase (30-40%), size and number of cavities in continuous phase increased; addition of NDF (10-20%) resulted irregular network with large number of cavities (SEM)	[13]
Effect of compound coagulants on quality of whole soybean curd	Commercial soybean seeds	Enzymatic treatment (transglutaminase, TGase)	-	Soaked soybeans were ground with high-speed mill then dispersed in water and heated to 50 °C then 95 °C; $CaCl_2$ and TGase were	Rupture strength after cooking: 406-769 g (for 500-6000 ppm TGase); Hardness after cooking: 759-868 g (for 500-6000		Irregular and porous gel structure was observed without TGase; tighter and less porous structure shown with increasing TGase concentration (SEM)	[10]

				added to soymilk at 50 °C to incubate then 95 °C; gels were molded under pressured of 16 g/cm² for 30 min	ppm TGase)			
Effect of high-speed shearing of okara on aggregation behaviour and microstructure of whole soybean curd	Commercial soybean seeds	High-speed shearing (HSS)	Soybean flour dispersed in water and treated with high-speed shearing (HSS) homogenizer then filtered by a 300-mesh sieve	Treated suspensions were heated at 95 °C and filtered by a 300-mesh seieve; 0.4% GDL was then added and incubated at 55 °C to form whole soybean curd	Gel strength: 27-55 g	-	Seed coat detected in whole soybean curd forming disordered gel structure; though okara fiber size decreased after HSS but the gel network became loose and less cohesive	[4]
Modification of okara fiber to improve its compatibility	Commercial okara insoluble dietary fiber (O-IDF)	Layer-by-layer coating of chitosan/pectin on okara dietary fiber	O-IDF was micronized in an ultrafine grinder and sieved through 400 mesh; chitosan coat was prepared (O-IDF/C) by dissolving chitosan in acetic acid (pH 4) then adding O-IDF to mixture dropwise and adjust pH to 4.5-6.5; pellet was obtained via centrifuge and spray-dried; pectin coat was prepared (O-IDF/C/P) by dispersing O-IDF/C in acetic acid and added dropwise to	Soaked soybeans were ground to removed okara; extracted soymilk was heated to 95 °C then 10 g/L of O-IDF and O-IDF/C/P were suspended in soymilk and homogenized in high-speed dispersion homogenizer	-	-	Spray-dried O-IDF had much coarse surfaces; chitosan-pectin coated okara particles showed smoother surface with no apparent cracks; coating of chitosan only resulted in thin films tightly adhered to the surface of the particles and no significant changes in	[120]

189

			pectin solution; treated solid okara obtained via centrifuge and spray-dry				size and shape (SEM) *Note: prepared gel was not imaged, only the okara particles were imaged*	
Evaluate properties of okara-soy gel prepared by mTGase	Commercial soybeans	High-pressure homogenization (HPH) and enzymatic treatment by TGase	Okara was separated from soymilk and suspended in water and ground in a high-speed mill; ground okara was subjected to high-pressure homogenization at 40-100 MPa	SPI mixed with 60% w/w ultrafine okara using a homogenizer and heated at 100 °C; TGase (30 U/g) was added to the mixture and incubated at 45 °C for 1 h	-	G': 150-1400 Pa; G": 10-140 Pa (0-10 Hz)	Okara without HPH had largest particle size composing of numerous fiber strands; HPH sheared okara fibers to smaller bundles; clustering of okara decreased as pressure increased but fiber flocculation was observed (CLSM)	[11]
Effect of heating condition on okara-tofu modified by enzymatic hydrolysis with cellulase and high-pressure homogenization	Commercial soybeans	Enzymatic hydrolysis with cellulase and high-pressure homogenization	Soaked soybeans were blanched at 100 °C then ground with water; slurry was mixed with commercial cellulase and heated at 50 °C; treated soymilk was homogenized at 30 Mpa by high pressure homogenizer	0.5 g of NaCl was added to 500 g of cooked whole cotyledon soymilk; then 1.75 g of CaSO$_4$ was added at 75 °C; after soymilk was cooled, it was pressed in a mold with 1 kg load for 40 min	Gel strength: 61-72 g (for heating at 90-95 °C, 5 min), 84-120 g (for boiling time of 0-6 min); Hardness: 68-109 g (for heating at 90-95 °C, 5 min), 68-95 g	-	-	[9]

					(for boiling time of 0-6 min)			
Examine okara-tofu modified with mTGase	Commercial soybeans	TGase treatment	An additional 0.15% w/w TGase was added to okara-soymilk mixture during tofu preparation and incubated at 50 °C for 240 min, before incubation at 85 °C to obtain TGase-induced high-fiber tofu (TG-HFT)	Soybeans were ground with water to separate soymilk from okara; 60% of the total okara was added back to soymilk and homogenized with a high-pressure homogenizer at 40 MPa to reduce size to < 50 um; okara-soymilk heated to 95 °C, then 0.3% w/w GDL was added and incubated at 85 °C to obtain high-fiber tofu (HFT)	Gel strength: 55 g for HFT and 110 g for TG-HFT	G': 600-1100 Pa for HFT, 720-1300 Pa for TG-HFT; G'': 40-160 Pa for HFT, 10-180 Pa for TG-HFT (0-10 Hz)	Tofu prepared without okara had continuous and smooth network with small and uniform pores; HFT had discontinuous protein network with large okara particles; TG-HFT also had discontinuity in the protein network but appears to be slightly more uniform (SEM)	[5]
Effects of different processing techniques on whole soybean curd	Commercial soybeans	Superfine grinding, Ultrasonic disruption, Cellulase enzymolysis	Superfine grinding: soybeans were ground in a pulverizer and further ground by a superfine pulverizer; power dispersed in water to prepare WSM; WSM was then treated with ultrasonic cleaner or with enzyme (cellulase)	Cleaned and soaked soybeans were ground; soy slurry was heated at 90 °C then 0.5% GDL, 0.07% MgCl2, and 0.02% MTGase were added to	Gel strength: 146-189 g; Hardness: 148-196 g (for the three treatment techniques)	-	Treatment of superfine grinding produced uniform honey-comb structure with small lumps embedded in protein network; treatment of ultrasonic disruption	[12]

				soymilk and incubated at 50 °C then 85 °C; curd was cooled and stored			resulted large and unevenly distributed lumps; Treatment by cellulase produce discontinuo us protein network with various-sized pores and lumps (SEM)	

Raw Data of Uniaxial Compression and Viscoelastic Measurements
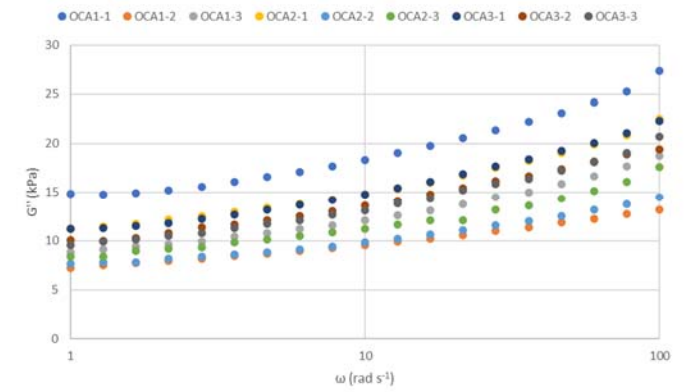
Stress-Strain Curves
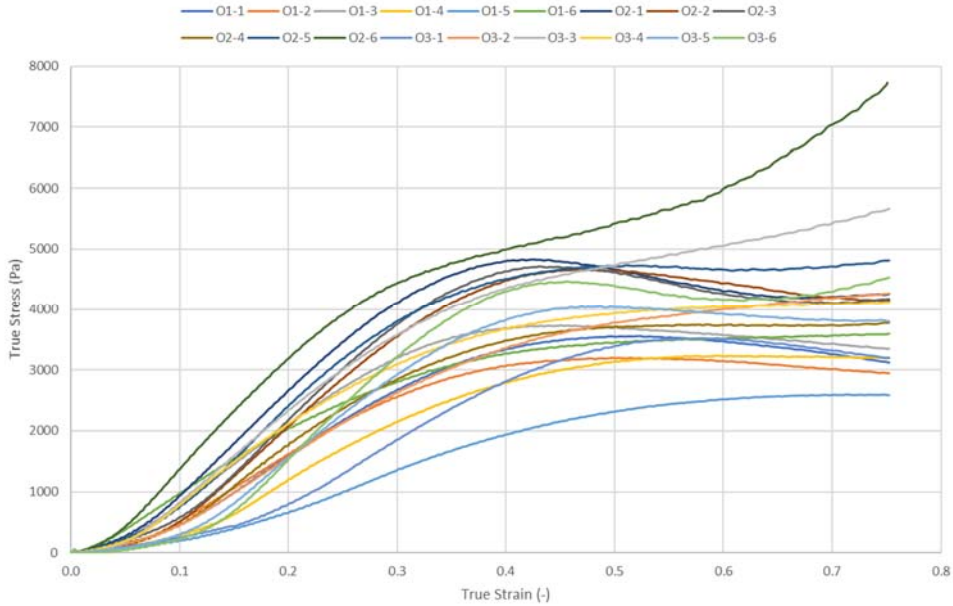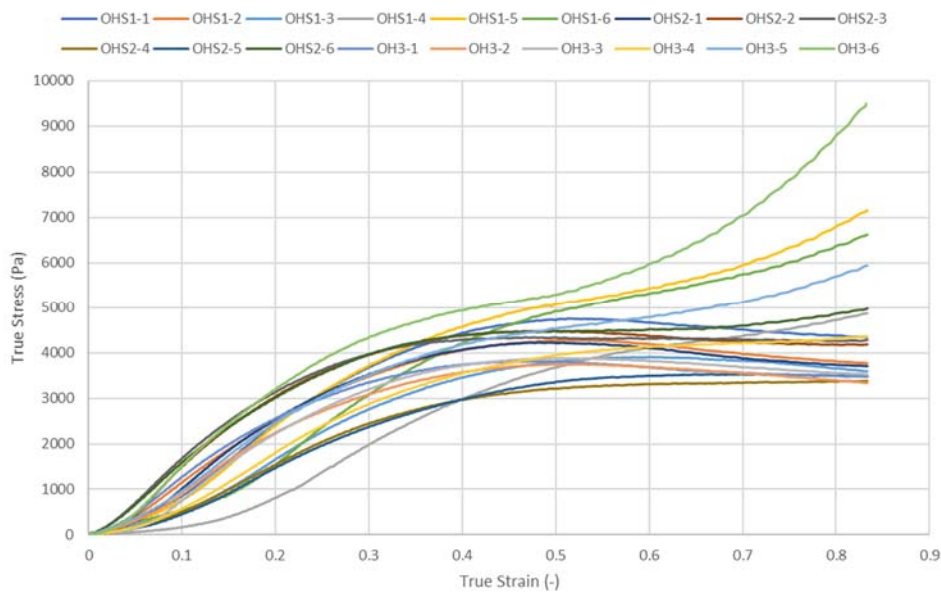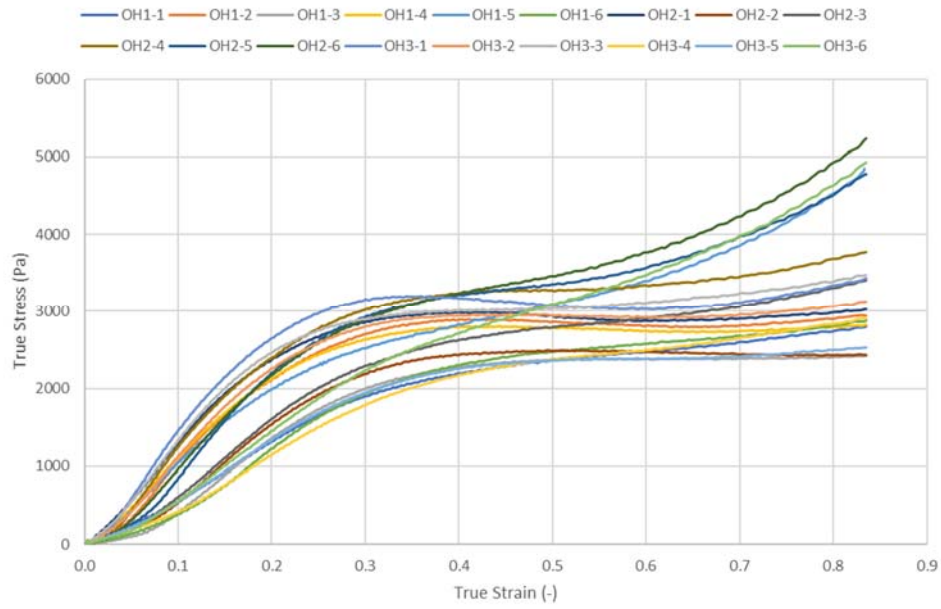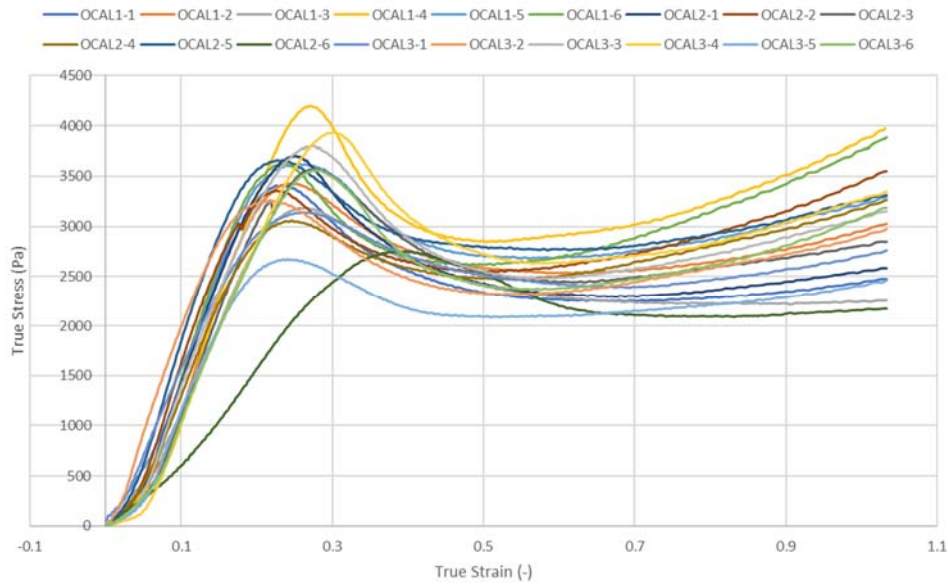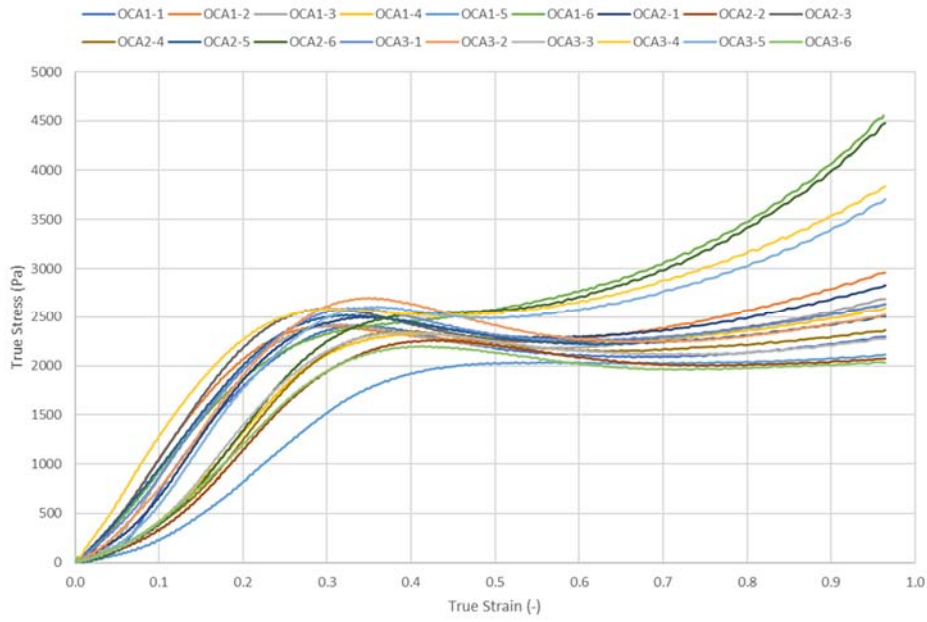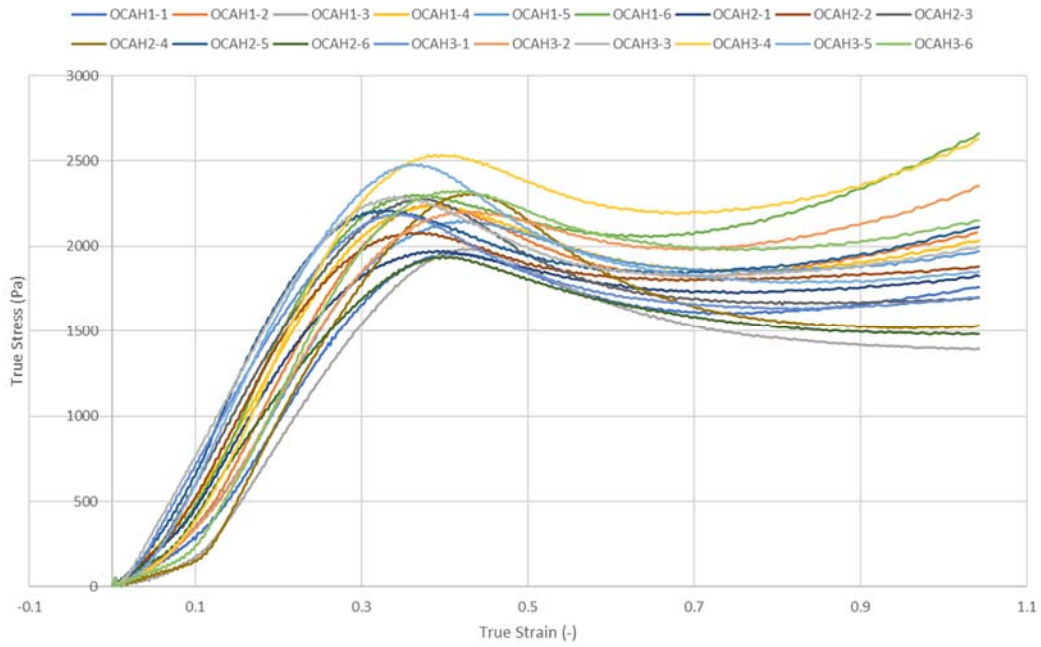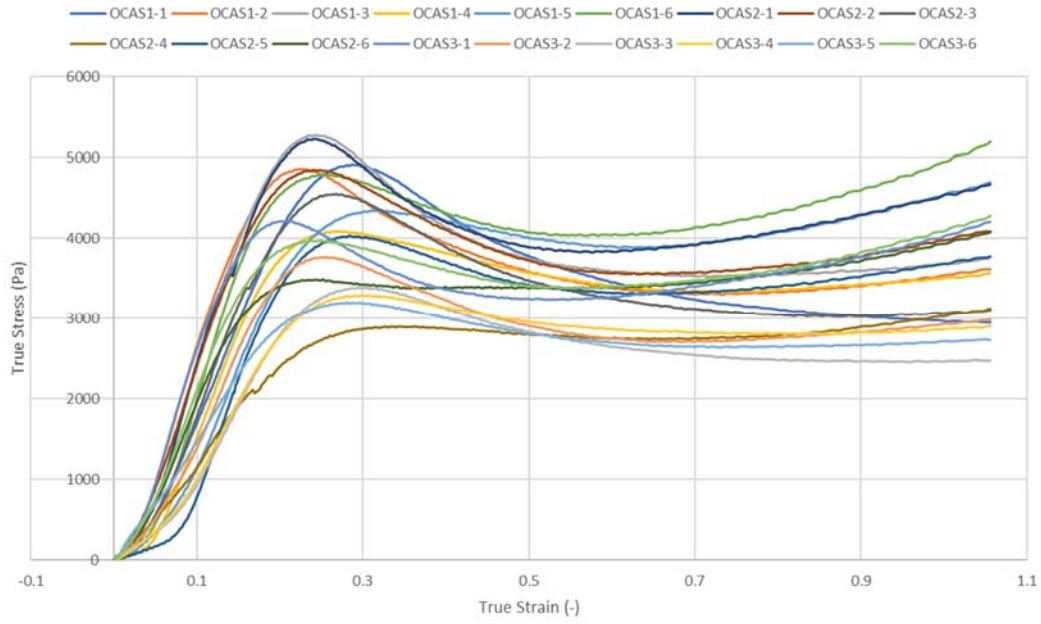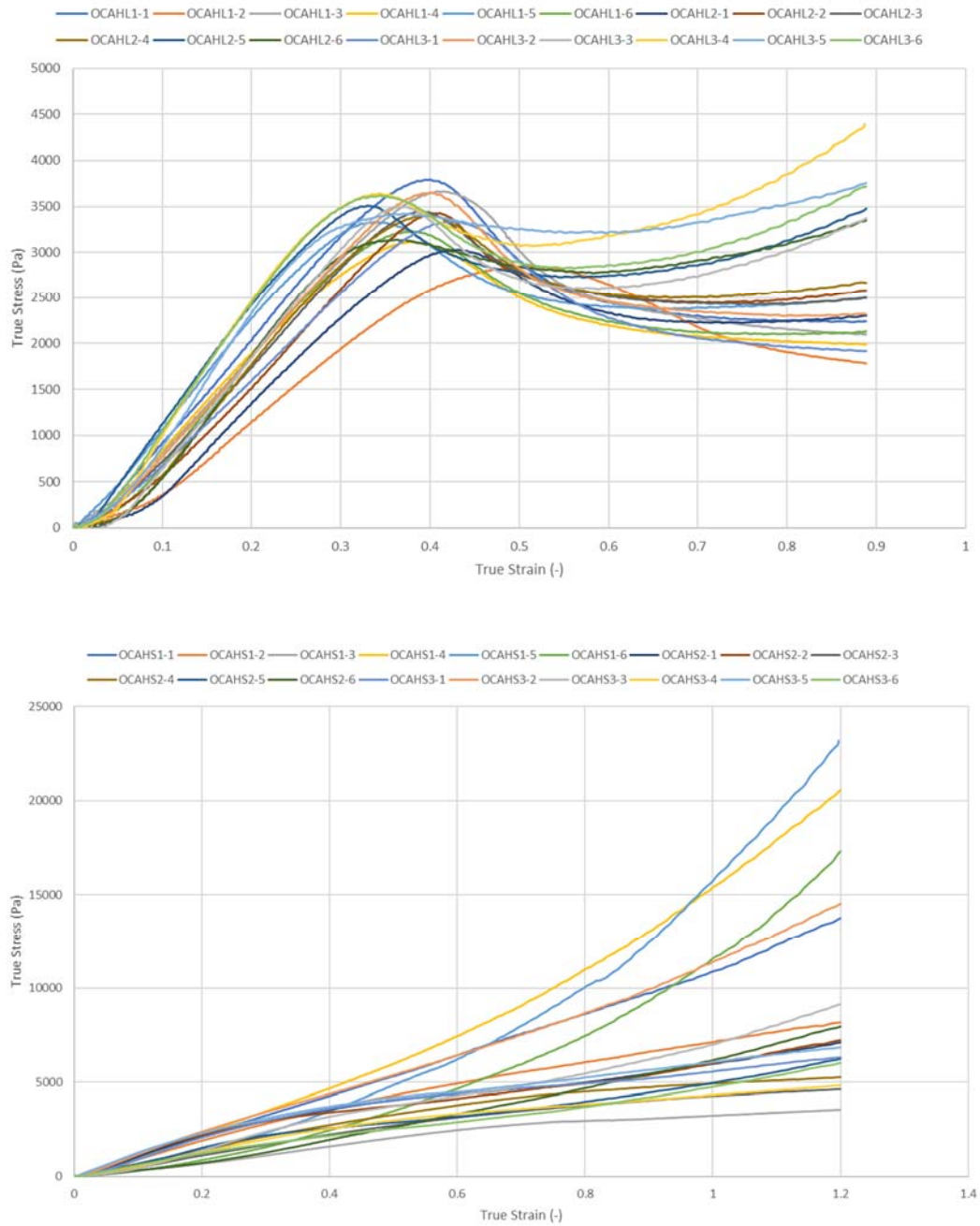
Figure S. 4 True stress-strain curves of untreated or citric-acid-treated okara soymilk gels. Abbreviations can be referred to the main text of the manuscript.
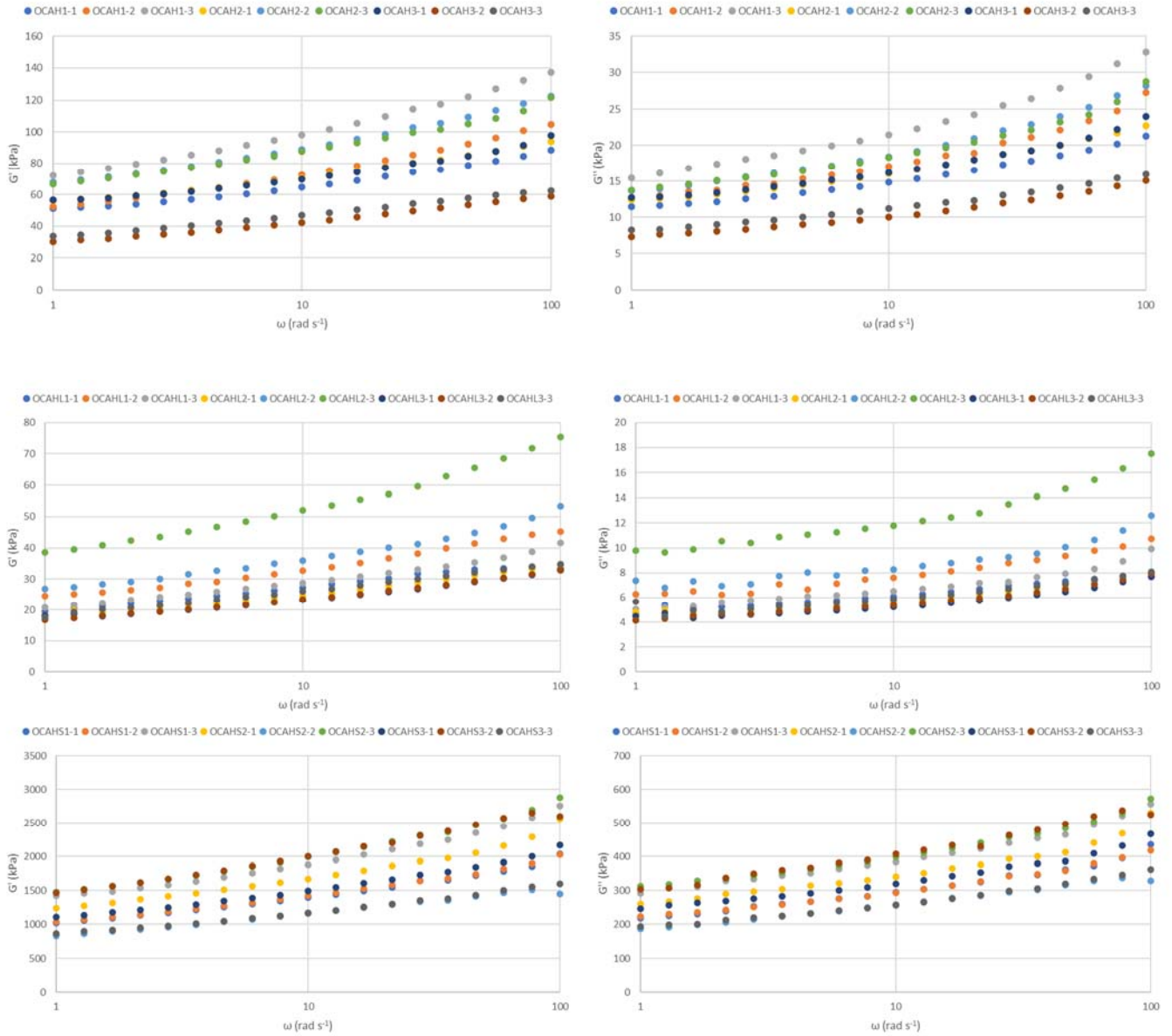
Frequency Sweep Plots
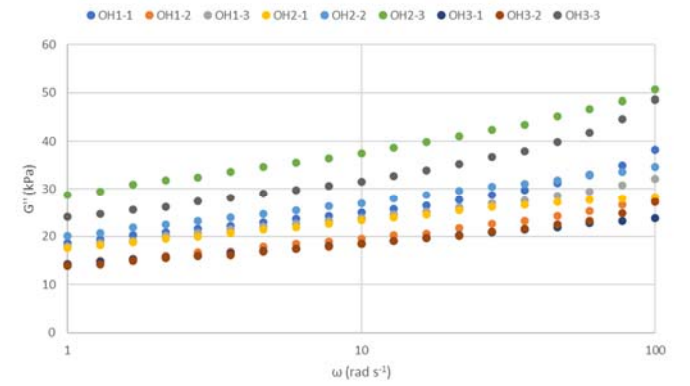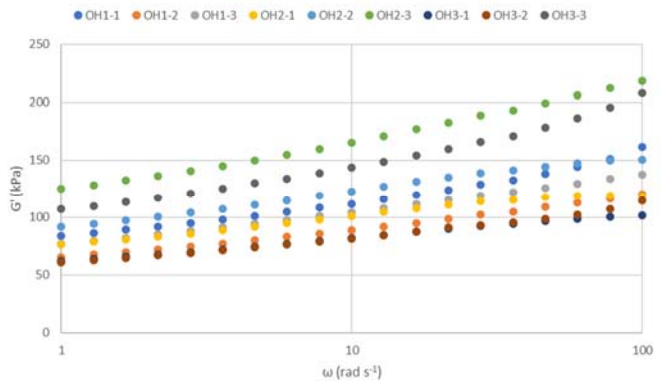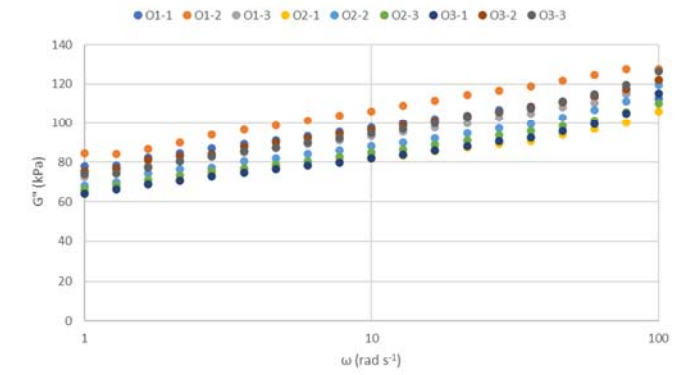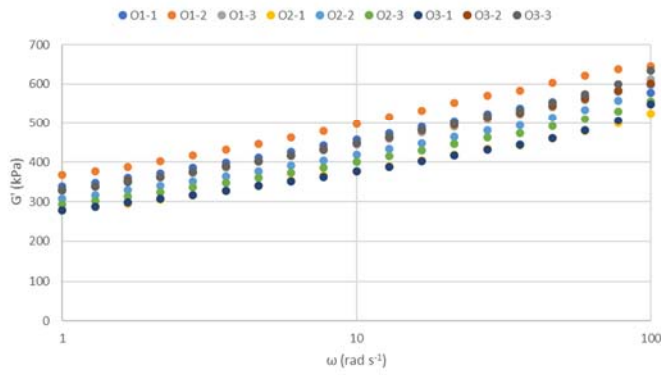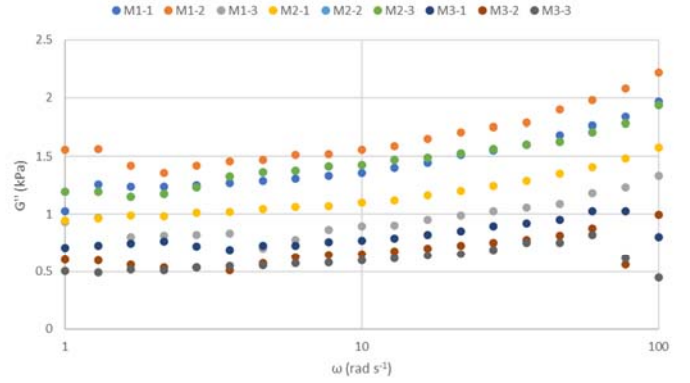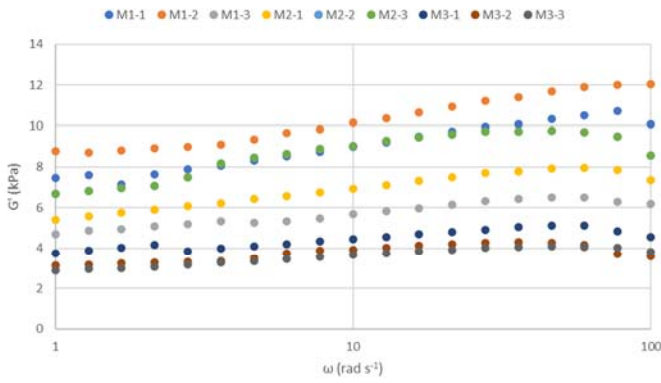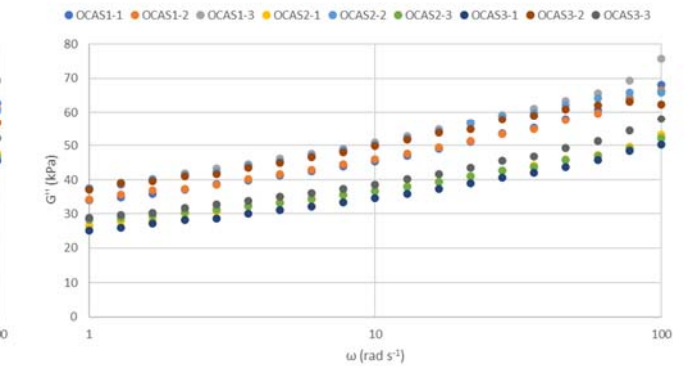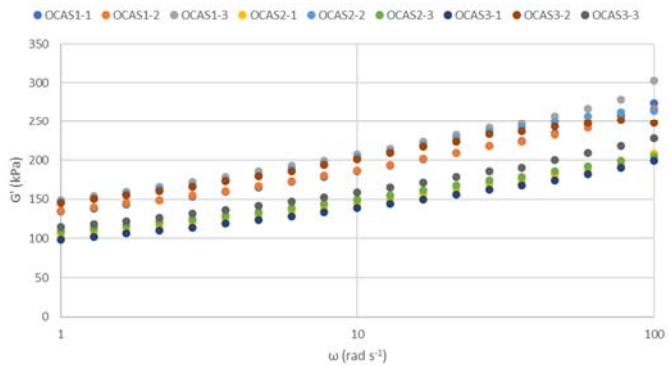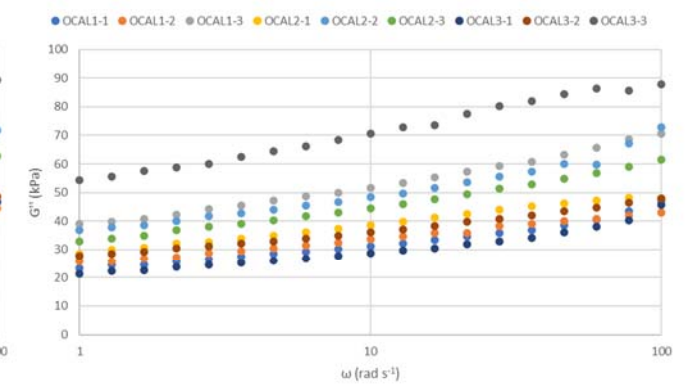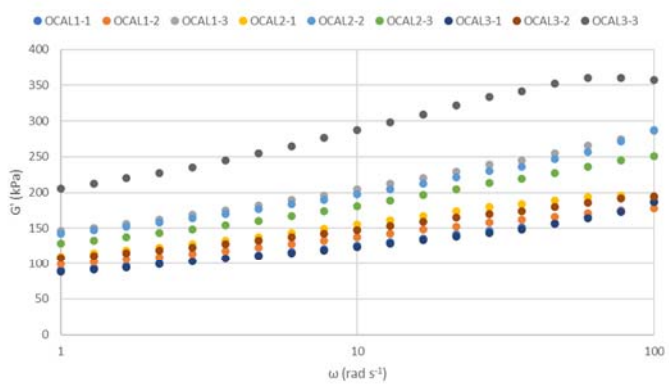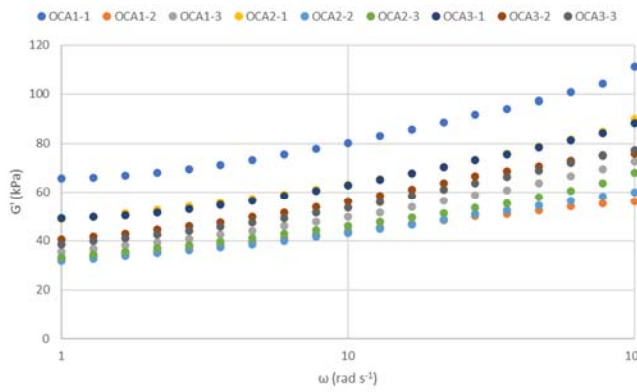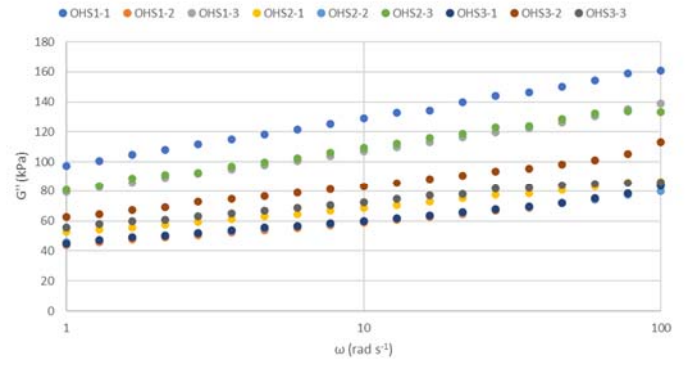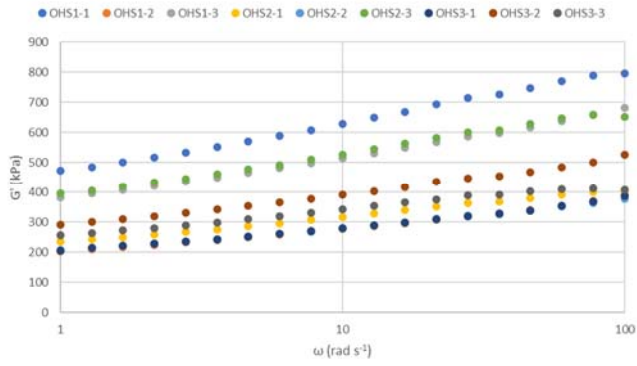
Figure S. 5 Storage (G') and loss (G'') moduli of untreated or citric-acid-treated okara soymilk gels as functions of angular frequency. Abbreviations can be referred to the main text of the manuscript.

Supporting Information

Table and Figure

Table S. 6 Thermal degradation properties of commercial products. Abbreviations: FM, fresh mozzarella; PM, pizza mozzarella; P, paneer; EFT, extra firm tofu; MFT, medium firm tofu; T, tempeh; VM, vegan mozzarella; VC, vegan cheddar.

Product	Degradation peak (°C, (decomposition rate, %/min))			Weight loss (%)				Mass at 600 °C (%)
	Peak 1	Peak 2	Peak 3	< 150 °C	150-240 °C	240-400 °C	400-600 °C	
FM	121 (1.3)	**331** **(8.2)**	-	6.3	4.4	63.9	9.1	16.2
PM	194 (1.3)	**336** **(8.6)**	-	14.0	4.8	63.2	6.1	12.0
P	122 (3.9)	**334** **(8.0)**	-	6.4	4.0	61.3	9.2	19.1
EFT	**328** **(5.5)**	-	-	4.0	5.2	56.0	14.3	20.4
MFT	**362** **(5.6)**	-	-	3.9	5.9	59.0	15.0	16.3
T	83 (2.2)	144 (2.3)	**335** **(3.6)**	22.9	6.9	43.3	11.8	15.0
VM	151 (2.4)	**306** **(8.2)**	-	3.0	5.3	70.9	10.8	10.0
VC	51 (4.0)	**124** **(8.5)**	311 (4.1)	42.7	3.7	41.9	2.4	9.3

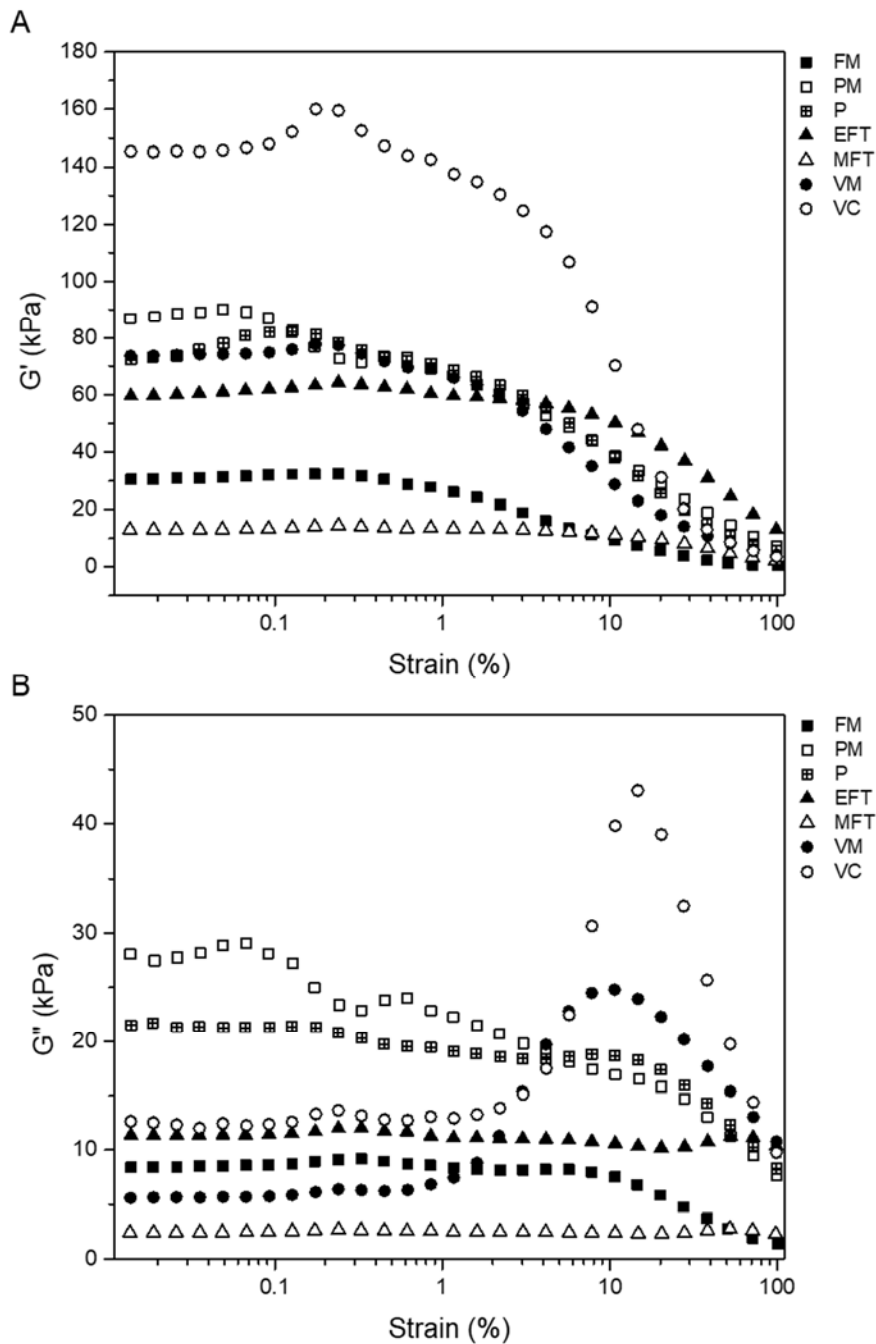*Bolded numbers are major degradation temperature peaks and corresponding rates.

Figure S. 6 Typical storage modulus, G' (A) and loss modulus, G'' (B) of commercial products as a function of strain. Abbreviations: FM, fresh mozzarella; PM, pizza mozzarella; P, paneer; EFT, extra firm tofu; MFT, medium firm tofu; VM, vegan mozzarella; VC, vegan cheddar.

Table S. 7 Yield strain of the commercial products and power law parameters estimated according to **Equation 12** and **Equation 13** of the main manuscript. Power law estimates expressed as means of 3 replicates ± standard deviation. Means in the same column that do not share a common superscript letter are significantly different. Tempeh was not evaluated due to its crumbly and heterogeneous structure. Abbreviations: FM, fresh mozzarella; PM, pizza mozzarella; P, paneer; EFT, extra firm tofu; MFT, medium firm tofu; VM, vegan mozzarella; VC, vegan cheddar.

| Product	Yield strain (%)	$G_0' \times 10^3$ (Pa)	n' (-)	R^2	$G_0'' \times 10^3$ (Pa)	n'' (-)	R^2
FM	0.8	278.8 ± 37.4^{ad}	0.14 ± 0.01^a	0.988 ± 0.011^a	81.1 ± 12.4^a	0.12 ± 0.01^{ac}	0.944 ± 0.033^{ab}
PM	0.2	51.6 ± 3.8^d	0.19 ± 0.01^d	0.998 ± 0.002^a	20.0 ± 1.1^d	0.13 ± 0.01^a	0.996 ± 0.003^a
P	1.1	641.7 ± 38.1^b	0.12 ± 0.00^b	0.958 ± 0.019^b	170.2 ± 8.9^b	0.11 ± 0.00^c	0.921 ± 0.025^{ab}
EFT	6.3	378.1 ± 41.0^{ab}	0.10 ± 0.00^b	0.994 ± 0.000^a	69.8 ± 8.3^a	0.12 ± 0.00^{ac}	0.986 ± 0.002^{ab}
MFT	7.7	115.5 ± 9.8^{ad}	0.11 ± 0.01^b	0.999 ± 0.000^a	21.7 ± 1.7^{cd}	0.12 ± 0.01^{ac}	0.995 ± 0.001^a
VM	1.1	665.1 ± 157.2^b	0.04 ± 0.01^c	0.990 ± 0.013^a	51.4 ± 15.0^{ac}	0.06 ± 0.01^b	0.885 ± 0.081^b
VC	2.0	1142.5 ± 270.7^c	0.05 ± 0.00^c	0.990 ± 0.007^a	82.0 ± 18.7^a	0.12 ± 0.00^{ac}	0.982 ± 0.014^{ab}
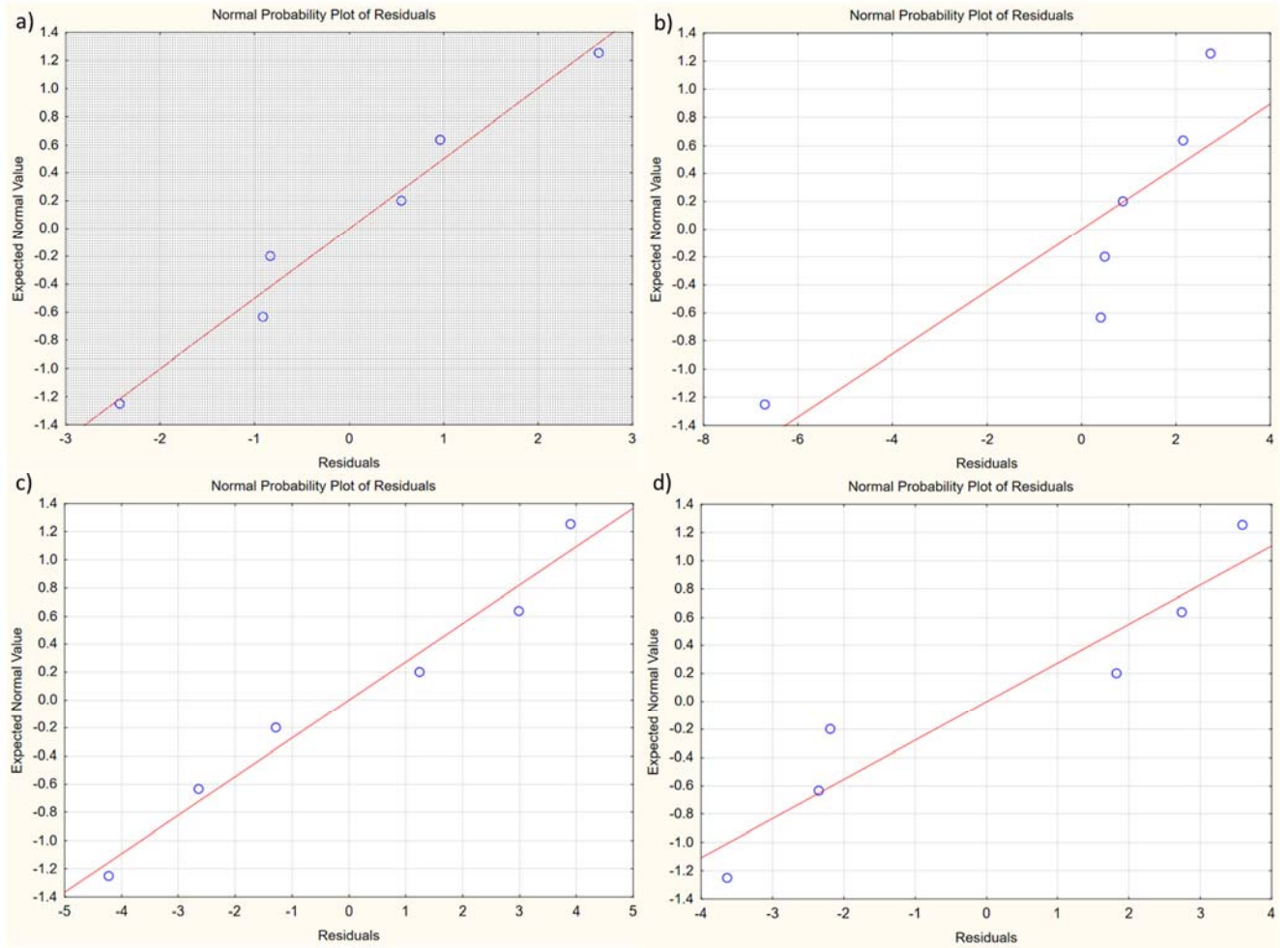
Figure S. 7 Normal probability plot of residuals for a) fat and yield strain, b) carbohydrate and fracture stress, c) carbohydrate and n', and d) moisture and fat.

Additional Table and Figure

Table S. 8 True fracture stress, true fracture strain and Young's modulus of commercial products. Values expressed as means of 7 replicates ± standard deviation. Tempeh was not evaluated due to difficulty in sample cutting because of its inhomogeneous structure. Means in the same column that do not share a common superscript letter are significantly different. Abbreviations: FM, fresh mozzarella; PM, pizza mozzarella; P, paneer; EFT, extra firm tofu; MFT, medium firm tofu; T, tempeh; VM, vegan mozzarella; VC, vegan cheddar.

Commercial products	Load cell used (N)	True fracture stress (kPa)	True Fracture strain (-)	Young's modulus (kPa)
FM	50	10.9 ± 1.5^a	1.67 ± 0.03^b	7.2 ± 1.1^a
PM	500	59.2 ± 9.4^b	0.54 ± 0.06^c	154.8 ± 28.6^b
P	500	49.4 ± 7.0^c	1.00 ± 0.04^a	66.0 ± 10.4^c
EFT	500	23.2 ± 4.0^d	1.04 ± 0.04^a	30.1 ± 4.5^{ac}
MFT	50	11.2 ± 1.9^a	1.06 ± 0.19^a	13.0 ± 2.1^a
VM	500	90.1 ± 4.6^e	0.48 ± 0.03^c	277.6 ± 12.3^d
VC	500	94.5 ± 5.1^e	0.29 ± 0.04^d	518.2 ± 50.8^e

Table S. 9 Yield strain or strain at end of LVR; range of dynamic moduli (G' and G'') and tan δ over angular frequency range of 1 – 100 rad/s for commercial products. Tempeh was not evaluated due to difficulty in sample cutting because of its inhomogeneous structure. Abbreviations: FM, fresh mozzarella; PM, pizza mozzarella; P, paneer; EFT, extra firm tofu; MFT, medium firm tofu; VM, vegan mozzarella; VC, vegan cheddar.

| Commercial products	Yield strain (%)	G' x 10^3 (Pa)	G'' x 10^3 (Pa)	tan δ
FM	0.8	293 – 531	88 – 147	0.27 – 0.30
PM	0.2	48 – 130	19 – 38	0.29 – 0.39
P	1.1	693 – 1161	184 – 296	0.25 – 0.27
EFT	6.3	388 – 624	73 – 128	0.19 – 0.21
MFT	7.7	116 – 189	22 – 39	0.19 – 0.21
VM	1.1	669 – 797	34 – 46	0.05 – 0.06
VC	2.0	1156 – 1460	81 – 135	0.07 – 0.09
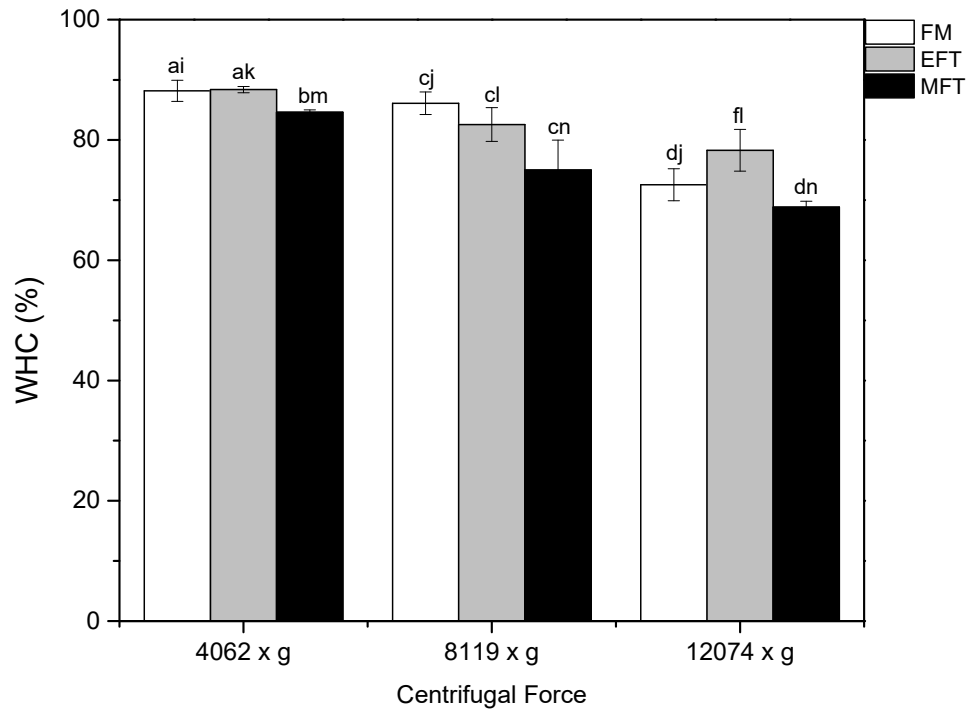
Figure S. 8 WHC of fresh mozzarella (FM), extra firm tofu (EFT) and medium firm tofu (MFT) at different centrifugal forces for 20 min. Values presented as average ± standard deviation (n = 3). Means at each centrifugal force across different products are statistically different if the first letter is different. Means for each product at different centrifugal forces are statistically different if the second letter is different.

Raw Data

Mechanical True Stress-True Strain Curves
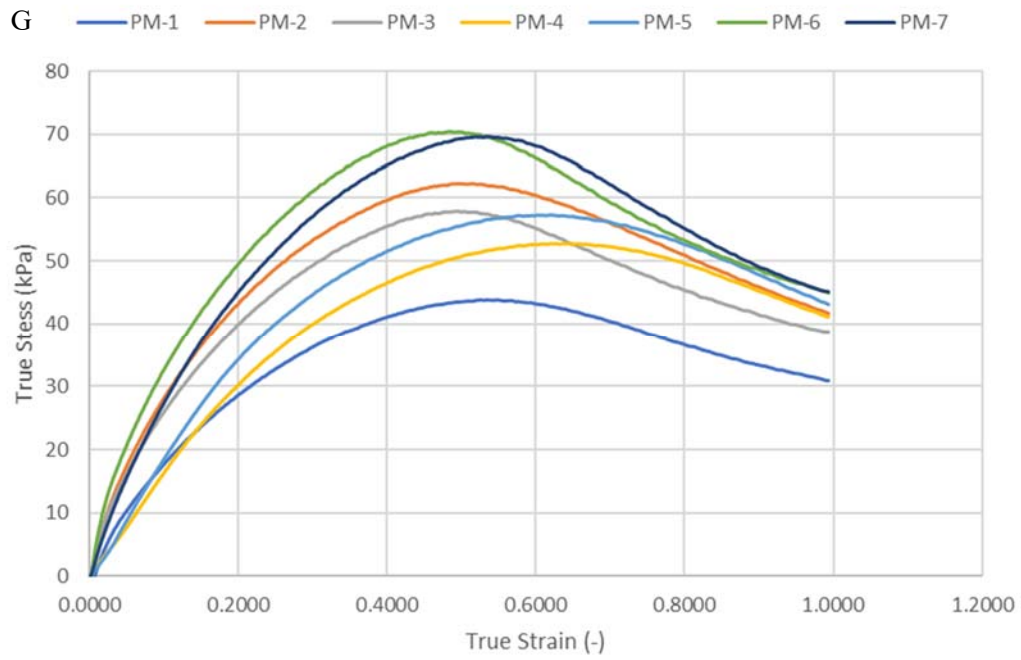

A

B

C

D

E

F
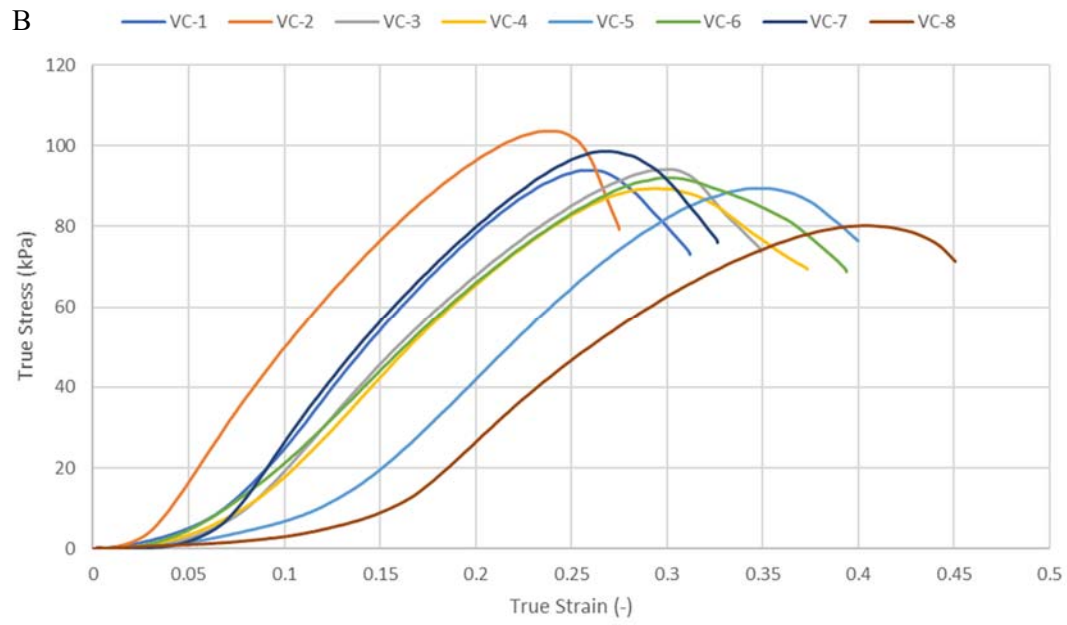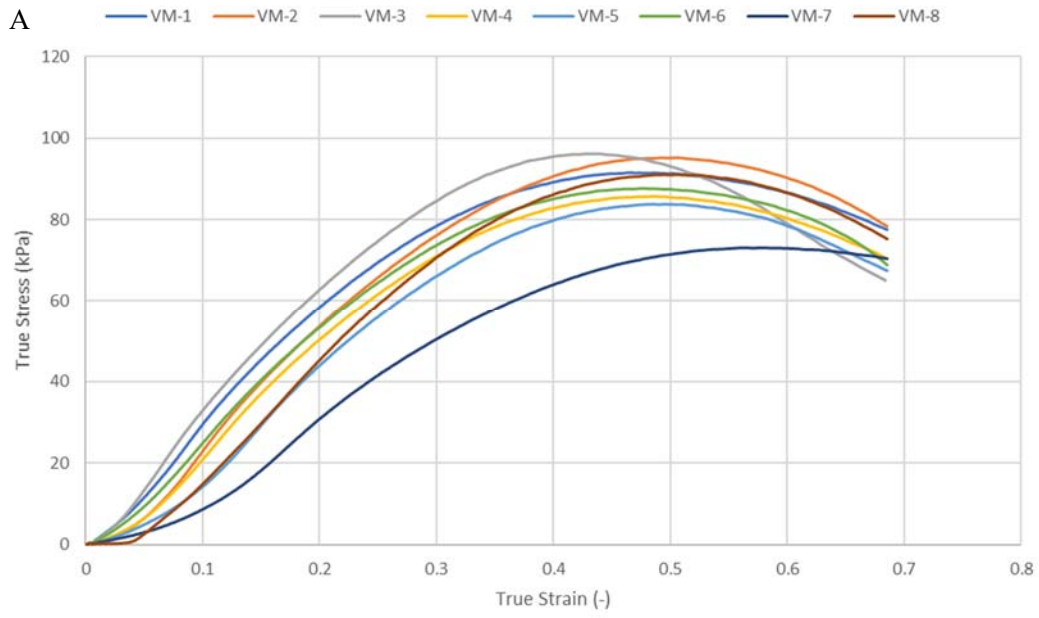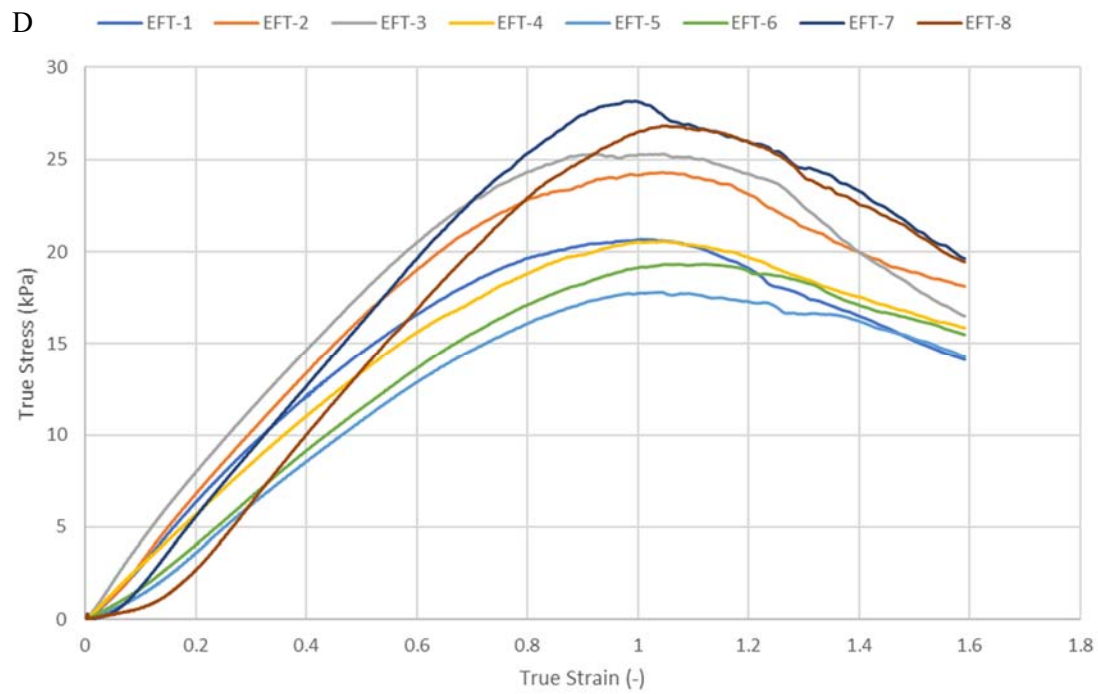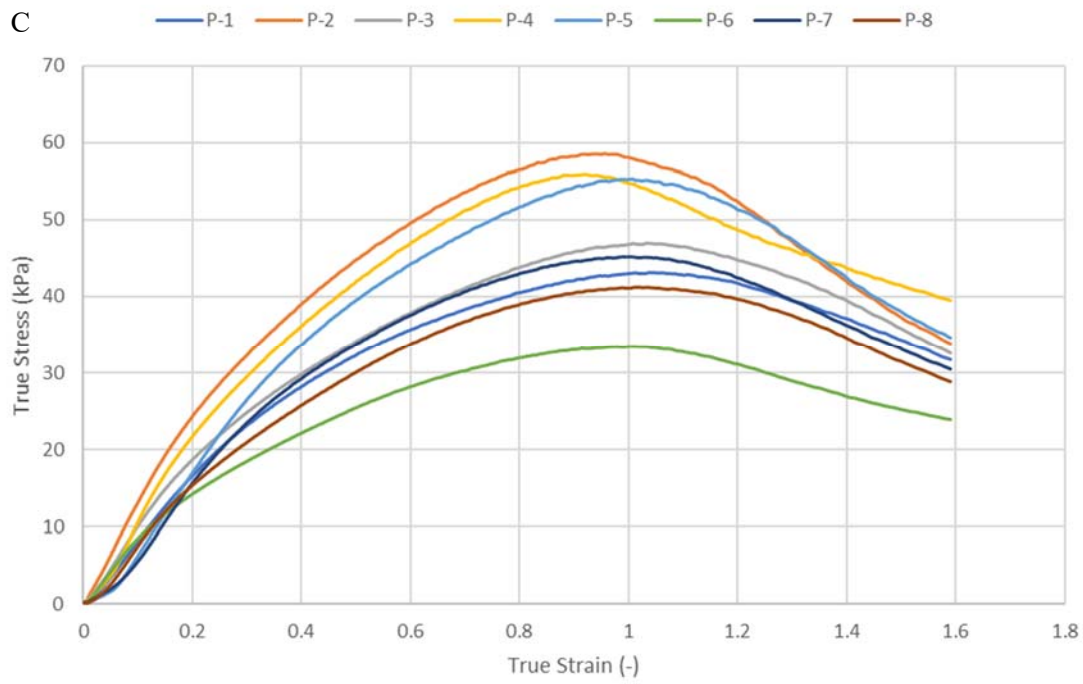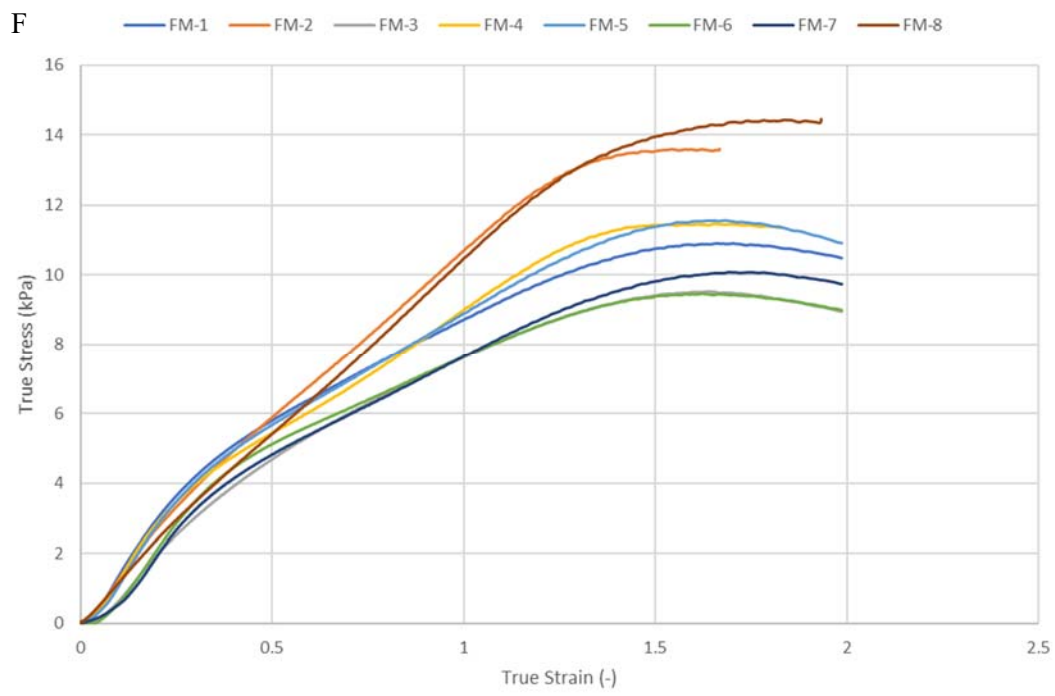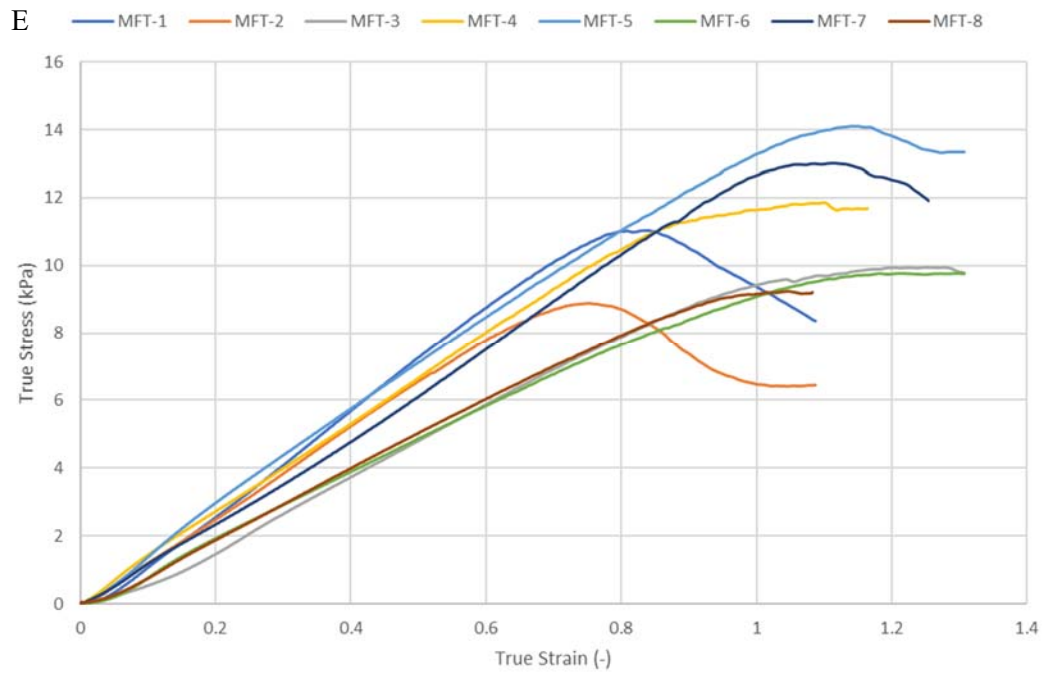
Figure S. 9 True stress-strain curves of the various commercial products with seven test replicates: (A) VM, (B) VC, (C) P, (D) EFT, (E) MFT, (F) FM, and (G) PM.
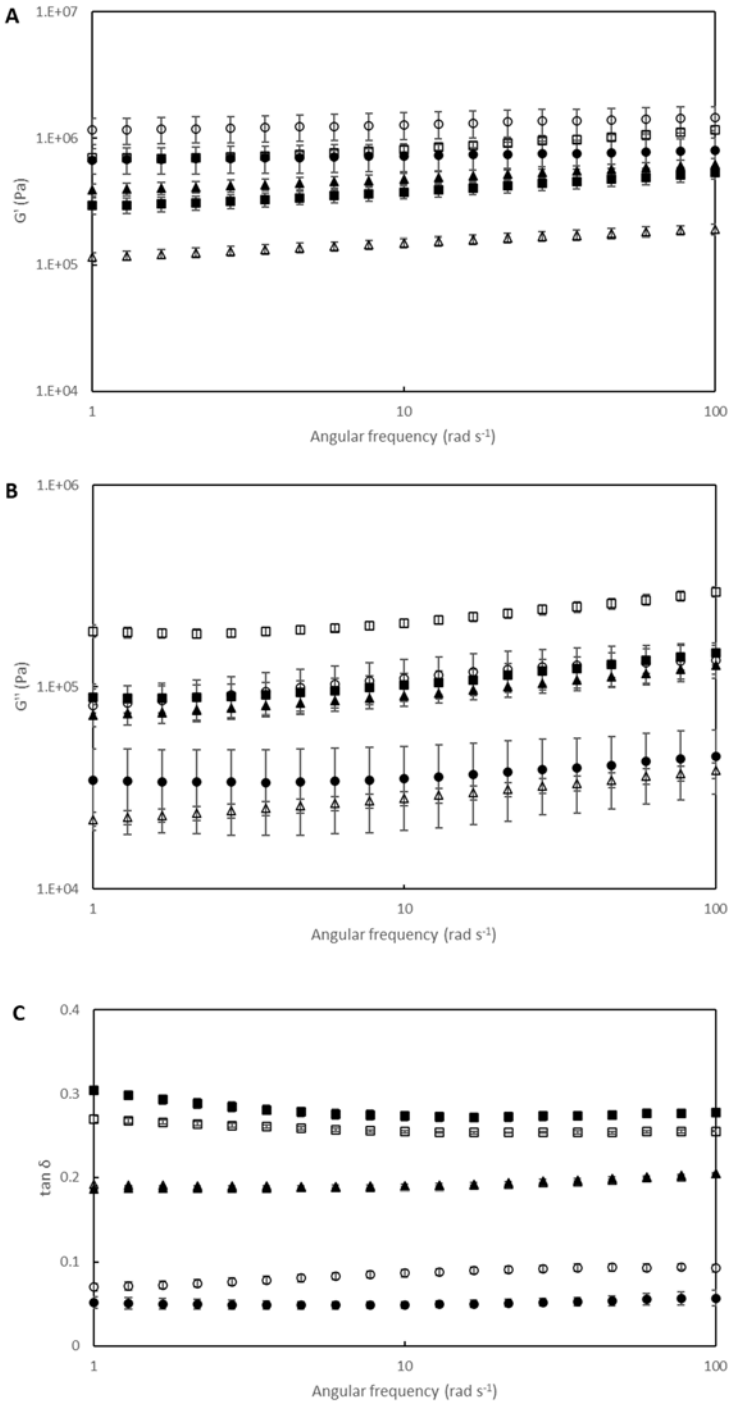
Viscoelastic Frequency Sweep

Figure S. 10 Storage modulus, G' (A), Loss modulus, G'' (B), and tan δ (C) of fresh mozzarella (■), paneer (□), extra firm tofu (▲), medium firm tofu (△), vegan mozzarella (●), and vegan cheddar (○), as a function of angular frequency (rad s^{-1}). Average ± standard deviation (n = 3).

Appendix C Supplementary Information for Comparisons

In the literature review of this thesis, comparisons were made by contrasting published experimental results. **Table S. 10** severs as an example of data used for comparison presented in **Table 2-5**.

Table S. 10 Supporting data of comparisons made in **Table 2-5**.

Coagulant	Coagulation rate	Texture	Microstructure	Taste
Gypsum ($CaSO_4$)	More than 8 min for curd formation based on visual observation [78]	Hardness: 416.8-458.5 g [78]; Hardness: 5828.5 N; Cohesiveness: 0.50; Springiness: 0.98; Chewiness: 2863.6 N [83]	SEM: larger pores, more uniformly rounded [84]; CLSM: fewer in number [83]	Sensory results of cooked gypsum (GYP) vs nigari (NGR) tofu [83]: Texture: 28 (GYP) & 48 (NGR) Flavour: 29 (GYP) & 47 (NGR) Overall: 24 (GYP) & 52 (NGR)
Nigari (bittern, mostly $MgCl_2$)	Rapid based on visual observation [74], [78], [77]	Hardness: 395.5-414.6 g [78]; Hardness: 4969.2 N; Cohesiveness: 0.47; Springiness: 0.99; Chewiness: 2334.0 N [83]	SEM: slightly more compact than gypsum [84]; CLSM: smaller pores with irregular size and shape [83]	Sensory results of uncooked GYP vs NGR tofu [83]: Texture: 48 (GYP) & 28 (NGR) Flavour: 47 (GYP) & 29 (NGR) Overall: 48 (GYP) & 28 (NGR)
Epsom ($MgSO_4$)	More than 8 min for curd formation based on visual observation [78]	Hardness: 292.5-293.4 g [78]	-	Sensory scores of Epsom (ES) vs Gypsum (GYP) tofu: Flavour: 4.3 (ES) & 6.2

				(GYP); Mouthfeel: 5.0 (ES) & 6.8 (GYP); Overall acceptability: 5.7 (ES) & 6.8 (GYP) [85]
Calcium chloride (CaCl2)	Rapid based on visual observation [78]	Hardness: 484.2-515.3 g [78]	-	-